Discrete symmetries, dynamical tadpoles, and the swampland

Memoria de Tesis Doctoral realizada por
Alessandro Mininno
presentada ante el Departamento de Física Teórica
de la Universidad Autónoma de Madrid
para optar al Título de Doctor en Física Teórica

Tesis Doctoral dirigida por
Ángel María Uranga Urteaga
Profesor de Investigación CSIC
en el Instituto de Física Teórica UAM-CSIC

Departamento de Física Teórica
Universidad Autónoma de Madrid

Instituto de Física Teórica
UAM-CSIC

Instituto de
Física
Teórica
UAM-CSIC

Universidad Autónoma
de Madrid

Junio de 2021

Disclaimer
The author received funding from "la Caixa" Foundation (ID 100010434) with fellowship code LCF/BQ/IN18/11660045 and from the European Union's Horizon 2020 research and innovation programme under the Marie Skłodowska-Curie grant agreement No. 713673.

Colophon
This document was typeset customizing KOMA-Script and LaTeX using the kaobook class. The source code of the original layout for the book is available at:
`https://github.com/fmarotta/kaobook`

To Martina and my family

This Ph.D. thesis is based on the following papers:

1. Eduardo García-Valdecasas, Alessandro Mininno, and Ángel M. Uranga. "Discrete Symmetries in Dimer Diagrams". In: *JHEP* 10 (2019), p. 091. DOI: 10.1007/JHEP10(2019)091. arXiv: 1907.06938 [hep-th]
2. Ginevra Buratti, José Calderón, Alessandro Mininno, and Ángel M. Uranga. "Discrete Symmetries, Weak Coupling Conjecture and Scale Separation in AdS Vacua". In: *JHEP* 06 (2020), p. 083. DOI: 10.1007/JHEP06(2020)083. arXiv: 2003.09740 [hep-th]
3. Alessandro Mininno and Ángel M. Uranga. "Dynamical Tadpoles and Weak Gravity Constraints". In: *JHEP* 05 (2021), p. 177. DOI: 10.1007/JHEP05(2021)177. arXiv: 2011.00051 [hep-th]

The aim of this thesis is to explain the results of the above papers, supplementing them with more background material of that present in the papers.
During my Ph.D. I collaborated also in the following projects:

4. Federico Carta and Alessandro Mininno. "No go for a flow". In: *JHEP* 05 (2020), p. 108. DOI: 10.1007/JHEP05(2020)108. arXiv: 2002.07816 [hep-th]
5. Federico Carta, Alessandro Mininno, Nicole Righi, and Alexander Westphal. "Gopakumar-Vafa hierarchies in winding inflation and uplifts". In: *JHEP* 05 (2021), p. 271. DOI: 10.1007/JHEP05(2021)271. arXiv: 2101.07272 [hep-th]
6. Federico Carta, Simone Giacomelli, Noppadol Mekareeya, and Alessandro Mininno. "Conformal Manifolds and 3d Mirrors of Argyres-Douglas theories". In: (May 2021). arXiv: 2105.08064 [hep-th]

Despite they have been original works where I made significant contributions, they will not be discussed in this document, because less pertinent to the discussion that I will develop in this thesis.

Acknowledgments

Many people have earned to be put in the acknowledgments of this thesis, but, by all means, one person deserves a special position: Ángel.
I thank you for teaching me everything I know about string theory. I thank you for having been there to explain me physics in a natural and clear way. I thank you for having listened to every question I asked you and having answered them comprehensively, wisely but always humbly. I thank you because you are the reason I know what I know, and I am writing this thesis. Many more things I wanted to learn from you, because three years are not sufficient to learn everything you know. However, thank you for putting me on this path, for guiding me, and I hope that now I am ready to continue by myself.

How not to continue without mentioning my friends and other collaborators in these three years: Federico. Everything I know of class $\mathcal{S}$ and non-Lagrangian theories I give it to you. Thank you for having been patient with me and having listened to me in our long Zoom calls of brainstorming. We have discussed and still are discussing many ideas of projects that we can do together, and I hope we will do. Our work together would have filled another Ph.D. thesis and I hope you know how grateful I am for your friendship and collaborations.

Speaking of collaborators, I think it is time to thank Alexander and Nicole. Our paper has not found space in this thesis, but I really enjoy working with you. Our Zoom calls, together with Federico, are always a source of interesting discussions and questions. I am really excited to come to Hamburg for working with you and having conversations about physics, books, movies, and TV series in person.

My collaborators at the IFT are the next people to thank: Eduardo, Ginevra and José.
Eduardo, I thank you for having answered to many of my doubts in my first year, when I was still trying to orient myself in the world of dimers that you mastered already. By the way, I did all our figures from scratch in Tikzpicture for this thesis because you know how much I hated Inkscape.
Ginevra, I thank you for sharing the office with me, for being my friend here in Madrid: my Italian friend in a foreign country. I remember very pleasantly our conversations about physics, gossip, movies, and TV series. I feel proudly responsible for your passion for Tarantino's movies!
José, my Swampland "Avenger", I thank you for our long discussions with Ginevra about discrete symmetries and monodromies. I really like your enthusiasm and your curiosity, despite I do not always understand your questions.

I need to thank my collaborators of the projects completed: Simone and Noppadol with whom I hope to work again in the future. I also thank my collaborators of the projects

been our beers at "your bar", our conversations about Chilean or Italian lifestyle, and the awful bureaucratic technicalities. I wish you good luck with everything.
I am not forgetting my other friends at the IFT: Joan and his memes, Sergio, Fran and Sergio with their songs and joyful presence, and all the others, thank you!

My Ph.D. would have been possible without my LaCaixa fellowship and my experience would have not been so enjoyable without my LaCaixitos: Max, Llorenç, Walter, Irene, Vicky, Michel, David, Miguel, Jose, Carol, Andrea and all the others that I cannot list because you are too many. Our first LaCaixa training in Girona has been fantastic, and I will always remember it. The second training would have been better if COVID-19 had allowed it. I will miss you all, and I thank you for having distracted me from work from time to time.

Special thanks go to my landlord Carlos, that let me stay in my wonderful apartment, and to Marceliano that many times helped me to fix small and big things there, and we had very interesting conversations about physics.

I would like to thank generically Spain. I fell in love for this country, for the city of Madrid, for its food, for its landscapes, and for its people. Spain welcomed me as I was one of them and I will always be grateful for that.

I would like to thank my Italian friends that I left Italy for pursuing my Ph.D. in Spain three years ago. I enjoyed our conversations on Telegram on the "Pannocchie" and "Perplessi" groups and I really hope to see you again in person one day. I would like to thank Damiano and Denise that came to Madrid before the pandemic and made me see places of Spain that I would have not visited alone.

Finally, I must thank the people to whom this thesis is dedicated: my family and Martina. I think that this time they deserve to understand what I am writing to them, so I will write in Italian.
Un ringraziamento, un abbraccio forte e un bacio vanno a mia madre. Te che da Bari tutti i giorni mi appoggi in tutte le mie decisioni e mi suggerisci sempre ciò che ritieni essere il meglio per me. Ti voglio bene e sappi che sempre ti ritengo vicino nonostante ci siano centinaia di chilometri che ci separano.
Un ringraziamento, un abbraccio forte e un bacio vanno anche a mio padre. Tu hai sempre sostenuto le mie scelte e mi hai aiutato come meglio potevi: ti voglio bene. Un abbraccio e un bacio vanno a Daniela che è sempre disponibile ad ascoltarti quando si ha bisogno e a Gabriele che sta crescendo in fretta e presto anche lui entrerà nel mondo universitario.

For the last person I must mention, I will switch to English again.
The last person that I will thank is Martina. She has always been there for me, whenever I was happy, stressed, sad, or excited. She always assured me with the kindest words when I needed someone to talk to. Despite we have been in different cities, we always tried to see each other whenever it was possible and every weekend or vacation was special.

My experience in Madrid ends here for now, but another one is opening soon in another country, and I am happy because you will be there for me.

Contents

List of Figures

List of Tables

Introduction

Introducción

Los dos logros más importantes de la Física del siglo pasado son la formulación del Modelo Estándar (ME) y la Relatividad General (RG). El primero es, quizás, la más importante Teoría de Campo Cuántico (TCC) jamás formulada y predice todas las partículas fundamentales descubiertas hasta la fecha. Ha sido comprobado experimentalmente durante décadas y la última partícula necesaria para completarlo, el bosón de Higgs, fue descubierta en el 2012 al CERN y no hay otras partículas elementales presentes en el modelo.
El ME es también una TCC que involucra solo tres de las interacciones fundamentales conocidas: la interacción fuerte, débil y electromagnética (estás últimas dos se unifican a energías superiores de la masa del bosón de Higgs en la interacción electro-débil). Sin embargo, la interacción gravitatoria se queda fuera, así el ME es una TCC en la que la gravedad está desacoplada.
Por otro lado, la gravedad tiene una descripción como teoría de campo clásica en la RG, en la que se asocia a la dinámica del espacio-tiempo. La RG también está muy bien comprobada experimentalmente y es responsable de la explicación de la dinámica de las galaxias y de la evolución del Universo. Una de las últimas confirmaciones de las predicciones de la RG son las ondas gravitacionales, detectadas en el 2016, uno de los primeros resultados teóricos de la RG.
ME y GR ofrecen muchos resultados interesantes, pero no son impecables.
El ME, por ejemplo, no contiene una explicación para las oscilaciones de los neutrinos (que se entienden mediante las masas de los neutrinos), o no explica por qué la masa del bosón de Higgs es tan pequeña en comparación con la escala donde los efectos gravitatorios se convierten relevantes, la escala de Planck. Este último problema puede solucionarse mediante una compleción ultravioleta (UV) del ME, considerado entonces una teoría de campo efectiva (TCE), válida hasta una determinada energía límite.
Una extensión natural del ME es el Modelo Estándar con Mínima Supersimetría (MEMS), donde se teoriza que cada partícula conocida tiene un compañero supersimétrico que difiere solo $1/2$ en el espín, y se relacionan mediante transformaciones supersimétricas. La supersimetría soluciona el problema de jerarquía descrito arriba, pero también impone una degeneración entre las masas de las partículas y sus supercompañeros. Puesto que no se ha observado degeneración alguna hasta ahora, si la supersimetría existe, se rompe a una determinada escala.
Otra razón para creer que el ME es una TCE es el número de parámetros libres presentes en la teoría y que tienen que ser fijados por los experimentos. Hay 18 parámetros libres, no predichos por el ME, y, en el lenguaje moderno de las TsCE, la presencia de un parámetro en una teoría corresponde a un valor de expectación del vacío (VEV) de un campo dinámico de otra TCQ. Este es el punto de vista que apoya la idea de que el ME no predice todo el espectro de partículas elementales.
Por último, ya hemos dicho que el ME no contiene la interacción gravitatoria, que está, en cambio, presente en una teoría clásica como la RG.
Por otro lado, la RG predice también la presencia de singularidades

en las soluciones de la ecuación de campo de Einstein, que no pueden ser resueltas con la teoría misma. Además, al ser la RG una teoría clásica, no puede capturar ningún efecto cuántico capaz de resolver estas singularidades.

La primera idea que viene en mente para resolver este problema, es hacer de la RG una TCC, es decir una teoría de Gravedad Cuántica (GC). Sin embargo, una cuantización directa de la RG conduce a divergencias, ya que la RG no es renormalizable. Esto significa que estas divergencias no pueden ser resueltas usando técnicas de renormalización y la teoría se vuelve mal definida a una escala donde los efectos cuánticos empiezan a ser relevantes, de nuevo, a la escala de Planck.
Nuevamente, en el lenguaje de las TsCE, esto podría significar que la RG es solamente válida hasta una determinada escala, y debería existir una teoría que es válida en el régimen ultravioleta. El más prometedor, si no el único, candidato que ofrece una teoría consistente de GC es la Teoría de Cuerdas (TC).
a idea de TC es considerar objectos de dimensión $1 + 1$ como partículas elementales en vez de objetos puntuales como en el ME. Estos objetos son las llamadas **cuerdas**. La longitud de la cuerda es dada por ls, que además fija la escala de energía a la cual estas cuerdas son apreciables. Generalmente, esta escala se encuentra cerca de la escala de Planck. Las cuerdas pueden ser abiertas o cerradas, y la diferente tipología de partículas que existen en nuestro Universo son vistas como diferentes modos de excitación de tales cuerdas. Las componentes del espacio-tiempo atravesadas por la cuerda mientras evoluciona en tiempo forma una hoja de universo (en ingles *worldsheet*, "WS"), y las interacciones son unívocamente determinadas considerando las diferentes topologías por el WS de la cuerda. Curiosamente, las ecuaciones del campo de Einstein surgen directamente a partir de la invariancia conforme del WS. El único parámetro libre en la teoría es la longitud de la cuerda ls, pero se cree que también puede ser un artefacto de la descripción perturbativa de la TC. Introduciendo la supersimetría en el WS, el número de dimensiones de espacio-tiempo de la TC se fijan a $D = 10 = 1 + 9$. Esto significa que hay seis dimensiones extra además del espacio-tiempo 4-dimensional que percibimos. El objetivo es compactificar tales dimensiones extras, de manera que no sean detectables a las escalas de energía accesibles experimentalmente.
Las cuerdas no son los únicos objetos predichos por la TC. Hay también objetos p-dimensionales extendidos, llamados p-branes, en la cual puede terminar una cuerda abierta. Ellos llevan cargas bajo campos gauge p-formas en la teoría. Cuando el acople de la cuerda crece suficientemente, las branas se convierten en los objectos fundamentales de la teoría, porque su masa se vuelve más pequeña de que la masa de la cuerda fundamental. Elegantemente, integrando todas la excitaciones masivas de cuerdas, TC se reduce a una teoría en 10d de supergravedad (SUGRA).
El hecho de que haya un parámetro libre, de nuevo, nos dice que debería existir otra teoría cuyo límite perturbativo es TC. Esta teoría es la llamada teoría M, y no se conoce, pero se cree que su límite de baja energía tiene que ser 11d SUGRA. Curiosamente, esta supuesta teoría no es una TC.

Declarar que estamos trabajando en un marco de TC no es suficiente para determinar unívocamente la tipología de teoría que estamos considerando. De hecho, hay cinco teorías de supercuerdas, pero, increíble-

mente, se relacionan todas mediante **dualidades**. Las teorías son

- tipo I, donde el número I se debe al número de gravitinos en la teoría. Se obtiene combinando cuerdas abiertas y cerradas no-orientadas de manera que sus inconsistencias individuales se cancelan. Preserva solamente 16 supercargas en 10d, es decir $\mathcal{N} = 1$.
- Tipo IIA, que es una teoría que contiene dos gravitinos con quiralidad opuesta, así que es una TC no quiral. Preserva áaxima supersimetría, es decir 32 supercargas o $\mathcal{N} = (1, 1)$ en 10d.
- Tipo IIB es también una teoría con dos gravitinos, pero con la misma quiralidad, así que es una TC quiral. También preserva máxima supersimetría, es decir $\mathcal{N} = (2, 0)$ in 10d.
- Las TsC heteróticas se obtienen estableciendo el sector levógiro como el de una TC bosónica y el sector dextrógiro como el de una supercuerda. Usando las cancelaciones de anomalías, los campos de materia pueden transformarse bajo $E_8 \times E_8$ o SO(32). Preservan 16 supercargas, es decir $\mathcal{N} = 1$ in 10d.

La red de dualidades se muestra en la Figura I:

- Tipo I y heterótica SO(32) tienen el mismo espectro sin masa y tienen las mismas acciones 10d SUGRA en el límite de baja energía.
- Tipo I es tipo IIB TC en orientifolds O9-planos.
- Tipo IIB es dual a tipo IIA bajo T-dualidad.
- 11d SUGRA compactificada en un circulo está relacionada con la acción efectiva de tipo IIA. Hay, entonces, una dualidad entre las dos teorías. En realidad, la dualidad es aún más fuerte, y habitualmente se llama dualidad de tipo IIA con M-teoría sobre un círculo. De hecho, es posible levantar los estados de tipo IIA que tienen cargas bajo de las p-formas de tipo IIA a teoría M. Las correspondientes p-branas son llamadas Mp-branas. Se construyen también como soluciones de 11d SUGRA. La aplicación de dualidad de las branas de tipe IIA y los objetos en teoría M se muestra en la Tabla I.
- Una discusión parecida, pero más difícil, puede ser hecha con la teoría M en $\mathbf{S}^1/\mathbb{Z}_2$ y $E_8 \times E_8$ TC heterótica.
- En fin, las dos TsC heteróticas están relacionadas usando T-dualidad.

Hay también otras dualidades que permiten de ir directamente desde una teoría a una otra, o también con teoría F.

No obstante todas las TsC parecen relacionadas unas con otras, hay todavía otro gran problema con las teorías de supercuerdas: TC necesita 10 dimensiones espacio-temporales para ser consistente y nosotros tenemos múltiples opciones de variedades que pueden ser usadas para compactificar las seis dimensiones extras. Además, la teoría en 4d resultante depende fuertemente de la variedad elegida y tenemos que tratar con un increíblemente gran conjunto de TsCE. Requeriendo que la cantidad de supersimetría en la TCE está reducida (pero no está totalmente rota) respecto de las 32 supercargas (o 16 por tipo I y TC heteroticas) de la teoría en 10d, usualmente, se escoge como variedad del espacio interno una Calabi-Yau (CY) compacta. Estas variedades son responsables de romper hasta 8 supercargas, e introduciendo planos de orientifolds o flujos, es posible romper hasta 8 supercargas, es decir $\mathcal{N} = 1$ in 4d.
La gran cantidad de TsCE que se puede obtener eligiendo diferentemente las CYs o los flujos toma el nombre de **Panorama de cuerdas** (en ingles *String landscape*). El número de vacíos posibles provenientes de TsCE

aparentemente distintas es del orden de 10^{272000} y de momento no hay ningún ejemplo de vació de cuerda que describa nuestro Universo. Esta es la razón por la que puede ser necesario cambiar de perspectiva. En lugar de buscar todas las TsCE posibles que provienen de TC, es más razonable entender cual son las reglas generales que una TCE acoplada con la gravedad debe satisfacer y mirar si admite una compleción en el UV hasta TC. Todas las TsCE que no son consistentes con TC (or con GC en general) se dicen que pertenecen al **Ciénaga** (en ingles *Swampland*).

El objetivo del programa del Ciénaga es, entonces, definir una serie de conjeturas (en la esperanza que se conviertan en teoremas) que todas las TsCE acopladas a la gravedad deben satisfacer. Cuando una TCE no satisface una de estas conjeturas, o pertenecen al Ciénaga, o la conjetura tiene que ser refinada para contemplar también esta TCE. El objetivo es formular principios bastante precisos que permitan seleccionar las TsCE que admiten una compleción en el UV hasta GC. Cuanto más refinada es la serie de conjeturas, más precisos son los limites que separan el Panorama del Ciénaga.

Muchas conjeturas del Ciénaga imponen limitaciones sobre la tipología de simetrías que son posibles en una TCE acoplada con la gravedad. Por ejemplo, una de las conjeturas más aclamadas dice que en una teoría de GC no pueden existir simetrías globales, y todas las simetrías tiene que ser gauge. Otra conjetura dice que la interacción gravitatoria tiene que ser la más débil de todas las interacciones en la TCE. Estas conjeturas se aplican a simetrías continuas y se cree que son válidas también en simetrías de gauge discretas. De hecho, en algunos contextos, la conjetura de "No simetrías globales" ha sida probada por todas las tipologías de simetrías. Pero, la función de las simetrías discretas en una teoría de CQ y en el programa de Ciénaga se encuentra todavía en desarrollo y no se comprende completamente.
Las simetrías discretas son estados fundamentales en muchas teorías de física más allá del ME. Pensamos al enigma del sabor, que trata de explicar el origin de las masas de los fermiones y sus mezclas. También se han considerado en el MEMS para explicar la estabilidad del protón. Sin embargo, sus orígenes permanece obscuros, y deberían ser investigadas a un nivel más fundamental. Es, entonces, interesante mirar qué limitaciones imponen las simetrías discretas al Panorama y al Ciénaga. En particular, pueden ser usadas, como veremos, como límite a la fuerza del acoplamiento de gauge de otras simetrías continuas en la teoría, o para justificar la presencia de separación de escala en vacíos de anti-de Sitter (AdS).

Muchas conjeturas de Ciénaga están hasta ahora tan bien testadas que pueden ser usadas para señalar inconsistencias en la TCE que se está estudiando. Esta es la situación, por ejemplo, de las teorías que tienen **tadpoles dinámicos**. Estos tadpoles no son topológicos, porque se asocian a campos dinámicos. La presencia de estos tadpoles habitualmente significa que la teoría no está en un mínimo de un potencial y está rodando bajo un potencial escalar. Es posible que si alguien elige ignorar los efectos de estos tadpoles, entonces alguna conjetura de Ciénaga no se satisfaga. El hecho de que la conjetura de Ciénaga esté violada significa que la solución de las ecuaciones de movimiento (EdM) no es correcta, y tiene que ser substituida con una solución que depende del tiempo que tiene en cuenta la presencia del tadpole dinámico. Es, entonces, posible

que la conjetura de Ciénaga es satisfecha, o que sea necesario modificarla de manera que sea válida en todo el espacio de campos.

Esquema de la tesis

La tesis contiene tres partes principales y una conclusión.

La primera parte contiene desde el Capítulo 1 a 4 y reúne todo el material de referencia necesario para entender los principales resultados de la tesis. En el Capítulo 1, empezamos con un resumen de la correspondencia AdS / TCC en la Sección 1.1. Esta correspondencia propone una equivalencia entre TC tipo IIB en AdS, especialmente $AdS_5 \times \mathbf{S}^5$, y la teoría de gauge $\mathcal{N} = 4$ superYang-Mills (SYM) en 4d. Además, extendemos la conjetura a un fondo general para las D3-branas que sondan una singularidad CY en la Sección 1.1.1. La CY es no-compacta y viene dada por un cono sobre una variedad de Sasaki-Einstein (SE) $\mathbf{X}_5$. La dualidad, entonces, relaciona TC tipo IIB en $AdS_5 \times \mathbf{X}_5$ con una teoría supersimétrica de campo conforme (TSCC), que vive en la D3-brana que sonda la punta del cono en la CY. Desde la generalización de la conjetura, explicamos como es posible construir vértices de bariones que son duales a operadores de bariones en la SCFT en la Sección 1.1.2. Es posible construir las TsSCC también en otras dimensiones espacio-temporales usando el principio holográfico. Por ejemplo, en la Sección 1.1.3, explicamos el modelo de Aharony-Bergman-Jafferis-Maldacena (ABJM), que es obtenido considerando la teoría M en $AdS_4 \times \mathbf{S}^7/\mathbb{Z}_k$. La teoría dual es una TSCC de Chern-Simons (CS) en 3d con grupo de gauge $U(N)_k \times U(N)_{-k}$.
La correspondencia relaciona todas las cantidades presentes en el lado gravitacional con una cantidad análoga en la TSCC. Por ejemplo, es posible reafirmar el principio de maximización de la carga central "a" que permite calcular las R-cargas de los campos en una TSCC con la minimización del volumen del espacio interno $\mathbf{X}_5$ en la teoría dual. Esto se llama **minimización del volumen** y lo explicamos enla Sección 1.1.4 y es útil para la discusión en el Capítulo 7.
Desde la Sección 1.2 empezamos a examinar compactificaciones de TC con orientifolds y flujos sobre variedad CY. Primero explicamos cuáles son la condiciones generales para compactificar con flujos en tipo II en la Sección 1.2.1 y luego damos algunas generalidades de variedades CY en la Sección 1.2.2. El procedimiento paso a paso para compactificar TC sobre CY es enseñado solo para tipo IIA desde la Sección 1.2.3 y haremos un ejemplo de estabilización de módulos en la Sección 1.2.3.4, donde explicamos DeWolfe-Giryavets-Kachru-Taylor (DGKT). Este ejemplo es importante para el Capítulo 6.

En el Capítulo 2 introducimos el concepto de teoría de gauge con **quivers** en la Sección 2.1. Para el caso de teorías de gauge tóricas, introducimos el **diagrama de dimer** y el suyo grafico dual, es decir el **quiver periodico**, en la Sección 2.2. Explicamos como es posible encontrar simetrías U(1) continuas usando el dimer (o quiver periódico) en la Sección 2.2.2. La novedad consiste en reformular estas técnicas usando **identidades geométricas**, introduciendo conceptos topológicos nuevos que son útiles para identificar simetrías globales U(1) usando los dimers. Esto está hecho en la Sección 2.3.1. Finalmente, explicamos como construir orbifolds

generales para teorías tóricas generales en la Sección 2.3.2. Este capítulo es importante para el Capítulo 5.

En el Capítulo 3, introducimos las simetrías discretas en TC. Primero, explicamos cómo simetrías discretas abelianas de gauge aparecen en teoría de campos, y su generalización a teoría de campos con dimensiones arbitrarias, en las Secciones 3.1 y 3.1.1. En la Sección 3.2, describimos las simetrías discretas de gauge que surgen naturalmente en compactificaciones de TC, centrándonos en aquellas asociadas al acoplamiento de Dvali-Kaloper-Sorbo (DKS). Los objetos con cargas bajo estas simetrías discretas son paredes de dominio (PD), que vamos a clasificar en compactificaciones sobre CY de tipo IIA. Finalmente, describimos cómo simetrías discretas surgen en TsCC tóricas en la Sección 3.3. Esta última sección es necesaria para la discusión en el Capítulo 5.

En el Capítulo 4, empezamos con un resumen del programa del Ciénaga, enumerando las conjeturas principales en la Sección 4.1. Desde la Sección 4.2, nos centramos en particular sobre las distintas versiones de la Conjetura de Gravedad Débil (CGD). Esta conjetura juega un papel importante en los Capítulos 6 y 7.

La segunda parte se centra en la relación entre simetrías discretas y el programa de Ciénaga. Contiene los Capítulos 5 y 6.
En el Capítulo 5, introducimos un nuevo kit para identificar el grupo de Heisenberg discreto que surge desde las TsCC que viven en D3-branas que sondan singularidades de orbifold generales de una CY 3-fold tórica general. Primero, explicamos cómo identificar la estructura de un grupo de Heisenberg discreto usando el dimer en Sección 5.2. Este grupo de Heisenberg puede ser realizado desde el espacio de cobertura de una teoría con orbifold y describimos como construirlo en manera sistemática En Sección 5.3. Desde la Sección 5.4. ofrecemos muchos ejemplos que ilustran nuestro procedimiento. Concluimos en la Sección 5.5 con comentarios sobre el dual gravitacional.

En el Capítulo 6, por fin, queremos entender cómo las simetrías discretas entran en el programa de Ciénaga. En la Sección 6.2, consideramos teorías de GC con simetrías de gauge discretas y continuas. Estudiamos la CGD para objetos Bogomol'nyi–Prasad–Sommerfield (BPS) presentes en la teoría y que tienen carga bajo una simetría discreta abeliana. Proponemos la Conjetura 6.1 que llamamos $\mathbb{Z}_k$ Conjetura de Acopiamiento Débil (CAD). Dicha conjetura dice que en una teoría de GC con una simetría discreta de gauge $\mathbb{Z}_k$ y una simetría continua de gauge con acoplamiento g, el acoplamiento de gauge debe escalar con $k^{-\alpha}$, donde α es un número de orden 1. A modo de ejemplo, en la Sección 6.3, usamos aquellas teorías cuyo grupo de Heisenberg ha sido identificado en el Capítulo 5. La historia se repite también con ABJM en la Sección 6.4. Ellos son presentes en modelos de intersección de branas, tal y como analizamos en la Sección 6.5. Desde la Sección 6.6, empezamos de estudiar simetrías discretas de 3-formas. Motivados por la estabilización de los módulos de DGKT en tipo IIA, que tiene una separación de escala en un vacío AdS en 4d, argumentamos que esta separación es debida a la presencia de estas simetrías discretas. Proponemos, entonces, un refinamiento de la Conjetura de la Distancia en AdS en la versión Fuerte (CDAF) en presencia de una simetría de gauge discreta $\mathbb{Z}_k$. Llamamos a la Conjetura 6.2 la Refinada Conjetura de la Distancia en AdS en la versión Fuerte

(RCDAF). También en este caso, apoyamos nuestra proposición con ejemplos usando las fórmulas de uniones, que revisamos en Apéndice A.

La tercera parte de la tesis, por otro lado, se centra en la interacción entre los tadpoles dinámicos, es decir tadpoles asociados a campos dinámicos, y la CGD con axiones. Contiene solo el Capítulo 7 y nuestras conclusiones son que, es posible que, en presencia de tadpoles dinámicos, la CGD no se satisfaga, siéndolo sólo en el mínimo del potencial. Primero, proponemos un vistazo de lo que está pasando en un contexto holográfico, usando las técnicas de minimización del volumen introducidas en la Sección 1.1.4. De hecho, en la Sección 7.2, aplicamos la minimización del volumen para calcular el volumen de 3-ciclos que son envueltos por D3-branas. Mostramso que la CGD se satisface solo si el volumen es minimizado, es decir si estamos en el mínimo del potencial. Desde la Sección 7.3, explicamos cómo calcular la reacción debida a la presencia de D-branas en diferentes configuraciones. Primero consideramos la reacción en configuraciones supersimétricas en la Sección 7.3.1, luego pasamos a las no supersimétricas en la Sección 7.3.2. Una vez que la configuración non-compacta está entendida, pasamos a discutir la presencia de tadpoles dinámicos en modelos de D7-branas desde la Sección 7.4. Consideramos una compactificación sobre toros con orientifold y flujos, que permiten la presencia de D7-branas móviles y ED3-branas y calculamos la reacción de las D7-branas, ligeramente desplazada de su mínimo, en los instantones. En la Sección refsec:the-clash, mostramos que la CGD no se satisface siempre si ignoramos la presencia del tadpole dinámico y nos quedamos con una solución que no depende del tiempo. El modelo explícito que analizamos se explica en detalle en la Sección 7.5.

La última parte se dedica a las conclusiones de esta tesis.

Además, complementamos la tesis con diferentes apéndices que permiten al lector entender mejor el contenido examinado en los diversos capítulos. En el Apéndice A explicamos las condiciones de uniones para vacíos en AdS. En el Apéndice B enumeramos los conceptos principales de geometría tórica, con el fin de introducir el concepto de diagrama tórico y su dual diagrama (p,q)-web en la Sección B.2. En el Apéndice C explicamos la anomalía de Freed-Witten (FW) en la Sección C.1 y introducimos la construcción de Hanany-Witten (HW) en la Sección C.2. Finalmente, en el Apéndice D listamos nuestras convenciones para las funciones modulares usadas en Capítulo 7.

Introduction

Two of the greatest achievements of Physics of the last century have been the formulation of the Standard Model (SM) and the General Relativity (GR). The former is, maybe, the most important Quantum Field Theory (QFT) that has been formulated and predicts all the fundamental particles that have been so far discovered. It has been tested for decades and the last particle that was necessary to complete the SM, i.e. the Higgs boson, which has been discovered in 2012 at CERN [7] and no more fundamental particles are present in the model.

The SM is also a QFT involving only three of the fundamental interactions that are known so far, i.e. the strong, the weak and the electromagnetic interaction (these last two unify at energies above the mass of the Higgs boson into the electro-weak interaction). However, the gravitational interaction is left out, so the SM is a QFT where gravity is decoupled.

The SM physics can be found in textbooks, e.g. [8–10]. While an introduction to GR can be found in [11, 12].

Gravity, on the other hand, has a classical field theory description in terms of GR, where it is associated with the dynamics of spacetime itself. GR is also very well tested by experiments, and it is responsible for explaining the dynamics of galaxies and the evolution of the Universe itself. One of the latest confirmations of the predictions of GR have been the gravitational waves, detected in 2016 [13] but they were one of the first theoretical results of GR.

SM and GR provide many interesting results, but they are not flawless. The SM, for instance, does not contain an explanation for the oscillations of the neutrinos (that it is understood in terms of neutrino masses), or it does not explain why the mass of the Higgs boson is so small compared to the scale where gravitational effects become relevant, i.e. the Planck scale. This last problem can be solved if one looks for Ultraviolet (UV) completion of SM, which is then considered as an Effective Field Theory (EFT) valid up to a certain energy cut-off.

A natural extension of the SM is the Minimal Supersymmetric Standard Model (MSSM), where it is theorized that each known particle has a supersymmetric partner which differs only by 1/2 in the spin, and they are related by supersymmetric transformations. Supersymmetry would solve the hierarchy problem described above, but it also imposes a degeneracy among the masses of particles and their superpartners. Since no degeneracy has been observed so far, if supersymmetry exists, it must be broken at some scale.

Rigid supersymmetry is nicely reviewed in [14] and references therein.

Another elegant reason to believe that SM is an EFT is given by the number of free parameters that are present in the theory that should be fixed by experiments. There are 18 free parameters that are not predicted by the SM and, in the modern language of EFTs, the presence of a parameter in a theory corresponds to the Vacuum Expectation Value (VEV) of some dynamical field of another QFT. This point of view supports the idea that the SM is not predicting the whole spectrum of fundamental particles.

Finally, we have already said that the SM does not contain the gravitational interaction, which is instead present in a classical theory such as GR.

On the other hand, GR predicts also the presence of singularities in the solutions of Einstein's field equation, that cannot be cured by the theory. Moreover, being GR a classical theory, it cannot capture any quantum effects that might cure such singularities.

The first idea that comes up to mind to solve this problem is to make GR a QFT, i.e. a theory of Quantum Gravity (QG). However, a straight forward quantization of GR leads to divergences, being GR non-Renormalizable. This means that such divergences cannot be cured using renormalization techniques and the theory becomes ill-defined at the scale in which quantum effects become relevant, i.e., again, the Planck scale.
Once again, in the EFT language, this might mean that GR is only valid up to a certain scale, and there must exist a theory that is valid in the UV regime. Such a theory is still not known.
The most promising, if not the only, candidate that provides a consistent theory of QG is String Theory (ST).

The discussion about ST is mainly based on [9].

The idea of ST is to consider $1 + 1$ dimensional objects as fundamental particles instead of point-like ones as in the SM. These objects are called **strings**. The length of the string is given by l_s and it sets the energy scale at which such strings become appreciable. Usually, such scale is close to the Planck scale. Strings can be open or closed, and the different kind of particles that are present in our universe are seen as different modes of excitation of such strings. The spacetime components spanned by the string while it evolves in time form a Worldsheet (WS), and the interactions are uniquely determined by considering the different topologies for the WS of the string. Interestingly, Einstein's field equations arise directly from the conformal invariance of the WS. The only free parameter in the theory is the string scale l_s but it is believed also that it might be an artifact of the perturbative description of ST.
Introducing supersymmetry on the worldsheet theory, we have also a constraint on the spacetime dimensions of the string theory framework, which is fixed to be $D = 10 = 1 + 9$. This means that there are an extra six dimensions in addition to the 4d spacetime we perceive. The aim is to compactify such extra dimensions so that they are undetectable at the energy scales that are currently accessible by experiments.
Strings are not the only objects that are predicted by ST. There are also extended p-dimensional objects, called p-branes, on which open strings can end. They carry charges under p-form gauge fields in the theory. When the string coupling grows large enough, they become the fundamental objects of the theory, since their mass becomes smaller than the mass of the fundamental strings. Nicely, integrating out all massive string excitations, ST reduces to be a 10d Supergravity (SUGRA) theory. The fact that there is a free parameter, once again, tells us that there should exist another theory whose perturbative limit is ST. Such theory is called M-theory, and it is not known, but it is believed that its low energy limit must be 11d SUGRA. Interestingly, this putative theory is not a string theory.

Declaring that we are working in a ST framework is not sufficient to uniquely determine the kind of theory we are going to consider. Indeed, there are five consistent superstring theories, but amazingly, they are all related by so-called **dualities**. The theories are

- Type I, where the number I states the number of gravitinos in the theory. It is obtained by combining open and closed unoriented strings in a way such that their individual inconsistencies cancel [9]. It preserves only 16 supercharges in 10d, i.e. $\mathcal{N} = 1$.
- Type IIA, which is a theory that contains two gravitinos with opposite chiralities, so it is a non-chiral string theory. It preserves

maximal supersymmetry, i.e., 32 supercharges or $\mathcal{N} = (1, 1)$ in 10d.
- Type IIB is instead the theory with two gravitinos but with the same chirality, so it is the chiral string theory. It also preserves 32 supercharges, i.e. $\mathcal{N} = (2, 0)$ in 10d.
- Heterotic string theories are obtained, taking the left sector to be that of a bosonic string theory, while the right sector to be that of the superstring. By anomaly cancellations, the matter fields can transform either under $E_8 \times E_8$ or SO(32). They preserve 16 supercharges, i.e. $\mathcal{N} = 1$ in 10d.

The web of dualities is showed in Figure I:

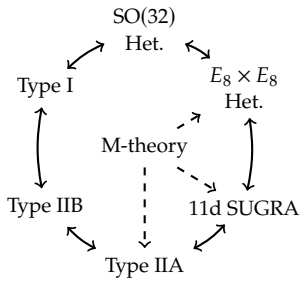

Figure I: Principal duality web of superstring theories.

- Type I and SO(32) Heterotic have the same massless spectrum, and they have the same low energy 10d SUGRA actions.[1]
- Type I is type IIB string theory on O9-planes orientifolds.
- Type IIB is dual to type IIA by T-duality.[2]
- 11d SUGRA compactified on a circle, is related to the effective action of type IIA. There is then a duality relating the two theories. Actually, the duality is even stronger, and it is usually stated as a type IIA / M-theory on a circle duality. Indeed, it is possible to lift the type IIA brane states charged under the type IIA p-form to M-theory. The corresponding p-branes are called Mp-branes. They can be constructed also as 11d SUGRA solutions. The duality map of the type IIA branes and the M-theory objects is in Table I from [9].
- A similar discussion, but trickier, can be done with the M-theory on $\mathbf{S}^1/\mathbb{Z}_2$ and $E_8 \times E_8$ heterotic duality. As a consequence, 11d SUGRA is also dual to $E_8 \times E_8$ heterotic string theory.
- Finally, the two heterotic string theories are related by T-duality.

1: Up to a change of variable.

2: There is also another duality that maps type IIB at weak coupling, to type IIB at strong coupling. This duality is known as S-duality.

There are also other dualities that allow one to go directly from one theory to the other, or also involve F-theory.

Despite all STs seem to be related one to the other, there is still another major problem with superstring theories: ST needs 10 spacetime dimensions in order to be consistent, and we have multiple choices of manifolds that can be used to compactify the extra six dimensions. Moreover, the resulting 4d theory depends strongly on the chosen manifold, and we need to deal with an incredibly large set of EFTs. Requiring that the amount of supersymmetry in the EFT is reduced (but not completely broken) with respect to the 32 supercharges (or 16 for type I and heterotic STs) of the 10d theory, usually, the manifold of the internal space is chosen to be a compact Calabi-Yau (CY). These manifolds are responsible

Type IIA	$\leftrightarrow$	M-theory on $\mathbf{S}^1$
D0-branes	$\leftrightarrow$	KK moments on 11d supergravitons
IIA string	$\leftrightarrow$	M2-branes wrapped on $\mathbf{S}^1$
D2-branes	$\leftrightarrow$	M2-branes
D4-branes	$\leftrightarrow$	M5-branes wrapped on $\mathbf{S}^1$
NS5-branes	$\leftrightarrow$	M5-branes
D6-branes	$\leftrightarrow$	KK monopoles

Table I: Relation between type IIA branes and Mp-branes.

to break up to 8 supercharges,[3] and introducing orientifold planes or fluxes, it is possible to break up to 4 supercharges, i.e. $\mathcal{N} = 1$ in 4d.
The large amount of EFTs that can be obtained by choosing differently CYs and fluxes take the name of **String landscape**. The number of possible vacua coming from apparently distinct EFTs is of the order of $\sim 10^{272000}$ and at the moment there is no known example of string vacuum that describes our universe.
This is the reason why it might be necessary to change perspective. Instead of looking at all possible EFTs that come from ST, it is more reasonable to understand what are the general rules that a EFT coupled to gravity must satisfy and look if it admits a UV completion to ST. All the EFTs that are inconsistent with ST (or QG in general) are referred to belong to the **Swampland**.

The aim of the Swampland is then that of defining a set of conjectures (in the hope that they become theorems) that all EFTs coupled to gravity must satisfy. Whenever an EFT does not satisfy one of these conjecture, either it belongs to the Swampland, or the conjecture must be refined to contemplate also this EFT. The purpose is to formulate principles precise enough that allow us to select the EFTs that admits a UV completion to QG. More refined is the set of conjectures, and more precise are the boundaries separating the Landscape from the Swampland.

Many Swampland conjectures set constraints on the kind of symmetries that are possible in a EFT coupled to gravity. For instance, one of the most acclaimed conjecture states that in a theory of QG there cannot be global symmetries, and all symmetries must be gauged. Another conjecture states that the gravitational interaction must be the weakest one among the interactions in a EFT. Such conjectures apply for continuous symmetries and are believed to hold also for discrete gauge symmetries. Indeed, in some context, the "No global symmetry" conjecture has been proved for any kind of symmetry. However, the rôle of the discrete symmetries in a theory of QG and in the Swampland program is still in development and not completely understood.
Discrete symmetries have been proved fundamental in many theories of physics beyond the SM. Let us think about the flavor puzzle, that aims to explain the origin of fermions masses and their mixing. They have been also invoked in the MSSM to explain the stability of the proton. However, their origin remains obscure, and they should be investigated at a more fundamental level. It is then interesting to see what kind of constraints the discrete symmetries imposes on the Landscape and the Swampland. In particular, they can be used, as we will see, as a bound on the gauge coupling strength of other continuous gauge symmetries in the theory, or to justify the presence of a separation of scale in a Anti-de Sitter (AdS) vacua.

Many Swampland conjectures are by now so tested that can be used also to show some inconsistency in the EFT that one is studying. This is the case, for instance, of theories that have **dynamical tadpoles**. Such tadpoles are not topological, but they are associated to dynamical fields. The presence of these tadpoles usually mean that the theory is not sitting at the minimum of a potential, but it is instead rolling down a slope of a scalar potential. It is possible that if one decides to ignore the effects of these tadpoles then some Swampland conjecture is not satisfied anymore. The fact that the Swampland conjecture is violated means that

3: We are considering CY 3-folds. For larger or smaller CYs the amount of broken supersymmetry is larger or smaller.

the solution to the Equations of motion (EoMs) is not the correct one, and it must be substituted with a time-dependent solution that takes into account the presence of the dynamical tadpole. It is then possible that the Swampland conjecture is restored, or it might be necessary to modify it so that it is valid in all field space.

Plan of the thesis

The thesis contains three main and one conclusive parts.

The first part contains Chapters 1 to 4 and it is collecting all the background materials that are necessary to understand the main results of the thesis.
In Chapter 1, we start with a review of the AdS / CFT correspondence in Section 1.1. This correspondence proposes an equivalence between type IIB string theory on AdS background, specifically $AdS_5 \times \mathbf{S}^5$, and $\mathcal{N} = 4$ SuperYang-Mills (SYM) gauge theory in 4d. We also extend the conjecture to general background for the D3-branes probing a CY singularity in Section 1.1.1. The CY is a non-compact CY given by the cone over a Sasaki-Einstein (SE) manifold $\mathbf{X}_5$. The duality then relates type IIB ST on $AdS_5 \times \mathbf{X}_5$ with a Supersymmetric Conformal Field Theory (SCFT) living on the worldvolume of the D3-brane probing the tip of the cone in the CY. From the generalization of the conjecture, we review how it is possible to construct baryonic vertices that are dual to baryonic operators in the SCFT in Section 1.1.2. It is possible to construct also SCFTs on different spacetime dimensions using the holographic principle. For instance, in Section 1.1.3 we review the Aharony-Bergman-Jafferis-Maldacena (ABJM) model, which is obtained considering M-theory on $AdS_4 \times \mathbf{S}^7/\mathbb{Z}_k$. The dual theory is a 3d Chern-Simons (CS) SCFT with gauge group $U(N)_k \times U(N)_{-k}$.
The correspondence relates every quantity on the gravity side to an analogous quantity on the SCFT. For instance, it is possible to restate the principle of a-maximization that allows the computation of the R-charges of the fields in a SCFT with the minimization of the volume of the internal space $\mathbf{X}_5$ in the gravity dual. This is usually called **Volume minimization**, and it is reviewed in Section 1.1.4, and it will be useful in the discussion in Chapter 7.
From Section 1.2 we start reviewing ST compactifications with orientifold and fluxes on CY manifold. We first explain what are the general conditions for compactifications with fluxes in type II in Section 1.2.1, and later we give some generalities on CY manifolds in Section 1.2.2. The step-by-step procedure to compactify string theory on CY is showed only for type IIA from Section 1.2.3, and we will make an example of moduli stabilization in Section 1.2.3.4, where we will review DeWolfe-Giryavets-Kachru-Taylor (DGKT). This example is important for Chapter 6.

In Chapter 2 we introduce the concept of **quiver** gauge theories in Section 2.1. For the case of toric gauge theories, we introduce the **dimer diagram** and its dual graph, i.e. **periodic quiver**, in Section 2.2. We review how it is possible to find continuous U(1) symmetries from the dimer (or periodic quiver) in Section 2.2.2. The novelty is on rephrasing such techniques using **geometric identities**, introducing new topological concepts that are useful to identify U(1) global symmetries using the

dimer. This is done in Section 2.3.1. Finally, we review how to construct general orbifolds for general toric theories in Section 2.3.2. This chapter is important for Chapter 5.

In Chapter 3, we introduce the discrete symmetries in ST. First, we review how Abelian discrete gauge symmetries appear in field theory, and their generalization to a field theory in arbitrary dimensions, in Sections 3.1 and 3.1.1. In Section 3.2, we describe the discrete gauge symmetries that arise naturally in ST compactifications, focusing on those associated to Dvali-Kaloper-Sorbo (DKS) couplings. The objects charged under these discrete symmetries are Domain Walls (DWs), that we will classify in type IIA CY compactifications. Finally, we describe how discrete symmetries arise in toric SCFTs in Section 3.3. This last section lays the foundations for what is discussed in Chapter 5.

In Chapter 4, we start with a review of the Swampland program, listing the principal conjectures in Section 4.1. From Section 4.2, we focus in particular on the various versions of the Weak Gravity Conjecture (WGC). Such conjecture plays an important rôle in Chapters 6 and 7.

The second part focuses on the relation between discrete symmetries and the swampland program. It contains Chapters 5 and 6.
In Chapter 5 we introduce new toolkits to identify the discrete Heisenberg groups that arise from the SCFTs living on D3-branes probing the general orbifold singularities of general toric CY 3-fold. We first explain how to identify the structure of a discrete Heisenberg group from the dimer in Section 5.2. Such Heisenberg group can be realized from the covering space of the orbifolded theory, and we describe how to construct it systematically in Section 5.3. From Section 5.4 we provide many examples that illustrate our procedure. We conclude in Section 5.5 with remarks on the gravity dual.

In Chapter 6, finally, we want to understand how discrete symmetries enter the Swampland program. In Section 6.2, we consider theories of QG with discrete and continuous gauge symmetries. We study the WGC for Bogomol'nyi–Prasad–Sommerfield (BPS) objects that are present in the theory and are charged under an Abelian discrete symmetry. We propose Conjecture 6.1 that we call $\mathbb{Z}_k$ Weak Coupling Conjecture (WCC). Such conjecture states that in a theory of QG with a $\mathbb{Z}_k$ discrete gauge symmetry and a continuous gauge symmetry with coupling g, the gauge coupling g must scale with $k^{-\alpha}$, where α is some order 1 number. As an example, in Section 6.3, we use those theories whose Heisenberg group has been identified in Chapter 5. The story is repeated also for ABJM in Section 6.4. They are also present in intersecting brane models, as we analyze in Section 6.5. From Section 6.6, we start to study discrete 3-form symmetries. Motivated by the DGKT type IIA moduli stabilization, which is a scale separated AdS vacuum in 4d, we argue that such scale separation is due to the presence of these discrete symmetries. We propose, then, a refinement of the Strong AdS Distance Conjecture (SADC) when a $\mathbb{Z}_k$ discrete gauge symmetry is present. We call Conjecture 6.2 the $\mathbb{Z}_k$ Refined Strong AdS Distance Conjecture (RSADC). Also for this case we support our proposal with examples using junction formulas, reviewed in Appendix A.

The third part of the thesis, instead, focuses on the interplay between dynamical tadpoles, i.e., tadpoles associated to dynamical fields, and the

axion WGC. It contains only Chapter 7 and our findings are that, it is possible that whenever the dynamical tadpoles are ignored, the WGC is not satisfied, being satisfied only at the minimum of the potential. We first propose a glimpse of what it is happening in an holographic context, using volume minimization techniques introduced in Section 1.1.4. In fact, in Section 7.2, we apply the volume minimization to compute the volume of 3-cycles that are wrapped by D3-branes. We show that the WGC is satisfied only if the volume is minimized, i.e. we are at the minimum of the potential. From Section 7.3, we review how to compute D-brane backreactions in various set-ups. First we consider supersymmetric backreactions in Section 7.3.1, then we move to non-supersymmetric one's in Section 7.3.2. Once that the non-compact set-up is understood, we move to discuss the presence of dynamical tadpoles in D7-brane models from Section 7.4. We consider a toroidal orientifold compactification with fluxes, that support mobile D7-branes and ED3-branes, and we compute the backreaction of the D7-branes, slightly moved off the minimum, to the instantons. In Section 7.4.3, we show that the WGC is not always satisfied if we ignore the presence of the dynamical tapdole, and we stick with a time-independent solution. The explicit model that we analyze is explained in detail in Section 7.5.

The last part is devoted to the conclusions of this thesis.

In addition, we supplement the thesis by various appendices that allow the reader to better understand the content discussed in the various chapters. In Appendix A we review the junction conditions for AdS vacua. In Appendix B we list the basic concepts of toric geometry, in order to introduce the concept of toric diagram and its dual (p, q)-web diagram in Section B.2. In Appendix C we review Freed-Witten (FW) anomaly in Section C.1, and we introduce Hanany-Witten (HW) construction in Section C.2. Finally, in Appendix D we list our conventions for the modular functions used in Chapter 7.

Background materials

Elements of string theory and string theory compactification

1

In this chapter, we review some basic concepts of string theory and string compactification. In particular, we introduce the correspondence between type IIB string theory on AdS and Conformal Field Theories (CFTs). We will focus mainly on AdS_5 / CFT_4 correspondence in Section 1.1 both in the original formulation and in its generalization (Section 1.1.1) for type IIB on $AdS_5 \times \mathbf{X}_5$, where $\mathbf{X}_5$ is a toric SE manifold. We then give in Section 1.1.2 a glimpse of how baryonic vertices can be constructed in the gravity side of the correspondence. We introduce the concept of volume minimization as gravity dual of the a-maximization for a 4d $\mathcal{N} = 1$ gauge theory in Section 1.1.4. We will just refer to other generalizations of the conjecture given by, for instance, the ABJM model in Section 1.1.3. In Section 1.2 we review type II compactification with fluxes, focusing in particular on type IIA string theory. The papers used to write this chapter are usually cited at the beginning of each section.

1.1 AdS / CFT correspondence

Section 1.1 is based on [15–19].

In [15], it has been proposed a groundbreaking equivalence between type IIB string theory on $AdS_5 \times \mathbf{S}^5$ and $\mathcal{N} = 4$ SYM gauge theory in 4d. The strong form of the correspondence is the following [19]:

Conjecture 1.1 [Strong Maldacena's AdS_5 / CFT_4 conjecture [15]]**.**

Type IIB string theory on $AdS_5 \times \mathbf{S}^5$ with radius R and N units of F_5 flux on $\mathbf{S}^5$ is dynamically equivalent to $\mathcal{N} = 4$ pure SU(N) SYM theory, with gauge coupling g_{YM}.

In particular, the following relations among the parameters are conjectured to hold:

$$g^2_{\text{YM}} = 2\pi g_s \text{ and } 2g^2_{\text{YM}} N = \frac{R^4}{\alpha'^2}\,. \tag{1.1}$$

It is instructive to see what are the arguments that brought Maldacena to come up with the conjecture in [15]. Following [17–19], we can first consider N parallel D3-branes spanning a 10d Minkowski space. For this set-up, we can consider two kinds of perturbative excitations: those coming from the closed string sector and those from the open string sector [17, 20, 21]. In the low energy limit, only the zero modes of the open and closed strings enter [18]. The closed string massless states give a gravity multiplet in 10d, while the open string massless states form a $\mathcal{N} = 4$ vector multiplet in 4d [17]. The two sectors decouple at low energy, so we get a $\mathcal{N} = 4$ SU(N) SYM in 4d[4] and a decoupled free 10-dimensional supergravity in flat space.
The second point of view we can take is that of a D3-brane solution of

4: More properly the gauge group on a stack of N D3-branes is U(N), but in the Infrared (IR) the U(1) decouples.

supergravity with N units of D3-brane flux [22]:

$$ds^2 = Z(r)^{-1/2}\eta_{\mu\nu}dx^\mu dx^\nu + Z(r)^{1/2}\left(dr^2 + r^2 d\Omega_5^2\right) , \tag{1.2}$$

with

$$F_5 = (1+\star)dZ^{-1}dx^0dx^1dx^2dx^3 \text{ where } Z(r) = 1 + \frac{4\pi\alpha'^2 g_s N}{r^4} . \tag{1.3}$$

The function $Z(r)$ in Eq. (1.3) becomes constant when r approaches infinity. The solution is then a 10d Minkowski flat space. When $r \to 0$, $Z(r)$ scales as r^{-4}, but the metric in Eq. (1.2) is heavily redshifted. The low energy theory consists, once again, of two decoupled sectors: the near horizon region of the geometry and a decoupled free 10-dimensional supergravity in flat space. Defining $R^4 = 4\pi\alpha'^2 g_s N$, the near horizon limit is obtained for $r \ll R$, so that $Z(r) \sim R^4/r^4$. The geometry in Eq. (1.2) becomes [17]

$$ds^2 = \frac{r^2}{R^2}\eta_{\mu\nu}dx^\mu dx^\nu + R^2\frac{dr^2}{r^2} + R^3 d\Omega_5^2 , \tag{1.4}$$

where we recognize the geometry of $AdS_5 \times \mathbf{S}^5$. Thus, we get the conjecture in Conjecture 1.1.

1.1.1 Generalization of the correspondence

Section 1.1.1 is based on [17, 18] and references therein.

The duality between type IIB supertring theory on $AdS_5 \times \mathbf{S}^5$ and $\mathcal{N} = 4$ SYM is not the only application of Conjecture 1.1. We can consider a more general background for the D3-branes. Namely, instead of D3-branes on a (1 + 9)d Minkowski space, we could consider a space as

$$ds^2 = ds^2_{\mathbf{M}_4} + dr^2 + r^2 ds^2_{\mathbf{X}_5} , \tag{1.5}$$

where $\mathbf{M}_4$ is a Minkowski space, while $dr^2 + r^2 ds^2_{\mathbf{X}_5}$ is a metric of a conic Ricci flat manifold $\mathbf{Y}_6$, such $\mathbf{X}_5$ is a suitable manifold at the base of cone. The metric of $\mathbf{X}_5$ is constrained by the Ricci-flatness condition of $\mathbf{Y}_6$ such that

$$R^{\mathbf{X}_5}_{mn} = 4g^{\mathbf{X}_5}_{mn} . \tag{1.6}$$

Considering D3-branes at the tip $r = 0$ of the cone, one can repeat the study of the spectrum at the low energy limit on the D3-branes and this is conjectured to be equivalent to the near horizon limit of type IIB supergravity on $AdS_5 \times \mathbf{X}_5$ with N units of self-dual 5-form flux through $\mathbf{X}_5$. One of the main difference is, however, the curvature radius R of AdS_5 that this time is related to the volume of $\mathbf{X}_5$ as follows:

$$R^4 = \frac{4\pi^2\alpha'^2 g_s N}{\text{Vol}(\mathbf{X}_5)} . \tag{1.7}$$

1.1.1.1 Orbifold singularities

Section 1.1.1.1 is based on [17, 18, 23] and references therein.

The simplest generalization of the conjecture is to consider D3-branes at orbifold singularities. This corresponds to consider the near horizon limit of D3-branes on $\mathbf{M}_4 \times \mathbb{R}^6/\Gamma$, where Γ is some finite subgroup of the rotation symmetry group $SO(6) \simeq SU(4)_R$. If $\Gamma \subset SU(2)$, supersymmetry

is broken to $\mathcal{N} = 2$ in the corresponding 4d SCFT, while, if $\Gamma \subset$ SU(3, supersymmetry is broken down to $\mathcal{N} = 1$ in 4d. On the gravity side, this corresponds to consider type IIB supergravity on $AdS_5 \times \mathbf{S}^5/\Gamma$. The simplest way to construct the field theory is to consider N D3-branes on the covering space of $\mathbb{R}^6/\Gamma$, i.e., $\mathbb{R}^6$. There are, then, dim Γ images of each D3-brane. The theory is obtained projecting the U(N dim Γ) $\mathcal{N} = 4$ SCFT over the modes that are invariant under Γ. This is done by specifying that Γ is acting on the Chan-Paton indices as that of a regular representation of Γ. We will construct in detail the field theory obtained by the orbifold projection in Section 2.3.2.

1.1.1.2 Non-orbifold singularities

Section 1.1.1.2 is based on [17, 18, 24, 25] and references therein.

Interesting are also the singularities constructed from the cone over $\mathbf{X}_5$ that, instead, are not coming from orbifolds. In this case, the theories are obtained requiring that $\mathbf{Y}_6 = C(\mathbf{X}_5)$ is a non-compact CY 3-folds. Since the holonomy of the manifold is reduced to SU(3), by our definition of CY, supersymmetry is reduced to only 4 supercharges, i.e., $\mathcal{N} = 1$ in 4d. If the cone is CY, then, also $\mathbf{X}_5$ as a name, and it is called **Sasaki-Einstein** manifold. The simplest SE is $\mathbf{S}^5$, and its cone is simply $\mathbb{C}^3$, i.e., the flat space. Historically, the second manifold for which an explicit metric was known is called $T^{1,1}$ [27]. This is a $\mathbf{S}^1$ bundle over $\mathbf{S}^2 \times \mathbf{S}^2$ and in the literature, it is usually expressed in terms of the coset space

We review some basic property of SE manifolds, in particular for the case of toric CYs, in Section 1.1.4. The interested readers can find them reviewed e.g. in [25, 26] and references therein.

$$T^{1,1} = \frac{\text{SU}(2) \times \text{SU}(2)}{\text{U}(1)} \,. \tag{1.8}$$

The exact metric for $T^{1,1}$ is known to be

$$ds^2_{T^{1,1}} = \frac{1}{6} \sum_{i=1}^{2} \left(d\theta_i^2 + \sin^2 \theta_i d\phi_i^2 \right) + \frac{1}{9} \left(d\psi - \sum_{i=1}^{2} \cos \theta_i d\phi_i \right)^2 \,, \tag{1.9}$$

that describes a circle bundle, where the circle ψ is fibered over $\mathbf{S}^2 \times \mathbf{S}^2$ [23, 27]. Its cone is CY and it is called **conifold**. The CY metric reads

$$ds^2_{\mathscr{C}(T^{1,1})} = dr^2 + r^2 ds^2_{T^{1,1}} \,, \tag{1.10}$$

which can be inserted in Eq. (1.2) and it corresponds to the near horizon limit of type IIB compactified on $AdS_5 \times T_{1,1}$ with N units of F_5 flux on $T^{1,1}$. The gauge theory obtained by probing the tip of the conifold singularity is a toric quiver gauge theory. We will consider this theory in Chapter 5 (see also Section 1.1.4.1 as an example of volume minimization applied to this example).
Another famous category of SE manifolds is that called $Y^{p,q}$. They constitute an infinite class of SE manifolds and the D3-branes probing the real cone constructed over them is associated to $\mathcal{N} = 1$ 4d SCFTs.

1.1.2 Baryons in AdS

Section 1.1.2 is based on [16, 17, 28–31] and references therein.

Another generalization of Conjecture 1.1 is to consider the near horizon limits of D3-branes on orientifolds. They are very similar to orbifolds, but there are no twisted sector states in this case. The orientifold cases are interesting because they break the same amount of supersymmetry

of D3-branes, so in the near horizon limit we still have a $\mathcal{N} = 4$ 4d SCFT. However, the projection would change the gauge group on the stack of the D-branes. There are two possible projections, giving either SO($2N$) gauge group[5] or USp($2N$) gauge group for the $\mathcal{N} = 4$ gauge theory in 4d. On the gravity side this corresponds to type IIB string theory on $AdS_5 \times \mathbf{S}^5/\mathbb{Z}_2 \equiv AdS_5 \times \mathbb{RP}^5$. However, from the gravity side we still need to see how it is possible to distinguish between the three possible gauge groups that arise on the SCFT. This is done implementing a discrete torsion on $\mathbb{RP}^5$. The Neveu–Schwarz − Neveu–Schwarz (NSNS) B_2 field can be turned on in the non-trivial cohomology class of $H^3\left(\mathbb{RP}^5, \tilde{\mathbb{Z}}\right) = \mathbb{Z}_2$.[6] It is also possible to turn on a similar discrete torsion for the Ramond − Ramond (RR) B-field. It turns out, then, there are four possible string theories on $AdS_5 \times \mathbb{RP}^5$: when there is no B-fields, the corresponding 4d SCFT is SO($2N$). The theory where B_{NSNS} is non-zero, it corresponds to 4d SCFT with gauge group USp($2N$). The theory where B_{RR} is non-zero corresponds to SO($2N + 1$) gauge theory.
The theory corresponding of SO($2N$) gauge group is particularly interesting because it allows a gauge invariant chiral superfield constructed with the Pfaffian. This operator is dual to a D3-brane wrapped around a 3-cycle in $\mathbb{RP}^5$, corresponding to the homology class $H_3\left(\mathbb{RP}^5, \mathbb{Z}\right) = \mathbb{Z}_2$. This is the first example of baryon operator in the AdS / CFT context.

5: In this case it is possible to add an additional D3-brane stuck on the orientifold, to get SO($2N + 1$) gauge groups.

6: $\tilde{\mathbb{Z}}_2$ is a twisted sheaf of integers [28].

The possibility of wrapping a D3-brane over a 3-cycle is possible only if there is no B-field turned on. This is consistent with the fact that this operator can be generated only if the group is SO($2N$).

Section 1.1.2.1 is based on [17, 29] and references therein.

1.1.2.1 Heisenberg group: a first encounter

This is not the only possibility to obtain a baryon operator from the AdS / CFT correspondence. Considering for instance D3-branes probing a conifold singularity, the dibaryon operator that can be constructed on the gauge theory side, corresponds to a D3-brane wrapped on an orbit of one of the two SU(2)'s in the definition of the $T^{1,1}$ coset space.
There are also many orbifold theories where it is possible to construct dibaryon operators. One example has been explored in [29], where they considered type IIB on $AdS_5 \times \mathbf{S}^5/\mathbb{Z}_3$. The presence of the orbifold generates torsion homologies for $\mathbf{S}^5/\mathbb{Z}_3$ where different branes may be wrapped on torsion cycles. A D3-brane wrapped on a torsion 3-cycle is a dibaryon operator. Interesting, since $H_1(\mathbf{S}^5/\mathbb{Z}_3, \mathbb{Z}) = \mathbb{Z}_3$, it is possible to turn on $\mathbb{Z}_3$ valued Wilson lines. This leads to triplets of D3-brane states, on which a discrete group acts faithfully. This group is a discrete **Heisenberg group**. We will see the action of the Heisenberg group at the level of the field theory in Section 3.3 while we will devote a complete chapter (Chapter 5) for the general analysis of the Heisenberg group on toric quiver gauge theories.

Discrete Heisenberg group

A discrete Heisenberg group $H_k(\mathbb{Z})$ is a non-Abelian nilpotent group with 2 generators, A and B, and one central element C. The generators, by definition, commute with the central element, while it is true the following commutation relation:

$$C = ABA^{-1}B^{-1}\,.$$

If the Heisenberg group is defined modulo p, where p is a prime number, the elements of the group satisfy

$$A^p = B^p = C^p = 1\,.$$

Section 1.1.3 is based on [2, 23, 32] and references therein.

1.1.3 ABJM model

What we are going to discuss in this section is the gravity dual of the ABJM theory [32]. On the SCFT side, this is a 3d supersymmetric $U(N)_k \times U(N)_{-k}$ CS matter theory, with $\pm k$ denoting the CS level. From the gravity perspective, it is possible to realize this theory considering an extension of Conjecture 1.1. Indeed, the AdS / CFT correspondence can also be established for other types of branes. An example is to consider 11d supergravity (or low energy limit of M-theory) on $AdS_4 \times \mathbf{S}^7/\mathbb{Z}_k$. The ABJM theory is then living on a stack of N M2-branes probing a $\mathbb{C}^4/\mathbb{Z}_k$

orbifold singularity, and the orbifold is acting on the $\mathbb{C}^4$ coordinates z_i as $z_i \longrightarrow e^{2\pi i/k} z_i$. The curvature radius of the covering $\mathbf{S}^7$ and the AdS_4 is given by

$$R^6 = 2^5 \pi^2 M_{P,11}^{-6} N k \,, \tag{1.11}$$

where we have used again the covering space perspective as in Section 1.1.1.1 to define the radius of the orbifolded space. Using this radius it is possible to describe this theory in type IIA. The type IIA limit arises as follows. The $\mathbf{S}^7$ is a $\mathbf{S}^1$ Hopf fibration over $\mathbb{CP}^3$, where the $\mathbb{Z}_k$ quotient acts on the $\mathbf{S}^1$. The radius of the $\mathbb{CP}^3$ factor is large whenever $Nk \gg 1$. From (1.11) we conclude that the M-theory description is valid whenever $k^5 \ll N$. When k increases, we end up in a weakly coupled regime, and we can reduce to type IIA string theory [32].

The type IIA background corresponds to a compactification on $AdS_4 \times \mathbb{CP}^3$ with internal and AdS radii R_s (see below), with N units of F_6 RR flux over $\mathbb{CP}^3$ (i.e., of F_4 flux over AdS_4) and k units of F_2 RR flux over $\mathbb{CP}^1 \subset \mathbb{CP}^3$ (due to the Hopf fibration of the M-theory $\mathbf{S}^1$).

The matching of string theory quantities to the 11d Planck scale is as follows. The 10d string coupling g_s is related to the M-theory radius $\mathcal{R} = R/k$ as

$$g_s = M_{P,11}^{3/2} \mathcal{R}^{3/2} \,, \tag{1.12}$$

that scales as

$$g_s \sim N^{1/4} k^{-\frac{5}{4}} \,. \tag{1.13}$$

The string scale M_s is related to the 11d Planck scale as

$$M_{P,11}^3 = \frac{M_s^3}{g_s} \,. \tag{1.14}$$

Therefore, in terms of M_s, the radius (1.11) becomes

$$R \sim N^{1/6} k^{1/6} g_s^{1/3} M_s^{-1} \,. \tag{1.15}$$

Finally, we need the radius R_s of $\mathbb{CP}^3$ from the string viewpoint. The type IIA metric is given by

$$ds_{IIA}^2 = R_s^2 \left(\frac{1}{4} ds_{AdS_4}^2 + ds_{\mathbb{CP}^3}^2 \right) \,, \tag{1.16}$$

where

$$R_s^2 \sim N^{1/2} k^{-1/2} M_s^{-2} \,. \tag{1.17}$$

In Chapter 6 we will use this theory to introduce the $\mathbb{Z}_k$ WCC and we will review the discrete symmetries present in both the M-theory and type IIA perspective of the ABJM model.

1.1.4 Volume minimization

Section 1.1.4 is based on [3, 18, 25, 33–36] and references therein.

In this section, we recall the key ideas in [25, 33]. Consider the AdS / CFT duality between 4d $\mathcal{N} = 1$ quiver gauge theories, obtained from D3-branes at a toric CY threefold singularity $\mathbf{Y}_6$, and type IIB string theory on $AdS_5 \times \mathbf{X}_5$, with the horizon $\mathbf{X}_5$ given by the base of the real cone $\mathbf{Y}_6$. The CY condition of $\mathbf{Y}_6$ implies that $\mathbf{X}_5$ is SE, and has at least

one U(1) symmetry (dual to the SCFT $U(1)_R$-symmetry). It is generated by the Reeb vector, obtained from the complex structure J of $\mathbf{Y}_6$ by

$$\xi = J\left(r\frac{\partial}{\partial r}\right) . \tag{1.18}$$

Using the condition that $\mathbf{X}_5$ is Einstein, it is possible to fix the normalization of the Ricci tensor as

$$\mathcal{R}_{mn} = 4g_{mn} . \tag{1.19}$$

This Ricci tensor can be obtained extremizing the Einstein-Hilbert action, which can be recast as the volume of $\mathbf{X}_5$ [33]

$$S[g] = \int_{\mathbf{X}_5} d^5x\sqrt{g}\left(\mathcal{R}_{\mathbf{X}_5} - 12\right) = 8\text{Vol}(\mathbf{X}_5) , \tag{1.20}$$

which in turn depends only on the Reeb vector ξ. This means that the problem of finding the metric for the SE manifold reduces to the minimization of the volume with respect to the Reeb vector. For toric $\mathbf{Y}_6$, the SE manifold $\mathbf{X}_5$ has at least an $U(1)^3$ isometry. Let us introduce the 3d vectors defining the toric fan data of $\mathbf{Y}_6$; since they lie on a plane, they are of the form $v_i = (1, w_i)$, with w_i giving the toric diagram of the geometry. The computation of the volume of $\mathbf{X}_5$ is done using the Duistermaat-Heckman formula and via localization, which boils down to simple closed formulas in the toric case. We write down the coordinates of $\xi = (3, b_2, b_3)$ as[7]

A review of toric geometry is in Appendix B.

7: By $\det(x, y, z)$, we mean the determinant of the matrix obtained by the vectors x, y and z as rows (or columns).

$$\text{Vol}(\mathbf{X}_5) \equiv \frac{\pi^3}{3}\sum_{i=1}^{d}\frac{\det(v_{i-1}, v_i, v_{i+1})}{\det(\xi, v_{i-1}, v_i)\det(\xi, v_i, v_{i+1})} , \tag{1.21}$$

The quantity Z is defined as the volume of a SE manifold, relative to that of the round sphere. It is an algebraic number given by

$$Z(b_2, b_3) \equiv \frac{1}{(2\pi)^3}\text{Vol}(\mathbf{X}_5) = \frac{1}{24}\sum_{i=1}^{d}\frac{\det(v_{i-1}, v_i, v_{i+1})}{\det(\xi, v_{i-1}, v_i)\det(\xi, v_i, v_{i+1})} , \tag{1.22}$$

The AdS solution thus corresponds to the configuration which minimizes this quantity with respect to the Reeb vector, a procedure known as Z-minimization. Incidentally, this provides the gravity dual of the a-maximization [37] in the holographic 4d $\mathcal{N} = 1$ SCFT.

In the toric case, we can be more precise in the expression of the volumes in terms of the toric data. For instance, let us consider a 3-cycle Σ_i of a SE manifold $\mathbf{X}_5$. Such a cycle has a volume that also can be expressed as a function of the Reeb vector and, in the toric case, using the fan data of $\mathbf{Y}_6$. It is another result in [33] that the volume of a 3-cycle as a function of ξ is

$$\text{Vol}(\Sigma_i) \equiv 2\pi^2\frac{\det(v_{i-1}, v_i, v_{i+1})}{\det(\xi, v_{i-1}, v_i)\det(\xi, v_i, v_{i+1})} . \tag{1.23}$$

From this expression it is possible to show that[8]

8: For details of the general proof for toric SE manifold, the reader can have a look at [33].

$$\text{Vol}(\mathbf{X}_5) = \frac{\pi}{6}\sum_{i=1}^{d}\text{Vol}(\Sigma_i) . \tag{1.24}$$

Finally, it is better to define R the radius of the AdS space and of the internal manifold $\mathbf{X}_5$. Eq. (1.21) and (1.23) become

$$\begin{aligned} \mathrm{Vol}\,(\mathbf{X}_5) &= \frac{\pi^3 R^5}{3} \sum_{i=1}^{d} \frac{\det\,(v_{i-1}, v_i, v_{i+1})}{\det\,(\xi, v_{i-1}, v_i)\det\,(\xi, v_i, v_{i+1})}\,, \\ \mathrm{Vol}\,(\Sigma_i) &= 2\pi^2 R^3 \frac{\det\,(v_{i-1}, v_i, v_{i+1})}{\det\,(\xi, v_{i-1}, v_i)\det\,(\xi, v_i, v_{i+1})}\,. \end{aligned} \tag{1.25}$$

This means that Eq. (1.24) is

$$\mathrm{Vol}\,(\mathbf{X}_5) = \frac{\pi R^2}{6} \sum_{i=1}^{d} \mathrm{Vol}\,(\Sigma_i)\,. \tag{1.26}$$

Notice, moreover, that we can define the Z-function normalizing the volume with respect to a 5-sphere of radius R and still get the same expression as in Eq. (1.22).

1.1.4.1 Example - $T^{1,1}$

The prototypical example of volume minimization for toric SE manifolds is given by $T^{1,1}$. This manifold has been already introduced in Section 1.1.1.2, namely Eq. (1.8), as an example of generalization of Maldacena's Conjecture 1.1 when the D3-branes probe a non-orbifold singularity. Constructing the cone over $T^{1,1}$, the dual theory is a quiver gauge theory with gauge group $\mathrm{SU}(N)_0 \times \mathrm{SU}(N)_1$, four $\mathcal{N} = 1$ bifundamental chiral fields and two $\mathcal{N} = 1$ adjoint gaugini. By a-maximization [37] we get that the R-charge of the bifundamental fields is $1/2$, while that of the gaugini is 1, and the central charge a is maximized to[9]

$$a = \frac{3}{32}\left(3\mathrm{tr}\,R^3 - 5\mathrm{tr}\,R\right) = \frac{27}{32}N^2\,, \tag{1.27}$$

where the trace is taken over all fermions in the theory.[10]

Let us consider the fan diagram of the conifold as in Figure 1.1a (the corresponding toric diagram, obtained by considering the section along the plane $x = 1$ is in Figure 1.1b). The fan vectors are

$$v_1 = (1,0,0)\,,\ v_2 = (1,1,0)\,,\ v_3 = (1,1,1)\,,\ v_4 = (1,0,1)\,. \tag{1.28}$$

Inserting these vectors in Eq. (1.22) and minimizing with respect to the Reeb vector $\xi = (3, b_2, b_3)$, we obtain a minimum at $\xi_{\min} = \left(3, \frac{3}{2}, \frac{3}{2}\right)$, for which

$$Z\,(\xi_{\min}) = \frac{2}{27}\,. \tag{1.29}$$

The volume of $T^{1,1}$ is then

$$\mathrm{Vol}(T^{1,1}) = \frac{16\pi^3}{27}\,. \tag{1.30}$$

We know from [38] (see also [16, 39]) that the central charges a and c of a SCFT are related to the cosmological constant Λ of the dual AdS space as

$$a = c = \pi^2 \Lambda^{-3/2}\,. \tag{1.31}$$

9: Although this technique is more general, for quiver SCFTs, $\mathrm{tr}\,R = 0$.

10: Recall that for any chiral fields containing a complex scalar with R-charge R there is a fermion with R-charge $(R-1)$.

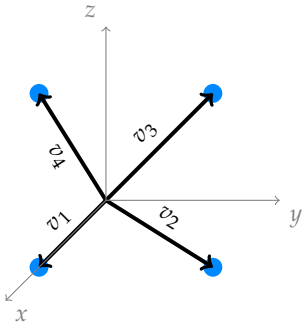

(a) Fan of the conifold.

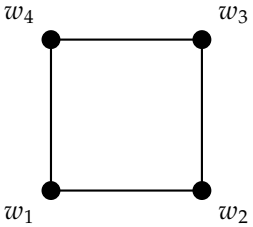

(b) Toric diagram of the conifold.

On the other hand, the cosmological constant can be found from (1.7) to be

$$\Lambda = \left(\frac{4\text{Vol}(\mathbf{X}_5)}{N^2\pi}\right)^{2/3} . \tag{1.32}$$

Putting everything together, we obtain

$$a = c = \frac{N^2\pi^3}{4\text{Vol}(\mathbf{X}_5)} , \tag{1.33}$$

that for the case of $T^{1,1}$, using Eqs. (1.27) and (1.29), we see that the two results match.

1.2 String theory compactification with fluxes

In string compactification, the first ansatz is that the background spacetime is a product

$$\mathscr{M}_{10} = \mathscr{M}_4 \times \mathbf{Y}_6 , \tag{1.34}$$

Section 1.2 is based on [9, 40] and references therein.

where $\mathscr{M}_4$ is a 4-dimensional non-compact manifold, while $\mathbf{Y}_6$ is a compact internal manifold. Generically, the 10d metric takes the following form

$$ds^2 = e^{2A(y)} g_{\mu\nu} dx^\mu dx^\nu + g_{mn} dy^m dy^n , \tag{1.35}$$

where $e^{2A(y)}$ is a non-trivial **warp factor** that depends on the internal coordinates, while $g_{\mu\nu}$ can be either Minkowski, de Sitter (dS) or AdS [40]. The effective 4d theory is obtained expanding all the fields into modes of the internal manifold $\mathbf{Y}$. This is a generalization of a Kaluza-Klein (KK) reduction, for a generic compactification.
Since we want that the non-compact space has maximal symmetry, the background should be purely bosonic (since all VEVs of the fermionic fields should vanish) [40]. In compactification with fluxes, this means that only F_4 in type IIA and F_5 in type IIB are allowed to have components along the non-compact directions. Moreover, demanding that the gravitino has zero VEV, we need a covariantly constant spinor on the 10d manifold. In the absence of fluxes, the consequence is that the warp factor is constant and the non-compact manifold must be Minkowski. At the same time, the internal manifold should have a constant spinor. If we want to preserve supersymmetry, we are forced to consider CY manifolds.

1.2.1 General conditions for compactifications with fluxes

Section 1.2.1 is based on [40–42] and references therein.

Before proceeding in explaining how to compactify type IIA on CY orientifold, it is better to review what are the general conditions that our theory must satisfy in order to be consistence. In particular, we will review the tadpole conditions both in type IIA and type IIB as well as the general Giddings-Kachru-Polchinski (GKP) construction [42].
Maldacena and Nuñez showed in [41] that the flux contribution to the energy momentum tensor is always positive. This means that, without considering localized sources or corrections to the EoMs, a de Sitter compactification is ruled out.[11] The introduction of localized sources also gives a positive contribution to the Einstein's equation, but, if one

11: It is still possible to obtain Minkowski space in the presence of F_1 flux.

introduces negative tension objects, it is possible to avoid the no-go theorem. Such objects are, indeed, the orientifold planes.[12]
If we want supersymmetric solutions, however, Einstein's equation is automatically satisfied, but we need to demand certain Bianchi identity conditions and the fluxes must also satisfy their EoMs. Let us define the NSNS flux has

$$H_3 = dB_2\,, \tag{1.36}$$

while the RR field strengths in 10d as

$$F_{p+1} = dC_p - H_3 \wedge C_{p-2} + m e^{B_2}\,, \tag{1.37}$$

where m is the Roman mass and the exponential is understood to be the formal expansion up to order $\frac{p+1}{2}$ of B_2.[13]
The RR field strengths are constrained by Hodge duality, i.e.,

$$F_{p+1} = (-1)^{\left\lfloor \frac{p+1}{2} \right\rfloor} \star F_{9-p}\,, \tag{1.38}$$

but both NSNS and RR fluxes must satisfy the following Bianchi identities:

$$dH_3 = 0\,,\ dF_{p+1} - H_3 \wedge F_{p+1} = 0\,. \tag{1.39}$$

Using the self-duality relations, such Bianchi identities also contain the EoMs for the fluxes, i.e.,

$$d\left(\star F_{p+1}\right) + H_3 \wedge \star F_{p+3} = 0\,, \tag{1.40}$$

that are valid for both type IIA and type IIB. From Eq. (1.40) and the requirement that we want to have a supersymmetric flux background with metric (1.35), we obtain the following EoMs:

$$\begin{aligned} dF_{p+1} - H_3 \wedge F_{p-1} &= 0\,, \\ d\left(e^{4A} \star F_{p+1}\right) - H_3 \wedge \left(e^{4A} \star F_{11-p}\right) &= 0\,. \end{aligned} \tag{1.41}$$

In a compact set-up, the integral of dF_{p+1} should be zero, but the contribution coming from the product with H_3 is usually positive if we require supersymmetry. The EoMs are satisfied if we introduce orientifolds that cancel the positive contributions. Such cancellations are usually called NSNS or RR **tadpole cancellations**, since we want zero net NSNS or RR charge for the solution. The charges can be fluxes or also localized sources.
In the following we will consider CYs that are simply connected, so the only possible source of tadpole cancellation conditions can come from D6-branes or O6-planes wrapped on a 3-cycle. The tadpole condition reads as[14]

$$N_{D6}(\Sigma_3) - 2N_{O6}(\Sigma_3) + \frac{m}{2\pi\sqrt{\alpha'}} \int_{\tilde{\Sigma}_3} H_3 = 0\,, \tag{1.42}$$

where N_{D6} and N_{O6} is the number or D6-branes and O6-planes, while $\tilde{\Sigma}_3$ is the dual 3-cycle to Σ_3.
In type IIB there are more sources of tadpole cancellation conditions. They come from D7-, D5- and D3-branes. Let us first consider the tadpole condition coming from the D7-branes. In the presence of N_{D7_a} D7-branes wrapping the 4-cycles $\tilde{\pi}_{D7_a}$, and calling $\tilde{\pi}'_{D7_a}$ the 4-cycle wrapped by the corresponding orientifold image of the D7-branes, the D7-brane tadpole

12: In the following we will focus on supersymmetric solutions, but the results just described are general for any kind of compactification with fluxes.

13: In type IIB there is no Roman mass and that term is not present.

14: Recall that for a O6$^-$-plane the charge is minus twice the charge of a D6-brane.

cancellation condition imposes

$$\sum_{D7_a} N_{D7_a} \left(\pi_{D7_a} + \pi'_{D7_a} \right) = 8 \sum_{O7_i} \pi_{O7_i} \,, \tag{1.43}$$

where π_{D7_a} or π_{O7_i} are the Poincaré dual cycles to the 4-cycles $\tilde{\pi}_{D7_a}$ or $\tilde{\pi}_{O7_i}$ wrapped by the branes. This condition is a cohomological expression, and it is constraining the number of D7-branes allowed in the compactification, in the presence of O7-planes. In particular, it tells us that in the presence of O7-planes, we are forced to introduce D7-branes in the set-up.
Considering D5-branes wrapped on a 2-cycle Σ_2, the Bianchi identify reads

$$N_{D5}(\Sigma_2) - N_{O5}(\Sigma_2) + \frac{1}{(2\pi)^2 \alpha'} \int_{\tilde{\Sigma}_4} H_3 \wedge F_1 = 0 \,, \tag{1.44}$$

where $\tilde{\Sigma}_4$ is the dual 4-cycle to Σ_2. Since $D3$-branes are point-like in the internal manifold, their tadpole cancellation conditions involve an integration over the whole 6d compactification space, giving[15]

$$N_{D3} - \frac{1}{4} N_{O3} + \frac{1}{(2\pi)^4 \alpha'^2} \int_{\mathbf{Y}_6} H_3 \wedge F_3 = 0 \,. \tag{1.45}$$

The integral gives the number of units of D3-charge induced by the 3-form fluxes:[16]

$$N_{\text{flux}} = \frac{1}{(2\pi)^4 \alpha'^2} \int_{\mathbf{Y}_6} H_3 \wedge F_3 \,. \tag{1.46}$$

Type IIB orientifold compactifications with D3- and D7-branes can be realized in F-theory compactifying on a CY 4-folds $\mathbf{X}_8$ with an elliptic fibrations π over a 3-fold base B_6. Using the F-theory construction, the tadpole cancellation imposes

$$N_{D3} + N_{\text{flux}} = \frac{\chi(\mathbf{X}_8)}{24} \,, \tag{1.47}$$

where χ is the Euler number of $\mathbf{X}_8$. Finally, the tadpole cancellation condition for NS5-branes is the same for both type IIA and type IIB. In the presence of these kinds of sources, the Bianchi identity for H_3 is modified such that

$$dH_3 = \rho_{NS5} \,. \tag{1.48}$$

In [42], GKP showed that if any localized sources have an energy momentum tensor T^{loc} satisfying

$$T^{\text{loc}} \geq 2T_3 \rho_3(x) \,, \tag{1.49}$$

where T_3 is the tension of a D3-brane, and ρ_3 is the energy density of the D3-brane, then the form of the solution is determined completely. In particular, a warped solution is obtained if

1. The internal components of the Ricci tensor and the axion-dilaton

15: $$q_{O3} = -\frac{1}{4} q_{D3} \,.$$

16: The presence of D3-brane charges can be also induced by the introduction of D7- or D5-branes. One may wonder, then, if it is possible to satisfy the tadpole condition in Eq. (1.45) tuning the fluxes so that the D3-branes contribution cancel. However, for supersymmetric backgrounds, one of the requirements is that

$$G_3 = F_3 - \tau H_3 \,,$$

where $\tau = C_0 + ie^{-\phi}$, is Imaginary Self-Dual (ISD). This condition implies that

$$\int_{\mathbf{Y}_6} H_3 \wedge F_3$$

is positive definite, so one must introduce O3-planes to cancel the fluxes and the D3-branes contributions [9].

τ, in string units, are [40]

$$R_{mn} = \frac{(2\pi)^8 \alpha'^4}{4} e^{2\phi} \partial_{\{m}\tau \partial_{n\}}\overline{\tau} + (2\pi)^7 \left(T^{D7}_{mn} - \frac{1}{8} g_{mn} T^{D7} \right) ,$$
$$\nabla^2 \tau = -ie^{\phi} (\nabla\tau)^2 - 4(2\pi)^7 e^{-2\phi} \frac{1}{\sqrt{-g}} \frac{\delta S_{D7}}{\delta \tau} , \tag{1.50}$$

where T^{D7} is the energy-momentum tensor of a D7-brane wrapped on some 4-cycles of the internal space.[17]

17: D7-branes arise naturally in the type IIB limit of F-theory.

2. The 5-form flux is given by

$$F_5 = (1 + \star) \left[d\left(e^{4A}\right) \wedge dx^0 \wedge dx^1 \wedge dx^2 \wedge dx^3 \right] . \tag{1.51}$$

3. The complex 3-form flux

$$G_3 = F_3 - \tau H_3 , \tag{1.52}$$

where $\tau = C_0 + ie^{-\phi}$, is ISD, namely

$$\star G_3 = iG_3 . \tag{1.53}$$

Primitive k-form

Let $(\mathbf{Y}, J)$ be a Kähler manifold of dimension n, we say that α is a primitive k-form, with $k \leq n$, if

$$\alpha \wedge J^{n-k+1} = 0 .$$

4. The inequality in Eq. (1.49) is saturated.

An important point is that GKP constructions do not impose supersymmetry *at priori*. Indeed, supersymmetric solutions impose G_3 to be ISD, i.e., G_3 must be $(2,1)$ and primitive, but also $G^{(0,3)} = 0$. In case in which the CY is not simply-connected, GKP allows for non-zero $(1,2)$ non-primitive components and a $(0,3)$ singlet piece.

1.2.2 Generalities on Calabi-Yau manifolds

Section 1.2.2 is based on [9, 43–47] and references therein.

We begin with the definition of CY manifold:

Definition 1.1 [Calabi-Yau].

A CY n-fold is a compact n-dimensional Kähler manifold $\mathbf{Y}_{2n}$ such that has a Kähler metric with global holonomy contained in SU(n).

There are other equivalent definitions of CY manifolds in the mathematical literature. Equivalent definitions include the following.

- A CY n-fold is a compact n-dimensional Kähler manifold $\mathbf{Y}_{2n}$ such that the canonical bundle of $\mathbf{Y}_{2n}$ is trivial.
- A CY n-fold is a compact n-dimensional Kähler manifold $\mathbf{Y}_{2n}$ such that it has a never-vanishing holomorphic n-form.

This definition implies that the first integral Chern class

$$c_1(\mathbf{Y}_{2n}) = \frac{1}{2\pi} \mathrm{tr}\, R , \tag{1.54}$$

where R is the Ricci form on $\mathbf{Y}_{2n}$, vanishes.[18]

18: Note that the inverse is not true.

In the physics literature, CYs are complex manifolds that have holonomy exactly equal to SU(n). In particular, for string compactifications in absence of fluxes where $\mathbf{Y}_6$ is CY 3-fold with holonomy equal to SU(3), the 4d effective theory preserves minimal supersymmetry.[19]

19: 4 real supercharges, i.e., $\mathcal{N} = 1$ in 4d.

By definition of complex manifold, we can define a **complex structure** I^n_m, such that [9]

$$I^n_a I^b_n = -\delta^b_a ,$$
$$\partial_{[n} I^p_{m]} - I^q_{[m} I^r_{n]} \partial_r I^p_q = 0 , \tag{1.55}$$

20: The Niejenhuis tensor is defined
$$N^p_{mn} = \partial_{[n} I^p_{m]} - I^q_{[m} I^r_{n]} \partial_r I^p_q \,.$$

where the last condition is the vanishing of the Niejenhuis tensor,[20] from which we can construct a set of complex coordinates

$$dz^j = dx^j + i I^j_k dy^k \;\text{ and }\; d\overline{z}^j = dx^j - i I^j_k dy^k \,. \tag{1.56}$$

A 2-form J can be introduced using the metric $g_{i\bar{j}}$:

$$J = g_{i\bar{j}} dz^i \wedge d\overline{z}^{\bar{j}} \,, \tag{1.57}$$

where the Kähler condition imposes J to be closed. This is usually called **Kähler form**. By definition of CY there must exist a unique non-vanishing 3-form Ω, called **holomorphic 3-form**, that satisfies

$$J \wedge \Omega = 0 \;\text{ and }\; \frac{1}{3!} J^3 = \frac{i}{2}^3 \Omega \wedge \overline{\Omega} \,. \tag{1.58}$$

When one performs a compactification on $\mathbf{Y}_6$, the fields are expressed in terms of harmonic forms of $\mathbf{Y}$, since they are related to the zero modes of the Laplacian in $\mathbf{Y}$. For the case of a complex manifold, p-forms can be classified in terms of their holomorphic and antiholomorphic indices. Indeed, we introduce a cohomology class $H^{p,q}(\mathbf{Y}_6)$ that contains representatives of harmonic forms with p holomorphic and q antiholomorphic indices, and we define $h^{p,q} = \dim H^{p,q}(\mathbf{Y}_6, \mathbb{Z})$. This is a generalization of the Betti numbers for a given manifold, that can be obtained as

$$b_k = \sum_{\substack{p,q=0 \\ p+q=k}}^{n} h^{p,q} \,, \tag{1.59}$$

for $k = 0, \ldots, 2n$. The CY condition imposes some constraints on the harmonic forms that are admissible, and usually the dimensions of the cohomology classes are represented in an **Hodge diamond**. For the case in which $\mathbf{Y}_6$ has exactly holonomy SU(3), the Hodge diamond has the following form

$$\begin{array}{ccccccc} & & h^{0,0} & & & & \\ & h^{1,0} & & h^{0,1} & & & \\ h^{2,0} & & h^{1,1} & & h^{0,2} & & \\ h^{3,0} & & h^{2,1} & & h^{1,2} & & h^{0,3} \\ & h^{3,1} & & h^{2,2} & & h^{1,3} & \\ & & h^{3,2} & & h^{2,3} & & \\ & & & h^{3,3} & & & \end{array} = \begin{array}{ccccccc} & & 1 & & & & \\ & 0 & & 0 & & & \\ 0 & & h^{1,1} & & 0 & & \\ 1 & & h^{2,1} & & h^{2,1} & & 1 \\ & 0 & & h^{1,1} & & 0 & \\ & & 0 & & 0 & & \\ & & & 0 & & & \end{array} \,. \tag{1.60}$$

The reasons why the Hodge diamond reduces to only 2 free parameters are the following:

- Complex conjugation already imposes $h^{p,q} = h^{q,p}$.
- Poincaré duality implies $h^{p,q} = h^{n-p,n-q}$.
- Since the only non-vanishing 3-form is Ω, then $h^{3,0} = h^{0,3} = 1$.
- Any $(p,0)$-form can be contracted with $\overline{\Omega}$ to give a (p,n)-form, and by Poincaré duality we obtain $h^{p,0} = h^{n-p,0}$.
- We also consider $\mathbf{Y}_6$ to be a compact and connected manifold, so that $b_0 = 1$, and analogously $h^{0,0} = h^{3,3} = 1$.
- For simplicity, it is also assumed $\mathbf{Y}_6$ to be simply connected, so $\pi_1(\mathbf{Y}_6) = 0$, and by Hurewicz's theorem, also $H_1(\mathbf{Y}_6, \mathbb{Z})$ is trivial. We conclude that $h^{1,0} = h^{0,1} = 0$.

Hurewicz's theorem

For any path-connected space $\mathbf{X}$ and positive integer n there exists a group homomorphism

$$h_* : \pi_n(\mathbf{X}) \to H_n(\mathbf{X}) \,.$$

In particular, for $n = 1$, there is an isomorphism between the abelianization of the first homotopy group and the first homology group.

We conclude that for a CY 3-fold there are only 2 degrees of freedom:

1. $h^{1,1}$ parameters that give $h^{1,1}$ real **Kähler moduli**.
2. $h^{2,1}$ parameters, that correspond to $h^{2,1}$ **complex structure moduli**.

We introduce a basis of harmonic $(1,1)$-forms ω_a (and their dual $\tilde{\omega}^a$) and a basis of harmonic 3-forms (α_A, β^B),[21] such that

$$\int_{\mathbf{Y}_6} \omega_a \wedge \tilde{\omega}^b = \delta_a^b \text{ and } \int_{\mathbf{Y}_6} \alpha_A \wedge \beta^B = \delta_A^B \,. \tag{1.61}$$

21: From now on, unless it is specified otherwise, we work in string units, but we want to keep the harmonic forms dimensionless. For this reason, it is better to think of them as $M_s^2\omega_a$ and $M_s^3\alpha_A$.

To summarize, the basis elements are in Table 1.1.

Cohomology group	Betti numbers	Basis
$H^{1,1}(\mathbf{Y}_6, \mathbb{Z})$	$h^{1,1}$	ω_a
$H^{2,2}(\mathbf{Y}_6, \mathbb{Z})$	$h^{1,1}$	$\tilde{\omega}^a$
$H^3(\mathbf{Y}_6, \mathbb{Z})$	$2h^{2,1}+2$	(α_A, β^B)
$H^{2,1}(\mathbf{Y}_6, \mathbb{Z})$	$h^{2,1}$	χ_A
$H^{3,3}(\mathbf{Y}_6, \mathbb{Z})$	1	$\mathrm{Vol}(\mathbf{Y}_6)$

Table 1.1: Cohomology groups and their corresponding basis for a CY 3-fold.

It is possible to introduce the intersection numbers for a CY manifold, given by

$$\begin{aligned} \mathcal{K}_{abc} &= \int_{\mathbf{Y}_6} \omega_a \wedge \omega_b \wedge \omega_c \,, \quad \mathcal{K}_{ab} = \int_{\mathbf{Y}_6} \omega_a \wedge \omega_b \wedge J \,, \\ \mathcal{K}_a &= \int_{\mathbf{Y}_6} \omega_a \wedge J \wedge J \,, \qquad \mathcal{K} = \int_{\mathbf{Y}_6} J \wedge J \wedge J \,. \end{aligned} \tag{1.62}$$

In particular, the volume of CY is $\mathcal{V} = \frac{1}{6}\mathcal{K}$.

1.2.3 Type IIA effective action

Section 1.2.3 is based on [9, 40, 44–46, 48–52] and references therein.

1.2.3.1 Type IIA compactification on CY

It is possible to write down the effective type IIA supergravity action in 10d. This is the low energy limit of type IIA superstring theory, for which we keep only the massless string modes. If we focus only on the bosonic Degrees of Freedom (DoFs), the theory contains a dilaton ϕ, a metric g, a 2-form B_2 from the NSNS sector, and a 1-form C_1 and a 3-form C_3 from the RR sector. We can define the corresponding field strengths for the p-forms, i.e.,

$$H_3 = dB_2 \,, \quad \tilde{F}_2 = dC_1 \text{ and } \tilde{F}_4 = dC_3 - C_1 \wedge H_3 \,, \tag{1.63}$$

so that the effective type IIA supergravity action in the string frame is[22]

$$\begin{aligned} S^{10d} =& \frac{1}{2\kappa_{10}^2} \int d^{10}x \sqrt{-g} \left(e^{-2\phi} \left(R + 4(\partial_\mu \phi)^2 - \frac{1}{2}|H_3|^2 \right) \right) + \\ & - \frac{1}{2\kappa_{10}^2} \int d^{10}x \sqrt{-g} \left(\left(|\tilde{F}_2|^2 + |\tilde{F}_4|^2 \right) \right) + S_{CS} \,, \end{aligned} \tag{1.64}$$

22: In our convention

$$|F_p|^2 = \frac{1}{p!} F_{\alpha_1 \ldots \alpha_p} F^{\alpha_1 \ldots \alpha_p} \,.$$

where $2\kappa_{10}^2 = (2\pi)^7 \alpha'^4$. In S_{CS} there are all the possible CS terms that can be written down containing the p-forms present in the theory,

$$S_{CS} \supset \int \sum_p H_3 \wedge dC_{2p-1} \wedge C_{7-2p} + \int \sum_p B_2 \wedge dC_{2p-1} \wedge F_{8-2p} \,, \quad (1.65)$$

where $p = 1, 2$ in the non-democratic notation.[23] Moving to the Einstein frame means to redefine $g \to g_E = g_s^{-1/2} e^{\phi/2} g$, where $g_s = e^{\langle\phi\rangle}$ is related to the VEV of the 10d dilaton. It is then possible to redefine $\kappa_{10} \to \kappa_{10} g_s$ and the 10d type IIA action becomes:

$$\begin{aligned} S^{10d} =& \frac{1}{2\kappa_{10}^2} \int d^{10}x \sqrt{-g_E} \left(\left(R_E + \frac{1}{2}(\partial_\mu \phi)^2 - \frac{1}{2} e^{-\phi} |H_3|^2 \right) \right) + \\ & - \frac{1}{2\kappa_{10}^2} \int d^{10}x \sqrt{-g_E} \left(\left(e^{3/2\phi} |\tilde{F}_2|^2 + e^{1/2\phi} |\tilde{F}_4|^2 \right) \right) + S_{CS} \,, \end{aligned} \quad (1.66)$$

23: When we will introduce fluxes, we can admit also $p = 0$, where F_0 corresponds to the Roman mass.

where it is understood that we are using g_E as metric also for the kinetic terms of the p-forms. We can proceed with the compactification in absence of fluxes by imposing the ansatz that the metric can be written as (1.35) and expanding the fields in the harmonic forms of $\mathbf{Y}_6$ in Table 1.1:

$$\begin{aligned} & C_1 = A_1(x) \,, \\ & B_2 = B_2(x) + b^a \omega_a \,, \ a = 1, \dots, h^{1,1} \,, \\ & C_3 = A_1^a \wedge \omega_a + \xi^A \alpha_A - \tilde{\xi}^A \beta_A \,, \ a = 1, \dots, h^{1,1} \text{ and } A = 1, \dots, h^{2,1} \,. \end{aligned} \quad (1.67)$$

The spectrum is then given by scalars $\left(b^a, \xi^A, \tilde{\xi}_A \right)$, one 1-form A_1 and $h^{1,1}$ 1-forms A_1^A and one 2-form B_2.
The deformations of the Kähler form J give rise to $h^{1,1}$ real scalars v^a. It is possible to relate these scalars with b^a, introducing $h^{1,1}$ complex fields

$$t^a = b^a + i v^a \,. \quad (1.68)$$

These variables parameterize the complexified Kähler cone and the Kähler moduli space $\mathcal{M}_{\text{ks}}$. A metric for the Kähler moduli space is given by

$$G_{ab} = \frac{3}{2\mathcal{K}} \int_{\mathbf{Y}_6} \omega_a \wedge \star \omega_b = -\frac{3}{2} \left(\frac{\mathcal{K}_{ab}}{\mathcal{K}} - \frac{3}{2} \frac{\mathcal{K}_a \mathcal{K}_b}{\mathcal{K}} \right) . \quad (1.69)$$

Introducing a Kähler potential

$$K^{\text{ks}} = -\ln \left[\frac{i}{6} \left(\mathcal{K}_{abc} \left(t - \bar{t} \right)^a \left(t - \bar{t} \right)^b \left(t - \bar{t} \right)^c \right) \right] = -\ln \frac{4}{3} \mathcal{K} \,, \quad (1.70)$$

the metric in Eq. (1.69) can be rewritten as

$$G_{ab} = \frac{\partial}{\partial t^a} \frac{\partial}{\partial t^b} K^{\text{ks}} \,. \quad (1.71)$$

We can allow also for deformations of the complex structure of $\mathbf{Y}_6$. They are parameterized by complex fields z^A and span the complex structure moduli space, $\mathcal{M}^{\text{cs}}$. The metric for the complex structure moduli space is

given by

$$G_{A\overline{B}} = -\frac{\int_{\mathbf{Y}_6} \chi_A \wedge \overline{\chi}_L}{\int_{\mathbf{Y}_6} \omega \wedge \overline{\Omega}} \,, \tag{1.72}$$

where

$$\chi_A = \frac{\partial}{\partial z^A}\Omega + \Omega \frac{\partial}{\partial z^A} K^{\rm cs} \,. \tag{1.73}$$

In Eq. (1.73) we have introduced the Kähler potential $K^{\rm cs}$ defined as

$$K^{\rm cs} = -\ln\left[i \int_{\mathbf{Y}_6} \Omega \wedge \overline{\Omega} \right] \,. \tag{1.74}$$

Expanding Ω in terms of (α_A, β^B), i.e.,

$$\Omega = \sum_{A=1}^{h^{2,1}} \left(Z^A \alpha_A - F_A \beta^A \right) \,, \tag{1.75}$$

we can define

$$Z^A = \int_{\mathbf{Y}_6} \Omega \wedge \beta^A \,, \;\; F^A = \int_{\mathbf{Y}_6} \Omega \wedge \alpha^A \,, \tag{1.76}$$

called **holomorphic periods**, the special coordinates are defined as $z^A = Z^A/Z^0$.[24]

We can put all the moduli together in $\mathcal{N} = 2$ multiplets for the type IIA supergravity action compactified on a CY manifold in Table 1.2.

Multiplet	Number	Components
Gravity multiplet	1	$(g_{\mu\nu}, A_1)$
Vector multiplets	$h^{1,1}$	(A_1^a, v^a, b^a)
Hypermultiplets	$h^{2,1}$	$\left(z^A, \xi^A, \tilde{\xi}_A\right)$
Tensor multiplet	1	$\left(B_2, \phi, \xi^0, \tilde{\xi}_0\right)$

Table 1.2: $\mathcal{N} = 2$ multiplets for type IIA supergravity action compactified on a CY manifold.

To state the 4d effective action for type IIA ungauged supergravity[25], we need to define the 4d dilaton

$$e^D = \frac{e^\phi}{\sqrt{\mathcal{V}}} \,, \tag{1.77}$$

and the effective action is[26]

$$\begin{aligned} S^{(4)}_{IIA} \propto & -\frac{1}{2}\int \left(R^{(4)}_E - \mathrm{Im}\,\mathcal{N}_{AB} F^A \wedge \star F^B - \mathrm{Re}\,\mathcal{N}_{AB} F^A \wedge F^B \right) + \\ & - \int \left(G_{ab} dt^a \wedge \star d\overline{t}^b + h_{uv} d\overline{q}^u \wedge \star d\overline{q}^v \right) \,. \end{aligned}$$

where we have put all the hypermultiplet sector inside the contribution $h_{uv} d\overline{q}^u \wedge \star d\overline{q}$, where h_{uv} is a quaternionic metric. The expansion can be found in [45]. Let us deconstruct Eq. (1.78). First $F^A = dA^A$, and G_{ab} is the Kähler moduli space metric. The gauge couplings of the vector

24: One of the periods Z^0 is unphysical because of the symmetry of the Kähler potential.

25: By "ungauged" we means in absence of background fluxes.

26: It is understood that F^A in the a 4d field strength, and it is not the holomorphic period introduced in Eq. (1.76).

In the expression for the type IIA action we have not explicitly written down the coupling in front of the action. By dimensional reduction, we need to rescale the Einstein metric by a factor

$$g^{(4)}_E \to \frac{\langle \mathcal{V} \rangle}{\mathcal{V}} g^{(4)}_E \,,$$

remembering that we want to keep the volume of the internal space as dimensionless. The 4d effective Planck mass is then defined as

$$M^2_{P,4} \propto \frac{\langle \mathcal{V} \rangle}{g_s^2} M_s^2 \,.$$

multiplets are encoded inside $\mathcal{N}_{AB}$, whose components are

$$\begin{aligned} \mathrm{Re}\,\mathcal{N} &= \begin{pmatrix} -\frac{1}{2}\mathcal{K}_{abc}b^a b^b b^c & \frac{1}{2}\mathcal{K}_{abc}b^b b^c \\ \frac{1}{2}\mathcal{K}_{abc}b^a b^c & -\mathcal{K}_{abc}b^c \end{pmatrix}, \\ \mathrm{Im}\,\mathcal{N} &= -\frac{\mathcal{K}}{6}\begin{pmatrix} 1+4G_{ab}b^a b^b & -4G_{ab}b^b \\ -4G_{ab}b^b & 4G_{ab} \end{pmatrix}. \end{aligned} \tag{1.78}$$

The interesting point is that the moduli space of type IIA compactification on CY manifold is given by a product of two moduli spaces:

$$\mathcal{M} = \mathcal{M}^{\mathrm{ks}} \times \mathcal{M}^{\mathrm{cs}}\,. \tag{1.79}$$

Moreover, the local structure of the moduli space is different between the two factors in the product. While the Kähler moduli space is a special Kähler manifold spanned by scalars in the vector multiplets (i.e., the deformations of the CY Kähler form), the complex structure moduli space is a quaternionic manifold spanned by scalars in the hypermultiplets (i.e., spanned by the complex structure deformations of $\mathbf{Y}_6$).

1.2.3.2 Type IIA compactification on CY orientifold

Special Lagrangian submanifold

A submanifold **M** of a symplectic manifold **Y** is **Lagrangian** if ω restricts to zero on **M** and $\dim \mathbf{Y} = 2\dim \mathbf{M}$. A submanifold **M** of a CY manifold is **special Lagrangian** if also $\mathrm{Im}\,\Omega$ restricts to zero on **M**. In this case, $\mathrm{Re}\,\Omega$ restricted to **M** is the volume form of the induced metric on **M** [53].

For the case of type IIA, the only orientifold that is consistent with supersymmetry is the O6-plane on the non-compact directions and wrapped on a Special Lagrangian 3-cycle of the internal CY. O6-planes can be included in the theory when the CY admits an isometric and antiholomorphic involution σ. Such σ is acting on the Kähler form and the holomorphic form as

$$\sigma^* J = -J \;\text{ and }\; \sigma^*\Omega = e^{2i\theta}\overline{\Omega}\,, \tag{1.80}$$

where σ^* is the pullback of σ and θ can be reabsorbed in the definition of Ω, so it can be set $\theta = 0$. The action of the orientifold is then defined by modding out from the type IIA spectrum all the fields that are not invariant under

$$\mathcal{O} = (-1)^{F_L}\Omega_p\sigma^*\,, \tag{1.81}$$

where F_L is the fermion number operator for the left-moving sector, and Ω_p is the worldsheet parity operator that exchanges left and right movers. Under $(-1)^{F_L}$, the dilaton ϕ, the metric g and B_2 are even, while the RR fields are odd. On the other hand, ϕ, g and C_1 are even under Ω_p, while B_2 and C_3 are odd. As a consequence, in order for the type IIA fields not to be projected out by the orientifold action, we need that ϕ, g and C_3 are even under the action of σ, while B_2 and C_1 must be odd.
In order to repeat the compactification of type IIA, this time, on CY orientifold, it is convenient to divide the cohomology groups $H^{p,q}$ in eigenspaces of σ^*:

$$H^{p,q} = H^{p,q}_+ \oplus H^{p,q}_-\,, \tag{1.82}$$

and we denote $h^{p,q}_\pm$ respectively the dimensions of the even and odd eigenspaces of $H^{p,q}$. The harmonic forms introduced in Table 1.1 are now split as in Table 1.3 where we have already imposed $h^{1,1}_\pm = h^{2,2}_\mp$. Since the volume form is odd, then $h^{0,0}_- = 0 = h^{3,3}_+$, while $h^{0,0}_+ = 1 = h^{3,3}_-$. We can expand the fields in the massless spectrum in terms of the new basis in Table 1.3. The involution σ acts only on the internal manifold, while the operators $(-1)^{F_L}\Omega_p$ act on the worldsheet theory, this means that there

Cohomology group	Betti numbers	Basis
$H^{1,1}_{+}(\mathbf{Y}_6,\mathbb{Z})$	$h^{1,1}_{+}$	ω_a
$H^{1,1}_{-}(\mathbf{Y}_6,\mathbb{Z})$	$h^{1,1}_{-}$	ω_a
$H^{2,2}_{+}(\mathbf{Y}_6,\mathbb{Z})$	$h^{1,1}_{+}$	$\tilde{\omega}^a$
$H^{2,2}_{-}(\mathbf{Y}_6,\mathbb{Z})$	$h^{1,1}_{-}$	$\tilde{\omega}^a$
$H^{3}_{+}(\mathbf{Y}_6,\mathbb{Z})$	$h^{2,1}+1$	(α_A,β^B)
$H^{3}_{-}(\mathbf{Y}_6,\mathbb{Z})$	$h^{2,1}+1$	(β^B,α_A)

Table 1.3: Cohomology groups and their corresponding basis for an orientifold CY 3-fold.

cannot be, for instance, a 2-form B_2 in the non-compact space. B_2 can be then expanded only in a basis ω_a of odd harmonic $(1,1)$-forms, resulting

$$B_2 = b^a \omega_a \,,\ a = 1,\dots,h^{1,1}_{-} \,. \tag{1.83}$$

Moreover, J is odd under the involution σ, so it can be expanded in a similar way, i.e., $J = v^a\omega_a$, and it can be combined in a set of complex coordinates:

$$t^a = b^a + iv^a \,. \tag{1.84}$$

The Kähler moduli space is parameterized by the same coordinates, but this time they are $h^{1,1}_{-}$ instead of $h^{1,1}$.
The RR field C_1 is odd under the orientifold, and since there are no 1-forms,[27] C_1 is projected out completely. The field C_3 is even under σ^*, and it has the following expansion:

27: Remember that we are considering simply-connected CYs

$$C_3 = c_3(x) + A^a_1 \wedge \omega_a + \xi^A\alpha_A - \tilde{\xi}_B\beta^B \,, \tag{1.85}$$

where A^a_1 are $h^{1,1}_{+}$ 1-forms, while ξ^A and ξ_B are $h^{2,1}+1$ scalar fields. The field c_3 has no physical DoF because it can be dualized to a scalar in 4d. The complex structure deformations can be found expanding Ω in the new basis of $H^3_{+}\oplus H^3_{-}$:

$$\Omega = \sum_{A,B=1}^{h^{2,1}+1} \left(Z^A\alpha_A - F_B\beta^B + Z^B\alpha_B - F_B\beta^B\right) \,. \tag{1.86}$$

The constraint in Eq. (1.80) imposes

$$\text{Im}\left(e^{-i\theta}Z^A\right) = 0 = \text{Re}\left(e^{-i\theta}F_B\right) \,,\ \text{Re}\left(e{-}i\theta Z^B\right) = 0 = \text{Im}\left(e^{-i\theta}F_A\right) \,, \tag{1.87}$$

this means that we project out $h^{2,1}$ reals scalars because of the first equation, while the second condition is a constraint on the periods of the CY. This constraint must be fulfilled so that Eq. (1.80) holds. In the previous section we have briefly mentioned the possibility that Ω is defined up to complex rescaling. This allowed us to reduce the number of complex structure deformations by 1 and remaining with $h^{2,1}$ periods. In the presence of orientifolds, it is more convenient to keep the scale invariance freedom, and to define a compensator $\mathscr{C} = e^{-D-i\theta}e^{1/2K^{\text{cs}}}$ so that we have

$$\mathscr{C}\Omega = \text{Re}\left(\mathscr{C}Z^A\right)\alpha_A + i\text{Im}\left(\mathscr{C}Z^B\right)\alpha_B - \text{Re}\left(\mathscr{C}F_B\right)\beta^B - i\text{Im}\left(\mathscr{C}F_A\right)\beta^A \,, \tag{1.88}$$

that depends on $h^{2,1}+1$ real parameters.
It turns out that $\mathcal{C}\Omega$ can be related to C_3, defining the complex combination

$$\Omega_c = C_3 + i\mathrm{Re}\,(\mathcal{C}\Omega)\,. \tag{1.89}$$

The complex structure deformations can be found in terms of $\mathcal{N}=1$ chiral multiplets:

$$\begin{aligned} N^A &= \frac{1}{2}\int_{\mathbf{Y}_6}\Omega_c\wedge\beta^A = \frac{1}{2}\xi^A + i\mathrm{Re}\,\left(\mathcal{C}Z^A\right)\,,\\ U_B &= i\int_{\mathbf{Y}_6}\Omega_c\wedge\alpha_B = i\tilde{\xi}_B - 2\mathrm{Re}\,\left(\mathcal{C}F_B\right)\,, \end{aligned} \tag{1.90}$$

and they are the complex structure moduli for type IIA orientifold compactifications. To summarize, the $\mathcal{N}=1$ spectrum is in Table 1.4.

Table 1.4: $\mathcal{N}=2$ multiplets for type IIA supergravity action compactified on a CY manifold.

Multiplet	Number	Components
Gravity multiplet	1	$g_{\mu\nu}$
Vector multiplets	$h^{1,1}_+$	A^a_1
Chiral multiplets	$h^{1,1}_-$	t^a
Chiral multiplets	$h^{2,1}+1$	N^A, U_B

The general expression for the action for type IIA orientifold compactifications is not useful for our purposes, and instead we refer to the literature cited at the beginning of Section 1.2.

1.2.3.3 Type IIA compactification on CY orientifold with fluxes

In the previous section, all the scalar components of the $\mathcal{N}=1$ multiplets have a flat potential. Indeed, at tree level the superpotential is trivial, but non-trivial background generate a scalar potential for the closed string moduli. If we consider compactifications on CY manifold with also the presence of non-trivial RR or NSNS fluxes as background, the CY geometry is not a solution anymore and a potential is generated.
To understand better the definition of fluxes in type IIA string theory, it is better to work in the democratic formulation for the RR potentials. There are indeed five p-forms, i.e., C_1, C_3, C_5, C_7 and C_9, linked by self-duality of their corresponding field strengths. The field strengths are indeed defined as

$$F_{2p} = dC_{2p-1} - H_3\wedge C_{2p-3} + me^{B_2}\,,\ p=1,\dots,5\,, \tag{1.91}$$

where B_2 is the NSNS field, and H_3 is its field strengths, while m is the mass parameter of IIA. The field strengths satisfy the following Bianchi identities:

$$d\left(e^{-B_2}\wedge F_{2p}\right)=0\,,\ dH_3=0\,. \tag{1.92}$$

If the internal manifold is compact, the Bianchi identities imply that H_3 and $e^{-B_2}\wedge F_{2p}$ are closed forms, and it is then possible to expand the forms in their harmonic and exact parts and to define

$$F_{2p}\to F_{2p}+F^{\mathrm{bg.}}_{2p}\ \text{ and }\ H_3\to H_3+H_3^{\mathrm{bg.}}\,, \tag{1.93}$$

where $F_{2p}^{\text{bg.}}$ and $H_3^{\text{bg.}}$ are the background fluxes. By quantization of the Page charges, the background fluxes can be characterized in terms of flux quanta, from which it is always possible to extract their integral parts. For instance, considering a basis of $\pi^a \in H_2^-(\mathbf{Y}_6, \mathbb{Z})$ 2-cycles, and their duals $\tilde{\pi}_a \in H_4^+(\mathbf{Y}_6, \mathbb{Z})$, we define

Remember that we are working in string units.

$$F_0^{\text{bg.}} = m\,, \quad \int_{\pi^a} F_2^{\text{bg.}} = m^a\,, \quad \int_{\tilde{\pi}_a} F_4^{\text{bg.}} = e_a\,, \quad \int_{\mathbf{Y}_6} F_6^{\text{bg.}} = e_0\,. \tag{1.94}$$

For the NSNS sector, we need to introduce a basis of $(\beta^K, \alpha_J) \in H_3^-(\mathbf{Y}_6, \mathbb{Z})$ odd 3-cycles, so that

$$\int_{B^K} H_3^{\text{bg.}} = h_K \text{ and } \int_{A_J} H_3^{\text{bg.}} = -h^J\,. \tag{1.95}$$

In the presence of fluxes, both Kähler and complex structure moduli are subjected to a superpotential. The RR fluxes generate a perturbative potential for the Kähler moduli:

$$W_{\text{ks}} = e_0 + e_a t^a + \frac{1}{2}\mathcal{K}_{abc} m^a t^b t^c + \frac{m}{6}\mathcal{K}_{abc} t^a t^b t^c\,, \tag{1.96}$$

while the NSNS fluxes are responsible for the superpotential for the complex structure moduli

$$W_{\text{cs}} = h_K N^K + h^J U_J\,. \tag{1.97}$$

1.2.3.4 An example of moduli stabilization in type IIA

Let us consider an example of type IIA orientifold compactification that will be useful in the discussion in Chapter 6. We briefly discuss a model of type IIA moduli stabilization on $\mathbf{T}^6/\mathbb{Z}_3^2$ orientifold done in [48], by DGKT. This model was fairly easy to analyze because it has no complex structure moduli, but only those corresponding to the size of the $\mathbf{T}^6$, three moduli for the B-field (one for each $\mathbf{T}^2$), the dilaton and a single axion coming from the compactification of C_3. The blow-ups of the 9 singular orbifold points generate further moduli for the metric and the B-field.

In the previous section we have focused on CYs that are simply connected, so, technically the torus is not a CY. However, in our set up, the resolved orientifold space has still a trivial H^1.

In the simplest set-up, they considered only F_0 and H_3 fluxes that contribute to the tadpole cancellation of the RR 7-form of the orientifold, and they also introduced F_4 fluxes that remained unbounded. The presence of the Roman mass $F_0 = m$, slightly modify the action in Eq. (1.64) and the definition of the RR forms in Eq. (1.63). We can indeed define [48]

$$\begin{aligned} H_3^{\text{total}} &= dB_2 + H_3^{\text{bg.}}\,, \\ \tilde{F}_2 &= dC_1 + mB_2\,, \\ \tilde{F}_4 &= dC_3 + F_4^{\text{bg.}} - C_1 \wedge H_3 - \frac{m}{2} B_2 \wedge B_2\,, \end{aligned} \tag{1.98}$$

and the action in (1.64), in the string frame becomes

$$\begin{aligned} S^{10d} =& \frac{1}{2\kappa_{10}^2}\int d^{10}x\sqrt{-g}\left(e^{-2\phi}\left(R+4(\partial_\mu\phi)^2-\frac{1}{2}|H_3^{\text{total}}|^2\right)\right)+ \\ &-\frac{1}{2\kappa_{10}^2}\int d^{10}x\sqrt{-g}\left(\left(|\tilde{F}_2|^2+|\tilde{F}_4|^2+m^2\right)\right)+S_{CS}\,. \end{aligned} \tag{1.99}$$

The CS action contains the terms in Eq. (1.65) but also

$$\begin{aligned} S_{CS} \supset -\frac{1}{2\kappa_{10}^2}\int \Big[&2B_2\wedge dC_3\wedge F_4^{\text{bg.}}+C_3\wedge H_3^{\text{bg.}}\wedge dC_3+ \\ &-\frac{m}{3}B_2\wedge B_2\wedge B_2\wedge dC_3+\frac{m^2}{20}B_2\wedge B_2\wedge B_2\wedge B_2\wedge B_2\Big]\,. \end{aligned} \tag{1.100}$$

We have restored α' for the moment, usually set to 1. Remember that the charge of an Op-plane is -2^{p-5} that of a Dp-brane.

Finally, the contribution of the orientifold O6 to the action is

$$S_{O6}=\frac{2}{(2\pi)^6\alpha'^{7/2}}\int_{O6}d^7\xi e^{-\phi}\sqrt{-g}-\frac{2\sqrt{2}}{(2\pi)^6\alpha'^{7/2}}\int C_7\,. \tag{1.101}$$

This set up has only one even α_0 and one odd β_0 3-cycle, and we can use the odd one to define the background $H_3^{\text{bg.}}$ flux:

$$H_3^{\text{bg.}}=-p\beta_0\,. \tag{1.102}$$

The tadpole condition for the RR C_7 of the orientifold imposes that

$$mp=-2\,, \tag{1.103}$$

so the Roman mass and the H_3 flux are bounded and they are order 1. The RR 3-form C_3 can be expanded in terms of the even 3-cycle α_0, and we call ξ the single modulus coming from this decomposition. The axion ξ and the dilaton ϕ combine into the complex axion-dilaton modulus. The stabilization of the 3-form axion ξ imposes

$$p\xi=e_0+e_ib_i-m\mathcal{K}b_1b_2b_3\,, \tag{1.104}$$

where the fluxes are defined in Eq. (1.94) and $\mathcal{K}$ is the triple intersection number of the $\mathbf{T}^6/\mathbb{Z}_3^2$ manifold.
In order to proceed with the stabilization, it is necessary to introduce the moduli v_i that will combine with b_i to become the Kähler moduli of the 4d effective theory. We call also

$$\mathcal{V}\equiv\int_{\mathbf{T}^6/\mathbb{Z}_3^2}\sqrt{g_6}=\mathcal{K}v_1v_2v_3\,, \tag{1.105}$$

the volume of the internal manifold, so that we can define the 4d dilaton

$$e^D=\frac{e^\phi}{\mathcal{V}^{1/2}}\,. \tag{1.106}$$

In terms of the moduli v_i, the fluxes e_i, p and m, and the 4d dilaton, the flux-induced potential reads

$$V(D,v)=\frac{m^2\mathcal{K}}{2|e_1e_2e_3|}e^{4D}v^3-\sqrt{2}|mp|e^{3D}+\frac{p^2}{4}\frac{e^{2D}}{v^3}\frac{|e_1e_2e_3|}{\mathcal{K}}+\frac{3}{2}\frac{e^{4D}}{v}\frac{|e_1e_2e_3|}{\mathcal{K}}\,. \tag{1.107}$$

Minimizing with respect to the moduli, it is possible to set

$$v_i = \frac{1}{e_i}\sqrt{\frac{5}{3}\left|\frac{e_1e_2e_3}{m\mathcal{K}}\right|}\,,\ e^D = |p|\sqrt{\frac{27}{160}\left|\frac{m\mathcal{K}}{e_1e_2e_3}\right|}\,, \tag{1.108}$$

and the minimum of the potential is negative:

$$V = -\frac{2}{3}\frac{|e_1e_2e_3|}{v\mathcal{K}}e^{4D}\,, \tag{1.109}$$

so the 4d spacetime is AdS.
The important point of this compactification is that the F_4 flux has not been bounded. Indeed, this solution depends on the value of the e_i, but nothing puts constraints on the values that the potential can get. In particular, it is possible to define

$$e_i = k\bar{e}_i\,, \tag{1.110}$$

where k is some integer number, which represents the Greatest Common Divisor (GCD) of the e_i, and k can be made arbitrarily large. Moreover, it is possible to find the scalings of the stabilized moduli with respect to k, e.g.,

$$v_i \sim k^{1/2}\,,\ \mathcal{V} \sim k^{3/2}\,,\ e^D \sim k^{3/2} \sim \xi\,. \tag{1.111}$$

The consequence of this behavior of the solution is that the KK modes scale with k differently than the 4d cosmological constant Λ, i.e.

$$\Lambda \sim k^{-9/2}\,,\ M_{KK}^2 \sim k^{-7/2}\,, \tag{1.112}$$

this means that in the limit in which $\Lambda \to 0$, there are states with mass of the order of the cutoff of the theory, such that

$$\Lambda \sim \frac{M_{\text{cutoff}}^2}{k}\,. \tag{1.113}$$

This is the starting point of the $\mathbb{Z}_k$ RSADC that we will introduce in Chapter 6. We are going indeed to show that the same scalings can be obtained by arguments based purely on the discrete symmetries that arise from the fluxes, and they are responsible for the separation of scale that this theory admits.

Elements of toric quiver gauge theories

2

In this chapter, we review the concept of quiver gauge theory in Section 2.1, in particular the relation with the theories introduced in Section 1.1.1. In Section 2.2 we introduce the dimer models and periodic quivers. We then review a way to define global U(1) symmetries from the dimer diagrams in Section 2.2.2. The novelty is from Section 2.3 where we introduce a new toolkit that allows to find U(1) global symmetries from geometric identities in the dimer (or periodic quiver). We also introduce the way in which a general orbifold for a general toric theory is constructed in Section 2.3.2.

2.1 Quiver gauge theories

In Section 1.1.1 we have considered D-branes probing a conifold singularity, giving rise to a SCFT. In particular, we focused on conifold singularities arising from the cone over a toric SE manifold that give rise to a toric CY 3-fold. The resulting theory, in the case of D3-branes probing such singularity, is SCFT with at least 4 real supercharges, i.e. $\mathcal{N} \geq 1$.

These theories may be represented using a **quiver** graph, i.e. a drawing made of nodes and arrows where each element in the drawing has a meaning in terms of the gauge and matter content of the SCFT [54]. In the case of 4d theories, it is usually used $\mathcal{N} = 1$ language. This means that a quiver is a graph made of circles, squares and arrows: a gauge group is associated to a circle node. Flavor symmetries are usually encoded in a square node, finally, to each arrow pointing from the group G_i to the group G_j, we associate a bifundamental $\mathcal{N} = 1$ chiral superfield in the fundamental representation of the group G_i and in the antifundamental representation of the group G_j, i.e. $\left(\square_i, \overline{\square}_j\right)$. Arrows that start and end on the same node are chiral superfields in the adjoint representation.

In Figure 2.1a and Figure 2.1b we show, as examples, the quiver of $\mathcal{N} = 4$ pure SU(N) SYM and the quiver of the conifold theory, arising from D3-brane probing the cone of $T^{1,1}$, i.e. $C\left(T^{1,1}\right)$. The quiver does not encode completely the superpotential that must be added to the graph.

In Figure 2.1b we are considering only regular N D3-branes that probe the CY singularity, so the ranks of the gauge groups are the same.

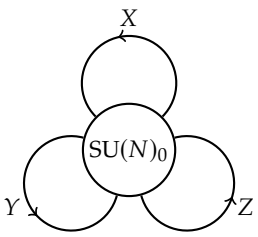

$$W = \text{tr}\ (XYZ - XZY)$$

(a) Quiver of $\mathbb{C}^3$.

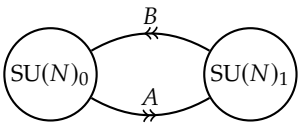

$$W = \varepsilon^{ij}\varepsilon^{kl}\text{tr}\left(A_i B_k A_j B_l\right)$$

(b) Quiver of the conifold.

Figure 2.1: Examples of quiver gauge theories.

2.2 Dimer diagrams and quiver gauge theories

2.2.1 Dimer diagram and periodic quiver

We have seen in Section 2.1 that the quiver graph does not encode directly the superpotential terms in the graph, and they must be added as extra information. For the case of gauge theories on D3-branes at toric CY 3-fold singularities, there is an efficient way to add it in a graph, using dimer diagrams [55–57]. These are bipartite tilings of $\mathbf{T}^2$. The bipartite

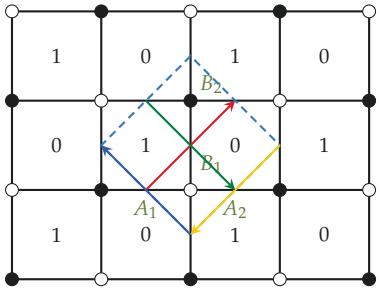

(a) Conifold.

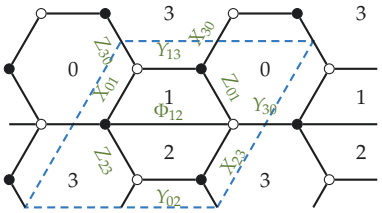

(b) dP_1.

Figure 2.2: Examples of dimer diagrams, their zig-zag paths and fundamental cells.

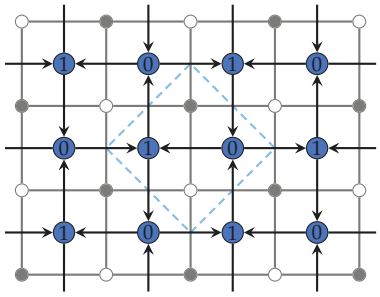

(a) Conifold.

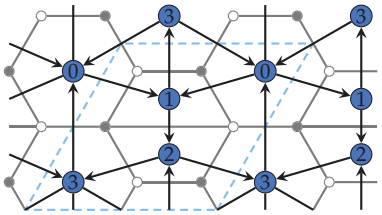

(b) dP_1.

Figure 2.3: Examples of periodic quivers.

property means that vertices can be colored black and white, with edges joining vertices of different colors; it endows edges with an orientation, e.g., from black to white nodes, and an orientation around vertices e.g. clockwise (resp. counter-clockwise) for black (resp. white) vertices.

The correspondence with the gauge theory is such that each face F_a corresponds to a gauge factor $SU(N_a)$. Actually, there is a $U(N_a)$ symmetry group, but the $U(1)_a$ factor is generically massive due to BF couplings with closed string modes [58] (often also involved in a Green-Schwarz mechanism to cancel mixed anomalies). These U(1)'s remain as (perturbatively exact) global symmetries and will play a prominent role in this section.

The correspondence also sets that each edge E_i, which separates faces F_a and F_b, corresponds to a bifundamental chiral multiplet $\left(\square_a, \overline{\square}_b\right)$ if one crosses E_i with positive orientation in going from F_a to F_b. Finally, black and white vertices, denoted by V_α or V'_α, respectively, introduce superpotential terms $\pm\mathrm{Tr}\,(\Phi_{E_1}\dots\Phi_{E_n})$, with $\{E_1,\dots,E_n\}$ is the ordered set of edges surrounding the vertex, and the sign is positive or negative for black and white nodes, respectively.

The dimer diagrams for the conifold and the dP_1 theory are shown in Figure 2.2. Figure 2.2a is the corresponding dimer diagram of the quiver in Figure 2.1b.

It will be convenient to introduce the periodic quiver as the dual of the dimer diagram. Namely, each face is replaced by a node, which we continue to denote by F_a; each edge E_i separating face F_a from face F_b is replaced by an oriented arrow (again denoted by E_i) between nodes F_a and F_b; and vertices V_α, V'_α now correspond to plaquettes of arrows with clockwise or counter-clockwise orientation, respectively. Namely, in the periodic quiver, nodes correspond to gauge factors, arrows to bifundamental matter, and plaquettes to superpotential couplings. The periodic quiver is similar to the standard quivers used to describe gauge theories, with the extra periodic structure providing also information about the superpotential. The periodic quivers for the conifold and dP_1 theories are given in Figure 2.3.

It will be useful to have in mind that these ingredients in the dimer and the periodic quiver allow to define a (co)homology in the corresponding diagrams, ultimately related to the (co)homology in the underlying 2-torus. We have collected this description in Section 2.3.

In the above description, we have considered general ranks N_a. In general, these are constrained by the cancellation of non-Abelian anomalies. Denoting the (net) number of bifundamentals $\left(\square_a, \overline{\square}_b\right)$ by I_{ab} (defined as an antisymmetric matrix, with negative entries indicating matter in the conjugate representation), the conditions are

$$\sum_a N_a I_{ab} = 0 \quad \forall b\,. \tag{2.1}$$

In a bipartite dimer, any face has an even number of edges,[28] so if we choose $N_a = N$ for all a there are cancellations among consecutive edges and the anomaly-cancellation constraints are satisfied. This corresponds to the so-called **regular** or dynamical D3-branes (which can move off

28: We consider a proper dimer diagram those that have more than two edges.

the singular point and explore the geometry). Choices of non-equal ranks include the so-called **fractional** branes, which can be regarded as higher-dimensional branes wrapped on the cycles collapsed at the singular point. In the following and in Chapter 5 we will focus on regular D-branes and mostly have the case $N = 1$ in mind.

The toric geometry associated to a given dimer diagram can be recovered in several (equivalent) ways. A very direct method is to introduce **zig-zag paths**. A zig-zag path in the dimer is a consecutive sequence of edges such that the path turns maximally to the left at e.g. black vertices and maximally to the right at white nodes. It can be depicted as a oriented path following edges and forced to cross them in the middle, see Figure 2.2a. Each edge is thus crossed by two oppositely oriented zig-zag paths. Zig-zag paths cannot self-intersect, and define (p, q) 1-cycles in the dimer 2-torus. Each such path corresponds to an external leg in the web diagram[29] corresponding to the toric 3-fold singularity, namely, the diagram dual to the toric data, see Figure 2.4b. For a brief discussion about toric diagrams and (p, q)-web diagrams, we refer to Appendix B.

Intuitively, this follows because the 3-fold geometry can be obtained as the mesonic moduli space of the gauge theory, and the zig-zag paths correspond to mesons of the gauge theory (obtained as the trace of the product of bifundamentals corresponding to the sequence of edges); notice that the F-term relations imply that mesons are only defined by the homology classes of the paths.

A more detailed method to obtain the 3-fold geometry is by introducing **perfect matchings**. A perfect matching in the dimer diagram is a set of edges such that each vertex in the dimer belongs to just one edge in the set, see Figure 2.5 for an example. There is no closed formula for the number of perfect matchings in a given dimer, but it is easily determined in most examples. At this point, one can recover the toric diagram as follows: regarding the perfect matchings p_A as 1-chains (with orientation of edges from black to white nodes), one can fix a reference matching p_0 and obtain a set of 1-cycles in the dimer given by $p_A - p_0$. The (p, q) labels of these 1-cycles correspond to the coordinates of points in the toric diagram of the 3-fold singularity, see Figure 2.4a. Note that this description is related to the previous paragraph because zig-zag paths can be obtained as differences of perfect matchings at consecutive external points in the toric diagram, namely, segments in the toric diagram dual to precisely external legs in the web diagram.

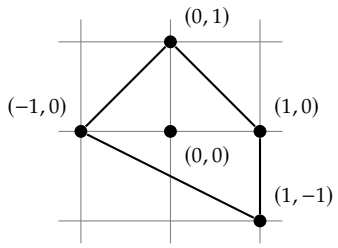

(a) Toric diagram.

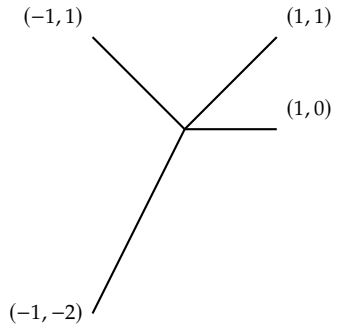

(b) (p, q)-web diagram.

Figure 2.4: dP_1 theory.

29: This correspondence is by defining a height function, defined as an integer-valued step-wise function increasing by one unit as one crosses the path (with positive orientation). The labels of the external leg in the web diagram are obtained as the jumps of the height function along the two basic 1-cycles in the 2-torus. In practice, this is equivalent (up to some relabeling) to just taking the (p, q) labels of the zig-zag path to be those of the external leg of the web diagram.

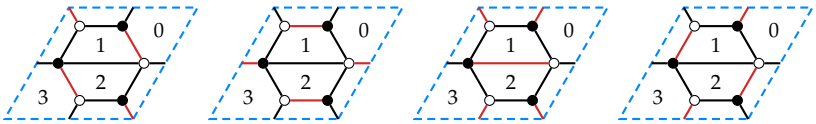

(a) p_1 **(b)** p_2 **(c)** p_3 **(d)** p_4

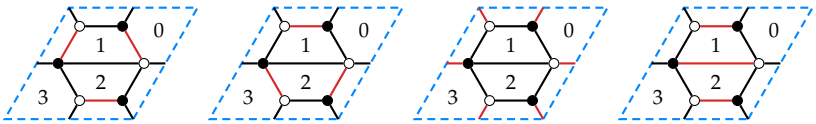

(e) s_1 **(f)** s_2 **(g)** s_3 **(h)** s_4

Figure 2.5: Set of perfect matchings for dP_1 theory.

An even more detailed relation with the toric description is by noticing that perfect matchings correspond to coordinates in the linear sigma model (or holomorphic quotient) description of the mesonic moduli space of the gauge theory. Let us review it, as it is useful to describe U(1) symmetries. In general, the bifundamentals are not useful coordinates to describe the moduli space, because they are constrained by the F-term conditions; perfect matchings are an efficient ingredient to solve these constraints automatically. The key idea is to define the bifundamentals in terms of the perfect matchings by the following relation

$$\Phi_{E_i} = \prod_A p_A^{k_{i,A}} , \tag{2.2}$$

where $k_{i,A} = 1$ if E_i belongs to the perfect matching p_A, and is zero otherwise. With this relation, all F-term constraints for the bifundamentals are solved automatically, with no restriction on the p_A. This is related to the fact that, from the definition of perfect matchings, any term in the superpotential is given by the product of all perfect matchings

$$W \sim \prod_A p_A . \tag{2.3}$$

On the other hand, the above relation (2.2) introduces a redundancy, as $\mathbb{C}^*$ transformations of the p_A which leave the Φ_{E_i} invariant. These are defined by a set of charges $q_{A,r}$ satisfying

$$\sum_A k_{i,A} q_{A,r} = 0 \quad \forall i . \tag{2.4}$$

The moduli space of F-flat directions is thus generated by the complex coordinates p_A modulo these $\mathbb{C}^*$ actions. In addition, to obtain the mesonic moduli space, we have to quotient by the U(1)'s associated to the faces of the dimer. A bifundamental Φ_{ab} in the $\left(\square_a, \overline{\square}_b\right)$ carries charges $(+1, -1)$ under $\mathrm{U}(1)_a \times \mathrm{U}(1)_b$, and we need to translate these to charges for the coordinates p_A. Denoting by $q_{i,a}$ the charge of the bifundamental Φ_{E_i} under $\mathrm{U}(1)_a$, we introduce a matrix of charges $q_{A,a}$ satisfying

$$q_{i,a} = \sum_A k_{i,A} q_{A,a} \quad \forall i . \tag{2.5}$$

The charges $q_{A,a}$ define $\mathbb{C}^*$ actions on the p_A which implement the $\mathrm{U}(1)_a$ actions at the level of perfect matchings. The mesonic moduli space is thus obtained as the quotient of the complex coordinates p_A by the $\mathbb{C}^*$ actions generated by the charges $q_{A,r}$ and $q_{A,a}$.

For illustration, consider one explicit example. In Figure 2.5 we see the perfect matchings for dP_1 theory. The moduli space of $F-$flat directions is found solving Eq. (2.4), which in our case, for instance, gives the following two $\mathbb{C}^*$ actions on the perfect matchings:

$$\left(\begin{array}{cccccccc} p_1 & p_2 & p_3 & p_4 & s_1 & s_2 & s_3 & s_4 \\ \hline 1 & 0 & -1 & 1 & -1 & -1 & 0 & 1 \\ -1 & -1 & 0 & -1 & 1 & 1 & 1 & 0 \end{array}\right) . \tag{2.6}$$

The other $\mathbb{C}^*$ actions can be found using Eq. (2.5), obtaining

$$\left(\begin{array}{cccccccc} p_1 & p_2 & p_3 & p_4 & s_1 & s_2 & s_3 & s_4 \\ \hline 0 & 0 & 0 & 0 & 0 & 0 & 1 & -1 \\ 0 & 0 & 0 & 0 & 1 & 0 & 0 & -1 \\ 0 & 0 & 0 & 0 & 0 & 1 & 0 & -1 \end{array}\right). \tag{2.7}$$

Combining the two matrices, you get the complete set of $\mathbb{C}^*$ actions on the perfect matchings which defines the mesonic moduli space. The kernel of the matrix is

$$\begin{pmatrix} 0 & -1 & 1 & 1 & 0 & 0 & 0 & 0 \\ 1 & 0 & 0 & -1 & 0 & 0 & 0 & 0 \\ -1 & 1 & -1 & 0 & 0 & 0 & 0 & 0 \end{pmatrix}. \tag{2.8}$$

The columns of this matrix are the coordinates of points in 3d. All points are on the plane defined by the equation $y = -x - z$ and, on that plane, the toric diagram of Figure 2.4a is reproduced.

2.2.2 Continuous U(1) symmetries

In the above discussion, it is implicit that the number of perfect matchings minus the number of $\mathbb{C}^*$ actions is equal to 3, so that the symplectic quotient defines a 3-fold. An important implication is that the resulting geometry enjoys a $\mathrm{U}(1)^3$ symmetry (namely, the toric action making it a **toric** geometry). Namely, $\mathbb{C}^*$ actions on the p_A which are orthogonal to those we are quotienting by. Labeling them with $m = 0, 1, 2$, their charges $q_{m,A}$ are given by the kernel of the combined matrix $(q_{A,a}|q_{A,r})$, namely satisfy:

$$\begin{aligned} \sum_A q_{m,A} q_{A,a} &= 0 \quad \forall a\,, \\ \sum_A q_{m,A} q_{A,r} &= 0 \quad \forall r\,. \end{aligned} \tag{2.9}$$

One of these U(1)'s (which we label with $m = 0$) is an R-symmetry,[30] whereas two linear combinations satisfying $\sum_A q_{m,A} = 0$, $m = 1, 2$, leave W in (2.3) invariant, and correspond to $\mathrm{U}(1)^2$ mesonic symmetries. In addition, there are $\mathrm{U}(1)_a$ symmetries associated to the faces. These correspond to baryonic symmetries, most of which are anomalous. The mixed $\mathrm{U}(1)_a - \mathrm{SU}(N_b)^2$ anomaly is given by

$$A_{ab} \propto N_a I_{ab} \quad \text{(no sum)}, \tag{2.10}$$

where N_a arises as a normalization of the $\mathrm{U}(1)_a$ generator and I_{ab} is defined as around (2.1). It is thus clear that, denoting by Q_a the generator of $\mathrm{U}(1)_a$, a general linear combination

$$Q_{\mathbf{B}} = \sum_a n_a Q_a \tag{2.11}$$

defines an anomaly free baryonic U(1) when the n_a satisfy the anomaly cancellation condition (2.1), namely

$$\sum_a n_a I_{ab} = 0\,. \tag{2.12}$$

30: In the superconformal case, the actual R-symmetry is in general a combination determined by a-maximization, see [24, 59]. We have used a-maximization in Section 1.1.4.1. As we have seen in Section 1.1.4, it is the field theory counterpart of the volume of the dual SE manifold minimization.

That is, there is an anomaly-free baryonic U(1) for coefficients n_a such that they could define a fractional brane. Let us emphasize, however, that for the anomaly-free baryonic U(1) to exist, it is not necessary that the fractional brane is present; hence our use of lowercase n_a instead of N_a in (2.11).

2.3 Some topological concepts in dimers and quivers

In this section, we introduce some (co)homological tools for dimer diagrams and their dual periodic quivers. The faces/nodes F_a, the edges/arrows E_i and the vertices/plaquettes V_α and V'_α can be regarded as the analogues of simplices in singular homology, hence we consider their formal linear combinations (with negative coefficients corresponding to reversing the orientation these objects carry), which we refer to as 0-, 1- and 2-chains.

On these diagrams, we can define p-forms as linear maps assigning a (in general, complex) number to every p-chain. For instance, in the dimer, we define 2-forms σ as assignments of numbers $\sigma(F_a)$ to the faces F_a, and similarly 1-forms $\lambda(E_i)$ and 0-forms $f(V_\alpha)$, $f(V'_\alpha)$. The assignments defining 2-, 1- and 0-forms in the dimer, when regarded in the quiver, define 0-, 1- and 2-forms. This can be regarded as a duality (in a construction known as quad-edge in computational physics), although we will not exploit it at present.

In the quiver there is a very natural realization of (co)homology. The boundary ∂V of a plaquette V (similarly for V') is the 1-chain given by the sum of the arrows surrounding it; the boundary ∂E of an edge E is the formal difference of the nodes at its tail and its head $\partial E = t(E) - h(E)$. Clearly $\partial^2 \equiv 0$, and we can define an homology. At the level of forms, we introduce an exterior derivative d as follows. For a 0-form f, we define df as the 1-form given by

$$df(E) = f(\partial E) = f(h(E)) - f(t(E)), \tag{2.13}$$

where $h(E)$, $t(E)$ denote the node at the head and tail of the arrow E. Similarly, for a 1-form λ, we define the 2-form $d\lambda$ by $d\lambda(F) = \lambda(\partial F)$. Finally, for a 2-form σ we define $d\sigma \equiv 0$. One clearly has $d^2 \equiv 0$ so this defines a cohomology. By defining integration by evaluation, d and ∂ obey Stokes' theorem. The above homology and cohomology are realizations of those of the underlying surface on which the quiver is embedded, in our case the 2-torus (or, as we occasionally focus on the infinite cover, $\mathbb{R}^2$).

The assignments of (continuous or discrete) charges to bifundamentals are used to define 1-forms λ on the quiver, and the conditions of invariance of the superpotential amount to closedness, $d\lambda = 0$. Non-trivial cohomology classes correspond to the mesonic U(1) symmetries, while exact forms $\lambda = df$ correspond to U(1) baryonic symmetries in the 2-torus.[31]

31: In Chapter 5 we will see that they are also related to the discrete B-symmetry in $\mathbb{R}^2$.

In the dimer, the notion of boundary and exterior derivative convenient for us but include a subtlety. We define the boundary $\tilde{\partial} F$ of a face F as the sum of the edges bounding it with their natural orientation (i.e., from

black to white vertices). This differs from the geometric intuition, where the boundary involves the same edges but with a weight ± determined by the incidence relation between the edge and the face (i.e., the chirality of the bifundamental). We use a tilde to emphasize this difference. We define the boundary $\tilde{\partial}E$ of and edge E as the difference between the corresponding black and white vertices, namely $\tilde{\partial}E = b(E) - w(E)$. Correspondingly, we define the exterior derivative $\tilde{d}$ as follows. For a 0-form f, we define $\tilde{d}f$ by

$$\tilde{d}f(E) = f\left(\tilde{\partial}E\right) = f(b(E)) - f(w(E))\,. \tag{2.14}$$

Similarly, for a 1-form λ we define $\tilde{d}\lambda(F) = \lambda\left(\tilde{\partial}F\right)$. Defining integration by evaluation, this obeys Stokes' theorem. However, in general $\tilde{d}^2 \neq 0$, $\tilde{\partial}^2 \neq 0$; there is a well-defined cohomology only if we restrict to 0-forms f which satisfy that for any face F, the value of f on the sum of black nodes equals its value on the sum of white nodes (and one may define homology in a similar restricted sense). Since these restrictions render these tools less natural, we simply use $\tilde{\partial}$ as a notational device. In terms of it, if the charge assignments under continuous or discrete symmetries are used to define a 1-form λ, the anomaly cancellation conditions read $\tilde{d}\lambda = 0$.

2.3.1 A new toolkit: U(1) global symmetries from Geometric Identities

Let us discuss global U(1) symmetries in the gauge theory from a more abstract perspective, using the topological intuitions in the dimer/quiver diagrams introduced in Section 2.3.

A U(1) symmetry is an assignment of charges to the edges E_i (or arrows E_i) in the dimer (resp. quiver) diagram of the gauge theory. We may regard this as a 1-form γ on the quiver, namely a map that to each arrow E_i assigns a number (the charge) $\gamma(E_i)$. Regarding the arrow as a 1-chain, this is also the integral of the 1-form over the 1-chain. One may also regard it as a 1-form in the dimer, which we also denote γ.

These charge assignments are constrained by demanding invariance of the superpotential. This means that for each plaquette V_α (or V'_α) in the quiver, with boundary given by a concatenation of arrows $\{E_1, E_2, \ldots, E_n\}$, the 1-form γ satisfies

$$\partial V_\alpha, \partial V'_\alpha \quad \rightarrow \quad \gamma(E_1) + \gamma(E_2) + \cdots + \gamma(E_n) = 0\,. \tag{2.15}$$

Recalling from Section 2.3 the definition of the exterior derivative, and using Stokes' theorem over the plaquette, we have

$$d\gamma = 0\,. \tag{2.16}$$

Regarding γ as realized in the dimer, these correspond to the so-called harmonic maps in the math literature. We stick to the nomenclature suggested by the notation, and refer to these as closed 1-forms in the periodic quiver.

As expected, closed 1-forms in finite graphs without torus periodicities must be exact, namely there exists a 0-form f in the quiver (namely, a map assigning a number $f(F_a)$ to each quiver node F_a) such that

$$\gamma = df \,. \tag{2.17}$$

Namely, if we denote by $h(E_i)$, $t(E_i)$ the head and tail of the arrow E_i, then

$$\gamma(E_i) = f(t(E_i)) - h(t(E_i)) \,. \tag{2.18}$$

Physically, if we denote $n_a \equiv f(F_a)$, this means that the charge assignment for edges given by γ is just inherited from the $\mathrm{U}(1)_a$ charges via a linear combination

$$Q = \sum_a n_a Q_a \,. \tag{2.19}$$

Namely, just like (2.11), with the only difference that we are not yet demanding the cancellation of anomalies. As explained above, such linear combinations in the toroidal graph correspond to (still possibly anomalous) baryonic U(1) symmetries. Hence, mesonic U(1) symmetries are defined as closed 1-forms (i.e. symmetries of the superpotential) which are not exact (i.e. are not baryonic), and correspond to combinations of the two independent homology classes of 1-forms in the 2-torus. Hence, we recover the $\mathrm{U}(1)^2$ mesonic symmetry.

Let us discuss the anomaly cancellation conditions more explicitly as follows. For each face F_a in the dimer (resp., node in the quiver), surrounded by a concatenation of edges (resp. arrows) $\{E_1, \ldots, E_m\}$, the mixed $\mathrm{SU}(N_a)^2$ anomaly cancellation conditions read

$$\tilde{\partial} F_a \quad \rightarrow \quad \gamma(E_1) + \cdots + \gamma(E_m) = 0 \,. \tag{2.20}$$

Note that since the natural orientation of edges does not allow to write this equation as over the boundary of F_a in the dimer, hence we use the notation $\tilde{\partial}$ for this 'signed' boundary.

In this language, an anomaly free U(1) symmetry is a charge assignment satisfying the conditions (2.15) and (2.20). These form an homogeneous linear system of equations, with the number of unknowns given by the number E of edges in the dimer, and with the number of equations given by the number V of vertices plus the number F of faces. Since the dimer is a tiling of the 2-torus, it satisfies

$$F + V = E \,. \tag{2.21}$$

Hence, the only non-trivial solution defining U(1) charges must require the existence of linear relations among the equations. Indeed, a general dimer always has two such relations, which we may write

$$\begin{aligned} \sum_\alpha \partial V_\alpha - \sum_\alpha \partial V'_\alpha = 0 \,, \\ \sum_a \tilde{\partial} F_a - \sum_\alpha \partial V_\alpha - \sum_\alpha \partial V'_\alpha = 0 \,. \end{aligned} \tag{2.22}$$

These can be regarded as **geometric identities** which the elements of the dimer/quiver diagrams satisfy. The two anomaly-free solutions which exist for any general dimer due to these universal geometric identities correspond to the $\mathrm{U}(1)^2$ mesonic symmetries.

In addition, we know that theories admitting fractional branes have additional anomaly-free baryonic U(1)'s. These correspond to linear combinations (2.11) satisfying (2.12). This requires that the above linear system of equations admits further geometric identities for theories admitting fractional branes. Indeed, in such cases it is possible to show that $\sum_a n_a \tilde{\partial} F_a$ can be recast as a combination of ∂V_α and $\partial V'_\alpha$. We will find explicit examples in later sections and chapters.

Incidentally, we would like to mention that, if we interpret $\gamma(E_i)$ not as charges, but as the exact anomalous dimensions for the bifundamental chiral multiplets, the above analysis is very closely related to the Leigh-Strassler characterization of marginal couplings in $\mathcal{N} = 1$ SCFTs [60] (see [61] for a discussion in the present context). Namely, the conditions of vanishing of the exact beta functions for the superpotential couplings (at V_α, V'_α) and for the gauge couplings (at F_a) form an inhomogeneous linear system of equations for $\gamma(E_i)$, whose associated homogeneous linear system is precisely given by the above, (2.15) and (2.20). Moreover, the inhomogeneous system of equations satisfies relations given precisely by the universal (2.22), allowing for the existence of a marginal coupling corresponding to the complexified coupling constant of the diagonal gauge group on the recombined regular brane. Additional geometric identities imply additional marginal couplings, associated to the gauge couplings of the corresponding fractional branes.

Let us conclude by mentioning the realization of these U(1) symmetries and marginal couplings in the holographic dual. For systems of D3-branes at toric singularities, there is a generic $U(1)^3$ isometry in the horizon, which includes the R-symmetry and the $U(1)^2$ mesonic symmetry. There is also a universal massless scalar, given by the axion-dilaton, dual to the marginal coupling. If the theory admits additional anomaly-free rank assignments (fractional branes), the gravity dual internal space $\mathbf{X}_5$ contains homology 3-cycles, supporting additional U(1)'s arising from integrating the RR 4-form over them; also, their dual 2-cycles produce additional massless scalars from integrating the NSNS and RR 2-forms, which are duals to the additional marginal couplings of the holographic dual gauge theory.

In Chapter 5 we will extend this matching to discrete symmetries. The natural arenas are then orbifolds.

2.3.2 General Orbifolds of General Toric Theories

Consider a general toric gauge theory with a dimer (resp. quiver) diagram with unit cell $\mathcal{C}$, with faces F_a, edges E_i and vertices V_α, V'_α. There is a general procedure to construct general Abelian $\mathbb{Z}_N$ orbifolds of this theory [62, 63] as follows. Denote by Q_1, Q_2 the two mesonic U(1)'s, normalized to have minimal charge ±1, and consider the linear combination

$$Q_\theta = p_1 Q_1 + p_2 Q_2 \quad p_1, p_2 \in \mathbb{Z}\,, \ \mathrm{GCD}(p_1, p_2) = 1\,. \tag{2.23}$$

Let us denote by k_{E_i} the charge under Q_θ of the bifundamental associated to the edge E_i. We consider the action of the generator θ of the orbifold

group $\mathbb{Z}_N$ to be given by

$$\theta : \quad \Phi_{E_i} \to \exp\left(2\pi i \frac{k_{E_i}}{N}\right) \Phi_{E_i} . \tag{2.24}$$

In addition, there is an action of θ on the gauge degrees of freedom, inspired by the action of Chan-Paton indices of D-branes. Namely, such that an object in the fundamental representation of $\mathrm{U}(N_a)$ transforms with an order N matrix

$$\gamma_{\theta,a} = \mathrm{diag}\left(\mathbf{1}_{n_{a,0}} , \ e^{2\pi i/N}\mathbf{1}_{n_{a,1}} , \ \ldots , \ e^{2\pi i(N-1)/N}\mathbf{1}_{n_{a,N-1}}\right) \tag{2.25}$$

and with its inverse on antifundamental representations.

The orbifold theory is obtained by removing fields of the parent theory which are not invariant under the combined action of the mesonic and gauge action. In particular, gauge bosons are singlets under the mesonic action, so demanding invariance of the generators λ_a of $\mathrm{U}(N_a)$ under the gauge action of $\gamma_{\theta,a}$

$$\lambda_a = \gamma_{\theta,a} \lambda_a \gamma_{\theta,a}^{-1} \tag{2.26}$$

breaks the group as follows

$$\bigotimes_a \mathrm{U}(N_a) \ \to \ \bigotimes_a \bigotimes_{r=0}^{N-1} \mathrm{U}(n_{a,r}) . \tag{2.27}$$

Here the treatment of the U(1)'s is as discussed above, namely, they are realized just as (potentially anomalous) global symmetries.

For an edge E_i separating two faces F_a, F_b in the dimer (respectively, an arrow with $t(E_i) = F_a$, $h(E_i) = F_b$ in the quiver), and with charge q_{E_i} under (2.23), the invariance of the bifundamental field Φ_{E_i}, regarded as a matrix is

$$\Phi_{E_i} = e^{2\pi i k_{E_i}/N} \gamma_{\theta,a} \Phi_{E_i} \gamma_{\theta,b}^{-1} , \tag{2.28}$$

leading to a projection pattern of the bifundamental E_i into a set of bifundamentals $E_{i,r}$ as follows

$$\left(\square_a , \overline{\square}_b\right) \ \to \ \bigoplus_{r=0}^{N-1} \left(\square_{a,r} , \overline{\square}_{b,r+k_{E_i}}\right) . \tag{2.29}$$

Finally, the superpotential of the orbifold theory is obtained by simply replacing the surviving fields in the superpotential terms of the parent theory. It is easy to see that a superpotential term in a vertex V_α (or V'_α), describing the interaction of a concatenated set of fields $\{E_1, \ldots, E_n\}$, leads to a set of superpotential terms $V_{\alpha,r}$ (resp. $V'_{\alpha,r}$) describing the interaction of the set of fields $\{E_{1,r}, \ldots, E_{n,r}\}$.

The orbifold theory is described by a dimer/quiver diagram whose unit cell $\mathscr{C}_N$ is obtained by taking N copies of the unit cell $\mathscr{C}$ of the parent theory. Hence, each ingredient of the parent theory has N descendant copies in the orbifold theory. We can be more explicit about how the different copies of $\mathscr{C}$ are adjoined to form $\mathscr{C}_N$, as follows, see Figure 2.6. Consider the infinite periodic array in $\mathbb{R}^2$ corresponding to the parent theory, and choose a unit cell $\mathscr{C}$, and two basis 1-cycles. The latter correspond to vectors in $\mathbb{R}^2$ defining the periodicities. The infinite copies of $\mathscr{C}$ can be labeled by two indices (r_1, r_2) according to their position in

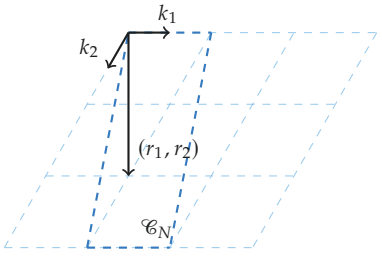

Figure 2.6: General orbifolding in a dimer using a periodic array of unit cells (in light blue). The final unit cell $\mathscr{C}_N$ is showed in blue.

the direction of the basic 1-cycles. Consider now mesons of the theory in $\mathscr{C}$, with winding numbers $(1,0)$ and $(0,1)$, and denote by k_1, k_2 the charges of these mesons under Q_θ (2.23), namely just the sums of the Q_θ charges k_{E_i} of the edges/arrows E_i involved in the corresponding meson. The mesons can be regarded as open paths in the infinite array, starting from a face in $\mathscr{C}$ to its copy face/node in the copies of $\mathscr{C}$ at the two independent adjacent positions. Now regarding the infinite array as the covering space for the orbifold theory, the open path joins a starting face/node $F_{a,r}$ with the faces/nodes $F_{a,r+k_1}$, $F_{a,r+k_2}$ in the two adjacent copies. In general, the copy of the face/node $F_{a,r}$ in the copy of $\mathscr{C}$ at the position (r_1, r_2) in the infinite array corresponds to the face/node $F_{a,r+r_1k_1+r_2k_2}$.

The integers k_1, k_2 determine the action of the orbifold on the mesons, namely, on the coordinates of the toric geometry. They are related to the construction of orbifolds in terms of toric data. Basically, the $\mathbb{Z}_N$ orbifold of any toric geometry is obtained by refining the 2-dimensional lattice by an order N vector, which in our present context is $(k_1, k_2)/N$. The action on the mesons is inherited from this by the standard relation between mesons and toric data as explained in Section 2.2.1. See Figure 5.12c for an example.

Note that in general, if e.g. $\mathrm{GCD}(k_1, N) = 1$, we may take the unit cell $\mathscr{C}_N$ of the orbifold theory as the N copies of $\mathscr{C}$ in the direction of the $(1,0)$ 1-cycle in $\mathscr{C}$. However, we prefer to work in the infinite array, and work for general k_1, k_2 with no special relation with N. On the other hand, notice that since all N copies of the unit cells arise in the infinite array, we may choose $\mathrm{GCD}(k_1, k_2) = 1$.

Discrete symmetries in string theory

3

In this chapter we introduce gauge and global discrete symmetries both in field theory and in string theory.
We review the general properties of discrete gauge symmetries in field theory in Section 3.1, and we show how naturally they arise in string compactifications in Section 3.2. Global discrete symmetries may be found on SCFTs in the context of AdS/CFT. They will play an important rôle in Chapter 5, and we explain the main properties in Section 3.3. Such global symmetries in the SCFT are gauged on the gravity side, and they are fundamental for the discussion in Chapter 6.

3.1 Abelian discrete gauge symmetries in field theory

Section 3.1 and its subsections are based on [8, 10, 51, 52, 64–69] and references therein.

Discrete Abelian gauge symmetries arise in the context of QFT when a $\mathfrak{u}(1)$ gauge symmetry is broken via the Higgs mechanism.[32] Let us consider a complex scalar field ϕ charged under a $\mathfrak{u}(1)$ symmetry with charge $k \in \mathbb{N}$. In 4d, the action for this theory contains

$$S \supset \int dx^4 \left(\partial_\mu \phi + ikA_\mu \phi\right)\left(\partial^\mu \bar{\phi} - ikA^\mu \bar{\phi}\right) . \tag{3.1}$$

32: See e.g. [8, 10] for a standard discussion on spontaneous symmetry breaking in QFT.

Suppose to give a non-trivial VEV v to ϕ, such that

$$\phi = \frac{1}{\sqrt{2}}(v + h)\, e^{2\pi i \eta} , \tag{3.2}$$

where h is the Higgs boson, while η is the massless Goldstone boson that will play the main rôle in the following. The action contains a kinetic term for η, which is the famous Stückelberg Lagrangian:

$$S \supset \frac{v^2}{2} \int dx^4 \left(\partial_\mu \eta + kA_\mu\right)^2 . \tag{3.3}$$

The scalar η enjoys a shift symmetry $\eta \simeq \eta + 1$ because it is a phase by its definition in Eq. (3.2) and it is usually called **axion**. Moreover, Eq. (3.3) is invariant under the following gauge transformation:

$$\begin{aligned} A_\mu &\longrightarrow A_\mu - \partial_\mu \Lambda , \\ \eta &\longrightarrow \eta + k\Lambda . \end{aligned} \tag{3.4}$$

Physically, the axion is usually gauged away giving a mass for the vector field. Technically, η transforms under a non-linear representation of $\mathfrak{u}(1)$ [69], and it signals that the symmetry $\mathfrak{u}(1)$ has been spontaneously broken. This interpretation makes clear why there is a discrete part of $\mathfrak{u}(1)$ left unbroken. Because of the shift symmetry of η, i.e. $\eta \simeq \eta + 1$, any transformation $\Lambda = \frac{n}{k}$, with $n \in \mathbb{N}$, leaves the action invariant. Such transformations are defined modulo k and they form the $\mathbb{Z}_k$ subgroup of U(1).

The objects that are electrically charged under A are $\mathbb{Z}_k$-charged particles with worldline L [51, 67]. They are described by Wilson line operators

$$W(L,n) \sim e^{2\pi i n \int_L A} \,. \tag{3.5}$$

The dual operators associated with these Wilson lines may be useful to realize that the symmetry is indeed $\mathbb{Z}_k$. The only 't Hooft operators that may be constructed are of the form $e^{2\pi i \eta}$ [67]. However, this operator is not gauge invariant, and it can be made gauge invariant if we attach to it k Wilson lines at the intersection point $P = \partial L$. The final operator is

$$H(P) \sim e^{2\pi i \eta(P)} W(L,k) \,, \tag{3.6}$$

which represents a process where k particles annihilate in P.

Let us consider $v = 1$ in Eq. (3.3). It is possible to dualize η in Eq. (3.3), defining

$$dB_2 = \star_4 d\eta \,. \tag{3.7}$$

Expanding the kinetic term, we obtain an interaction which is usually called **BF-coupling**:

$$S \supset k \int A \wedge dB_2 = k \int B_2 \wedge F_2 \,, \tag{3.8}$$

where $F_2 = dA$. The coefficient of the BF-coupling is also the order of the discrete symmetry $\mathbb{Z}_k$. Such couplings are very frequent in string theory compactifications also in their generalized forms that we will introduce in Section 3.1.1.

Such a dual formulation is useful to make manifest also another "emergent" $\mathbb{Z}_k$ discrete gauge symmetry [67]. Indeed, dualizing the gauge field such that

$$d\tilde{A} = \star_4 dA \,, \tag{3.9}$$

the action is

$$S \supset \frac{1}{2} \int d^4x \left(\partial_\mu \tilde{A}_\nu + k B_{\mu\nu} \right)^2 \,. \tag{3.10}$$

The action in Eq. (3.10) is invariant under the following transformations[33]

$$\begin{aligned} B_2 &\longrightarrow B_2 + d\Lambda_1 \,, \\ \tilde{A} &\longrightarrow \tilde{A}_1 - k\Lambda_1 \,. \end{aligned} \tag{3.11}$$

33: Note also that there is also another gauge transformation: $\tilde{A} \longrightarrow \tilde{A} + d\Theta$.

The emergent symmetry in this case is once again a $\mathbb{Z}_k$ symmetry[34] but the objects that are charged under it are different. We are now considering $\mathbb{Z}_k$-charged strings along a worldsheet S described by a Wilson line operator

34: Although in general it may differ.

$$W(S,n) \sim e^{2\pi i n \int_S B_2} \,. \tag{3.12}$$

To make the gauge symmetry manifest, we can once again consider the dual 't Hooft operators naively given by $e^{2\pi i \int_C \tilde{A}}$, where $C = \partial S$ is the junction line where they are inserted. To make such operators gauge

invariant, we need to add k strings on S that ends on C, i.e.,

$$H(C) \sim e^{2\pi i \int_C \tilde{A}} W(S,k)\,. \tag{3.13}$$

In complete analogy with the example in Eq. (3.6), such operator represents k strings that annihilate along C.

An interesting phenomenon that involves both $\mathbb{Z}_k$-charged particles and strings is the following: when a charge n particle defined as in Eq. (3.5) is moved around a charge p string as in Eq. (3.12), the wavefunction of the particle picks an Aharonov-Bohm phase $e^{2\pi i \frac{np}{k}}$. This means that it corresponds to a gauge transformation $n \longrightarrow n + np$. This is a way in which is it possible to detect the presence of a discrete symmetry.

We end this section with a bit of nomenclature. The theory in Eq. (3.3) is usually called "electric" theory, and the $\mathbb{Z}_k$-charged particle is the fundamental object, while the charged strings are called codimension-2 **topological defects**. In Eq. (3.10), the $\mathbb{Z}_k$-charged string is the fundamental object, while the charged particle is its topological defect. In this case, the theory is called "magnetic".

3.1.1 Generalization to arbitrary dimension

We have seen in Section 3.1 that it is not always the case that the gauge symmetry involves a scalar field and a 1-form gauge potential A. Indeed, the magnetic theory has a 1-form and 2-form playing, respectively, the rôle of the charged object and the gauge field. Suppose there is a $\mathbb{Z}_k$ gauge symmetry involving a $(p-1)$-form η_{p-1} and a p-form gauge potential A_p. The gauge transformation will be

Notice that we recover the electric theory in Section 3.1 for $p = 1$ and the magnetic theor for $p = 2$.

$$\begin{aligned} A_p &\longrightarrow A_p + d\Lambda_{p-1}\,, \\ \eta_{p-1} &\longrightarrow \eta_{p-1} - k\Lambda_{p-1}\,. \end{aligned} \tag{3.14}$$

Let us consider a D-dimensional gauge theory action[35]

35: As for the case with $p = 2$, there is also another gauge symmetry: $\eta_{p-1} \longrightarrow \eta_{p-1} + d\Theta_{p-2}$.

$$S \supset \frac{1}{2}\int_{\mathcal{M}_D} \left|d\eta_{p-1} + kA_p\right|^2\,. \tag{3.15}$$

This theory can be obtained with an analogous Higgs mechanism of that shown in Section 3.1 in $D = 4$. In this case the $\mathfrak{u}(1)$ gauge symmetry associated to A_p is broken to a $\mathbb{Z}_k$ subgroup. The Wilson lines in this case are representing $(p-1)$-branes with worldvolume S_p charged under the $\mathbb{Z}_k$ symmetry.

The action in Eq. (3.15) can be dualized by defining a $(D-p-1)$-form B_{D-p-1} and a $(D-p-2)$-form gauge potential $\tilde{A}_{D-p-2}$ from which we obtain

$$S \supset \frac{1}{2}\int_{\mathcal{M}_D} \left(d\tilde{A}_{D-p-2} + kB_{D-p-1}\right)^2\,. \tag{3.16}$$

This action is invariant under[36]

36: Remember that there is also the shift $\tilde{A}_{D-p-2} \longrightarrow \tilde{A}_{D-p-2} + d\Theta_{D-p-3}$.

$$\begin{aligned} B_{D-p-1} &\longrightarrow B_{D-p-1} + d\Lambda_{D-p-2}\,, \\ \tilde{A}_{D-p-2} &\longrightarrow \tilde{A}_{D-p-2} - k\Lambda_{D-p-2}\,. \end{aligned} \tag{3.17}$$

The generalization is straightforward for any kind of p-form gauge symmetry and in any dimension. The objects charged in this case are $\mathbb{Z}_k$-charged $(D-p-2)$-branes with worldvolume S_{D-r-1}. However, since we are dealing with branes for both the theory and its dual, there is no obvious identification of fundamental and topological defect objects.

Of particular interest is the generalization of the BF-coupling for general D-dimensional theory and p-form gauge symmetry. Starting, for instance, from Eq. (3.15) and expanding the square, we can isolate the term

$$S \supset k \int_{\mathcal{M}_D} dA_p \wedge B_{D-p-1} = k \int_{\mathcal{M}_D} F_{p+1} \wedge B_{D-p-1} \,, \tag{3.18}$$

where we have already integrated by parts the action.[37] Imposing $D = 4$ and $p = 2$, we obtain the BF-coupling of Eq. (3.8), however, here we see more possible couplings that signal the presence of a $\mathbb{Z}_k$ gauge symmetry.

37: Analogously, we can start from Eq. (3.16) and we obtain a coupling for the dual theory equal to

$$k \int_{\mathcal{M}_D} H_{D-p} \wedge A_p \,,$$

with $H_{D-p} = dB_{D-p-1}$.

One of the couplings that will play an important rôle in Chapter 6 is the so-called DKS coupling [66, 70]. Such coupling is a particular kind of BF-coupling when the B-field is a 0-form. For the particular case of $D = 4$, denoting $B_0 = b$, we obtain from Eq. (3.18)

$$S \supset k \int_{\mathcal{M}_4} b F_4 \,. \tag{3.19}$$

3.2 Discrete gauge symmetries in string theory

In Section 3.1.1 we generalized the BF-couplings to generic dimensions and p-form symmetry. String theory compactifications with background fluxes (see e.g. [9, 40, 49, 50] for reviews) offer a large number of examples in which such couplings arise naturally. As an example, it is sufficient to consider a KK reduction of the 10d CS couplings of the type II action as in Eq. (1.65), i.e.,

$$S_{\text{type II}} \supset \int_{\mathcal{M}_{10}} \sum_p H_3 \wedge F_p \wedge C_{7-p} + \int_{\mathcal{M}_{10}} \sum_p B_2 \wedge F_p \wedge F_{8-p} \,, \tag{3.20}$$

where B_2 is NSNS 2-form potential and $H_3 = dB_2$. The RR n-form potentials are given by C_n, while F_{n+1} are their field strengths. The distinction between type IIA and type IIB is given by n being, respectively, even or odd.

The presence of non-trivial background fluxes modifies the possible branes that can wrap cycles in the internal space. This is because the branes must satisfy the constraints coming from FW anomaly conditions [64, 65] (reviewed in Appendix C). The compactification of Eq. (3.20), which generate generalized BF-couplings may be also interpreted as wrapped branes on homologically non-trivial cycles in the internal space that are charged under the corresponding discrete gauge symmetry signaled by the BF-couplings. As explained in Section 3.1, the presence of the discrete symmetry is also shown from the annihilation of charged objects in a set of the order of the discrete symmetry. In this context, such wrapped branes decay in sets of the degree of the discrete symmetry, due to the

processes allowed by the presence of the fluxes. This phenomenon is usually called **flux catalysis** [51].

In Chapter 6 we will discuss mainly the presence of DKS couplings, that, as said in Section 3.1.1, in 4d are BF-couplings associated to a 3-form gauge symmetry. From the string compactification perspective, these terms are generated compactifying B_2 (resp. C_3) of Eq. (3.20) along 2-cycles (resp. 3-cycles) of the internal manifold. From the 4d effective theory, the charged objects are strings coming from NS5-branes wrapped on the dual 4-cycles (resp. D4-branes wrapped on 3-cycles), inducing the correct monodromy for the axion-like particle. Such objects suffer from FW anomalies that must be canceled by attaching to them domain walls. The domain wall is unstable, and a number of them may decay to nucleate a hole, whose boundary is the string itself. Let us do an example in type IIA backgrounds using the convention for the harmonic forms introduced in Section 1.2.2. Suppose to compactify B_2 on a basis of 2-cycles ω_a. Axionic strings arise from NS5-branes wrapped on the dual 4-cycles of ω, i.e., PD(ω_a). In the presence of the Roman mass, i.e., a background RR-flux F_0^{flux}, the axionic string develops an FW anomaly, that must be canceled emitting a D6-brane wrapped in the 4-cycle Poincaré dual of ω. The number of D6-branes that must be emitted is proportional to the amount of F_0^{flux}. A summary with all the domain walls present in type IIA compactification on CY orientifold is in Table 3.1 [52].

Table 3.1: 4d axionic strings and their corresponding domain walls arising from Dp- and NS5-branes wrapped on cycles of the CY manifold $\mathcal{M}_6$ with background fluxes and orientifold.

Axion	Brane	Flux	Domain Wall	Rank
$B_2 = b^a \omega_a$	NS5 on PD(ω_a)	$F_0^{\text{flux}} = m$	D6 on PD(ω_a)	m
$B_2 = b^a \omega_a$	NS5 on PD(ω_a)	$F_2^{\text{flux}} = m^a \omega_a$	D4 on PD$\left(F_2^{\text{flux}} \wedge \omega_a\right)$	$\mathcal{K}_{abc} m^c$
$B_2 = b^a \omega_a$	NS5 on PD(ω_a)	$F_4^{\text{flux}} = e_a \tilde{\omega}^a$	D2 at a point in $\mathcal{M}_6$	e_a
$C_3 = \xi^I \alpha_I$	D4 on PD(α_I)	$H_3^{\text{flux}} = h_J \beta^J$	D2 at a point in $\mathcal{M}_6$	$-h_J$
$C_3 = -\tilde{\xi}_I \beta^I$	D4 on PD$\left(\beta^I\right)$	$H_3^{\text{flux}} = h^J \alpha_J$	D2 at a point in $\mathcal{M}_6$	h^J

From Table 3.1 it is possible to understand how FW anomaly is cured by the domain wall for a generic flux. Given the 4d axionic string, in the presence of a background RR-flux F_{2p}^{flux}, when F_{2p} is non-trivial when restricted to the 4-cycles, a FW anomaly is developed where the NS5-brane is wrapped. Such anomaly is cured by emitting a D$(6-2p)$-brane wrapping the $(4-2p)$-cycle in the Poincaré dual class of the cycles wrapped by the NS5-brane [52]. In Appendix C, the reader will find a brief explanation of how FW anomalies work and also their relations with the more familiar HW construction in the non-compact case in terms of branes.

3.2.1 Domain wall gauge couplings in type IIA CY compactifications

In this section we derive the gauge coupling constants for domain walls present in type IIA CY flux compactifications, in particular we will try to obtain the relevant domain walls that are present in [48].[38] We review the computation in [71] following the conventions in [48]. Recall the type IIA

38: A review of the construction in [48] has been done in Section 1.2.3.4.

$|F_p|^2 = \frac{1}{p!} F_{\alpha_1 \dots \alpha_p} F^{\alpha_1 \dots \alpha_p}$.

supergravity action in Eq. (1.78) in the 10d string frame. In the presence of fluxes, we may consider the following modification

$$\begin{aligned} S^{10d} =& \frac{1}{2\kappa_{10}^2} \int d^{10}x \sqrt{-g} \left(e^{-2\phi} \left(R + 4(\partial_\mu \phi)^2 - \frac{1}{2} |H_3^{\text{total}}|^2 \right) \right) + \\ & - \frac{1}{2\kappa_{10}^2} \int d^{10}x \sqrt{-g} \left(\left(|\tilde{F}_2|^2 + |\tilde{F}_4|^2 + m_0^2 \right) \right) + S_{CS} \,, \end{aligned} \tag{3.21}$$

where $2\kappa_{10}^2 = (2\pi)^7 \alpha'^4$ and the definitions of the field strengths are

$$\begin{aligned} H_3^{\text{total}} &= dB_s + H_3^{\text{bg}} \,, \\ \tilde{F}_2 &= dC_1 + mB_2 \,, \\ \tilde{F}_4 &= dC_3 + F_4^{\text{bg}} - C_1 \wedge H_3 - \frac{m}{2} B_2 \wedge B_2 \,. \end{aligned} \tag{3.22}$$

The CS action contains also a prefactor $(2\kappa_{10})^{-1}$ in front. We define an adimensional internal volume by $\bar{\mathcal{V}} = M_s^6 \mathcal{V}$ and perform the dimensional reduction in the string frame. For instance, the kinetic term for the 4d field strength associated to the 10d F_4 reads

$$S_{4d}^{\text{kin}} \supset -\frac{M_s^2}{2} \int d_4x \sqrt{-g_4} \bar{\mathcal{V}} |\mathcal{F}_4|^2 \,, \tag{3.23}$$

where $\mathcal{F}_4 = dC_3$. To move back to the Einstein frame, we choose a reference scale a, and define the 4d dilaton $D(x)$ as

$$a = \frac{\langle \bar{\mathcal{V}} \rangle}{e^{2\langle \phi \rangle}} \,, \; e^{2D} = \frac{e^{2\phi}}{\bar{\mathcal{V}}} \,. \tag{3.24}$$

Therefore, the Einstein frame kinetic terms take the form

$$S_E^{\text{kin}} \supset \frac{M_s^2}{2a} \int d^4x \sqrt{-g_E} R_E - \frac{a^2 M_s^2}{2} \int d^4x \sqrt{-g_E} \bar{\mathcal{V}} e^{-4D} |\mathcal{F}_4|^2 \,, \tag{3.25}$$

where the products are now done using g_E as a metric.

To obtain 4d gauge 3-forms, we perform a KK reduction of 10d p-forms along suitable harmonic (p−3)-forms in the internal space. In the notation of [72],

$$C_3 = c_3^0 \,, \; C_5 = c_3^a \wedge \omega_a \,, \; C_7 = \tilde{d}_{3a} \wedge \tilde{\omega}^a \text{ and } C_9 = \tilde{d}_3 \wedge \omega_6 \,. \tag{3.26}$$

They correspond to the relevant 4-forms $\mathcal{F}_4^0$, $\mathcal{F}_4^a$, $\tilde{\mathcal{F}}_{4,a}$ and $\tilde{\mathcal{F}}_4$ associated with D2-, D4-, D6- and D8-branes.

Notice that we need to normalize the gauge fields by the coefficient in front of the D-brane CS term, in order for the charges to be properly quantized. For a Dp-brane this introduces factors of $\mu_p \propto \alpha'^{(p+1)/2} \sim M_s^{(p+1)}$ in the forthcoming gauge couplings. Namely, in order to be consistent, we need to keep the harmonic forms as adimensional, so the generic CS action is

$$S_{CS}^{(p)} \sim M_s^3 \int_{W_3 \times \gamma_{p-2}} c_3 \wedge \omega_{p-2} \,, \tag{3.27}$$

where we have called $c_3 \wedge \omega_{p-2}$ collectively each decomposition in (3.26). The normalization consists in redefining the RR 3-form by a factor M_s^3, so that there is no prefactor in front of the CS action. The effect of such

redefinition on (3.25) is just a change in the prefactor in front of the kinetic terms of the gauge fields,

$$S_E^{\text{kin}} \supset \frac{M_s^2}{2a}\int d^4x\sqrt{-g_E}R_E - \frac{a^2}{2M_s^2}\int d^4x\sqrt{-g_E}\bar{\mathcal{V}}e^{-4D}|\mathcal{F}_4|^2\,. \quad (3.28)$$

We are almost done with the definition of the coupling constants, but first we need the following quantities:

$$M_s^2 \propto \frac{e^{2\langle\phi\rangle}}{\langle\bar{\mathcal{V}}\rangle}M_{P,4}^2 = a^{-1}M_{P,4}^2\,,$$
$$K_K = -\ln(8\bar{\mathcal{V}})\,,\ K_Q = 4D\,,\ K = K_K + K_Q\,.$$

Substituting in (3.28) and including the other 4-forms, we obtain [71]

$$\begin{aligned} S_E^{kin} =& \frac{\pi}{2M_{P,4}^4}\int\frac{e^{-K}}{8}\left[\mathcal{F}_4^0\wedge\star\mathcal{F}_4^0 + 4g_{ab}\mathcal{F}_4^a\wedge\star\mathcal{F}_4^b\right] + \\ &+\frac{\pi}{2M_{P,4}^4}\int\frac{e^{-K}}{8}\left[\frac{1}{4\bar{\mathcal{V}}^2}g^{ab}\tilde{\mathcal{F}}_{4|a}\wedge\star\tilde{\mathcal{F}}_{4|b} + \frac{1}{\bar{\mathcal{V}}^2}\tilde{\mathcal{F}}_4\wedge\star\tilde{\mathcal{F}}_4\right], \end{aligned} \quad (3.29)$$

where

$$g_{ab} = \frac{\partial^2 K_K}{\partial t^a\partial\bar{t}^b} \quad (3.30)$$

is the metric in the Kähler moduli space with $t^a = v^a + ib^a$.
Recalling the example in Section 1.2.3.4, we can now specialize to a toroidal orbifold compactification. The Kähler potential is

$$K_K = -\ln(8v^1v^2v^3) = -\ln((t^1+\bar{t}^1)(t^2+\bar{t}^2)(t^3+\bar{t}^3))\,, \quad (3.31)$$

so

$$g_{ab} = \frac{1}{4}\,\text{diag}\left((v^1)^{-2},(v^2)^{-2},(v^3)^{-2}\right)\,. \quad (3.32)$$

We rewrite the action according to this metric obtaining

$$\begin{aligned} S_E^{kin} =& \frac{\pi}{2M_{P,4}^4}\int\frac{e^{-K}}{8}\left[\mathcal{F}_4^0\wedge\star\mathcal{F}_4^0 + \sum_{i=1}^{3}\left(\frac{1}{(v^i)^2}\mathcal{F}_4^i\wedge\star\mathcal{F}_4^i\right)\right] \\ &+\frac{\pi}{2M_{P,4}^4}\int\frac{e^{-K}}{8}\left[\sum_{i=1}^{3}\left(\frac{(v^i)^2}{\bar{\mathcal{V}}^2}\tilde{\mathcal{F}}_{4|i}\wedge\star\tilde{\mathcal{F}}_{4|i}\right) + \frac{1}{\bar{\mathcal{V}}^2}\tilde{\mathcal{F}}_4\wedge\star\tilde{\mathcal{F}}_4\right]. \end{aligned} \quad (3.33)$$

We are finally able to read the coupling constants of all kinds of domain walls:

$$\frac{1}{g_0^2} = \frac{\pi e^{-K}}{8M_{P,4}^4}\,,\ \frac{1}{g_i^2} = \frac{\pi e^{-K}}{8M_{P,4}^4(v^i)^2}\,,\ \frac{1}{g_{\tilde{i}}^2} = \frac{\pi e^{-K}(v^i)^2}{8M_{P,4}^4\bar{\mathcal{V}}^2}\,,\ \frac{1}{g_{\tilde{4}}^2} = \frac{\pi e^{-K}}{8M_{P,4}^4\bar{\mathcal{V}}^2}\,. \quad (3.34)$$

3.3 Discrete global symmetries in SCFTs

Section 3.3 is based on [1, 29, 73–76].

In Section 1.1.2 we have introduced certain kinds of baryons coming from wrapped branes on torsion cycles. In particular, it is possible to

associate three operators, namely, A, B and C that count the number of wrapped branes on different torsion cycles. For instance, in the set-up where NS5- and D5-branes were wrapping torsion 3-cycle, they can be counted respectively by the operators A and B. By HW transition, when these branes cross, a D3-brane can be created or destroyed. We can then consider C to be the operator that counts the number of wrapped D3-branes on torsion 1-cycles, and we realize that these three operators form a discrete **Heisenberg group** modulo some integer number q that depends on the structure of the quiver. It is possible to identify these operators also in the corresponding SCFT engineered by the brane set-up. The operators A, B and C will correspond to transformations on the quiver and on the fields that [73]:

See Appendix C for a review on HW constructions.

The definition of discrete Heisenberg group has been given in Section 1.1.2.1.

- Leave the superpotential invariant.
- Cancel the anomaly for all the SU(N) gauge groups.

The easiest examples where the Heisenberg group can be found are in 4d quiver gauge theories with p SU(N) gauge group in a complete quiver graph with different multiplicities.[39] We have already encountered the gravity dual of these SCFT when we considered orbifold singularities $\mathbb{Z}_p$ in Section 1.1.1.1 and the SCFTs are obtained by N D3-branes probing an orbifold $\mathbb{Z}_p$ singularity of $\mathbb{C}^3$.
As pioneered in [29], and further explored in [73] (see also [74–76]) there are several examples of orbifolds of simple geometries. Let us consider, for instance, the $\mathbb{Z}_3$ orbifold of $\mathbb{C}^3$ whose quiver is showed in Figure 3.1. The theory has 3 gauge groups SU$(N)_i$ and there is a manifest global discrete symmetry, with generator A acting as $i \to i+1$ on the labels of the SU(N)'s and on the fields, namely

39: A complete quiver graph is a quiver with n nodes all joined among each other by arrows with different multeplicities and directions.

$$A\begin{pmatrix} X_{i\,i+1} \\ Y_{i\,i+1} \\ Z_{i\,i+1} \end{pmatrix} = \begin{pmatrix} X_{i+1\,i+2} \\ Y_{i+1\,i+2} \\ Z_{i+1\,i+2} \end{pmatrix}, \tag{3.35}$$

where the labels are meant to be taken modulo 3. This is just a $\mathbb{Z}_3$ rotation of the theory, which in the context of orbifolds of $\mathbb{C}^3$ is often referred to as quantum symmetry (as it is a symmetry of the quantum worldsheet theory, in the sense of the α' expansion). This discrete group can be accompanied by a further symmetry generator B, defined as phase rotations of the bifundamentals, such that the symmetry is enhanced to the discrete Heisenberg group.

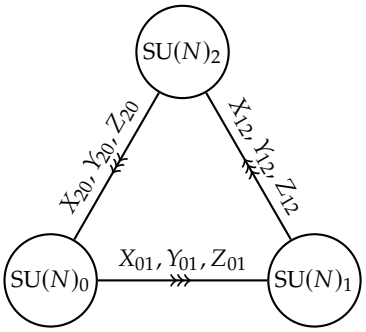

Figure 3.1: Quiver for the orbifold $\mathbb{C}^3/\mathbb{Z}_3$. The superpotential is omitted.

We can define $\omega = \exp[2\pi i/(3N)]$, so that on top of the global SU(3) symmetry, acting on the fields associated to the three complex planes, there is a global symmetry B under which the fields transform, for instance, as

$$\begin{aligned} B\begin{pmatrix} X_{01} \\ Y_{01} \\ Z_{01} \end{pmatrix} &= \omega\begin{pmatrix} X_{01} \\ Y_{01} \\ Z_{01} \end{pmatrix}, \\ B\begin{pmatrix} X_{12} \\ Y_{12} \\ Z_{12} \end{pmatrix} &= \omega^{-1}\begin{pmatrix} X_{12} \\ Y_{12} \\ Z_{12} \end{pmatrix}, \\ B\begin{pmatrix} X_{20} \\ Y_{20} \\ Z_{20} \end{pmatrix} &= \begin{pmatrix} X_{20} \\ Y_{20} \\ Z_{20} \end{pmatrix}. \end{aligned} \tag{3.36}$$

The actions A and B satisfy the commutation relation

$$AB = CBA\,, \tag{3.37}$$

where the action of C is

$$\begin{aligned} C\begin{pmatrix} X_{01} \\ Y_{01} \\ Z_{01} \end{pmatrix} &= \omega^{-2}\begin{pmatrix} X_{01} \\ Y_{01} \\ Z_{01} \end{pmatrix}, \\ C\begin{pmatrix} X_{12} \\ Y_{12} \\ Z_{12} \end{pmatrix} &= \omega\begin{pmatrix} X_{12} \\ Y_{12} \\ Z_{12} \end{pmatrix}, \\ C\begin{pmatrix} X_{20} \\ Y_{20} \\ Z_{20} \end{pmatrix} &= \omega\begin{pmatrix} X_{20} \\ Y_{20} \\ Z_{20} \end{pmatrix}, \end{aligned} \tag{3.38}$$

and commutes with both A and B so it is central. Hence, we recover a discrete Heisenberg group H_3, also known as Δ_{27}.

There are examples of other orbifolds of $\mathbb{C}^3$ studied for instance, in [73]. In the case of $\mathbb{C}^3/\mathbb{Z}_5$, whose quiver is in Figure 3.2, we can call $W_{i\,i+1} = (X_{i\,i+1}, Y_{i\,i+1})$, while we keep $Z_{i\,i-2}$ as it is. Let us also define $\omega = \exp[2\pi i/(5N)]$, so that the Heisenberg algebra is given by

$$\begin{aligned} B\,(W_{01}, W_{12}, W_{23}, W_{34}, W_{40}) &= \left(W_{01}, \omega W_{12}, \omega^2 W_{23}, \omega^3 W_{34}, \omega^{-6} W_{40}\right), \\ B\,(Z_{03}, Z_{14}, Z_{20}, Z_{31}, Z_{42}) &= \left(\omega^3 Z_{03}, \omega^6 Z_{14}, \omega^{-1} Z_{20}, \omega^{-3} Z_{31}, \omega^{-5} Z_{42}\right), \\ C\,(W_{01}, W_{12}, W_{23}, W_{34}, W_{40}) &= \left(\omega W_{01}, \omega W_{12}, \omega W_{23}, \omega W_{34}, \omega^{-4} W_{40}\right), \\ C\,(Z_{03}, Z_{14}, Z_{20}, Z_{31}, Z_{42}) &= \left(\omega^3 Z_{03}, \omega^3 Z_{14}, \omega^{-2} Z_{20}, \omega^{-2} Z_{31}, \omega^{-2} Z_{42}\right). \end{aligned} \tag{3.39}$$

In Chapter 5 we will be able to find a procedure to extract the B and C symmetries for a given toric quiver gauge theory using dimers. Our technique allows uncovering discrete global symmetries in the fields theories on D3-branes at singularities given by general orbifolds of general toric CY 3-fold singularities.

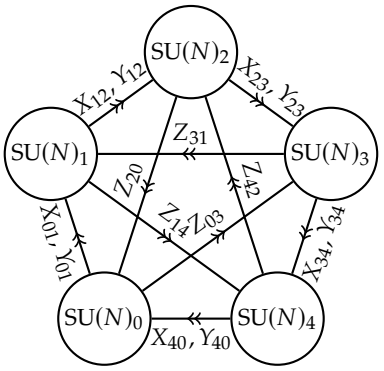

Figure 3.2: Quiver for the orbifold $\mathbb{C}^3/\mathbb{Z}_5$. The superpotential is omitted.

We have reviewed dimer diagrams and the construction of a general orbifold of a general toric CY 3-fold in Chapter 2.

The swampland program and Weak Gravity Conjectures

4

In this chapter we are going to give an overview of the swampland program developed in string phenomenology in the last decade. After a short list of the principal conjectures in Section 4.1, we are going to focus on the WGC (Section 4.2) which is the conjecture that is mostly used in Chapters 6 and 7. The content of this chapter is based on the reviews [77–79] and the papers [2, 3].

4.1 The swampland program

The Swampland program has the aim of defining a set of criteria to determine if an EFT can be completed into QG in the UV [78]. The **Swampland** is given by all the EFT that cannot be completed to QG, while the other theories are in the **Landscape**. In the years there have been nice reviews [77–79] where one can find more detailed information about the Swampland program. We are just going to review the relevant topics for the discussion in the next chapters.
The Swampland program then tries to give conjectures or criteria that all EFT must satisfy in order to hopefully have a UV completion to QG. These conjectures are based on string theory constructions, general QG arguments and microscopic physics [78]. When an EFT does not satisfy a conjecture, then the theory might be in the swampland or the conjectures are not refined enough to contemplate that theory.
A way, for instance, to prove that a conjecture must be refined, is to actually find a UV completion of the EFT. If the theory has a string theory 10d uplift, even if it was violating some conjectures, then, the conjectures must be refined in order to include also such EFT. If the 10d uplift is missing, then, the EFT might be in the swampland for the set of conjectures that have been so far formulated.
One possibility to make the Swampland program more precise is to prove the conjectures, and make them theorems. This is the reason many attempts have been done not only to find a mathematical and physical proof for the conjectures to hold, but also to find connections among the conjectures, so to make easier the proof of all of them, whenever it was possible to prove one of them.
In the following we will list only the most important conjectures and those that are relevant for the two conjectures we will propose in Chapter 6. In particular, the different formulations of the WGC will be discussed in Section 4.2. A schematic picture of how the conjectures are related one to the others is showed in Figure 4.1.

We start with the following conjecture:

Conjecture 4.1 [No Global Symmetries [67, 80]]**.**

A theory with a finite number of states, coupled to gravity, can have

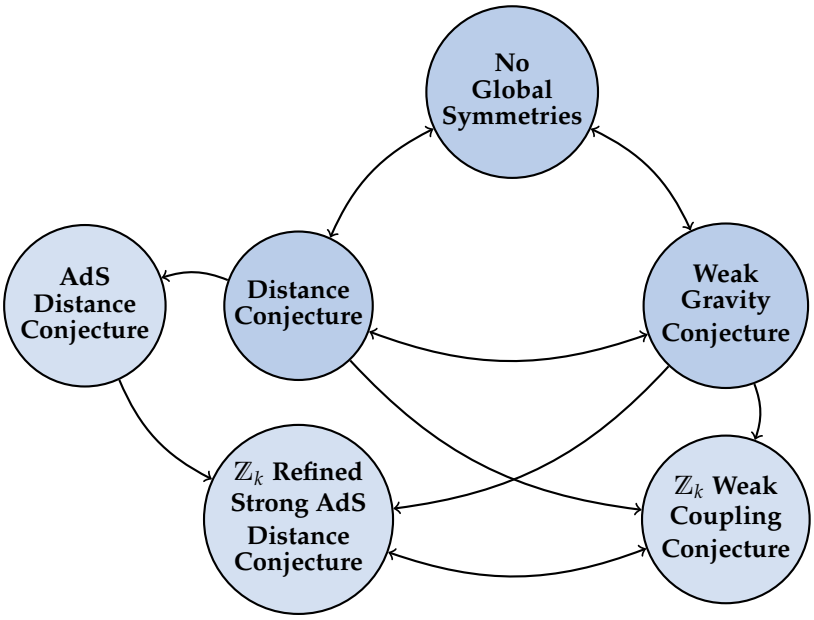

Figure 4.1: Map of relevant conjectures for our discussion inspired by [79]. We also added the two conjectures we will formulate in Chapter 6 with their connections to the already known conjectures.

no exact global symmetries [78].

It is probably the better established conjecture, and it has been proved in the context of AdS / CFT very recently in [81].
Related to that conjecture there is the Swampland Distance Conjecture (SDC) [82]. Such conjecture considers a theory, coupled to gravity, with a moduli space $\mathcal{M}$ which is parameterized by the VEV of some field ϕ that has no potential. Let us start from a point $P \in \mathcal{M}$ and we consider the geodesic distance $d(P,Q)$ between P and another point in the moduli space Q. The conjecture states that

Conjecture 4.2 [Swampland Distance Conjecture (SDC) [82]]**.**

There exists an infinite tower of states, with an associated mass scale M, such that

$$M(Q) \sim M(P)e^{-\alpha d(P,Q)}\,, \tag{4.1}$$

where α is some order 1 positive constant.

The geodesic distance between two points P and Q is defined as

$$d(P,Q) \equiv \int_\gamma \sqrt{g_{ij}\frac{\partial\phi^i}{\partial s}\frac{\partial\phi^j}{\partial s}}ds\,, \tag{4.2}$$

where γ is the shortest geodesic connecting the points P and Q, and ds is the line element along the geodesic [78]. The metric g_{ij} is defined from the kinetic terms of the fields ϕ^i in the action of the theory we are considering, i.e.

$$S \supset M_{P,D}^{d-2}\int d^Dx\sqrt{-h}\left[\frac{R}{2} - g_{ij}(\phi^i)\partial\phi^i\partial\phi^j\right]. \tag{4.3}$$

For the specific case in which we are considering a theory coupled to

gravity in an AdS vacuum, there exists a consequence of the SDC that involves the cosmological constant Λ:

Conjecture 4.3 [AdS Distance Conjecture (ADC) [83]]**.**

Any AdS vacuum has an infinite tower of states that becomes light in the flat space limit $\Lambda \to 0$, satisfying

$$m \sim |\Lambda|^{\alpha} , \tag{4.4}$$

where α is some order 1 positive constant.

For the case of supersymmetric AdS vacua, there is a stronger version of the ADC, namely

Conjecture 4.4 [Strong AdS Distance Conjecture (SADC] [83])**.**

For supersymmetric AdS vacua $\alpha = \frac{1}{2}$.

In Chapter 6 we are actually going to propose a refinement of this last conjecture in the presence of $\mathbb{Z}_k$ Abelian gauge symmetries coming from 3-forms gauge potentials.

4.2 Weak Gravity Conjectures

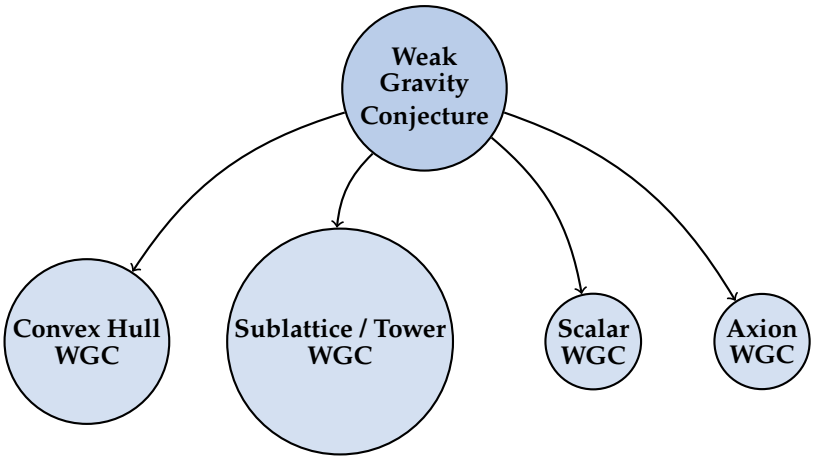

Figure 4.2: Principal refined versions of the WGC.

The WGC is maybe one of the most famous Swampland conjecture. It was formulated for the first time in [84] for a 4d theory coupled to gravity with a U(1) gauge symmetry, with gauge coupling g. It is usually formulated in two ways and they are, respectively the **Electric** WGC and the **Magnetic** WGC.

Conjecture 4.5 [4d Electric Weak Gravity Conjecture [84]]**.**

There exists a particle in the theory with mass m and charge q

satisfying

$$m \leq gqM_{P,4}\,. \tag{4.5}$$

Conjecture 4.6 [4D Magnetic Weak Gravity Conjecture [84]]**.**

The cutoff scale Λ of the EFT is bounded from above by the gauge coupling

$$\Lambda \lesssim gM_{P,4}\,. \tag{4.6}$$

Roughly speaking, then, the WGC is stating that gravity is the weakest interaction. The original argument at support of this conjecture was based on the decay of extremal Black Holes (BHs), in order to avoid BH remnants [77–79].

The first generalization that can be done to Conjecture 4.5 is in the case when there are multiple U(1) gauge symmetries. It was argued in [85] that there should be still a bound on the spectrum of particles, based on a **convex hull** condition. Suppose to consider a theory coupled to gravity with multiplet U(1) gauge symmetries with gauge coupling g_i. We then introduce the variable

$$z_i \equiv \frac{g_i q_i M_{P,4}}{m_i}\,, \tag{4.7}$$

where q_i is the charge with respect to the symmetry g_i of the particle with mass m_i. The conjecture is the following:

Conjecture 4.7 [Convex Hull WGC [85]]**.**

A theory with multiplet U(1)'s must have a spectrum of particles with charge-to-mass ratio vectors z_i, whose convex hull includes the unit ball.

The natural question is about which states must satisfy the WGC. At the moment the statement of the conjecture is only an indication that there should be states satisfying it, but there is no indication on how many of them and at which energy scale it must be satisfied for those state. The best version of the WGC that contains information about the kind of states that must satisfy the WGC is the **Sublattice** WGC [86–88] or the **Tower** WGC [89].

Conjecture 4.8 [Sublattice / Tower WGC [86–89]]**.**

For every site $\mathbf{q}$ of the charge lattice, there is a positive integer n such that there is a superextremal state with charge $n\mathbf{q}$ satisfying the WGC.[40]

40: For the case of the Sublattice WGC, the integer n is universal. For the case of the Tower WGC the integer depend on $\mathbf{q}$ [79].

For the moment, we focused on 4d EFTs but one can ask what are the generalizations to D-dimensional EFT and also what are the corresponding WGCs for objects that are not particles. In the case in which a

D-dimensional EFT contains scalars, for instance, there is a version for the WGC as follows.

Conjecture 4.9 [Scalar WGC [90]].

Given an EFT coupled to gravity with some massless scalar fields ϕ_i, there must exist a state with mass m satisfying:

$$g^{ij}\partial_{\phi_i} m \partial_{\phi_j} m \geq \frac{D-3}{D-2} m^2 \,, \tag{4.8}$$

where g_{ij} is the field metric.

Finally, in the case in which a D-dimensional EFT contains U(1) gauge symmetries come from generic p-forms with kinetic terms [78]:

$$\mathscr{L} \supset \frac{1}{2g_p^2} \left|F_{p+1}\right|^2 \,, \tag{4.9}$$

$$\left|F_{p+1}\right|^2 = \frac{1}{(p+1)!} F_{\mu_1 \cdots \mu_{p+1}} F^{\mu_1 \cdots \mu_{p+1}} \,.$$

Conjectures 4.5 and 4.6 become

Conjecture 4.10 [Electric WGC [86]].

A D-dimensional theory with a p-form field, should have a $(p-1)$-dimensional object with charge q_p and tension T_p satisfying

$$\frac{p(D-p-2)}{D-2} T_p^2 \leq q_p^2 g_p^2 \left(M_{P,D}^D\right)^{D-2} \,. \tag{4.10}$$

Conjecture 4.11 [Magnetic WGC].

The cutoff scale Λ of the EFT is bounded from above by the gauge coupling

$$\Lambda \lesssim \left(g^2 M_{P,D}^{D-2}\right)^{\frac{1}{2(p+1)}} \,. \tag{4.11}$$

The case of $p = 0$ is not covered in Conjecture 4.10. Indeed, this case was already present in [84], and it is the axion-instanton case. Suppose to consider the following effective Lagrangian [78]:

Note that Conjecture 4.11 already contemplate that case.

$$\mathscr{L} \supset -f^2 (\partial a)^2 + \Lambda^4 \sum_q e^{-qS} \left(1 - \cos(qa)\right) \,, \tag{4.12}$$

where f is the axion decay constant and S is the instanton action with instanton number q. The WGC for this set-up is

Conjecture 4.12 [Axion WGC [84]].

An axion with decay constant f must couple to instantons with

action S, such that

$$fS \leq M_{P,4}\,. \tag{4.13}$$

It is possible to modify Conjecture 4.10 so that it contains also the case $p = 0$, since the Axion WGC is related to the extended gravitational instantons solution [91]. In the presence of a dilaton, with dilatonic coupling α, Conjecture 4.10 becomes

$$\left[\frac{\alpha^2}{2} + \frac{p(D-p-2)}{D-2}\right] T_p^2 \leq q_p^2 g_p^2 \left(M_{P,D}^D\right)^{D-2}\,. \tag{4.14}$$

Moreover, it is possible to extend Conjecture 4.7 in the case of multiple axions, defining

$$z_i \equiv \sum_j \frac{M_{P,4}}{f_{ij} S_i} e_i\,, \tag{4.15}$$

where e_i are some orthonormal set of basis vectors [78] and requiring their convex hull to include the unit ball. Also Conjecture 4.9 gets modified when we consider axionic couplings. In the presence of a canonically normalized scalar field ϕ, the Axion WGC becomes

$$f^2 S^2 + f^2 \left(\partial_\phi S\right)^2 M_{P,4}^2 \leq M_{P,4}^2\,. \tag{4.16}$$

Discrete symmetries and swampland

Discrete Symmetries in Dimer Diagrams

5

We apply dimer diagram techniques to uncover discrete global symmetries in the fields theories on D3-branes at singularities given by general orbifolds of general toric CY 3-fold singularities. The discrete symmetries are discrete Heisenberg groups, with two $\mathbb{Z}_N$ generators A, B with commutation $AB = CBA$, with C a central element. This fully generalizes earlier observations in particular orbifolds of $\mathbb{C}^3$, the conifold and $Y_{p,q}$. The solution for any orbifold of a given parent theory follows from a universal structure in the infinite dimer in $\mathbb{R}^2$ giving the covering space of the unit cell of the parent theory before orbifolding. The generator A is realized as a shift in the dimer diagram, associated to the orbifold quantum symmetry; the action of B is determined by equations describing a 1-form in the dimer graph in the unit cell of the parent theory with twisted boundary conditions; finally, C is an element of the (mesonic and baryonic) non-anomalous U(1) symmetries, determined by geometric identities involving the elements of the dimer graph of the parent theory. These discrete global symmetries of the quiver gauge theories are holographically dual to discrete gauge symmetries from torsion cycles in the horizon, as we also briefly discuss. Our findings allow to easily construct the discrete symmetries for infinite classes of orbifolds. We provide explicit examples by constructing the discrete symmetries for the infinite classes of general orbifolds of $\mathbb{C}^3$, conifold, and complex cones over the toric del Pezzo surfaces, dP_1, dP_2 and dP_3.
The chapter is organized as follows. In Section 5.2 we describe the general structure of the discrete Heisenberg groups, and in Section 5.2.1 we uncover their origin from an underlying structure of a 1-form defined on the infinite dimer in $\mathbb{R}^2$ of the parent theory. We exploit this understanding solving by inspection the discrete symmetries for general orbifolds of $\mathbb{C}^3$, in Section 5.2.2, and of the conifold, in Section 5.2.3. In Section 5.3 we provide a systematic procedure to construct the explicit solution for the discrete symmetries of a general orbifold of a general toric singularity, in terms of equations for 1-forms on the graph of the parent theory dimer/quiver in its unit cell (with twisted boundary conditions). Section 5.4 is devoted to the explicit construction of the discrete symmetries in infinite families of orbifolds. In Sections 5.4.1 and 5.4.2 we recover the discrete symmetries for orbifolds of $\mathbb{C}^3$ and the conifold, and in Section 5.4.3 we construct the discrete symmetries for the infinite class of general orbifolds of the dP_1 theory. Further examples are in Sections 5.4.4 and 5.4.5. Finally, Section 5.5 contains a sketch of the realization of these symmetries in the gravity dual, in terms of torsion classes in the 5d horizon geometry.

5.1 General motivations

Discrete symmetries are key to our understanding of quantum field theory and the SM, and it is an interesting question to address their realization in fundamental theories like string theory. In particular, the

general arguments about absence of global symmetries in theories of QG (see [80, 92, 93] for early viewpoints, and, e.g., [67, 94] and references therein, for more recent discussions) suggest that discrete symmetries should have a gauge nature in such theories [95–102] (see [81, 103, 104] for recent discussions in the swampland [77, 78, 105] context).

Discrete gauge symmetries have been studied in string theory from different perspectives. Abelian gauge symmetries and their application to MSSM-like models have been explored in D-brane models in [51, 106–109]. Non-Abelian discrete gauge symmetries in 4d string compactifications were systematically studied in [110]. In fact, the first appearance of non-Abelian discrete gauge symmetries in string theory arose in [29] in the gravity dual of the quiver gauge theory on D3-branes at the $\mathbb{C}^3/\mathbb{Z}_3$ singularity. This was subsequently generalized to other particular orbifolds of $\mathbb{C}^3$, the conifold and $Y_{p,q}$ in [73, 76]. The symmetries were constructed as global discrete symmetries of the quiver theory, by laboriously solving the conditions of invariance of the superpotential and cancellation of discrete gauge anomalies. The symmetries correspond to discrete Heisenberg groups, with $\mathbb{Z}_N$ generators A, B anticommuting to a central element C, namely $AB = CBA$. In the gravity dual, the discrete symmetries arise from torsion homology cycles, and the non-Abelian nature is encoded in brane creation effects among the $\mathbb{Z}_N$ charged objects [29], or alternatively in the KK reduction of CS terms for torsion forms with non-trivial relations [110].

In this chapter, we apply the powerful description of D3-branes at toric CY 3-fold singularities in terms of dimer diagrams [55–57] to unravel the underlying structure of discrete symmetries in general orbifolds of general toric singularities. We find discrete Heisenberg groups for the whole class of theories, generalizing earlier results for particular examples. We show that the discrete symmetry structure for any orbifold of a given parent theory follows from a universal structure in the infinite dimer in $\mathbb{R}^2$ giving the covering space of the unit cell of the parent theory. The general structure is as follows. The generator A is realized as a shift in the dimer diagram, associated to the orbifold quantum symmetry; the action of B is determined by equations describing a 1-form in the dimer graph in the unit cell of the parent theory with twisted boundary conditions. The element C is a discrete subgroup of the non-anomalous U(1) symmetries (mesonic and baryonic, if present), determined by a simple set of equations related to geometric identities among the elements of the dimer graph in the parent theory.

Our findings allow to easily construct the discrete symmetries for infinite classes of orbifolds. To illustrate the power of our methods, we provide explicit examples by constructing the discrete symmetries for general orbifolds of $\mathbb{C}^3$, conifold, and complex cones over the toric del Pezzo surfaces, dP_1, dP_2 and dP_3.

These discrete global symmetries of the quiver gauge theories are holographically dual to discrete gauge symmetries from torsion cycles in the horizon, as we also briefly discuss. Our techniques thus provide the largest ensemble of discrete gauge symmetries in string theory models, in this case in AdS. They thus provide a natural setup to explore the properties of discrete symmetries in AdS QG, with interesting interplay

with holography and hopefully with the swampland constraints for AdS vacua [81, 83, 103, 111].

5.2 Structure of the Discrete Heisenberg group

It is possible to rederive the generators of the Heisenberg group that we have introduced in Section 3.3 in terms of dimer diagrams.[41] In the construction of Section 2.3.2, there is a manifest global discrete symmetry, with the generator A acting as $r \to r+1$ on the labels of the N copies of the fields of the parent theory, namely

$$\begin{aligned} A: F_{a,r} &\to F_{a,r+1} \quad \Rightarrow \quad \mathrm{SU}(n_{a,r}) \to \mathrm{SU}(n_{a,r+1}) \\ E_{i,r} &\to E_{i,r+1} \quad \Rightarrow \quad \Phi_{E_{i,r}} \to \Phi_{E_{i,r+1}} \\ V_{\alpha,r} &\to V_{\alpha,r+1} \quad (\text{similar for } V'_{\alpha,r})\,. \end{aligned} \tag{5.1}$$

41: Dimer diagrams have been introduced in Chapter 2.

This is just a $\mathbb{Z}_N$ rotation of the theory, which, as we have said in Section 3.3, in the context of orbifolds of $\mathbb{C}^3$ is often referred to as quantum symmetry (as it is a symmetry of the quantum worldsheet theory, in the sense of the α' expansion).

Using the notation introduced in Section 2.3.2, this transformation corresponds to a shift of the unit cell of the parent theory $\mathscr{C}$ in the $\mathscr{C}_N$, which in fact is most easily discussed in the infinite periodic array in $\mathbb{R}^2$. The shifts of $\mathscr{C}$ to the adjacent unit cells in the two independent directions correspond to the operations A^{k_1} and A^{k_2}, respectively. Since $\mathrm{GCD}(k_1, k_2) = 1$, by Bezout's theorem there exist integers r_1, r_2 such that $r_1 k_2 + r_2 k_2 = 1$, hence A corresponds to the shift of the unit cell $\mathscr{C}$ to its copy in the position (r_1, r_2). The B and C generators act on the fields as we shown in the examples in Section 3.3, only this time we are going to use dimers to uncover the discrete global symmetry.[42] We are looking for this structure on general orbifolds of general toric geometries. As explained above, the symmetry A corresponds to the shift $r \to r+1$, which implements an order N cyclic permutation among the gauge factors, acting correspondingly on the bifundamentals and superpotential terms. In addition, we look for an action B under which the different bifundamental fields $E_{i,r}$ will transform with charges $b_{E_{i,r}}$, which in general depend on r. The actions A and B should anticommute to an action C, under which the bifundamentals $E_{i,r}$ transform with charges c_{E_i}, which, in order for C to be central (and in particular commute with A), must be independent of r.

42: See, for instance, Figure 5.1 for the corresponding dimer diagram of the quiver in Figure 3.1.

The procedure to construct the solution for these charges in general orbifolds of general toric theories is explained in Section 5.3. Before entering this discussion, it is useful to introduce an important viewpoint.

5.2.1 Discrete symmetries from the covering space

Consider a given parent geometry, and the quotients defined by a $\mathbb{Z}_N$ group with generator θ defined by an action (2.23) associated to the two integers (p_1, p_2). As discussed, there is a $\Gamma = \mathbb{Z}_N$ quantum symmetry whose generator we denote by A_N, to emphasize its order. We also have

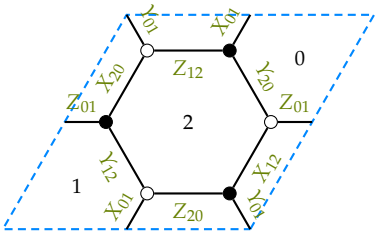

Figure 5.1: Dimer diagram for the orbifold $\mathbb{C}^3/\mathbb{Z}_3$.

a $\mathbb{Z}_N$ generated by B_N, under which bifundamentals have charges $b_{E_i,r}$ defined modulo N.

In this section, we are going to uncover the existence of the most important structure for the B symmetry for the family of orbifolds of a given parent theory, for fixed (k_1, k_2), but different orders N.

The first observation is that it is useful to regard the charge assignments for the B_N symmetry in the infinite periodic array in $\mathbb{R}^2$, with periodicities (for fixed k_1, k_2) depending on N. This is motivated by the following argument. We regard the set of B_N charges $b_{E_{i,r}}$ as defined for arbitrary $r \in \mathbb{Z}$, hence on the infinite periodic dimer/quiver, but satisfying the periodicity $b_{E_{i,r}} = b_{E_{i,r+N}} \mod N$. We also have to impose the condition that B_N leaves the superpotential invariant, and that it has no mixed anomaly with the gauge factors. These can be written

$$\begin{aligned} \sum_{\partial V_{\alpha,r}} b_{E_{i,r}} &= 0\,, \\ \sum_{\tilde{\partial} F_{a,r}} b_{E_{i,r}} &= 0\,. \end{aligned} \tag{5.2}$$

Here the equations have to be satisfied modulo N. However, we now show that they actually must be satisfied as equations for integers, without resorting to the mod N condition, as follows.

It is a familiar fact that quotienting the orbifold theory by the quantum symmetry Γ, one recovers the parent theory back. Similarly, if we consider some non-prime order $N = pN'$ with $p, N' \in \mathbb{Z}$, and consider the element $(A_N)^{N'}$, it generates a $\mathbb{Z}_p$ subgroup $\Gamma' \subset \Gamma$. Quotienting the theory by Γ' should result in a theory which is a $\mathbb{Z}_{N'}$ quotient of the parent, with the same pair (k_1, k_2). This merely corresponds to considering the unit cell $\mathcal{C}_N$ of the $\mathbb{Z}_N$ orbifold, and imposing the identification $r \to r + p$ on all elements to achieve a unit cell $\mathcal{C}_{N'}$ for the $\mathbb{Z}_{N'}$ orbifold theory. Going back to the infinite periodic version, we have an initial set of charges $b_{E_{i,r}}$ (defined mod N) and we are changing from a periodicity set by N to a periodicity set by N'. The requirement that the initial charges are compatible with the symmetry $B_{N'}$ of the discrete Heisenberg group of the $\mathbb{Z}_{N'}$ theory implies that $b_{E_{i,r}} = b_{E_{i,r+p}}$ mod N'. Transferring this to the set of constraints (5.2), and we find that they must be obeyed **modulo** N'. Considering N's large enough, or rather, with large enough number of divisors, it is easy to convince oneself that the equations (5.2) have to be obeyed in $\mathbb{Z}$, without use of the mod N conditions.

In other words, the family of $\mathbb{Z}_N$ theories, for fixed (k_1, k_2) and varying N, has B charges inherited from a universal assignment of integer charges $b_{E_{i,r}} \in \mathbb{Z}$, in the infinite periodic quiver/dimer i.e. $r \in \mathbb{Z}$. The charges for the theory of a given N are obtained by restricting the integer charges modulo N. The fact that this is compatible with the periodicities $b_{E_{i,r}} = b_{E_{i,r+N}}$ mod N, for any N, implies that (5.2) have to be obeyed directly, not modulo N.

In the following, we ignore the subindex N in the discrete symmetry generators like B, C, and mostly work in whole families of $\mathbb{Z}_N$ orbifolds, for fixed (k_1, k_2), but varying N. As anticipated, this is most efficiently done by working on the infinite periodic array, with B charges realized as integer charges therein.

The fact that the constraints (5.2) are defined without using the modulo N condition has an interesting implication. In the language of Section 2.3, the set of charges can be regarded as defining a 1-form γ, namely $\gamma(E_{i,r}) = b_{E_{i,r}}$. Then the invariance of the superpotential requires the 1-form to be closed

$$d\gamma = 0\,. \tag{5.3}$$

As explained above, solutions in the dimer 2-torus correspond to continuous U(1) mesonic (for non-exact $\gamma \neq df$) or baryonic (for exact $\gamma = df$) symmetries. This, together with the above considerations, suggests to look for symmetries defined by 1-forms γ defined on the covering infinite periodic array. In $\mathbb{R}^2$, any closed form must be exact $\gamma = df$; hence, we introduce a 0-form f on the infinite periodic array. More concretely, using a label r for the infinite set of faces/nodes, we assign an integer $n_a \equiv f(F_r)$ to each face of the (infinite) dimer (resp. node of the infinite quiver). This amounts to choosing a formal infinite linear combination of the $\mathrm{U}(1)_{a,r}$ generators $Q_{a,r}$

$$Q_B = \sum_{a,r} n_{a,r} Q_{a,r}\,. \tag{5.4}$$

So that a bifundamental associated to an edge E separating faces F_r and F_s (resp. an arrow from node $F_{a,r}$ to node $F_{b,s}$) has an associated B charge

$$b_E = \gamma(E) = n_{a,r} - n_{b,s}, \text{ for } t(E) = F_{a,r}\,,\ h(E) = F_{b,s}\,. \tag{5.5}$$

The values of n_r are further constrained by the cancellation of anomalies. In the following, we use the description in terms of the linear combination Q_B to construct the discrete symmetries in several infinite classes of models, by solving the anomaly cancellation conditions by inspection. A systematic procedure to solve general orbifolds of general geometries is given in Section 5.3.

5.2.2 The infinite class of general orbifolds of $\mathbb{C}^3$

Consider the infinite class of general orbifolds of $\mathbb{C}^3$,defined by a generator θ acting as

$$x \to e^{2\pi i k_1/N} x\,,\ y \to e^{2\pi i k_2/N} y\,,\ z \to e^{2\pi i k_3/N} z\,, \tag{5.6}$$

with $k_1 + k_2 + k_3 = 0$, so we take the twist vector $(k_1, k_2, -k_1 - k_2)/N$. The notation k_1, k_2 is chosen with hindsight to agree with their meaning in Section 2.3.2.

The parent theory of D3-branes in flat space $\mathbb{C}^3$ has three adjoints, X, Y, Z. They are the basic mesons parameterizing $\mathbb{C}^3$, so the orbifold action on them is inherited from (5.6). They carry charges $(1,0)$, $(0,1)$ and $(-1,-1)$ under the mesonic $\mathrm{U}(1)^2$, so this action corresponds to the Q_θ combination (2.23) with $p_1 = k_1$, $p_2 = k_2$.

In the orbifold, the gauge group is a product of unitary factors $\mathrm{U}(n)_r$, with $r = 0, \ldots, N-1$, and there are bifundamental fields

$$X_{r,r+k_1}\,,\ Y_{r,r+k_2}\,,\ Z_{r,r+k_3}\,, \tag{5.7}$$

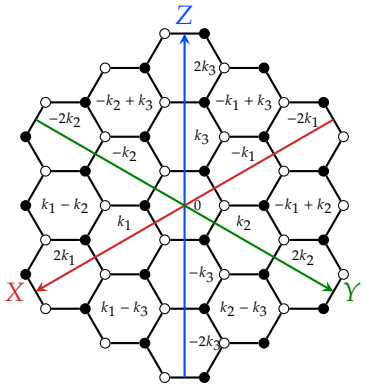

Figure 5.2: Dimer diagram for a general $\mathbb{C}^3/\mathbb{Z}_N$ orbifold.

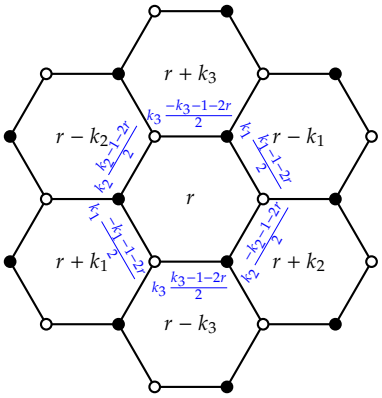

Figure 5.3: General face and B-charges (in blue) for bifundamentals for a general $\mathbb{C}^3/\mathbb{Z}_N$ orbifold.

where the subindices denote the bifundamental representation, i.e. Φ_{rs} transforms in the $\left(\square_r, \overline{\square}_s\right)$. All information, including the cubic superpotential, is encoded in a honeycomb dimer, where now the unit cell contains N different faces, labeled by $r = 0, \ldots, N-1$, and where the index of the faces changes by k_1 and k_2 between neighboring faces, in the two independent directions (and hence, by $-k_1 - k_2$ in the third, not linearly independent, direction). As explained, we prefer to consider the general class of orbifolds for arbitrary N, by considering the infinite periodic array in $\mathbb{R}^2$, as shown in Figure 5.2.

As explained above, the generator A of the Heisenberg group is realized as the action $r \longrightarrow r+1$. On the other hand, the generator B can be obtained from the combination (5.4), dropping the index a since there is only one face in the parent theory. The anomaly cancellation condition for the coefficients n_r thus reads

$$n_{r+k_1} - n_{r-k_1} + n_{r+k_2} - n_{r-k_2} + n_{r+k_3} - n_{r-k_3} = 0\,. \tag{5.8}$$

It is not difficult to use known examples to try and infer a viable solution to the anomaly conditions, given by

$$n_r = \frac{r(r+1)}{2}\,. \tag{5.9}$$

This will be rederived in Section 5.4.1 from a general procedure, but for the moment we take it at face value. Using the charges for bifundamentals (5.5), see Figure 5.3, it is straightforward to check that the anomalies for an arbitrary face cancel.

We can now extract the charges under the C symmetry. From the commutation relation $AB = CBA$ and the fact that C is central, we have $AB^{k_1} = C^{k_1}B^{k_1}A$, which implies that the charges of the different bifundamentals under the C symmetry can be obtained from the difference of charges of two copies of the bifundamental related by $r \longrightarrow r+k_1$. The result is that for bifundamentals of X, Y or Z kind, the C-charge is given by

$$Q_C(E) = k_i \text{ with } i = 1,2,3 \text{ for bifundamentals of } X\,,\ Y\,,\ Z \text{ kind.} \tag{5.10}$$

It is straightforward to check that the anomalies cancel, and that periodicities are satisfied. This follows directly from the fact that the C-charges must be equal for all copies of a given bifundamental. This means that the C-charge can be defined on the dimer of the 2-torus **of the parent theory**. In other words, it is part of the mesonic $\mathrm{U}(1)^2$ symmetry of the $\mathbb{C}^3$ theory (note that there are no baryonic U(1)'s in this case), as is moreover clear from the above explicit charges.

Given this universal solution, we can now find the discrete symmetry for any $\mathbb{Z}_N$ orbifold by interpreting the labels $r \mod N$, and thus recovering the unit cell $\mathscr{C}_N$ of the orbifold theory as dictated by the corresponding identifications of faces in the infinite dimer. It is easy to check that the set of B charges for the bifundamentals respects the corresponding periodicities as follows. Consider moving in the direction of $r \longrightarrow r+k_1$, until we hit r again (mod N). If we denote $\mathrm{GCD}(k_1, N) = p$, this will happen after N/p steps, so we have an identification $r \sim r + k_1 N/p$. The charges of all the bifundamentals charged under $\mathrm{U}(1)_r$ shifts by

an amount $k_i k_1 N/p$ (with $i = 1,2,3$ for fields of the X, Y or Z kind, respectively), which is $0 \mod N$ in all cases. Clearly, a similar result is obtained for the identifications in the directions $r \to r+k_2$ or $t \to r+k_3$.

Hence, we have explicitly constructed the discrete Heisenberg groups H_N for all orbifolds $\mathbb{C}^3/\mathbb{Z}_N$ with twist vector $(k_1, k_2, -k_1 - k_2)/N$. We invite the reader to check that this general solution reproduces all known examples of discrete symmetries in orbifolds of $\mathbb{C}^3$, in particular those of Section 5.2.

5.2.3 The infinite class of general orbifolds of the conifold

We now consider the infinite class of general orbifolds of the conifold. As shown in Figure 2.2a, the conifold theory is described by two factors $\mathrm{SU}(M)_0 \times \mathrm{SU}(M)_1$, and bifundamentals A_1, A_2 in the $\left(\square, \overline{\square}\right)$, and B_1, B_2 in the $\left(\overline{\square}, \square\right)$. We define the orbifold by the action of its generator θ on these fields

$$\begin{aligned} \theta : A_1 &\to e^{2\pi i \frac{p_1}{N}} A_1 \,, \; A_2 \to e^{-2\pi i \frac{p_1}{N}} A_2 \\ B_1 &\to e^{2\pi i \frac{p_2}{N}} B_1 \,, \; B_2 \to e^{-2\pi i \frac{p_2}{N}} B_2 \,. \end{aligned} \tag{5.11}$$

This agrees with the notation (2.23), by noticing that the charges of A_1, A_2, B_1, B_2 under the mesonic $\mathrm{U}(1)^2$ symmetries[43] are $(1,0)$, $(-1,0)$, $(0,1)$, $(0,-1)$.

Introducing the mesons

$$x = A_1 B_1 \,, \; y = A_2 B_2 \,, \; z = A_1 B_2 \,, \; w = A_2 B_1 \,, \tag{5.12}$$

which satisfy $xy = zw$, the orbifold action is

$$\begin{aligned} \theta : x &\to e^{2\pi i \frac{p_1+p_2}{N}} x \,, \; y \to e^{2\pi i \frac{-p_1-p_2}{N}} y \,, \\ z &\to e^{2\pi i \frac{p_1-p_2}{N}} z \,, \; w \to e^{2\pi i \frac{-p_1+p_2}{N}} w \,. \end{aligned} \tag{5.13}$$

Hence, in the notation of Section 2.3.2, we have $k_1 = p_1+p_2$, $k_2 = p_1-p_2$.

The dimer of this theory is shown in Figure 5.4. Note that in this case, there are two faces F_a in the parent theory, and hence two kinds of faces $F_{a,r}$ in the quotient, $r \in \mathbb{Z}$, shown in different background colors for clarity. The label displayed in the figure corresponds to the index r of the corresponding kind of face.

The A symmetry acts by $r \to r+1$ as usual. To build the B symmetry, we consider a general linear combination (5.4). The anomaly cancellation conditions are

$$n_{a,r+p_1} + n_{a,r-p_1} - n_{a,r+p_2} - n_{a,r-p_2} = 0 \text{ for } a = 0,1 \,. \tag{5.14}$$

The condition for $a = 0$ and $a = 1$ decouple, and this makes it easy to find solutions. In particular, we can take

$$n_{0,r} = r \,, \; n_{1,r} = 0 \,. \tag{5.15}$$

43: In this case, they are part of a larger $\mathrm{SU}(2)^2$ global symmetry.

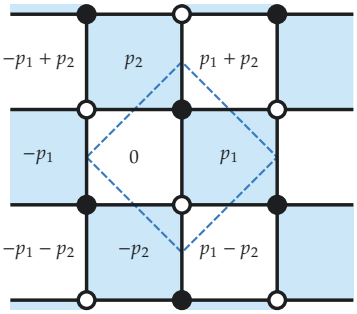

Figure 5.4: Dimer for general orbifold of the conifold. We show a unit cell of the parent theory with its two faces, and we display different background colors for their images.

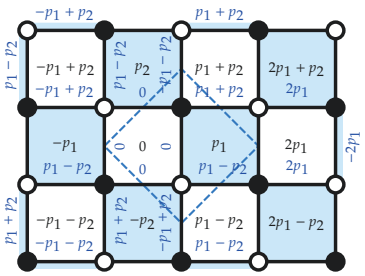

Figure 5.5: B-charges for general orbifold of the conifold. We take colored faces to have zero coefficient in the linear combination of U(1), while the coefficient for white faces is just its label. Hence, the charges of edges around a white face are just given by the face label, with a sign corresponding to the bifundamental orientation.

The charges obtained are shown in Figure 5.5, where the white faces are taken to correspond to $n_{1,r} = 0$, and the colored faces to $n_{0,r} = 0$. Hence, the charges for edges around a face correspond to the face label weighted by the orientation of the bifundamental. It is straightforward to check that the anomalies for an arbitrary face cancel.

The charge C can be read as the jumps in the B charges as one acts with the shifts corresponding to A, and read

$$Q_C(A_1) = 1\,,\ Q_C(A_2) = 1\,,\ Q_C(B_1) = -1\,,\ Q_C(B_2) = -1. \tag{5.16}$$

As is clear from these charges, the C symmetry is actually an element of the baryonic U(1) of the parent theory.

The above results will be rederived in Section 5.4.2 from a general procedure.

5.3 Discrete Symmetries in Orbifolds of Toric Geometries: General solution

In this section, we provide a systematic recipe to construct the discrete symmetries of general orbifolds of general toric theories, by formulating the problem in the framework of the unit cell $\mathscr{C}$ of the parent theory. Morally, the problem amounts to solving for the set of charges (eventually, B-charges) for the edges/arrows in $\mathscr{C}$, with a twisted boundary condition encoding the information of the orbifold action.

We start with a short recap of the main lessons from the previous section. Given a toric theory, we consider the infinite periodic array for its dimer/quiver diagram, and label the copies of the ingredients (faces/nodes, edges/arrows, vertices/plaquettes) in the basic unit cell with an index $r \in \mathbb{Z}$. Considering a unit cell $\mathscr{C}$, the orbifold is defined by two integers (k_1, k_2), which specify the jumps $r \to r + k_i$ in the labels of ingredients as one moves from $\mathscr{C}$ to the adjacent unit cells in the two independent directions. For fixed (k_1, k_2), this defines a family of orbifolds, with an extra parameter N specifying the order of the $\mathbb{Z}_N$ quotient.

For a given N, there is a discrete Heisenberg group H_N acting as a discrete symmetry of the theory. However, it is useful to consider the generators A, B, C, with $AB = CBA$, of the symmetry in general, without explicit reference to N. This is done by considering the infinite array of the dimer/quiver diagram as the natural structure on which the symmetry acts. In particular, the motion by one unit cell in the two independent directions corresponds to the application of A^{k_i}, $i = 1, 2$. Moreover, the B-charges for the edges/arrows $E_{i,r}$ are defined as integer charges $Q_B(E_{i,r}) = b_{E_{i,r}}$ for the edges/arrows in the infinite array, satisfying the conditions (5.2) of invariance of the superpotential and anomaly cancellation, exactly and not just mod N. Finally, the commutation relations of the Heisenberg group imply that the C-charges for $E_{i,r}$ are defined as r-independent integers $Q_C(E_{i,r}) = c_{E_i}$ in the infinite array, namely satisfying the periodicity of the unit cell $\mathscr{C}$ of the parent theory (hence, again independent of N). From this universal structure, the discrete symmetry generators for a particular choice of N are obtained

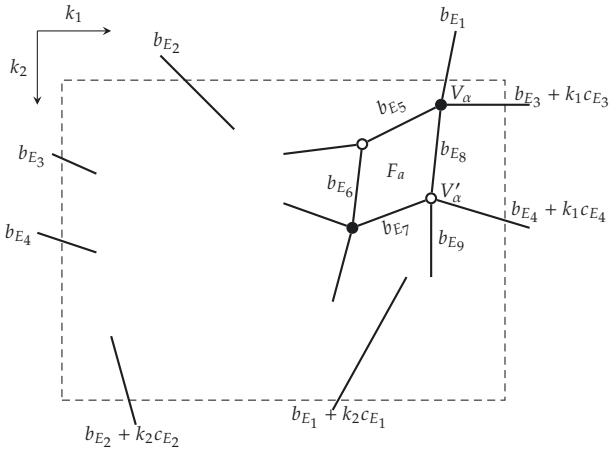
k_1
k_2
b_{E_2}
b_{E_1}
V_α
$b_{E_3} + k_1 c_{E_3}$
b_{E_5}
b_{E_3}
b_{E_8}
F_a
b_{E_6}
V'_α
$b_{E_4} + k_1 c_{E_4}$
b_{E_4}
b_{E_7}
b_{E_9}
$b_{E_2} + k_2 c_{E_2}$
$b_{E_1} + k_2 c_{E_1}$

must satisfy

$$\gamma\left(\partial V_\alpha\right) = \gamma\left(\partial V'_\alpha\right) = 0\,,\ \gamma\left(\tilde{\partial} F_a\right) = 0\,. \tag{5.19}$$

These equations are just (2.15) and (2.20). This shows that C is a discrete subgroup of the anomaly-free U(1) symmetries of the theory. This includes the $U(1)^2$ mesonic symmetries Q_1, Q_2. In addition, there are in general $N_{\mathbf{B}}$ baryonic U(1)'s which we denote by $Q_{\mathbf{B}_i}$. Incidentally, we recall that these U(1)'s arise from linear relations among the above equations, due to the geometric identities. The result is that the C charge is a combination of these symmetries,

$$Q_C = m_1 Q_1 + m_2 Q_2 + \sum_{1=1}^{N_{\mathbf{B}}} m_{\mathbf{B}_i} Q_{\mathbf{B}_i}\,. \tag{5.20}$$

So the actual number of unknowns is given by E from the B-charges and $2 + N_{\mathbf{B}}$ from the coefficients in the above combination for the C-charges.

Consider now the superpotential invariance and anomaly cancellation constraints the B-charges have to obey. These are given by (5.19) where now γ is the 1-form defined by the B-charges. Notice, however, that, since the B-charges do not satisfy the periodicities of the unit cell $\mathscr{C}$, this defines a **twisted** 1-form. In order to work with standard forms, we define the 1-form γ by $\gamma(E_i) = b_{E_i}$, so the constraints correspond to an inhomogeneous linear set of equations for the b_{E_i}, whose associated homogeneous system is precisely (5.19), and the inhomogeneous terms are combinations of the C-charges c_{E_i}. The number of equations is $F + V$, where F is the number of faces/nodes and V the number of vertices/plaquettes in $\mathscr{C}$. We may be tempted to consider that this defines a unique solution for the b's in terms of the c's, but additional care is required. Remember that the homogeneous system of equations is not linearly independent, since there are $2 + N_{\mathbf{B}}$ linear relations arising from the geometric identities. This implies that, for the inhomogeneous system to admit solutions, the inhomogeneous terms must satisfy non-trivial consistency constraints. Namely, evaluating the geometric identities with the (twisted) B-charge assignments, the dependence on the b_{E_i} disappears (because they are well-defined in $\mathscr{C}$ and hence obey the identity automatically), and we obtain certain combinations of the C-charges c_{E_i} for some edges; these combinations must be zero for the inhomogeneous system to admit solutions. This provides $2 + N_{\mathbf{B}}$ constraints on the c'_{E_i}, which are just enough to fix the $2 + N_{\mathbf{B}}$ coefficients (5.20) and thus determine the C-charges.

We may now take the inhomogeneous system of equations for the b_{E_i} and solve it in terms of the c_{E_i}. Since the number of independent equations (again, due to the geometric identities) is $F + V - 2 - N_{\mathbf{B}}$, the solutions for the b_{E_i} are unique up to $(2 + N - N_{\mathbf{B}})$ free parameters. But this is expected, since the discrete symmetry B-charges can only be defined up to the addition of an arbitrary combination of the $2 + N_{\mathbf{B}}$ continuous U(1) global symmetries.

In our procedure to solve for the B-charges we have not used the description in terms of the linear combination (5.4), which we exploited in the examples in Sections 5.2.2 and 5.2.3. Instead, the equations of invariance of the superpotential are written as part of our general linear system

and handled simultaneously with the anomaly cancellation conditions. This is because, whereas the twisting of B-charges along the periodic directions in the unit cell $\mathscr{C}$ are easy to understand, it is a priori not clear how the coefficients $n_{a,r}$ change as one moves in these periodic directions. On the other hand, given a solution for the B and C-charges, it is easy to go back to the linear combination (5.4) and disclose these transformation properties as follows.

Consider the unit cell $\mathscr{C}$ and pick a face/node $F_{a_0,0}$ in the dimer/quiver, for which we choose $n_{a_0,0} = 0$ without loss of generality. Now we may propagate to neighboring faces/nodes by crossing edges / following arrows and obtain the corresponding values of $n_{a,0}$ by adding the B charges of the edges crossed / arrows followed. A particularly interesting case is the behavior when we propagate from a face/node $F_{a,0}$ in $\mathscr{C}$ to the copy $F_{a,r_1k_1+r_2k_2}$ located in the copy of $\mathscr{C}$ located in the position (r_1, r_2) with respect to the two basic directions, in the infinite dimer/quiver diagram. To propagate from the initial to the final face/arrow, we may pick any path, since the result is path independent. For instance, we can pick edges/arrows forming a meson $M_{1,0}$ in the direction of k_1 (resp. $M_{2,0}$ in the direction of k_2) in $\mathscr{C}$, and we can follow the sequence of r_1 mesons M_{1,s_1} for $s_1 = 0, \ldots, r_1 - 1$, to reach F_{a,r_1k_1}, and then follow the sequence of r_2 mesons $M_{2,r_1k_2+s_2k_2}$ for $s_2 = 0, \ldots, r_2 - 1$to reach $F_{a,r_1k_1+r_2k_2}$. Using the B- and C-charges, we have

$$\begin{aligned} n_{a,r_1k_1+r_2k_2} - n_{a,0} &= \sum_{s_1=0}^{r_1-1} (b_{M_1} + k_1 s_1 c_{M_1}) + \\ &\quad + \sum_{s_2=0}^{r_2-1} (b_{M_2} + k_1 r_1 c_{M_2} + k_2 s_2 c_{M_2}) \\ &= r_1 b_{M_1} + r_2 b_{M_2} + r_1 r_2 k_1 c_{M_2} + \\ &\quad + \frac{r_1(r_1-1)}{2} k_1 c_{M_1} + \frac{r_2(r_2-1)}{2} k_2 c_{M_2} \,, \end{aligned} \tag{5.21}$$

where we have dropped sub-indices for charges in the unit cell $\mathscr{C}$ at $r = 0$.

Note that mesons carry no baryonic charge, hence the C-charges appearing above only have the mesonic contributions. From the above, we can easily understand different patters of growth of the n's with the r's: if the Q_C linear combination (5.20) involves the mesonic U(1)'s, the C-charges in the above equation are active, and the n's grow quadratically with the r's; if the Q_C linear combination does not contain the mesonic $U(1)'s$, then the above C-charges vanish and the n's grow linearly with the r's. This underlies the different behavior of the n_i's for $\mathbb{C}^3$ and the conifold, as we see in the examples in the next section.

5.4 Examples of Discrete Symmetries for Infinite Classes of Orbifolds

In this section, we illustrate the procedure of the previous section, by applying it to systematically construct the discrete symmetries for several infinite classes of orbifolds of different geometries.

5.4.1 General orbifolds of $\mathbb{C}^3$

We consider the general orbifolds of the $\mathbb{C}^3$ theories described in Section 5.2.2. The dimer and unit cell of the parent $\mathbb{C}^3$ are shown in Figure 5.7. There are no baryonic U(1)'s, and the mesonic charges are in Table 5.1 where the last column shows the charges under the combination $Q_C = m_1 Q_1 + m_2 Q_2$.

	Q_1	Q_2	Q_C
X	1	0	m_1
Y	0	1	m_2
Z	-1	-1	$-m_1 - m_2$

Table 5.1: Mesonic charges for parent $\mathbb{C}^3$.

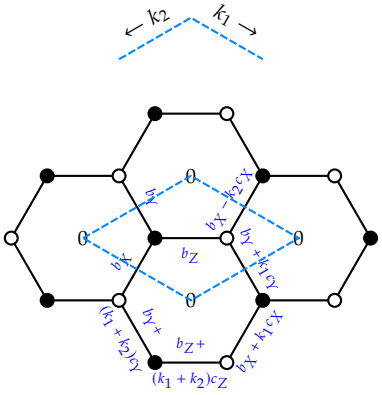

Figure 5.7: Unit cell in the dimer diagram for $\mathbb{C}^3$. We display the charge assignments corresponding to the B-charges.

There are two geometric identities in the graph. Denoting V and V' the black and white nodes and F the unique face, they are given by

$$\begin{aligned} \partial V - \partial V' &= 0 \\ \tilde{\partial} F - \partial V - \partial V' &= 0\,. \end{aligned} \tag{5.22}$$

Consider now a general orbifold, and consider the B-charge assignment in Figure 5.7. The conditions of invariance of the superpotential terms in the black and white nodes, and anomaly cancellation are

$$\begin{aligned} V &\rightarrow b_X + b_Y + b_Z = 0 \\ V' &\rightarrow b_X - k_2 c_X + b_Y + k_1 c_Y + b_Z = 0 \\ F &\rightarrow 2b_X + k_1 c_X + 2b_Y + k_1 c_Y + (k_1 + k_2) c_Y + \\ &\quad + 2b_Z + (k_1 + k_2) c_Z = 0\,. \end{aligned} \tag{5.23}$$

To extract the consistency conditions for the charges c_{E_i}, we use the geometric combinations (5.22), and obtain

$$\begin{aligned} -k_2 c_X + k_1 c_Y &= 0 \\ k_1 c_X + (2k_1 + k_2) c_Y + (k_1 + k_2) c_Z &= 0\,. \end{aligned} \tag{5.24}$$

Expressing the charges in terms of $Q_C = m_1 Q_1 + m_2 Q_2$ in the table above, the equations reduce to

$$-k_2 m_1 + k_1 m_2 = 0\,. \tag{5.25}$$

Choosing $m_1 = k_1$, $m_2 = k_2$ to yield integer C-charges, we have

$$c_X = k_1\,,\ c_Y = k_2\,,\ c_Z = -k_1 - k_2\,. \tag{5.26}$$

These C-charges ensure that Eqs. (5.24) admit a solution for the B-charges. The equations reduce to

$$b_X + b_Y + b_Z = 0\,. \tag{5.27}$$

As explained above, this determines the B-charges up to the action of mesonic $\mathrm{U}(1)^2$. One may choose the latter to set $b_X = b_Y = 0$ and then obtain $b_Z = 0$. Alternatively, we can recover the general solution in Section 5.2.2 by solving (5.27) with the values

$$\begin{aligned} b_X &= -\frac{k_2}{2} + \frac{k_2^2}{2}\,, \\ b_Y &= k_1 k_2 - \frac{k_1}{2} + \frac{k_1^2}{2}\,, \\ b_Z &= \frac{k_1 + k_2}{2} - \frac{(k_1 + k_2)^2}{2}\,. \end{aligned} \tag{5.28}$$

	Q_1	Q_2	$Q_{\mathbf{B}}$	Q_C
A_1	1	0	1	$m_1 + m_{\mathbf{B}}$
A_2	-1	0	1	$-m_1 + m_{\mathbf{B}}$
B_1	0	1	-1	$m_2 - m_{\mathbf{B}}$
B_2	0	-1	-1	$-m_2 - m_{\mathbf{B}}$

Table 5.2: Mesonic charges for parent conifold.

5.4.2 General orbifolds of the conifold

Consider the orbifolds of the conifold discussed in Section 5.2.3. The dimer diagram with a unit cell and ansatz for the B-charge assignment is shown in Figure 5.8. There are two mesonic U(1)'s and one baryonic U(1). The latter is associated to the existence of one kind of fractional brane, so it corresponds to the overall U(1) on one of the faces, say face 1. The charges of the different fields under these U(1)'s, and under a general combination $Q_C = m_1 Q_1 + m_2 Q_2 + m_{\mathbf{B}} Q_{\mathbf{B}}$, are in Table 5.2.

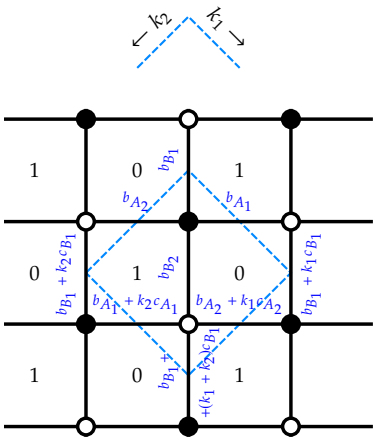

Figure 5.8: Dimer diagram with a unit cell for the conifold. We display the charge assignments corresponding to the B-charges.

The geometric identities correspond to the two generic ones, and one associated to the fractional brane. They can be written

$$\begin{aligned} &\partial V - \partial V' = 0 \\ &\tilde{\partial} F_1 + \tilde{\partial} F_2 - \partial V - \partial V' = 0 \\ &\tilde{\partial} F_1 - \partial V = 0\,. \end{aligned} \tag{5.29}$$

Using the B-charge assignments in Figure 5.8, the constraints from invariance of the superpotential terms at the two nodes, and anomaly cancellation on the two faces, are

$$\begin{aligned} \partial V &\rightarrow b_{A_1} + b_{B_1} + b_{A_2} + b_{B_2} = 0 \\ \partial V' &\rightarrow b_{A_1} + k_2 c_{A_1} + b_{B_1} + (k_1 + k_2) c_{B_1} + b_{A_2} + k_1 c_{A_2} + b_{B_2} = 0 \\ \tilde{\partial} F_1 &\rightarrow b_{A_1} + b_{B_1} + k_1 c_{B_1} + b_{A_2} + k_1 c_{A_2} + b_{B_2} = 0 \\ \tilde{\partial} F_2 &\rightarrow b_{A_1} + k_2 c_{A_1} + b_{B_1} + k_2 c_{B_1} + b_{A_2} + b_{B_2} = 0\,. \end{aligned} \tag{5.30}$$

Taking combinations of these equations as in the geometric identities, we obtain the consistency conditions for the C-charges (there are only two independent ones)

$$\begin{aligned} &k_2 c_{A_1} + (k_1 + k_2) c_{B_1} + k_1 c_{A_2} = 0 \\ &k_2 (c_{A_2} - c_{B_1}) = 0\,. \end{aligned} \tag{5.31}$$

Expressing them in terms of the generator $Q_C = m_1 Q_1 + m_2 Q_2 + m_{\mathbf{B}} Q_{\mathbf{B}}$ as in the table above, the equations imply

$$m_1 = m_2 = 0\,,\ m_{\mathbf{B}} \text{ arbitrary.} \tag{5.32}$$

Taking the minimal choice to obtain integer charges, we let $m_{\mathbf{B}} = 1$, and have

$$c_{A_1} = c_{A_2} = 1\,,\ c_{B_1} = c_{B_2} = -1\,. \tag{5.33}$$

Replacing into (5.31) leads to the unique constraint

$$b_{A_1} + b_{B_1} + b_{A_2} + b_{B_2} = 0\,. \tag{5.34}$$

These charges are as usual defined modulo the action of the two mesonic and the baryonic U(1) symmetries. The simplest solution is to use them to set $b_{A_1} = b_{A_2} = b_{B_1} = 0$ and then we get $b_{B_2} = 0$. This actually leads to the solution found in Section 5.2.3.

5.4.3 General orbifolds of the dP$_1$ theory

To illustrate the power of our method, we construct the discrete symmetries for a new infinite class of theories. They correspond to general orbifolds of the dP$_1$ theory. The dimer diagram with a unit cell and ansatz for the B-charge assignment is shown in Figure 5.9. There are two mesonic U(1)'s and one baryonic U(1). The latter is associated to the existence of one kind of fractional brane, given by $N_0 = 1$, $N_1 = 3$, $N_2 = 0$, $N_3 = 2$. The charges of the different fields under these U(1)'s, and under a general combination $Q_C = m_1 Q_1 + m_2 Q_2 + m_{\mathbf{B}} Q_{\mathbf{B}}$, are in Table 5.3.

Table 5.3: Mesonic charges for parent dP$_1$.

	Q_1	Q_2	$Q_{\mathbf{B}}$	Q_C
X_{30}	0	1	1	$m_2 + m_{\mathbf{B}}$
X_{01}	−1	0	−2	$-m_1 - 2m_{\mathbf{B}}$
X_{23}	−1	0	−2	$-m_1 - 2m_{\mathbf{B}}$
Y_{30}	1	0	1	$m_1 + m_{\mathbf{B}}$
Y_{02}	1	0	1	$m_1 + m_{\mathbf{B}}$
Y_{13}	1	0	1	$m_1 + m_{\mathbf{B}}$
Z_{30}	0	0	1	$m_{\mathbf{B}}$
Z_{01}	−1	−1	−2	$-m_1 - m_2 - 2m_{\mathbf{B}}$
Z_{23}	−1	−1	−2	$-m_1 - m_2 - 2m_{\mathbf{B}}$
Φ_{12}	1	1	3	$m_1 + m_2 + 3m_{\mathbf{B}}$

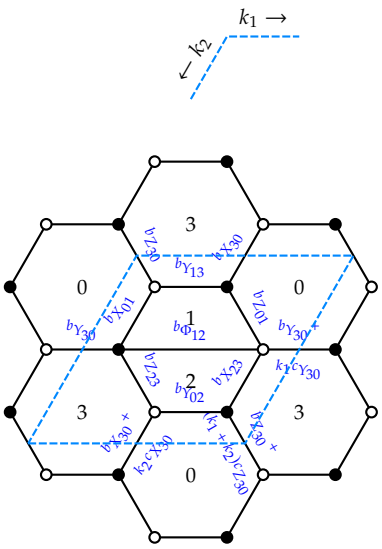

Figure 5.9: Dimer diagram with a unit cell for the dP$_1$ theory. We display the charge assignments corresponding to the B-charges.

The geometric identities correspond to the two generic ones, and one associated to the fractional brane. They read

$$\begin{aligned}
&\partial V_1 + \partial V_2 + \partial V_3 - \partial V_1' - \partial V_2' - \partial V_3' = 0 \\
&\tilde{\partial} F_0 + \tilde{\partial} F_1 + \tilde{\partial} F_2 + \tilde{\partial} F_3 - (\partial V_1 + \partial V_2 + \partial V_3) - \left(\partial V_1' + \partial V_2' + \partial V_3'\right) = 0 \\
&\tilde{\partial} F_0 + 3\tilde{\partial} F_1 + 2\tilde{\partial} F_3 - 3\partial V_1 - 2\partial V_2 - \partial V_3 - 2\partial V_1' + \partial V_3' = 0\,.
\end{aligned} \tag{5.35}$$

Using the B-charge assignments in Figure 5.9, the constraints from invariance of the superpotential terms at the three nodes, and anomaly

cancellation on the four faces, are

$$\begin{aligned}
\partial V_1 &\rightarrow b_{Z_{30}} + b_{Y_{13}} + b_{X_{01}} = 0 \\
\partial V_2 &\rightarrow k_1 c_{Y_{30}} + b_{Y_{30}} + b_{Z_{01}} + b_{X_{23}} + b_{\Phi_{12}} = 0 \\
\partial V_3 &\rightarrow k_2 c_{X_{30}} + b_{X_{30}} + b_{Y_{02}} + b_{Z_{23}} = 0 \\
\partial V_1' &\rightarrow b_{X_{30}} + b_{Y_{13}} + b_{Z_{01}} = 0 \\
\partial V_2' &\rightarrow (k_1 + k_2)\, c_{Z_{30}} + b_{Z_{30}} + b_{X_{23}} + b_{Y_{02}} = 0 \\
\partial V_3' &\rightarrow b_{Y_{30}} + b_{Z_{23}} + b_{X_{01}} + b_{\Phi_{12}} = 0 \\
\tilde{\partial} F_0 &\rightarrow b_{Y_{02}} + b_{Z_{30}} + (k_1 + k_2) c_{Z_{30}} + b_{X_{01}} + (k_1 + k_2) c_{X_{01}} + b_{Y_{30}} + \\
&\quad + (k_1 + k_2) c_{Y_{30}} + b_{Z_{01}} + k_2 c_{Z_{01}} + b_{X_{30}} + k_2 c_{X_{30}} = 0 \\
\tilde{\partial} F_1 &\rightarrow b_{Y_{13}} + b_{Z_{01}} + b_{X_{01}} + b_{\Phi_{12}} = 0 \\
\tilde{\partial} F_2 &\rightarrow b_{X_{23}} + b_{Y_{02}} + b_{Z_{23}} + b_{\Phi_{12}} = 0 \\
\tilde{\partial} F_3 &\rightarrow b_{X_{23}} + b_{Y_{30}} + k_1 c_{Y_{30}} + b_{Z_{23}} + k_1 c_{Z_{23}} + b_{X_{30}} + (k_1 + k_2) c_{X_{30}} + \\
&\quad + b_{Y_{13}} + (k_1 + k_2) c_{Y_{13}} + b_{Z_{30}} + (k_1 + k_2) c_{Z_{30}} = 0 \,.
\end{aligned} \tag{5.36}$$

The consistency conditions for the C-charges are

$$\begin{aligned}
& k_2 c_{X_{30}} + k_1 c_{Y_{30}} - (k_1 + k_2)\, c_{Z_{30}} = 0 \\
& (k_1 + k_2)\, c_{X_{01}} + (k_1 + k_2)\, c_{X_{30}} + k_2 c_{Y_{30}} + (k_1 + k_2)\, c_{Y_{13}} + k_1 c_{Z_{23}} + \\
& + k_2 c_{Z_{01}} + (k_1 + k_2)\, c_{Z_{30}} = 0 \\
& (k_1 + k_2)\, c_{X_{30}} + (k_1 + k_2)\, c_{Y_{13}} + k_1 c_{Z_{23}} + 2k_1 c_{Z_{30}} + 2k_2 c_{Z_{30}} = 0 \,.
\end{aligned} \tag{5.37}$$

Using the C-charges as in the table above, the system reduces to

$$\begin{aligned}
& k_1 m_1 + k_2 m_2 = 0 \\
& 2k_1 + m_{\mathbf{B}} + k_2 (m_1 + m_2 + 4 m_{\mathbf{B}}) = 0 \,.
\end{aligned} \tag{5.38}$$

To obtain integer C-charges, we choose

$$\begin{aligned}
m_{\mathbf{B}} &= k_2 (k_1 - k_2) \,, \\
m_1 &= 2k_2 (k_1 + 2k_2) \,, \\
m_2 &= -2k_1 (k_1 + 2k_2) \,.
\end{aligned} \tag{5.39}$$

And obtain

$$\begin{aligned}
c_{X_{30}} &= -(k_1 + k_2)(2k_1 + k_2) & c_{Y_{13}} &= 3k_2 (k_1 + k_2) \\
c_{X_{01}} &= -2k_2 (2k_1 + k_2) & c_{Z_{30}} &= k_2 (k_1 - k_2) \\
c_{X_{23}} &= -2k_2 (2k_1 - k_2) & c_{Z_{01}} &= 2\left(k_1^2 - k_2^2\right) \\
c_{Y_{30}} &= 3k_2 (2k_1 + k_2) & c_{Z_{23}} &= 2\left(k_1^2 - k_2^2\right) \\
c_{Y_{02}} &= 3k_2 (k_1 + k_2) & c_{\Phi_{12}} &= -(k_1 - k_2)(2k_1 + k_2) \,.
\end{aligned} \tag{5.40}$$

The solutions for the B-charges are

$$\begin{aligned}
b_{X_{01}} &= -b_{Z_{30}} - b_{Y_{30}} + k_2\left(k_1^2 - k_2^2\right)\\
b_{X_{23}} &= -b_{Z_{30}} - b_{Y_{30}} - 3k_1k_2(k_1+k_2)\\
b_{Y_{02}} &= +b_{Y_{30}} + k_2(k_1+k_2)(2k_1+k_2)\\
b_{Y_{13}} &= +b_{Y_{30}} + k_2\left(k_1^2 - k_2^2\right)\\
b_{Z_{01}} &= -b_{X_{30}} - b_{Y_{30}} - k_2\left(k_1^2 - k_2^2\right)\\
b_{Z_{23}} &= -b_{X_{30}} - b_{Y_{30}}\\
b_{\Phi_{12}} &= +b_{X_{30}} + b_{Y_{30}} + b_{Z_{30}} + k_2\left(k_1^2 - k_2^2\right)\ .
\end{aligned} \tag{5.41}$$

where $b_{X_{30}}, b_{Y_{30}}, b_{Z_{30}}$ are left as undetermined parameters encoding the freedom to shift charges by the global $\mathrm{U}(1)^3$ symmetry.

5.4.4 General orbifolds of the dP_2 theory

We now construct the discrete symmetries for the general orbifolds of the dP_2 theory. The dimer diagram with a unit cell and the B-charge assignment is shown in Figure 5.10. There are two mesonic and baryonic U(1)'s. The charges of the different fields under these U(1)'s, and under a general combination $Q_C = m_1Q_1 + m_2Q_2 + m_{\mathbf{B}_1}Q_{\mathbf{B}_1} + m_{\mathbf{B}_2}Q_{\mathbf{B}_2}$, are in Table 5.4.

Table 5.4: Mesonic charges for parent dP_2.

	Q_1	Q_2	$Q_{\mathbf{B}_1}$	$Q_{\mathbf{B}_2}$	Q_C
X_{10}	0	$-\frac{1}{2}$	3	-1	$-\frac{1}{2}m_2 + 3m_{\mathbf{B}_1} - m_{\mathbf{B}_2}$
X_{21}	0	0	-4	0	$-4m_{\mathbf{B}_1}$
X_{32}	$-\frac{1}{2}$	0	3	1	$-\frac{1}{2}m_1 + 3m_{\mathbf{B}_1} + m_{\mathbf{B}_2}$
X^1_{43}	0	$-\frac{1}{2}$	-1	-1	$-\frac{1}{2}m_2 - m_{\mathbf{B}_1} - m_{\mathbf{B}_2}$
X^2_{43}	0	$\frac{1}{2}$	-1	-1	$\frac{1}{2}m_2 - m_{\mathbf{B}_1} - m_{\mathbf{B}_2}$
X^1_{04}	$-\frac{1}{2}$	0	-1	1	$-\frac{1}{2}m_1 - m_{\mathbf{B}_1} + m_{\mathbf{B}_2}$
X^2_{04}	$\frac{1}{2}$	0	-1	1	$\frac{1}{2}m_1 - m_{\mathbf{B}_1} + m_{\mathbf{B}_2}$
X_{20}	0	$\frac{1}{2}$	-1	-1	$\frac{1}{2}m_2 - m_{\mathbf{B}_1} - m_{\mathbf{B}_2}$
X_{31}	$\frac{1}{2}$	0	-1	1	$\frac{1}{2}m_1 - m_{\mathbf{B}_1} + m_{\mathbf{B}_2}$
X_{14}	$-\frac{1}{2}$	$\frac{1}{2}$	2	0	$-\frac{1}{2}m_1 + \frac{1}{2}m_2 + 2m_{\mathbf{B}_1}$
X_{42}	$\frac{1}{2}$	$-\frac{1}{2}$	2	0	$\frac{1}{2}m_1 - \frac{1}{2}m_2 + 2m_{\mathbf{B}_1}$

On dP_2 there are two kinds of fractional branes given by:

1. $N_0 = 0, N_1 = 2, , N_2 = 0, N_3 = 1, N_4 = 1$;
2. $N_0 = 1, N_1 = 0, N_2 = 0, N_3 = 1, N_4 = 0$.

The geometric identities correspond to the two generic ones, and two

associated to fractional branes. They read

$$\begin{aligned}
&\partial V_1 + \partial V_2 + \partial V_3 - \partial V_1' - \partial V_2' - \partial V_3' = 0 \\
&\tilde{\partial} F_0 + \tilde{\partial} F_1 + \tilde{\partial} F_2 + \tilde{\partial} F_3 + \tilde{\partial} F_4 - (\partial V_1 + \partial V_2 + \partial V_3) + \\
&- \left(\partial V_1' + \partial V_2' + \partial V_3'\right) = 0 \\
&2(2\tilde{\partial} F_1 + \tilde{\partial} F_3 + \tilde{\partial} F_4) + \partial V_1 - \partial V_2 - \partial V_3 - 5\partial V_1' - \partial V_2' - 3\partial V_3' = 0 \\
&\tilde{\partial} F_0 + \tilde{\partial} F_3 + \partial V_2 - \partial V_1' - \partial V_2' - \partial V_3' = 0\,.
\end{aligned} \tag{5.42}$$

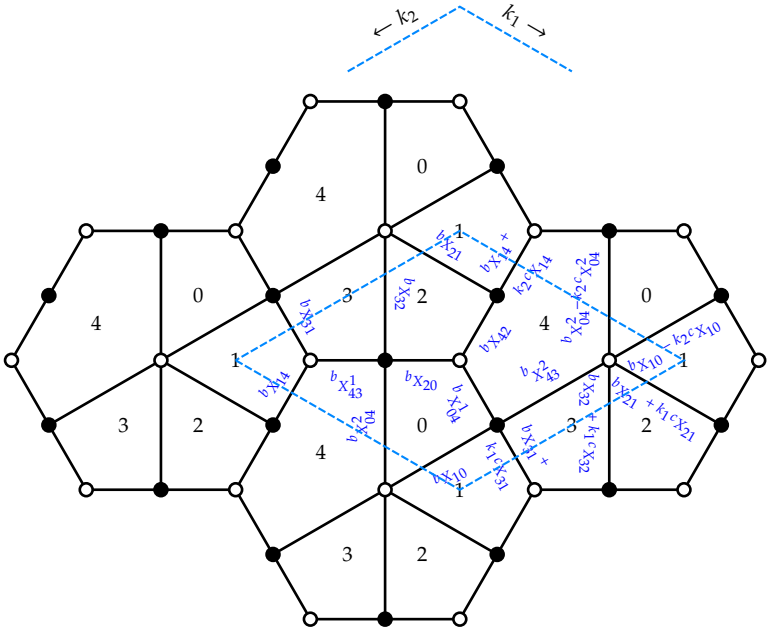

Figure 5.10: Dimer diagram with a unit cell for the dP_2 theory. We display the charge assignments corresponding to the B-charges.

Using the B-charge assignments in Figure 5.10, the constraints from invariance of the superpotential terms at the six nodes, and anomaly cancellation on the five faces, are

$$\begin{aligned}
\partial V_1 \;&\rightarrow\; b_{X_{32}} + b_{X_{43}^1} + b_{X_{04}^2} + b_{X_{20}} = 0 \\
\partial V_2 \;&\rightarrow\; -k_2 c_{X_{14}} + b_{X_{14}} + b_{X_{21}} + b_{X_{42}} = 0 \\
\partial V_3 \;&\rightarrow\; k_1 c_{X_{31}} + b_{X_{31}} + b_{X_{43}^2} + b_{X_{10}} + b_{X_{04}^1} = 0 \\
\partial V_1' \;&\rightarrow\; b_{X_{31}} + b_{X_{14}} + b_{X_{43}^1} = 0 \\
\partial V_2' \;&\rightarrow\; b_{X_{20}} + b_{X_{42}} + b_{X_{04}^1} = 0 \\
\partial V_3' \;&\rightarrow\; b_{X_{32}} + k_1 c_{X_{32}} + b_{X_{21}} + k_1 c_{X_{21}} + b_{X_{10}} - k_2 c_{X_{10}} + b_{X_{04}^2} + \\
&\quad -k_2 c_{X_{04}^2} + b_{X_{43}^2} = 0 \\
\tilde{\partial} F_0 \;&\rightarrow\; b_{X_{10}} + b_{X_{04}^2} + b_{X_{20}} + b_{X_{04}^1} = 0 \\
\tilde{\partial} F_1 \;&\rightarrow\; k_1 c_{X_{31}} + b_{X_{31}} + k_1 c_{X_{14}} + b_{X_{14}} + (k_1 + k_2)\, c_{X_{21}} + b_{X_{21}} + \\
&\quad + b_{X_{10}} = 0 \\
\tilde{\partial} F_2 \;&\rightarrow\; b_{X_{32}} + b_{X_{21}} + b_{X_{20}} + b_{X_{42}} = 0 \\
\tilde{\partial} F_3 \;&\rightarrow\; k_1 c_{X_{31}} + b_{X_{31}} + k_1 c_{X_{32}} + b_{X_{32}} + k_1 c_{X_{43}^1} + b_{X_{43}^1} + b_{X_{43}^2} = 0 \\
\tilde{\partial} F_4 \;&\rightarrow\; -k_2 c_{X_{14}} + b_{X_{14}} - k_2 c_{X_{04}^2} - k_2 c_{X_{43}^1} + b_{X_{43}^1} + b_{X_{43}^2} + b_{X_{04}^2} + \\
&\quad + b_{X_{42}} + b_{X_{04}^1} = 0\,.
\end{aligned} \tag{5.43}$$

Using the C-charges as in the table above, the system reduces to

$$\begin{aligned} & k_2\,(m_1 - m_2) + k_1 m_1 = 0 \\ & -2k_2\,(4m_{\mathbf{B}_1} - m_1 + m_2) + \frac{1}{2}k_1\,(-8m_{\mathbf{B}_1} + 4m_{\mathbf{B}_2} + 3m_1 + m_2) = 0 \\ & \frac{1}{2}k_1\,(4m_{\mathbf{B}_1} + m_1 - m_2) - k_2\,(m_2 - m_1) = 0\,. \end{aligned} \tag{5.44}$$

To obtain integer C-charges, we choose

$$\begin{aligned} m_{\mathbf{B}_1} &= \frac{k_1}{4}(k_1 + 2k_2)\,, \\ m_1 &= k_1 k_2\,, \\ m_2 &= k_1(k_1 + k_2)\,, \\ m_{\mathbf{B}_2} &= \frac{1}{4}\left(k_1^2 + 8k_1k_2 + 8k_2^2\right)\,. \end{aligned} \tag{5.45}$$

And we obtain

$$\begin{aligned} c_{X_{42}} &= 2k_2(k_1 + k_2) & c_{X^2_{54}} &= -2k_2(k_1 + k_2) \\ c_{X_{43}} &= (k_1 + 2k_2)(k_1 + k_2) & c_{X^1_{15}} &= k_2(k_1 + 2k_2) \\ c_{X_{25}} &= k_1(k_1 + k_2) & c_{X^2_{15}} &= 2k_2(k_1 + k_2) \\ c_{X_{32}} &= -k_1(k_1 + 2k_2) & c_{X_{31}} &= -2k_2(k_1 + k_2) \\ c_{X_{21}} &= -k_2(k_1 + 2k_2) & c_{X_{53}} &= k_1 k_2 \\ c_{X^1_{54}} &= -(k_1 + 2k_2)(k_1 + k_2)\,. \end{aligned} \tag{5.46}$$

The solutions for the B-charges are

$$\begin{aligned} b_{X_{21}} &= -b_{X_{42}} - b_{X_{25}} - b_{X_{32}} \\ b_{X^1_{54}} &= -b_{X_{42}} - b_{X_{25}} \\ b_{X^2_{54}} &= -b_{X_{43}} + b_{X_{25}} - 2k_1k_2(k_1 + k_2) \\ b_{X^1_{15}} &= b_{X_{43}} + b_{X_{32}} \\ b_{X^2_{15}} &= b_{X_{42}} + k_1k_2(k_1 + k_2) \\ b_{X_{31}} &= -b_{X_{43}} + b_{X_{25}} - k_1k_2(k_1 + k_2) \\ b_{X_{53}} &= -b_{X_{25}} - b_{X_{32}} + k_1k_2(k_1 + k_2)\,, \end{aligned} \tag{5.47}$$

where $b_{X_{42}}, b_{X_{43}}, b_{X_{25}}, b_{X_{32}}$ are left as undetermined parameters encoding the freedom to shift charges by the global $\mathrm{U}(1)^4$ symmetry.

5.4.5 General orbifolds of the dP_3 theory

We now construct the discrete symmetries for the general orbifolds of the dP_3 theory. The dimer diagram with a unit cell and the B-charge assignment is shown in Figure 5.11.

There are two mesonic U(1)'s and three baryonic U(1)'s. The charges of the different fields under these U(1)'s, and under a general combination $Q_C = m_1Q_1 + m_2Q_2 + m_{\mathbf{B}_1}Q_{\mathbf{B}_1} + m_{\mathbf{B}_2}Q_{\mathbf{B}_2} + m_{\mathbf{B}_3}Q_{\mathbf{B}_3}$, are in Table 5.5.

On dP_3, instead, there are three kinds of fractional branes given by:

1. $N_0 = 0\,,\ N_1 = 1\,,\ N_2 = 0\,,\ N_3 = 0\,,\ N_4 = 1\,,\ N_5 = 0$;

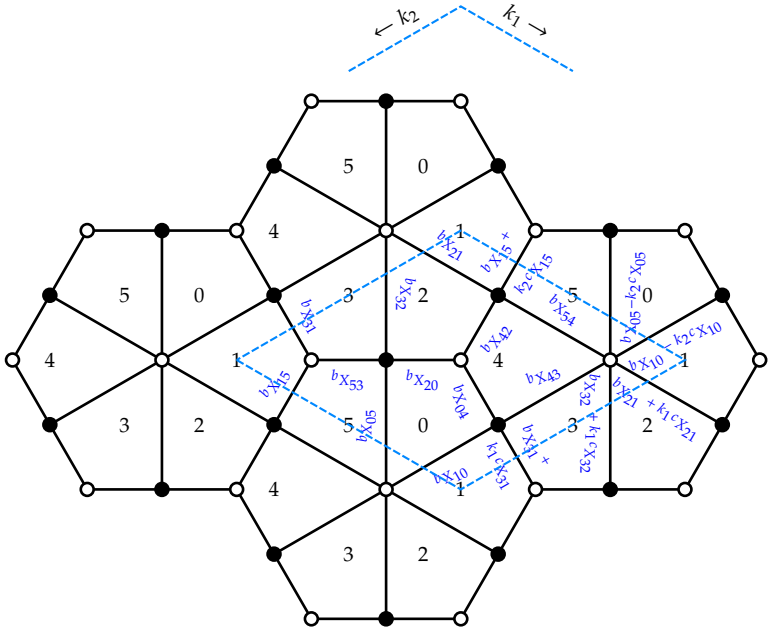

Figure 5.11: Dimer diagram with a unit cell for the dP_3 theory. We display the charge assignments corresponding to the B-charges.

Table 5.5: Mesonic charges for parent dP_3.

	Q_1	Q_2	$Q_{\mathbf{B}_1}$	$Q_{\mathbf{B}_2}$	$Q_{\mathbf{B}_3}$	Q_C
X_{10}	-1	0	1	0	-1	$-m_1 + m_{\mathbf{B}_1} - m_{\mathbf{B}_3}$
X_{54}	0	0	-1	1	-1	$-m_{\mathbf{B}_1} + m_{\mathbf{B}_2} - m_{\mathbf{B}_3}$
X_{32}	0	-1	0	-1	-1	$-m_2 - m_{\mathbf{B}_2} - m_{\mathbf{B}_3}$
X_{43}	-1	1	1	0	1	$-m_1 + m_2 + m_3 + m_{\mathbf{B}_3}$
X_{21}	1	0	-1	1	1	$m_1 - m_{\mathbf{B}_1} + m_{\mathbf{B}_2} + m_{\mathbf{B}_3}$
X_{05}	1	0	0	-1	1	$m_1 - m_{\mathbf{B}_2} + m_{\mathbf{B}_3}$
X_{31}	1	0	-1	0	0	$m_1 - m_{\mathbf{B}_1}$
X_{04}	1	-1	-1	0	0	$m_1 - m_2 - m_{\mathbf{B}_1}$
X_{15}	-1	0	1	-1	0	$-m_1 + m_{\mathbf{B}_1} - m_{\mathbf{B}_2}$
X_{42}	0	0	1	-1	0	$m_{\mathbf{B}_1} - m_{\mathbf{B}_2}$
X_{53}	0	0	0	1	0	$m_{\mathbf{B}_2}$
X_{20}	-1	1	0	1	0	$-m_1 + m_2 + m_{\mathbf{B}_2}$

2. $N_0 = 0\,,\ N_1 = 0\,,\ N_2 = 1\,,\ N_3 = 0\,,\ N_4 = 0\,,\ N_5 = 1$;
3. $N_0 = 1\,,\ N_1 = 0\,,\ N_2 = 1\,,\ N_3 = 0\,,\ N_4 = 1\,,\ N_5 = 0$.

The geometric identities correspond to the two generic ones, and three associated to fractional branes. They read

$$\begin{aligned}
&\partial V_1 + \partial V_2 + \partial V_3 - \partial V_1' - \partial V_2' - \partial V_3' = 0\\
&\tilde{\partial} F_0 + \tilde{\partial} F_1 + \tilde{\partial} F_2 + \tilde{\partial} F_3 + \tilde{\partial} F_4 + \tilde{\partial} F_5 - (\partial V_1 + \partial V_2 + \partial V_3) +\\
&- \left(\partial V_1' + \partial V_2' + \partial V_3'\right) = 0\\
&\tilde{\partial} F_1 + \tilde{\partial} F_4 - \partial V_2 - \partial V_3 = 0\\
&\tilde{\partial} F_2 + \tilde{\partial} F_5 - \partial V_1 - \partial V_2 = 0\\
&\tilde{\partial} F_0 + \tilde{\partial} F_2 + \tilde{\partial} F_4 - 2\partial V_2' - \partial V_3' = 0\,.
\end{aligned} \tag{5.48}$$

Using the B-charge assignments in Figure 5.11, the constraints from invariance of the superpotential terms at the six nodes, and anomaly cancellation on the six faces, are

$$\begin{aligned}
\partial V_1 &\rightarrow b_{X_{32}} + b_{X_{20}} + b_{X_{05}} + b_{X_{53}} = 0 \\
\partial V_2 &\rightarrow -k_2 c_{X_{15}} + b_{X_{15}} + b_{X_{54}} + b_{X_{42}} + b_{X_{21}} = 0 \\
\partial V_3 &\rightarrow k_1 c_{X_{31}} + b_{X_{31}} + b_{X_{10}} + b_{X_{04}} + b_{X_{43}} = 0 \\
\partial V_1' &\rightarrow b_{X_{31}} + b_{X_{15}} + b_{X_{53}} = 0 \\
\partial V_2' &\rightarrow b_{X_{20}} + b_{X_{04}} + b_{X_{42}} = 0 \\
\partial V_3' &\rightarrow b_{X_{32}} + k_1 c_{X_{32}} + b_{X_{21}} + k_1 c_{X_{21}} + b_{X_{10}} - k_2 c_{X_{10}} + b_{X_{05}} + \\
&\quad -k_2 c_{X_{05}} + b_{X_{54}} + b_{X_{43}} = 0 \\
\tilde{\partial} F_0 &\rightarrow b_{X_{10}} + b_{X_{04}} + b_{X_{20}} + b_{X_{05}} = 0 \\
\tilde{\partial} F_1 &\rightarrow k_1 c_{X_{31}} + b_{X_{31}} + k_1 c_{X_{15}} + b_{X_{15}} + (k_1 + k_2)\, c_{X_{21}} + b_{X_{21}} + \\
&\quad + b_{X_{10}} = 0 \\
\tilde{\partial} F_2 &\rightarrow b_{X_{32}} + b_{X_{21}} + b_{X_{20}} + b_{X_{42}} = 0 \\
\tilde{\partial} F_3 &\rightarrow k_1 c_{X_{31}} + b_{X_{31}} + k_1 c_{X_{32}} + b_{X_{32}} + k_1 c_{X_{53}} + b_{X_{53}} + b_{X_{43}} = 0 \\
\tilde{\partial} F_4 &\rightarrow b_{X_{42}} + b_{X_{04}} + b_{X_{43}} + b_{X_{54}} = 0 \\
\tilde{\partial} F_5 &\rightarrow b_{X_{15}} - k_2 c_{X_{15}} + b_{X_{54}} + b_{X_{05}} - k_2 c_{X_{05}} + b_{X_{53}} + k_2 c_{X_{53}} = 0\,.
\end{aligned} \tag{5.49}$$

Using the C-charges as in the table above, the system reduces to

$$\begin{aligned}
& k_2 m_1 + k_1 m_2 = 0 \\
& (k_1 + k_2)\, m_{\mathbf{B}_3} = 0 \\
& k_2 \left(m_{\mathbf{B}_3} + m_1 \right) = 0 \\
& k_1 \left(m_{\mathbf{B}_1} - m_1 + m_2 \right) - k_2 \left(m_{\mathbf{B}_2} - m_{\mathbf{B}_1} \right) = 0\,.
\end{aligned} \tag{5.50}$$

To obtain integer C-charges, we choose

$$\begin{aligned}
m_{\mathbf{B}_1} &= -k_2\,, \\
m_1 &= 0\,, \\
m_2 &= 0\,, \\
m_{\mathbf{B}_2} &= -k_2 - k_1\,, \\
m_{\mathbf{B}_3} &= 0\,.
\end{aligned} \tag{5.51}$$

And we obtain

$$\begin{aligned}
c_{X_{42}} &= k_2 & c_{X_{54}} &= -k_2 \\
c_{X_{43}} &= k_1 + k_2 & c_{X_{16}} &= k_1 + k_2 \\
c_{X_{26}} &= k_1 & c_{X_{15}} &= k_2 \\
c_{X_{32}} &= -k_1 & c_{X_{53}} &= k_1 \\
c_{X_{65}} &= -k_1 & c_{X_{64}} &= -k_1 + k_2 \\
c_{X_{21}} &= -k_2 & c_{X_{31}} &= k_1 + k_2\,.
\end{aligned} \tag{5.52}$$

The solutions for the B-charges are

$$\begin{aligned}
b_{X_{21}} &= -b_{X_{42}} - b_{X_{26}} - b_{X_{32}} \\
b_{X_{54}} &= -b_{X_{43}} + b_{X_{26}} - k_1 k_2 \\
b_{X_{16}} &= b_{X_{42}} - b_{X_{65}} + k_1 k_2 \\
b_{X_{15}} &= b_{X_{43}} + b_{X_{32}} \\
b_{X_{53}} &= -b_{X_{26}} - b_{X_{32}} - b_{X_{65}} + k_1 k_2 \\
b_{X_{64}} &= -b_{X_{42}} - b_{X_{26}} \\
b_{X_{31}} &= -b_{X_{43}} + b_{X_{26}} + b_{X_{65}} - k_1 k_2 \,,
\end{aligned} \tag{5.53}$$

where $b_{X_{42}}$, $b_{X_{43}}$, $b_{X_{26}}$, $b_{X_{32}}$, $b_{X_{65}}$ are left as undetermined parameters encoding the freedom to shift charges by the global $\mathrm{U}(1)^5$ symmetry.

5.5 Some remarks on the gravity dual

In this section, we sketch some main ingredients about the realization of the discrete symmetries in the gravity dual. It was established in [29], that the discrete symmetries in the $\mathbb{C}^3/\mathbb{Z}_3$ theory are associated to torsion classes in the 5d horizon $\mathbf{S}^5/\mathbb{Z}_3$ of the orbifold theory (see also [73] for other geometries), such that objects charged under the generators of the discrete Heisenberg group correspond to branes wrapped on torsion cycles. In a general orbifold, for the 5d horizon $\mathbf{X}_5 = \mathbf{S}^5/\mathbb{Z}_N$, the generator of $H_3(\mathbf{X}_5, \mathbb{Z}) = \mathbb{Z}_N$ is a torsion 3-cycle, such that wrapped D5- and NS5-branes produce 5d codimension 2 objects, around which the theory experiences monodromies associated to the A and B generators. The non-Abelian nature of the discrete gauge symmetry followed because two torsion 3-cycles intersect over a torsion 1-cycle in $H_1(\mathbf{X}_5, \mathbb{Z}) = \mathbb{Z}_N$; hence when the wrapped NS5- and D5-branes associated to the A and B actions are crossed in 5d, one generates, by the HW effect [112],[44] a D3-brane wrapped on the torsion 1-cycle. This precisely corresponds to the element C in the discrete Heisenberg group. Alternatively, one can characterize the discrete symmetry by the representations formed by (di)baryons, which are realized in the gravity side as D3-branes wrapped in 3-cycles with non-trivial torsion 1-cycles, on which one can turn on $\mathbb{Z}_N$ valued Wilson lines; this leads to N-plets of D3-brane states, on which the discrete Heisenberg group acts faithfully.

44: We review HW constructions in Appendix C.

We expect a similar mechanism to work in general orbifold theories, and hence are led to looking for such 3-cycles in the horizon geometry of general orbifolds of general toric theories. The 3-cycles on the SE 5d horizon of CY 3-fold singularities have been extensively studied in the context of the holographic description of baryons, and it is well-established that calibrated 3-cycles are in correspondence with non-compact holomorphic 4-cycles in the CY 3-fold singularity ([30], also for instance, [113–116]). In the toric setup, the non-compact 4-cycles were described in [117] (see also [118]) in terms of pairs of punctures; namely, in the type IIA mirror geometry, the non-compact 4-cycle becomes a non-compact 3-cycle, which is described as a 1-cycle in the mirror Riemann surface, which comes in through a puncture and goes out through another puncture. In particular, consider the baryonic operator corresponding to antisymmetrizing the indices of a given bifundamental;

the corresponding 4-cycle has as mirror a 3-cycle corresponding to two punctures which are mirror to the two zig-zag paths crossing the bifundamental. This leads to a one-to-one correspondence between such baryons and holomorphic 4-cycles in the toric singularity.

The description in terms of pairs of punctures is manifest also in the original type IIB picture for the non-compact 4-cycles bounded by adjacent external legs in the web diagram; in this case the non-compact 4-cycle is defined by the equation $p_i = 0$ of vanishing of the linear sigma model coordinate corresponding to the perfect matching p_i at the corresponding external point in the toric diagram,[45] see Figure 5.12.

When one performs a $\mathbb{Z}_N$ orbifold of a parent theory, the toric diagram of the original theory is the same as the original one, but in a refined lattice, such that the original is an index-N sub-lattice of the final one. Now recall that points of the toric diagram correspond to perfect matchings of the dimer; although there is in general not a one-to-one map for general points in the toric diagrams of the parent and quotient theory, there is such one-to-one map for **external** points, as follows. Consider an external point p_i of the toric diagram of the parent theory; this corresponds to a perfect matching p_i of the dimer in the parent unit cell $\mathcal{C}$; we can now obtain a perfect matching of the dimer of the orbifold theory with unit cell $\mathcal{C}_N$ by simply replicating p_i N times in the N copies of $\mathcal{C}$ in $\mathcal{C}_N$. In brief, there is a one-to-one correspondence between external perfect matchings of the toric diagrams of the parent and quotient geometries, and similarly between external legs of the web diagrams, and hence among 4-cycles, see Figure 5.12. Hence, the topology of the 4-cycle in the orbifold is that of the parent 4-cycle, quotiented by the $\mathbb{Z}_N$ action. At the level of the horizon, the 3-cycle defined by the 4-cycle in the orbifold theory is a quotient of the 3-cycle of the 4-cycle in the parent theory modded out by the $\mathbb{Z}_N$ action. This is the origin of the torsion classes, as follows.

An easy to check important feature is that the pairing of (p, q) labels of two external legs (namely, the quantity $p_1 q_2 - q_1 p_2$ for legs of labels (p_1, q_1), (p_2, q_2)) picks up a factor of N in going from the parent to the orbifold theory. Hence, all the pairings are multiples of N in any $\mathbb{Z}_N$ orbifold of a general toric singularity. This introduces a subtlety in the relation between 4-cycles and baryonic operators, in the sense that the geometric 4-cycle is actually related to an N-plet of baryonic operators. Focusing on the simplest baryonic operators, obtained by antisymmetrizing indices on a given bifundamental, this implies that we have an N-plet of bifundamentals; they are just the N copies of the bifundamental of the parent theory in the orbifold theory. These N copies form a representation of the discrete Heisenberg groups, with the A generator acting as a shift and B- and C-charges as determined in earlier sections. The holographic duals of the baryons associated to these bifundamentals are given by D3-branes wrapped on the 3-cycle with different $\mathbb{Z}_N$-valued Wilson lines turned on.

It would be interesting to pursue the gravitational dual description of the Heisenberg group, and in particular to unveil the geometric interpretation of the B- and C-charges, and their interplay with the mesonic and baryonic U(1)'s for general orbifolds of general toric geometries. In this direction

45: For simplicity, in this section we carry out the discussion for theories with no parallel external legs.

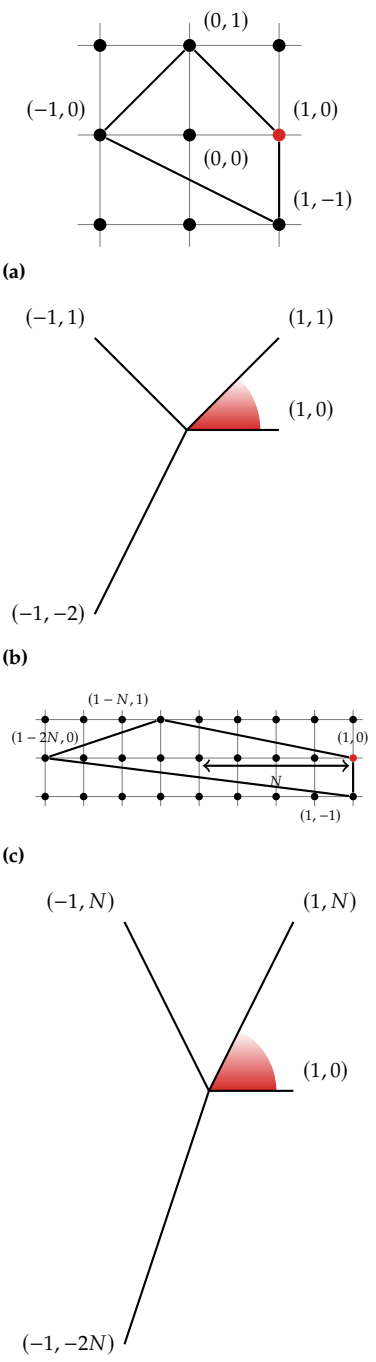

Figure 5.12: Toric and web diagrams of the dP_1 theory and its quotient. We have highlighted in red the perfect matching and wedge related to an example of non-compact 4-cycle.

is the discussion about the rôle of discrete symmetries in the swampland program described in Chapter 6.

Discrete Symmetries, Weak Coupling Conjecture and Scale Separation in AdS Vacua

6

We argue that in theories of QG with discrete gauge symmetries, e.g. $\mathbb{Z}_k$, the gauge couplings of U(1) gauge symmetries become weak in the limit of large k, as $g \to k^{-\alpha}$ with α a positive order 1 coefficient. The conjecture is based on black hole arguments combined with the Weak Gravity Conjecture (or the BPS bound in the supersymmetric setup), and the species bound. We provide explicit examples based on type IIB on $AdS_5 \times \mathbf{S}^5/\mathbb{Z}_k$ orbifolds, and M-theory on $AdS_4 \times \mathbf{S}^7/\mathbb{Z}_k$ ABJM orbifolds (and their type IIA reductions). We study AdS_4 vacua of type IIA on CY orientifold compactifications, and show that the parametric scale separation in certain infinite families is controlled by a discrete $\mathbb{Z}_k$ symmetry for domain walls. We accordingly propose a refined version of the SADC, including a parametric dependence on the order of the discrete symmetry for 3-forms.
The organization of the chapter is given in the next section.

6.1 General motivations

By now, there is a substantial number of swampland conjectures constraining effective field theories to be compatible with QG [82, 84, 105, 111, 119, 120] (see [77, 78] for reviews). They have led to interesting insights into phenomenological applications of string theory models.

Interestingly, many of these works focus on the properties of continuous gauge symmetries, whereas far fewer results have been obtained to constrain discrete symmetries (for some results, see [67, 81, 103], and also [104]), and mostly focus on the constraint that global discrete symmetries, just like global continuous symmetries, are forbidden in QG (see [95–97, 99–102] for early literature). Discrete gauge symmetries are an interesting area with exciting applications in Beyond Standard Model (BSM) phenomenology and string model building [51, 107, 108, 110, 121–123]. The scarcity of swampland constraints on them is partially explained by the fact that discrete symmetries lack long-range fields or tunable parameters like coupling constants, so there are fewer handles to quantitatively constrain their properties or their impact on other quantities of the theory.

In this work, we overcome this difficulty by considering theories with both discrete and continuous gauge symmetries, and uncover interesting quantitative links among them. For simplicity, we focus on Abelian $\mathbb{Z}_k$ and U(1) symmetries. In theories with a U(1) gauge symmetry, considerations about evaporation of charged black holes lead to the WGC [84], by demanding that the black hole should remain (sub)extremal throughout the process. To put it simply, considering an extremal black hole with $M = gQ$ (in Planck units), the theory must contain particles with mass m and charge q, with $m \leq gq$, such that the black hole can decay without becoming superextremal. This is the WGC. The marginal case in which the WGC particles saturate the inequality $m = q$ has been

further proposed to correspond to supersymmetric situations, in which it often corresponds to a BPS bound.

If the theory enjoys a further $\mathbb{Z}_k$ discrete gauge symmetry, one can consider any such classical black hole solution and endow it with discrete $\mathbb{Z}_k$ charge, with no change in the classical solution, as this charge does not source long-range fields (see e.g. [124], and also [125] for a recent perspective), and study their decay as in the WGC. In particular, we may consider extremal black holes carrying $\mathbb{Z}_k$ charge and derive a striking result, the $\mathbb{Z}_k$ WCC which schematically is the statement that in a theory with a discrete $\mathbb{Z}_k$ gauge symmetry and a U(1) gauge symmetry with coupling g, the gauge coupling scales as $g \sim k^{-\alpha}$ for large k, with α a positive order 1 coefficient.

The derivation and some qualifications to this statement are discussed in Section 6.2. In particular, we also relate this statement with diverse versions of swampland distance conjectures.

As we will see, the derivation is most precise in the supersymmetric case, in which the WGC bound saturates, but we believe it holds far more generally, as we will illustrate in concrete string theory examples. In particular, in Section 6.3 we study $AdS_5 \times \mathbf{S}^5/\mathbb{Z}_k$ vacua (and generalization to general toric[46] theories $AdS_5 \times \mathbf{X}_5/\mathbb{Z}_k$), in which there is a discrete Heisenberg group $H_k(\mathbb{Z})$, associated to torsion classes in $\mathbf{S}^5/\mathbb{Z}_k$ [1, 29, 73], as we have seen in Sections 1.1.2.1 and 3.3 and Chapter 5. This is generated by elements A, B, each generating a $\mathbb{Z}_k$ symmetry, with commutation relations $AB = CBA$, with C a central element. In the effective 5d theory (namely at scales below the KK scale, and thus at long distance compared with the AdS radius as well) there is at least one U(1) gauge symmetry, corresponding to the R-symmetry of the holographic dual SCFT, whose coupling, as we show, obeys the WCC. In addition, for $\mathbf{S}^5/\mathbb{Z}_k$, and in fact for any toric theory $\mathbf{X}_5/\mathbb{Z}_k$, there are two additional U(1)'s (the mesonic global symmetries in the dual SCFT), which also satisfy the WCC.

46: By toric, in this context we mean that the CY3 obtained as the real cone over the SE 5d variety, is toric.

In Section 6.4 we discuss an analogous exercise in 4d by considering in Section 6.4.1 the case of M-theory on $AdS_4 \times \mathbf{S}^7/\mathbb{Z}_k$, which provides the gravity dual to the ABJM theories [32]. The U(1) symmetry corresponds to an isometry of the internal space, and the discrete symmetry is also related to torsion classes in $\mathbf{S}^7/\mathbb{Z}_k$, although it has an intricate structure not reducible to just $\mathbb{Z}_k$. This is further clarified using the type IIA perspective in Section 6.4.2, in which the discrete gauge symmetry is shown to have order $k^2 + N^2$, and the U(1) symmetry is a linear combination of different RR p-form gauge symmetries, with a second linear combination that is massive due to a Stückelberg coupling. We discuss these systems and show how the corresponding WCC is duly satisfied.

In Section 6.6 we turn to exploiting these considerations in theories in which the $\mathbb{Z}_k$ charged objects are not particles (or their dual objects, e.g. strings in 4d), but rather 4d domain walls. In particular, we consider the type IIA AdS_4 vacua obtained in CY orientifold compactification with NSNS and RR fluxes. In Section 6.6.1 we review a class of compactifications with fluxes scaling with a parameter k, shown in [48] to have parametric scale separation controlled by k. These vacua would violate the SADC proposed in [83], an issue on which our analysis sheds important insights. In Section 6.6.2 we show that these systems are

higher p-form analogues of the type IIA vacua of Section 6.4.2, with a continuous 3-form symmetry arising from a massless linear combination, and the discrete symmetry arising from a second linear combination made massive by a 3-form Stückelberg mechanism (see [66, 70], also [121]), also called DKS mechanism. In Section 6.6.3 we discuss the role of the discrete $\mathbb{Z}_k$ symmetry in fixing the scaling of the moduli with k. In Section 6.6.4 we use tensions of BPS domain walls to recover the vacuum energy scalings, and show that AdS vacua with trivial 3-form discrete symmetry have no scale separation, while the above scaling family of AdS vacua with a non-trivial 3-form discrete symmetry displays scale separation controlled by k, as follows. The scale separation relation between the KK scale m_{KK} and the 4d cosmological constant Λ is given by the species bound

$$\Lambda = \frac{m_{\rm KK}^2}{k} \,. \tag{6.1}$$

We accordingly formulate the following $\mathbb{Z}_k$ RSADC: In supersymmetric AdS_4 vacua with a discrete symmetry associated to $\mathbb{Z}_k$-charged domain walls, the ratio between the KK scale and Λ is $m_{\rm KK} \sim (k\Lambda)^{1/2}$.

This provides an underlying rationale for the seemingly violation of the strong ADC by the family of scaling AdS solutions in type IIA vacua with field strength fluxes. It would be interesting to test it in other setups, and even exploit it in applications to holography.

Our work is an important step in understanding the nature of discrete gauge symmetries in QG, and their non-trivial interplay with continuous gauge symmetries. As in other swampland constraints, although the arguments for the $\mathbb{Z}_k$ WCC are admittedly heuristic, there is a substantial amount of evidence from concrete, very rigorous, string vacua supporting it. We have argued that discrete symmetries for 3-forms play an important role in the problem of scale separation, and provided a rationale to embed it in a refined AdS Distance Conjecture. We thus expect they may be relevant in other swampland criteria, like the de Sitter constraint.

6.2 The $\mathbb{Z}_k$ Weak Coupling Conjecture

In this section we consider theories of QG with discrete and continuous gauge symmetries. For simplicity, we focus on a $\mathbb{Z}_k$ discrete symmetry and a U(1) gauge symmetry. Generalizations to multiple U(1)'s and discrete groups could be worked out similarly. Notice that in this chapter we are interested in the properties of the theory at large k, hence many of our expressions should be regarded as the leading approximation in an $1/k$ expansion.

6.2.1 A black hole argument

For concreteness, we focus on 4d theories, although the results extend to other dimensions (as we will see, e.g., in the examples of Section 6.3). The strategy is to use black hole evaporation as a guiding principle to derive new swampland constraints, as we now review in two familiar situations.

6.2.1.1 Review of some mass bound derivations

Let us briefly recall one such derivation for the WGC [84]. The idea is to consider extremal black holes, with mass M and charge Q, satisfying $M = gQM_P$, where g is the U(1) gauge coupling (in units in which the minimal charge is 1). Requiring the decay of such extremal black holes, while preventing them from becoming superextremal, leads to the familiar statement of the Weak Gravity Conjecture, namely, that there must exist some particle in the theory with mass m and charge q such that

$$m \leq gqM_P. \tag{6.2}$$

There are different versions of the WGC (see [78] for a review with references), including the lattice [86] and sublattice [88] versions, but we stick to the basic one above.

Let us consider a black hole (possibly charged under the U(1) or not), carrying a discrete $\mathbb{Z}_k$ charge. The analysis now follows [126]. Even though this is a gauge symmetry, it does not have long-range fields, so it does not affect the classical black hole solution, neither its evaporation in the semiclassical approximation, which thus does not allow to eliminate the $\mathbb{Z}_k$ charge. Since we are interested in the large $k$behavior, this would lead to a too large number of remnants. Hence, when the black hole radius reaches some cutoff value Λ^{-1} it starts peeling off its $\mathbb{Z}_k$ charge. If we denote by m the mass of the $\mathbb{Z}_k$ charged particles, the mass of the black hole at the cutoff scale should suffice to emit $\mathcal{O}(k)$ of such particles, that is

$$M_P^2\Lambda^{-1} \gtrsim km\,. \tag{6.3}$$

The cutoff radius is intuitively of the order of the inverse mass of the emitted particle, hence we consider $\Lambda \sim \beta m$, with β some unknown coefficient encoding model dependent information about the black hole and its evaporation process. Consequently, we obtain

$$m^2 \lesssim \frac{M_P^2}{k}\,. \tag{6.4}$$

This is often known as the species bound [126], although in the present context, k does not correspond to the number of species, rather it relates to the order of the discrete symmetry.[47]

47: Actually, to account for the fact that the particle needs not be minimally charged under $\mathbb{Z}_k$, we should point out that the role of k above should actually be played by the number of emitted particles. Hence the factor appearing in relations like (6.4) may differ from the order of the discrete group by a factor of the particle charge, see some examples in Sections 6.4 and 6.6.

Keeping in mind the unknown factors in the discussion, we take the above relation as controlling the scaling of suitable $\mathbb{Z}_k$ charged particles in the limit of large k. Namely, there must exist some $\mathbb{Z}_k$ charged particle whose mass must scale as $m \lesssim k^{-1/2}M_P$.

In the following, we will apply this constraint to black holes charged under continuous U(1) symmetries. One may worry that the derivation in [126] did not include such charges, i.e., it implicitly assumed Schwarzschild black holes. However, there are analogous arguments for charged (in fact extremal) black holes in theories with U(1) gauge groups, leading to identical results. For concreteness, the classical solutions we are taking are the extremal Reissner-Nordström black holes in 4d space-time dimensions. They have vanishing Hawking temperature, so the analysis in [126] is not directly applicable. Extremal black holes can discharge through Schwinger radiation [127–129]. Whenever the electric field is

much larger than the background curvature, this happens essentially in flat space [130]. In this case, the production rate has an exponential suppression

$$\Gamma \sim e^{-\frac{m^2}{qE}} \sim e^{-\chi} , \tag{6.5}$$

where m and q are the mass and charge of the emitted particle and E is the electric field, given by

$$E = \frac{g^2}{4\pi}\frac{Q}{r^2} . \tag{6.6}$$

As we will argue in Section 6.2.1.2, the simplest way in which this kind of black hole is able to get rid of both continuous and discrete charges while remaining subextremal is in the presence of a $\mathbb{Z}_k$ WGC particle. Let us assume that this particle is actually BPS,

$$m = gqM_P . \tag{6.7}$$

As a consequence, the black hole will remain extremal throughout the whole evaporation process.

From (6.5) and (6.6), we notice that the maximum particle production will happen close to the horizon, so in this order of magnitude analysis we will approximate the whole radiation as the contribution of that region.

From the extremality condition, we can relate the horizon radius and the charge of the BH with its mass through

$$r_h \sim \frac{M_{BH}}{M_P^2} , \; gQ \sim \frac{M_{BH}}{M_P} . \tag{6.8}$$

They lead to

$$E \sim g\frac{M_P^3}{M_{BH}} . \tag{6.9}$$

Introducing (6.7) and (6.9) in (6.5) we can estimate the factor in the exponential suppression of the production rate of the $\mathbb{Z}_k$ WGC particle to be

$$\chi \sim \frac{mM_{BH}}{M_P^2} . \tag{6.10}$$

The black hole will be able to efficiently evaporate the discrete charge when

$$M_{BH} \lesssim \frac{M_P^2}{m} . \tag{6.11}$$

With this condition being true, the black hole should still have enough mass to radiate $\mathcal{O}(k)$ particles (assuming the $\mathbb{Z}_k$ WGC particle to have unit discrete charge), which means

$$M_{BH} \gtrsim km . \tag{6.12}$$

Finally, from the two conditions (6.11) and (6.12), we obtain the following bound for the mass of the $\mathbb{Z}_k$ WGC particle:

$$m^2 \lesssim \frac{M_P^2}{k} . \tag{6.13}$$

This is the species bound in [126]. We have shown that the bound also applies to extremal black holes emitting $\mathbb{Z}_k$ WGC particles via Schwinger effect.

6.2.1.2 The $\mathbb{Z}_k$ Weak Gravity Conjecture

In the above discussion, the mass of the $\mathbb{Z}_k$ particle we are constraining is thought of as the lightest one. However, in the following we argue that we can use a similar argument to constrain not only the lightest $\mathbb{Z}_k$ charge particle, but also the one with the smallest ratio q/m between its U(1) charge and its mass. Namely, the WGC particles.

Consider an extremal black hole with mass M and charge Q, and endow it with a large $\mathbb{Z}_k$ charge. The black hole can try to peel off its $\mathbb{Z}_k$ charge by emitting $\mathbb{Z}_k$ charged particles, but this would decrease its mass while keeping its charge fixed, thus becoming superextremal. The simplest way to prevent this is that there exists some $\mathbb{Z}_k$ charged particle which is also charged under the U(1) with charge q, and such that it satisfies the WGC bound $m \leq gqM_P$. In other words, the simplest resolution is that the WGC particles carry $\mathbb{Z}_k$ charge. We may dub this result as the $\mathbb{Z}_k$ **Weak Gravity Conjecture**.

This is a remarkable result, but is actually a little of an overstatement. It may well happen that the WGC particles are neutral and do not saturate the WGC bound, and the evaporation of the black hole by emission of WGC particles makes it sufficiently subextremal so as to be able to subsequently emit enough $\mathbb{Z}_k$ charged particles (not obeying the WGC bound) to peel off its discrete charge without ever getting superextremal. Interestingly, notice that this is only possible if the WGC particles satisfy the strict WGC bound, not the equality, and hence, according to the extended WGC version in [111], it is possible only in non-supersymmetric theories. Thus, our derivation above is strictly valid in the supersymmetric setup, and in our examples we will indeed focus on supersymmetric examples. We, however, still consider the argument as interestingly compelling also in non-supersymmetric models, and hence keep an open mind about its general validity and that of its implications, to which we turn.

6.2.1.3 The $\mathbb{Z}_k$ Weak Coupling Conjecture

The fact that the WGC particles, whose defining feature has to do with the U(1) gauge symmetry, know about the $\mathbb{Z}_k$ symmetry implies that there are cross constraints among the U(1) and the $\mathbb{Z}_k$ symmetry. Indeed, let us consider a relaxed version of the $\mathbb{Z}_k$ bound (6.4), by stating that the $\mathbb{Z}_k$ charged particles involved in the black hole decay should have mass scaling as

$$m \sim k^{-\alpha} M_P \,, \tag{6.14}$$

with α an order 1 coefficient, obeying some bound $\alpha \geq 1/2$ to satisfy (6.4). On the other hand, the particles that extremal black holes use to peel off their $\mathbb{Z}_k$ charge are WGC particles, hence obey

$$m \sim gqM_P \,. \tag{6.15}$$

We thus obtain that the gauge coupling of the U(1) must depend on k and should become weak fast enough in the large k limit, as

$$g \sim k^{-\alpha} \,. \tag{6.16}$$

We thus propose this to be a general swampland constraint, as follows:

Conjecture 6.1 [$\mathbb{Z}_k$ Weak Coupling Conjecture]**.**

In a quantum gravity theory with a discrete $\mathbb{Z}_k$ gauge symmetry and a U(1) gauge symmetry with coupling g, the gauge coupling scales as $g \sim k^{-\alpha}$ for large k, with α a positive order 1 coefficient.

We note that, in the case of multiple U(1) gauge symmetries, a similar BH argument leads to a $\mathbf{Z}_k$ Weak Coupling Conjecture for any rational direction in charge space, much in the spirit of the WGC for multiple U(1)'s [85]. Since the gauge coupling of any linear combination follows from those in some basis in the charge lattice, in this case it suffices that the couplings of these independent U(1) obey the $\mathbf{Z}_k$ Weak Coupling Conjecture. We also note that in the case of multiple discrete symmetries, the conjecture applies to each discrete symmetry independently.

The above intertwining between the properties of discrete and continuous symmetries is completely unexpected from the viewpoint of the low energy effective field theory, where these parameters are uncorrelated and would seem to be completely free choices. As with other swampland constraints, it is amusing that QG manages to impose its own plans.

A simple illustration of how this interplay works in intersecting brane modes is discussed at the heuristic level in Section 6.5. More concrete examples will follow in the upcoming sections.

6.2.2 Distance Conjectures

Before moving to concrete examples, it is interesting to explore the relation between the $\mathbb{Z}_k$ WCC and the SDC. The WCC states that gauge couplings scale to zero for large k, thus approaching a global symmetry and hence presumably leading to the appearance of a tower of states becoming light.

An intuitive picture of this implication is as follows. Consider a 4d version of the $\mathbb{Z}_k$ WCC with $g \sim k^{-\alpha}$. For simplicity, and following many examples in string theory, we consider g to belong to a complex modulus

$$S = \frac{1}{g^2} + i\theta \tag{6.17}$$

and assume a Kähler potential

$$K(S, \bar{S}) = -\log(S + \bar{S}) \,. \tag{6.18}$$

In this moduli space, the distance as a function of $s = \mathrm{Re}\, S$ as one

approaches infinity reads

$$d \sim \int \frac{ds}{s} \sim \log s \,. \tag{6.19}$$

The SDC states that there is a tower of states becoming light as $s \to \infty$ with masses

$$m_{\rm tw} \sim M_P e^{-\gamma d} \,, \tag{6.20}$$

with γ an order 1 coefficient, for d measured in Planck units. In our case we have

$$m_{\rm tw} \sim M_P k^{-1/2\alpha\gamma} \,. \tag{6.21}$$

Hence, there is a $\mathbb{Z}_k$ Distance Conjecture stating that there is a tower of states with masses becoming light as a negative power of k. This is just a rederivation of the 'species' bound cutoff [126].

The above argument where g is dealt with as a modulus going to infinite distance in moduli space does not correspond to the general $\mathbb{Z}_k$ WCC, since at least some gauge couplings may not correspond to fundamental moduli. For instance, consider the intersecting brane toy model in Section 6.5. There, the moduli remain at fixed location in moduli space, and we instead change the discrete wrapping numbers for some D-branes. Hence, the origin of the tower should be a different one, as is easily argued. In a configuration in which one stack of branes has wrappings scaling with k, the angles between that stack of branes and others will scale as $\theta \sim k^{-1}$ (to see that, consider e.g. the cycles $(1,0)$ and $(k,1)$ in a rectangular $\mathbf{T}^2$ with radii (R_1, R_2). They have intersection angle θ with $\tan\theta = k^{-1}R_2/R_1$, hence $\theta \sim k^{-1}$). As discussed in [131, 132] there is a tower of string states with masses given by

$$m_{\rm tw}^2 \sim M_s \theta \sim k^{-1} \,. \tag{6.22}$$

This again nicely reproduces the 'species' bound cutoff.

6.3 $\mathbf{AdS}_5 \times \mathbf{S}^5$ orbifolds

In this section, we consider type IIB string theory on $\mathrm{AdS}_5 \times \mathbf{S}^5/\mathbb{Z}_k$. The discussion can be easily extended to general toric orbifold theories $\mathrm{AdS}_5 \times \mathbf{X}_5/\mathbb{Z}_k$, but the 5-sphere case will suffice to illustrate the main points. We study general $\mathbb{Z}_k$ actions compatible with supersymmetry, namely acting as SU(3) in the underlying $\mathbb{C}^3$. We also note that, although these vacua do not display scale separation, we may discuss the 5d physics essentially in the same sense as in the AdS / CFT correspondence, whose dictionary and results we use freely in this section. Moreover, our final statement involves gauge couplings for U(1) symmetries, which can be observed at arbitrarily long distances, in particular at energies well below the KK scale.

As pioneered in [29] (see also [73–76] for other examples) and generalized in [1], there is a discrete gauge symmetry in the AdS_5 theory, corresponding to the discrete Heisenberg group $H_k(\mathbb{Z})$. This group has been the main focus of Chapter 5. It is defined by two non-commuting

$\mathbb{Z}_k$ symmetries generated by A, B (hence $A^k = 1$, $B^k = 1$) satisfying

$$AB = CBA\,, \tag{6.23}$$

with C a central element (also generating a further $\mathbb{Z}_k$, and possibly mixing with other anomaly free baryonic U(1)'s, if present).

Generalizing [29], the particles charged under the discrete symmetry are D3-branes wrapped on torsion 3-cycles carrying non-trivial flat gauge bundles (discrete Wilson lines and 't Hooft loops). The minimally charged particle is obtained by wrapping the D3-brane on a maximal $\mathbf{S}^3/\mathbb{Z}_k$. We are interested in the mass of this particle, and in particular in its scaling with k. It is a simple exercise, as this is just analogous to a giant graviton in the parent $AdS_5 \times \mathbf{S}^5$ theory [31].

6.3.1 The D3-brane particle mass computation

In the KK reduction from 10d to 5d, the 5d Planck mass $M_{P,5}$ in terms of the string scale is

$$M_{P,5}^3 = \frac{M_s^8 R^5}{g_s^2 k}\,. \tag{6.24}$$

We are ignoring numerical factors, e.g., in the volume of $\mathbf{S}^5$. Above, R is the curvature radius of $\mathbf{S}^5$, which is also the AdS_5 radius. Note that in order to get a theory with N units of RR 5-form flux over $\mathbf{S}^5/\mathbb{Z}_k$, the parent theory is the $AdS_5 \times \mathbf{S}^5$ solution corresponding to Nk D3-branes, and the usual relation between the radius R and N is modified to

$$R^4 = 4\pi\alpha'^2 g_s N k\,. \tag{6.25}$$

Hence

$$R \sim M_s^{-1} g_s^{1/4} N^{1/4} k^{1/4}\,, \tag{6.26}$$

where we have dropped the numerical factors.

The mass m of the D3-brane particle[48] in 5d is

$$m = \frac{M_s^4 R^3}{g_s k}\,. \tag{6.27}$$

48: Notice that for our purposes it does not matter if we are in the string or Einstein frame, since this introduces factors that depend on dynamical fields, but does not change the scaling with k, which goes into the constant part (reference value).

We wish to express the mass in terms of the 5d Planck scale. From (6.24) and (6.26) we get

$$M_s \sim M_{P,5} g_s^{1/4} N^{-5/12} k^{-1/12} \quad , \quad R \sim M_{P,5}^{-1} N^{2/3} k^{1/3}\,. \tag{6.28}$$

Hence

$$m \sim M_{P,5} N^{1/3} k^{-1/3}\,. \tag{6.29}$$

Note that the k-dependence reproduces the 5d version of the relation (6.4) [126]

$$m^3 \sim \frac{M_{P,5}^3}{k}\,. \tag{6.30}$$

This result fits nicely with the expectation for the mass of a particle charged under $\mathbb{Z}_k$.

Notice that, as mentioned in Section 6.2.1, the coefficient in (6.30) is not necessarily the order of the discrete symmetry (which we recall is the Heisenberg group $H_k(\mathbb{Z})$) but the number of particles emitted to peel off the black hole charge. We also note that the factor of N in (6.29) is presumably related to the precise nature of the cutoff Λ in the black hole argument in Section 6.2.1.1. It would be interesting to explore this dependence in more detail, but we leave this for future work.

6.3.1.1 Comparison with the BPS formula and WCC

The above states are not the lightest carrying charges under the $\mathbb{Z}_k$ subgroups of the Heisenberg group. In fact, there are charged particle states arising from fundamental strings and D1-branes wrapped on torsion 1-cycles on the internal geometry. What is special about the above D3-brane particle states is that they are BPS. Just like giant gravitons in $AdS_5 \times \mathbf{S}^5$, they carry N units of momentum along a maximal $\mathbf{S}^1$, determined by the $\mathbb{Z}_k$ action. In the 5d theory, there is a KK $U(1)_R$, which is precisely the gravity dual of the R-symmetry of the holographic SCFT. In the SCFT, the D3-brane particle states are dibaryons of the form $\det \Phi_{ij}$, with Φ denoting a generic bifundamental chiral multiplet in the quiver gauge theory. It has R-charge N, and conformal dimension $\Delta = N$. Using the AdS / CFT dictionary, we then expect the masses of these particles to be given by

$$m = \frac{N}{R} \,. \tag{6.31}$$

The fact that these states are BPS means that they should saturate the WGC conjecture bound, in other words, the BPS mass formula

$$m = \left(g M_{P,5}^{1/2}\right) N M_{P,5} \,. \tag{6.32}$$

This is the standard $m = gQ$ in Planck units, with charge $Q = N$ and g being the gauge coupling of the U(1).

In these relations, there is no manifest dependence on k, which could be puzzling from the viewpoint of the black hole arguments. As we however know, the resolution is that, on these general grounds, the gauge coupling g **must** scale with k, at large k, in particular

$$g \sim k^{-1/3} \,. \tag{6.33}$$

This is easily checked by computing the gauge coupling. In the KK reduction from 10d to 5d, the prefactor of the gauge kinetic term is

$$\frac{1}{g^2} = \frac{M_s^8 R^5}{g_s^2 k} R^2 \,. \tag{6.34}$$

The first factor is just the 10d prefactor times the volume of $\mathbf{S}^5/\mathbb{Z}_k$, and the R^2 comes from the rescaling of the mixed components of the metric into a dimensionful gauge field, such that the charges are quantized in integers.

Using our above expressions, we get

$$g \sim R^{-1} M_{P,5}^{-3/2} \,, \tag{6.35}$$

which means

$$g M_{P,5}^{1/2} = N^{-2/3} k^{-1/3} \,. \tag{6.36}$$

So, in terms of this gauge coupling, the mass (6.29) turns into (6.32). Hence, we recover a very explicit confirmation of our heuristic argument in Section 6.2.

Let us conclude with some general remarks.

- In addition to $\mathrm{U}(1)_R$ there are in general (in fact, for general toric theories) two extra mesonic U(1) symmetries, arising from isometries of the internal 5d manifold. The direct computation of their 5d gauge couplings proceeds as above, thus leading to a scaling compatible with the WCC.
- In addition to D3-brane charged particles, there are 5d membranes of real codimension 2, which implement monodromies associated to the discrete group elements. As in the Abelian case, these objects are charged under a dual discrete gauge symmetry (this can be made more manifest by introducing non-harmonic forms to represent the torsion classes [106, 110]). However, since these objects are not charged under any continuous symmetry, we lack a good handle to constrain their properties, and we will not discuss them further.

6.3.2 The $\mathbb{Z}_k$ Distance Conjectures

It is interesting to explore the relation between the $\mathbb{Z}_k$ WCC and the AdS Distance Conjecture in the present setup where, using (6.28), going to large k implies going to large R. This is a decompactification limit (note that the orbifold only reduces lengths in $\mathbf{S}^5$ in some directions, so the KK scale remains R^{-1}), in which also the AdS cosmological constant goes to zero, approaching flat space. Hence, we can apply the AdS Distance Conjecture, which, e.g. in its strong version (as we have supersymmetry) establishes that there should be a tower of states with masses scaling as

$$m_{\mathrm{tw}} \sim \frac{1}{R} \sim M_{P,5} N^{-2/3} k^{-1/3} \,, \tag{6.37}$$

where we have also kept the dependence on N. From the $1/R$ dependence, it is clear the tower corresponds to KK modes. These are the familiar particles dual to single trace chiral primary mesonic operators of the dual SCFT, extensively studied in the literature [16], see [17]. Note that, even though the scaling with k is the same as for wrapped D3-branes, KK modes are lighter due to the relative factor of N.

6.3.3 A further subtlety

The above discussion has overlooked an important subtlety. The discrete symmetry $\mathbb{Z}_k$ (in fact the full discrete Heisenberg group) is intertwined with the U(1) in the following sense. Since the D3-branes are charged under the U(1) with charge N, a set of k D3-branes carries no discrete $\mathbb{Z}_k$ charge, but carries kN units of momentum and cannot decay to the vacuum. In fact, the instanton processes removing the discrete $\mathbb{Z}_k$ charge (which correspond to a D3-brane wrapped on the 4-chain whose boundary is k times the torsion 3-cycle) produce simultaneously N

particles each carrying momentum k on the circle (whose radius is R/k due to the orbifold).

The situation is very analogous to the one we will encounter in M-theory and type IIA compactifications in Section 6.4, so we postpone the discussion. Suffice to say that in this kind of situation, the actual discrete symmetry has order $k^2 + N^2$, heuristically corresponding to the fact that the discrete charge may be eliminated via emission of k D3-branes (each with charge k under the discrete group) and N KK modes (each with charge N under the discrete group). In the regime where the gravity description of $\mathbf{S}^5/\mathbb{Z}_k$ is valid, we need large $R^4 \sim Nk$ and large $R/k \sim N^{1/4}k^{-3/4}$, hence $N \gg k^3$, and the order of the gauge group is effectively dominated by the N^2 term, corresponding to emission of N KK modes. Hence, the actual discrete symmetry in this regime is an effective $\mathbb{Z}_N$.

It is straightforward to repeat the above computations for the KK mode particles. The mass is given by k/R, as corresponds to mesonic operators of dimension k (or multiples of it) due to the orbifold action. We obtain the relations and scalings

$$m \sim M_{P,5} N^{-2/3} k^{2/3} \,, \;\; m \sim g k M_{P,5}^{3/2} \,, \;\; g M_{P,5}^{1/2} = N^{-2/3} k^{-1/3} \,. \tag{6.38}$$

Here g is obviously the same as in (6.36), but we repeat it for convenience. Happily, it is clear that g obeys a $\mathbb{Z}_N$ WCC. Notice also that the discretely charged KK modes fit more nicely with the black hole argument in Section 6.2.1. It seems more manageable to emit KK particles than D3-brane particles, as the latters extend to a very large size in the internal dimension.

As anticipated, we will re-encounter a very similar situation in M-theory compactifications in the next section, with the additional handle of a type IIA reduction, which makes these aspects far more intuitive. We refer the reader to those sections for details.

6.4 M-theory orbifolds and ABJM

In this section we study the WCC in M-theory on $\mathrm{AdS}_4 \times \mathbf{S}^7/\mathbb{Z}_k$ and its type IIA reduction, which provide the gravity dual of the ABJM gauge theories [32]. These theories display interesting new subtleties as compared with earlier cases. Some have been partially discussed in the ABJM literature, so we can again profit from the holographic dictionary.

6.4.1 M-theory on $\mathbf{AdS}_4 \times \mathbf{S}^7/\mathbb{Z}_k$

Let us now consider M-theory on $\mathrm{AdS}_4 \times \mathbf{S}^7/\mathbb{Z}_k$. This theory has been introduced in Section 1.1.3 and is the dual to the ABJM theories, which correspond to $\mathrm{U}(N)_k \times \mathrm{U}(N)_{-k}$ CS matter theories,[49] with $\pm k$ denoting the CS level.

The curvature radius of the covering $\mathbf{S}^7$ and the AdS_4 is given in Eq. (1.11)

49: Actually, as mentioned below and pointed out in [32] the global structure is different such that there are gauge invariant dibaryons for arbitrary N, k.

We are interested in studying gauge symmetries in the 4d theory. The 4d Planck scale is given by

$$M_{P,4}^2 = \frac{M_{P,11}^9 R^7}{k} \,. \tag{6.39}$$

Hence we have

$$R \sim M_{P,11}^{-1} N^{1/6} k^{1/6} \,, \tag{6.40}$$

and then

$$M_{P,11} \sim M_{P,4} N^{-7/12} k^{-1/12} \,, \; R \sim M_{P,4}^{-1} N^{3/4} k^{1/4} \,. \tag{6.41}$$

There are two relevant symmetries. There is a U(1) isometry, surviving from the underlying isometry of $\mathbf{S}^7$ which decomposes as SO(8) $\rightarrow$ SU(4) $\times$ U(1) under the orbifold action $z_i \rightarrow e^{2\pi i/k} z_i$. It is a continuous gauge symmetry in AdS_4. In addition, the internal space has a non-trivial torsion group $H_5\left(\mathbf{S}^7/\mathbb{Z}_k\right) = \mathbb{Z}_k$ which allows to obtain 4d particles by wrapping M5-branes on the torsion 5-cycle. In the covering space, the minimal charge particle is essentially an M5-brane giant graviton, similar to those in the $AdS_4 \times \mathbf{S}^7$ theory. In particular, it carries N units of momentum on the $\mathbf{S}^1$ associated to the U(1) symmetry.

This seems a perfect candidate for a WGC particle charged under the discrete symmetry, so we consider its properties in analogy with the D3-brane particles in Section 6.3. Its mass is given by

$$m_{\mathrm{M5}} \sim \frac{M_{P,11}^6 R^5}{k} = M_{P,4} N^{1/4} k^{-1/4} \,, \tag{6.42}$$

where, in the last equation, we have used (6.41). Note that we recover the AdS / CFT dictionary relation

$$m_{\mathrm{M5}} = \frac{N}{R} \,, \tag{6.43}$$

indicating that the M5-brane particle is dual to an operator of conformal dimension N, as befits a dibaryon.

We can compare this mass with the WGC bound (BPS bound), by computing the gauge coupling. This is just given by the KK reduction of the 11d Einstein terms and gives

$$g^{-2} \sim M_{P,11}^9 \left(R^7 k^{-1}\right) R^2 \,. \tag{6.44}$$

Note that we have taken the normalization factor R^2, which holds when GCD$(N,k) = 1$. This is because in that normalization, the charges under the U(1) are KK modes of momentum multiple of k (since the radius is R/k due to the orbifold action), and M5-branes, whose charges are multiples of N. Then by Bezout's lemma, the minimal charge quantum is 1. For the general case GCD$(N,k) = r$, we would have a factor $(R/r)^2$. We proceed with the coprime case in what follows. As pointed out in [32], the existence of gauge invariant dibaryon operators for general N (not a multiple of k) implies a specific choice of the global structure of the gauge group of the holographically dual ABJM field theory, see Footnote 49.

Using (6.41) we have

$$g^{-2} \sim N^{3/2} k^{1/2} \quad \rightarrow \quad g \sim N^{-3/4} k^{-1/4} \,. \tag{6.45}$$

So we get the WGC/BPS relation

$$m_{\text{M5}} = M_{P,4} g N \,. \tag{6.46}$$

It is interesting that in the large k limit we recover a weak coupling scaling result $g \sim k^{-1/4}$, but that this decrease is slower than the critical$g \sim k^{-1/2}$ required by the black hole evaporation argument. The resolution of this point reveals two interesting related subtleties: the actual discrete gauge symmetry of the theory is not just $\mathbb{Z}_k$, and the wrapped M5-branes are not the only states charged under the discrete symmetry. Indeed, as mentioned in [32], a set of k wrapped M5-brane particles can unwrap, but they do not decay to the vacuum, but rather turn into N KK states with momentum along the U(1) circle (which, due to the $\mathbb{Z}_k$ orbifold, is quantized in multiples of k). In other words, there are instantons (given by M5-branes wrapped on the $\mathbb{CP}^3$ base of the Hopf fibration of $\mathbf{S}^7/\mathbb{Z}_k$), which emit k M5-branes and N minimal momentum KK modes. As will be more intuitively explained in Section 6.4.2, there is a discrete symmetry of order $N^2 + k^2$, under which a wrapped M5-brane has charge k and a minimal momentum KK mode has charge N. Thus, KK modes provide a possible alternative to allow for black hole decay, which in fact is dominated by processes of emission of N such KK modes. Hence, the gauge coupling needs to obey a WCC with respect to N. Let us thus check this point.

The KK particle mass is given by

$$m_{\text{KK}} = \frac{k}{R} \,. \tag{6.47}$$

This constitutes the holographic dictionary relation for an operator of conformal dimension k. These are constructed with k copies of a bifundamental field, as required by gauge invariance under the level-k U(1)'s of the holographic dual field theory [32].

Using (6.41) we have

$$m_{\text{KK}} = M_{P,4} N^{-3/4} k^{3/4} \,, \tag{6.48}$$

and with (6.45) we obtain

$$m_{\text{KK}} = M_{P,4} g k \,. \tag{6.49}$$

Hence, these are WGC particles charged under the discrete symmetry, and the gauge coupling (6.45) obeys a WCC bound with respect to N.

6.4.2 Type IIA description of ABJM vacua

We may now describe the type IIA version of the previous section, which makes some above points more intuitive, and provides a good warm-up for the coming sections. For details on how to move from the M-theory

perspective to type IIA we refer to Section 1.1.3. We can now compute the 4d Planck mass:

$$M_{P,4}^4 \sim M_s^8 g_s^{-2} R_s^6 \,, \tag{6.50}$$

and combine with (1.17), (6.50) and (1.13) to obtain

$$\begin{aligned} R_s &\sim N k^{-1} M_{P,4}^{-1} g_s^{-1} \sim M_{P,4}^{-1} N^{3/4} k^{1/4} \,, \\ M_s &\sim N^{-3/4} k^{3/4} M_{P,4} g_s \sim M_{P,4} N^{-1/2} k^{-1/2} \,. \end{aligned} \tag{6.51}$$

Let us now consider the gauge symmetries in the 4d theory in this type IIA string compactification. The SU(4) symmetry arises as the isometry of the internal $\mathbb{CP}^3$. On the other hand, there are additional U(1) gauge fields arising from the 10d RR fields, concretely the 10d RR 1-form potential and the 10d RR 3-form potential integrated over $\mathbb{CP}^1 \subset \mathbb{CP}^3$. We should however notice that there are Stückelberg couplings arising from the 10d CS coupling $B_2 \wedge F_2 \wedge F_6$, of the form[50]

$$N B_2 \wedge F_2 + k B_2 \wedge F_2' \,, \tag{6.52}$$

where $F_2' = \int_{\mathbb{CP}^2} F_6$. This implies that the massless U(1) linear combination is

$$J = k Q_0 - N Q_4 \,. \tag{6.53}$$

Here the generators Q_0, Q_4 are labeled by the objects charged under the corresponding U(1)'s, namely D0-branes and D4-branes wrapped on $\mathbb{CP}^2$. Note that our sign convention differs from [32].

The orthogonal linear combination

$$Q_{\text{broken}} = N Q_0 + k Q_4 \,, \tag{6.54}$$

corresponds to a massive U(1), which is broken by instanton effects, and only a discrete subgroup remains. The instanton corresponds to an NS5-brane wrapped on $\mathbb{CP}^3$, since it couples magnetically to B_2. It suffers from FW anomalies due to the F_6 and F_2 fluxes, so it emits N D0-branes and k wrapped D4-branes. Hence, the total violation of Q_{broken} is $N^2 + k^2$. This is the order of the gauge group. However, notice that at the level of the black hole (and of the WCC), what is actually relevant is the number of particles required to be emitted, namely N D0-branes (contributing charge N each) and k D4-branes (contributing charge k each). The type IIA internal space is large compared with the string scale if $N \gg k$, so the limit of large order of the discrete gauge group scales as N^2 and the black hole decay is dominated by the emission of N D0-branes. In the arguments below, this is one particular instance in which the relevant coefficient in scaling relations is not the order of the discrete symmetry, but the number of emitted particles.

Notice also that we are recovering in possibly more intuitive terms the discussion of the earlier M-theory setup, with wrapped D4-branes corresponding to wrapped M5-branes and D0-branes corresponding to KK modes of the M-theory circle.

Let us discuss the masses of the D4- and D0-brane particles and the U(1)

50: For further discussion of CS couplings and swampland constraints see [133].

gauge couplings. They scale as

$$\begin{aligned} m_{\mathrm{D0}} &= g_s^{-1} M_s \sim M_{P,4} N^{-3/4} k^{3/4} \,, \\ m_{\mathrm{D4}} &= g_s^{-1} M_s^5 R_s^4 \sim M_{P,4} N^{1/4} k^{-1/4} \,. \end{aligned} \tag{6.55}$$

We already notice that the D0-brane mass decreases with N faster than the 'species' bound reviewed in Section 6.2.1.1, ensuring that black holes can get rid of their discrete charge by emitting D0-branes. Let us turn to check the implication for gauge couplings and verify the $\mathbb{Z}_N$ WCC.

The 4d gauge couplings for the U(1)'s generated by Q_0 and Q_4 are given by

$$\begin{aligned} \frac{1}{g_0^2} &\sim M_s^8 R_s^6 M_s^{-2} \\ \frac{1}{g_4^2} &\sim M_s^8 R_s^6 \left(M_s^{-5} R_s^{-4} \right)^{-2} \,. \end{aligned} \tag{6.56}$$

The first common factor arises from the reduction of the 10d kinetic term for RR fields on the $\mathbb{CP}^3$, while the last factors arise from the normalization of the gauge fields by the coefficient of the D-brane CS term, so that the charges are integer numbers. Using the familiar relations above, we obtain the scalings

$$\begin{aligned} g_0^{-2} &\sim N^{3/2} k^{-3/2} \,, \\ g_4^{-2} &\sim N^{-1/2} k^{1/2} \,. \end{aligned} \tag{6.57}$$

The coupling constant associated to the massless combination (6.53) is

$$g^{-2} = \frac{k^2}{g_0^2} + \frac{N^2}{g_4^2} \sim N^{3/2} k^{1/2} \,, \tag{6.58}$$

and, as explained, its scaling satisfies the WCC with respect to N

$$g \sim N^{-3/4} k^{-1/4} \,. \tag{6.59}$$

As expected, the D0- and D4-brane particles satisfy the BPS/WGC bound, in agreement with the result for wrapped M5-branes and KK modes in (6.46), (6.49)

$$\begin{aligned} m_{\mathrm{D4}} &= M_{P,4} g N \,, \\ m_{\mathrm{D0}} &= M_{P,4} g k \,. \end{aligned} \tag{6.60}$$

Notice also that $g \sim 1/R$ in Planck units, so the above masses imply conformal dimensions N and k for the holographically dual operators, as is by now familiar.

6.5 Discrete symmetries in intersecting brane models

Discrete symmetries are ubiquitous in models of intersecting branes (see [9] for a review), as pioneered in [107]. In this section, we use them to

illustrate the interplay of $\mathbb{Z}_k$ and U(1) gauge symmetries, and the scalings implied by the WCC.

Let us start by recalling the basic setup. Consider a compactification of type IIA on a CY space $\mathbf{X}_6$ quotiented by the orientifold[51] action $\Omega\mathcal{R}(-1)^{F_L}$, where $\mathcal{R}$ is an antiholomorphic $\mathbb{Z}_2$ involution of $\mathbf{X}_6$, which introduces O6-planes. Let us denote $[\Pi_{\rm O6}]$ the total homology class of the 3-cycles wrapped by the O6-planes. Introducing a symplectic basis $[\alpha_i]$, $[\beta_i]$ of 3-cycles even and odd under $\mathcal{R}$, respectively, we may expand

$$[\Pi_{\rm O6}] = \sum_i r^i_{\rm O6}[\alpha_i] + s^i_{\rm O6}[\beta_i]\,, \tag{6.61}$$

with $r^i_{\rm O6}$, $s^i_{\rm O6}$ some coefficients of order 1-10.

51: Note that the orientifolds are not essential for the argument, but we choose to introduce them to better connect with the literature on intersecting brane models.

The O6-planes are charged under the RR 7-form, so, as we reviewed in Section 1.2.1, to cancel its tadpoles we introduce D6-branes. We consider stacks of N_A overlapping D6$_A$−branes wrapped on 3-cycles Π_A, and their orientifold image D6$_{A'}$−branes on 3-cycles $\Pi_{A'}$. In terms of the basis, we have

$$[\Pi_A] = \sum_i r^i_A[\alpha_i] + s^i_A[\beta_i]\,,\ [\Pi_{A'}] = \sum_i r^i_A[\alpha_i] - s^i_A[\beta_i]\,. \tag{6.62}$$

The RR tadpole condition reads

$$\sum_A 2r^i_A + r^i_{\rm O6} = 0 \quad \forall i\,. \tag{6.63}$$

In addition, there are K-theory RR tadpole conditions [134], which we skip in this sketchy discussion.

In these models, there are Stückelberg couplings for the U(1)$_A$, of the form

$$\sum_A N_A s^i_A b_{2,i} \wedge F_A\,. \tag{6.64}$$

F_A is the field strength of the U(1) gauge field on the D6$_A$−branes, and the 4d 2-forms $b_{2,i}$ arise from the KK compactification of the RR 5-form C_5 as

$$b_{2,i} = \int_{\beta_i} C_5\,. \tag{6.65}$$

This makes some U(1)'s massive. Let us consider linear combinations of the U(1)$_A$ generators Q_A

$$Q = \sum_A c_A Q_A\,, \tag{6.66}$$

with c_A being coprime integers, to preserve charge integrality. The Stückelberg coupling for the field strength F of the U(1) generated by A is

$$\left(\sum_A c_A N_A s^i_A\right) b_{2,i} \wedge F\,. \tag{6.67}$$

Hence, the condition for a U(1) to remain massless is

$$\sum_A c_A N_A s^i_A = 0 \quad \forall i\,. \tag{6.68}$$

If not, the U(1) is broken, remaining only as an approximate global symmetry, broken by non-perturbative D2-brane instanton effects [135–137]. The condition that a discrete $\mathbb{Z}_k$ subgroup remains as an exact discrete gauge symmetry is

$$\sum_A c_A N_A s_A^i = 0 \mod k \quad \forall i \,. \tag{6.69}$$

Generically, to achieve this for a large k, a possibility[52] is to have $s_A^i \sim k$, at least for some A, for all i. This implies that there is some brane which is wrapped on a very large (i.e. multiply wrapped) cycle. This implies that in general any unbroken U(1), given by a linear combination (6.66) satisfying (6.68), will also involve that particular Q_A with a coefficient of order k. This implies that the gauge coupling of the unbroken U(1) scales as

$$\frac{1}{g^2} = k \text{ hence } g \sim k^{-1/2} \,. \tag{6.70}$$

Although this is not quite a rigorous argument, it is a good illustration of how the interplay between U(1) gauge couplings and $\mathbb{Z}_k$ symmetries arises, as a consequence of the fact that, to achieve a large order $\mathbb{Z}_k$ discrete symmetry, one needs to use parametrically large cycles, thus parametrically scaling gauge couplings to zero. Hence, intersecting brane models provide an intuitive mechanism for the WCC.

52: This is not the only one, but we stick to it as an illustrative example.

6.6 Discrete 3-form symmetries and scale separation in AdS solutions

In [83] it is proposed that in AdS vacua with cosmological constant Λ, the limit $\Lambda \to 0$ is accompanied by a tower of states becoming light as

$$m \sim |\Lambda|^\alpha \,. \tag{6.71}$$

The strong version of this conjecture is that $\alpha = 1/2$, which is the case in many/most string solutions (see below for examples). We focus on this version and phrase the conjecture as a ratio of scales[53]

$$\frac{m^2}{\Lambda} \sim \mathcal{O}(1) \,. \tag{6.72}$$

53: Note that Λ has dimension mass^2.

The states in the tower are typically KK states, and we use this term in the following. The conjecture implies that one cannot achieve a (parametric) separation of the KK scale and the scale of the cosmological constant. In fact, a problem that has been pervasive in holography literature is the search of gravity duals of QCD or 4d SCFT with conformal anomaly coefficients $a \neq c$. Scale separation is also an important intermediate step in constructions attempting to realize de Sitter vacua in string theory [138, 139]. Hence, it is an important question which merits attention.

There are systematic constructions of AdS_4 vacua in string theory in type IIA compactifications on CY orientifolds with NSNS and RR fluxes [48, 140] (see [141] for a recent generalization to general CYs). As already noticed in the literature, there is a family of vacua in [48] (see also [140]) claimed to achieve scale separation, thus violating the strong form of the conjecture. In this section we show that this family enjoys a $\mathbb{Z}_k$

discrete symmetry arising from 3-form gauge symmetries broken by a topological coupling to an axion, of the kind considered in [66, 70], together with a continuous 3-form symmetry.Hence,e it provides a setup in which a $\mathbb{Z}_k$ WCC for 3-form gauge fields is at work. The tension of the corresponding BPS domain walls can be related to the vacuum energy, and introduces additional factors of k in (6.72), thus explaining the parametric scale separation, that is controlled by the parameter k. This symmetry is consistently absent in other AdS vacua with no scale separation, hence provides a rationale for the existence of scale separation in this family, and suggests the proper generalization of (6.72) in the presence of domain wall $\mathbb{Z}_k$ symmetries.

6.6.1 Review of scaling AdS_4 vacua with scale separation

In this section we review some key elements of the family of models with scale separation, following [48] (see also [140] for related classes of type IIA AdS vacua).

Consider type IIA on a CY threefold modded out by an orientifold action introducing O6-planes. The O6-planes introduce a tadpole for the RR 7-form, which is canceled by (possibly present) D6-branes, and a combination of the $F_0 \equiv m$ Romans mass flux parameter and H_3 NSNS field strength flux on 3-cycles. Although it is possible to introduce it, we consider the RR F_2 field strength fluxes to be zero.[54] On the other hand, we introduce RR F_4 field strength fluxes on a basis of 4-cycles $\tilde{\Sigma}_{\tilde{i}}$

$$\int_{\tilde{\Sigma}_{\tilde{i}}} F_4 = e_{\tilde{i}} \in \mathbb{Z} \,. \tag{6.73}$$

We do not introduce RR F_6 flux over the CY, and only consider it when generated by monodromies, see Section 6.6.3. Some details on the 4d effective action of this theory are provided in Sections 1.2.3.4 and 3.2.1, and here we streamline the key facts. Whereas the fluxes $F_0 = m$ and H_3 are constrained to be $\mathcal{O}(1)$ due to the tadpole conditions, the fluxes for F_4 are unconstrained and can be taken large. The scaling solutions are achieved in the large k limit of

$$e_{\tilde{i}} \sim \bar{e}_{\tilde{i}} k \,, \tag{6.74}$$

where the $\bar{e}_{\tilde{i}}$ are $\mathcal{O}(1)$ quantities. Note that we have renamed the scaling parameter of [48] as k to make better contact with earlier sections, and to emphasize its forthcoming role as related to a discrete gauge symmetry.

Although we keep much of the upcoming discussion general, it is useful to consider explicit examples, like those introduced in Section 1.2.3.4. A simple class is obtained by taking toroidal orbifolds $\mathbf{T}^6/\mathbb{Z}_3$, whose untwisted sector is given by 3 Kähler moduli associated to the 3 underlying $\mathbf{T}^2$'s. Their volumes, measured in string units, are denoted by v_i, $i = 1, 2, 3$, with the overall volume being $\mathcal{V} \sim v_1 v_2 v_3$. They are complexified by the axions from the NSNS 2-form over the 2-tori b_i. We ignore twisted sectors, and refer the reader to [48] for details. Since $h_{2,1} = 0$, there is only one axion ξ from the period of the RR 3-form over the 3-cycle; it combines with the 4d dilaton e^D to form a complex modulus.

54: Actually, by monodromies in suitable axions [121] the F_2 flux can be generated due to the presence of F_0 flux. This follows from a DKS coupling, and intertwines non-trivially with similar DKS coupling to appear in Section 6.6.2. We keep our simplified discussion for $F_2 = 0$, and refer the reader to [72, 142] for further information on the more general framework.

In the scaling limit, [48] found a supersymmetric AdS_4 minimum (which we refer to as the DGKT solution) with the following values for the 4d moduli

$$v_i, b_i \sim k^{1/2}\,,\ \bar{\mathcal{V}} \sim k^{3/2}\,,\ e^{-D}, \xi \sim k^{3/2}\,. \tag{6.75}$$

This implies that

$$M_s^2 \sim e^{2D} M_{P,4}^2 \sim k^{-3} M_{P,4}^2\,, \tag{6.76}$$

and that the following relevant quantities of the 4d effective action, evaluated at the minimum, and measured in 4d Planck units, scale as

$$W \sim k^{3/2}\,,\ e^{\mathcal{K}} \sim k^{-15/2}\,,\ \Lambda \sim k^{-9/2}\,. \tag{6.77}$$

One may evaluate the KK scale as

$$m_{\rm KK} \sim \bar{\mathcal{V}}^{-1/6} M_s \sim k^{-7/4} M_{P,4} \tag{6.78}$$

(incidentally, it coincides with the mass scale for other massive moduli, so it provides a general cutoff of the 4d theory).

This leads to a relation of the type (6.71)

$$m_{\rm KK}^2 \sim \Lambda^{7/9}\,, \tag{6.79}$$

and hence to a seeming parametric violation of the strong version of the conjecture. In [143] the problem was considered in a family of IIA compactifications with geometric fluxes. The back-reaction of the latter [144] implied a modification of $m_{\rm KK}$ which restored the scaling predicted by the strong AdS Distance Conjecture. This mechanism, however, is not clearly available in the present context, where geometric moduli are absent. In the following sections we propose the scale separation is physical in these cases, and find a rationale in terms of underlying symmetries.

6.6.2 The discrete 3-form symmetry

In this section, we address the backbone of the solution to the above conundrum. First, notice that we have rewritten the strong conjecture as in the form (6.72) with hindsight. Indeed, taking this ratio, we find that in the DGKT family

$$\frac{m_{\rm KK}^2}{\Lambda} \sim k\,. \tag{6.80}$$

Alternatively, we may express the vacuum energy Λ in terms of the UV cutoff scale $m_{\rm KK}$ as

$$\Lambda \sim \frac{m_{\rm KK}^2}{k}\,. \tag{6.81}$$

Recalling that Λ has dimension 2, this is extremely reminiscent of the type of relation one finds in theories with a $\mathbb{Z}_k$ discrete gauge symmetry, see (6.4). Moreover, since the left hand side quantity is the vacuum energy, the relevant charged objects should be related to the structure of the vacuum.

We now show that there is indeed an effective $\mathbb{Z}_k$ symmetry acting on the domain walls changing the fluxes in the vacuum. The structure is

controlled by topological couplings of the 10d theory. In fact, we will study them without assuming the vacuum solution described in the previous section, and show that the scaling relations found there are a consequence of these topological couplings, or equivalently of the discrete symmetry structure.

Therefore, we start with the general CY (orientifold) compactification, and consider the basis of 4-cycles $\tilde{\Sigma}_i$ and their dual 2-cycles Σ_i. We recall the F_4 flux structure and introduce 4d axions from B_2 as

$$\int_{\tilde{\Sigma}_i} F_4 = k\bar{e}_{\tilde{i}} \,, \quad \int_{\Sigma_i} B_2 = \phi_i \tag{6.82}$$

(these axions were denoted by b_i in the toroidal setup above). In addition, we introduce a symplectic basis of orientifold-odd 3-cycles α_a and orientifold-even 3-cycles β_a, and introduce the NSNS H_3 fluxes and RR axions

$$\int_{\alpha_a} H_3 = p_a \,, \quad \int_{\beta_a} C_3 = \xi_a \,. \tag{6.83}$$

In addition, there is a Romans mass flux parameter $F_0 = m$.

Let us initially focus on the dynamics of Kähler moduli, hence ignore ξ_a, which will be reintroduced later on. Most of the discussion is general, although we eventually apply it to the toroidal orbifold for illustration.

The dimensional reduction of the 10d CS coupling $F_4 \wedge F_4 \wedge B_2$ leads to the 4d topological coupling

$$k \left(\sum_i \bar{e}_{\tilde{i}} \phi_i \right) F_4 \,. \tag{6.84}$$

This makes the 3-form massive, by eating up the 2-form dual to a linear combination of axions. The overall factor k implies that there is a discrete $\mathbb{Z}_k$ symmetry under which domain walls are charged [51]. This confirms we are on the right track. In fact, although certain modifications are about to come in, in the large k limit this $\mathbb{Z}_k$ discrete symmetry determines the properties of the system.

The situation is actually slightly more subtle, because of the following. The scalars ϕ_i also appear in couplings with other 4-forms, arising from the 8-form as

$$F_{4,\tilde{i}} = \int_{\tilde{\Sigma}_i} F_8 \,. \tag{6.85}$$

Hence, including the reduction of the 10d coupling $F_0 B_2 \wedge F_8$, the complete set of topological couplings is

$$m \sum_i \phi_i F_{4,\tilde{i}} + k \left(\sum_i \bar{e}_{\tilde{i}} \phi_i \right) F_4 \,. \tag{6.86}$$

This means that the combination $\phi' \equiv \sum_i \bar{e}_{\tilde{i}} \phi_i$ also couples to other 4-forms. To isolate that dependence, introduce the generators Q' and Q_i of 3-form U(1) symmetries for C_3 and $C_{3,i}$, and consider the linear combination

$$Q' = \sum_i \bar{e}_{\tilde{i}} Q_i \,. \tag{6.87}$$

The topological coupling for the corresponding 4-form F_4' is

$$m\left(\sum_i \bar{e}_{\tilde{i}}\phi_i\right)F_4' = m\phi' F_4' \,. \tag{6.88}$$

Hence, we can isolate the axion ϕ' with its couplings to the 4-forms F_4, F_4' as

$$\phi'\left(mF_4' + kF_4\right) \,. \tag{6.89}$$

It is interesting that we have this universal sector decoupled (at the topological level) from other axions and 4-forms, and hence independent of the details of the underlying CY compactification space.

Since there is only one axion and two 4-forms, there is clearly a massless 3-form corresponding to the combination

$$Q_{\mathrm{U}(1)} = kQ' - mQ = \sum_i e_{\tilde{i}}Q_{\tilde{i}} - mQ \,. \tag{6.90}$$

In the second equality we have recast the combination in terms of the original 4-forms. It is straightforward to check, using (6.86), that $Q_{\mathrm{U}(1)}$ is indeed free from topological couplings to scalars, hence remains an unbroken 3-form gauge symmetry.

The combination appearing in (6.89), namely,

$$Q_\perp = mQ' + kQ = \sum_i m\bar{e}_{\tilde{i}}Q_{\tilde{i}} + kQ \,, \tag{6.91}$$

is broken to a discrete subgroup. To better understand its structure, consider the string emitting a number of domain walls, and let us compute the violation of conservation of $Q_\perp$. The relevant string couples to the dual to ϕ, namely it is given by an NS5-brane wrapped on the linear combination of 4-cycles $\sum_i \bar{e}_{\tilde{i}}\tilde{\Sigma}_i$. Due to the presence of m, it emits $m\bar{e}_{\tilde{i}}$ D6-branes wrapped on $\tilde{\Sigma}_i$; due to the presence of $e_{\tilde{i}}$ units of 4-form flux over $\tilde{\Sigma}_i$, it emits $\sum_i \bar{e}_{\tilde{i}}e_{\tilde{i}}$ D2-branes. Since each D6-brane on $\tilde{\Sigma}_i$ violates $Q_{\tilde{i}}$ in 1 unit, and each D2-brane violates Q in 1 unit, we have a total violation of Q_{broken} by

$$\Delta Q_\perp = \sum_i \left(\bar{e}_{\tilde{i}}\right)^2\left(k^2 + m^2\right) \,. \tag{6.92}$$

Although it would seem that at large k the symmetry is of order k^2, notice that it suffices to have k D2-branes (plus a number of D6's sub-leading in the $1/k$ approximation) to annihilate into a string. It is only that one D2-brane implies a violation of k units of Q_{broken}, from the way we built the linear combination. So it is an effective $\mathbb{Z}_k$ for D2-branes.

Notice that this system realizes a 3-form version of the theories with discrete and continuous U(1) symmetries (for 1-forms) we described in earlier sections. In particular, the structure of two underlying U(1)'s with one linear combination broken by a topological coupling is completely analogous to the discussion of the type IIA gravity dual of ABJM theories in Section 6.4.2.[55]

55: With the notational difference that the roles of N, k are now played by k, m, respectively.

6.6.3 Scaling relations for moduli from discrete symmetries

In analogy with the ABJM system, the D2- and D6-brane domain walls are BPS, and their tensions must relate to their charges under the unbroken $Q_{\mathrm{U}(1)}$,

$$T_{\mathrm{DW}} = g Q_{\mathrm{U}(1)} M_{P,4}^4 \,. \tag{6.93}$$

The gauge coupling g for $Q_{\mathrm{U}(1)}$ is derived from those of the 3-form symmetries associated to Q and $Q_{\tilde{i}}$, see (6.90). We denote them g_2, $g_{6,\tilde{i}}$ respectively, to indicate that the charged objects are D2-branes and D6-branes on $\Sigma_{\tilde{i}}$. We have

$$\frac{1}{g^2} = k^2 \sum_i \left(\tilde{e}_{\tilde{i}}\right)^2 \frac{1}{g_{6,\tilde{i}}^2} + m^2 \frac{1}{g_2^2} \,. \tag{6.94}$$

The fact that both D2- and D6-branes can satisfy the BPS condition (6.93), implies that, in the large k limit, their gauge couplings must relate as

$$g_{6,\tilde{i}} \sim k g_2 \,. \tag{6.95}$$

It is easy to express the ratio of these gauge couplings in terms of microscopic compactification parameters and **derive** that the scaling for v reproduces (6.75). We offer a simplified discussion here, referring the reader to Section 3.2.1 for a supergravity-friendly derivation. For concreteness, we also focus on the toroidal case. The inverse gauge couplings squared are

$$\begin{aligned} \frac{1}{g_2^2} &= M_s^2 \bar{\mathcal{V}} \left(M_s^{-3}\right)^2 = M_s^{-4} \bar{\mathcal{V}} \,, \\ \frac{1}{g_{6,\tilde{i}}^2} &= M_s^2 \bar{\mathcal{V}} \left(M_s^{-3} \frac{v_i}{\bar{\mathcal{V}}}\right)^2 = M_s^{-4} \frac{(v_i)^2}{\bar{\mathcal{V}}} \,, \end{aligned}$$

where the first factor arises from the 10d coupling and the terms in parentheses arise from normalization of charges to integers, and we recall that $\bar{\mathcal{V}} = v_1 v_2 v_3$. We have that

$$\frac{g_{6,\tilde{i}}}{g_2} = \frac{\bar{\mathcal{V}}}{v_i} \tag{6.96}$$

and comparing with (6.95) for different i's gives

$$v_i \sim k^{1/2} \,, \; \bar{\mathcal{V}} \sim k^{3/2} \,. \tag{6.97}$$

A more direct, and possibly more general, route to the scaling relations for moduli is to use the monodromy relations. The fact that, e.g., F_4 has topological couplings to axions implies that the flux N of F_6 over the CY changes as the axions wind across their periods. Indeed, the above discussion is slightly oversimplified, since the fluxes experience a more intricate set of axion monodromies. These have been studied systematically in [72], and appeared implicitly in [48]. They just follow from the nested structure of 10d CS terms, or equivalently of the 10d

modified Bianchi identity for F_6, which implies

$$F_6 = dC_5 + F_4 \wedge B_2 + F_2 \wedge B_2 \wedge B_2 + F_0 B_2 \wedge B_2 \wedge B_2 + H_3 \wedge C_3 \,. \quad (6.98)$$

Hence, restricting to our setup with only F_0, F_4 and H_3, the effective 4d theory can depend only on the combination

$$N + k\bar{e}_{\tilde{i}}\phi_i + m\kappa_{ijk}\phi_i\phi_j\phi_k + p_a\xi_a \quad (6.99)$$

(where sums over repeated indices are implicit). Here κ_{ijk} is the triple intersection number. For instance, $\kappa_{123} = 1$ for the torus. This implies that it is possible to generate F_6 flux from m by performing a monodromy in b_1 to generate F_2 on the first $\mathbf{T}^2$, followed by a monodromy in b_2 to generate F_4 on the $\mathbf{T}^4$ transverse to the third coordinate, and one in b_3 to generate F_6 on the CY.

This is a more complete version of the topological couplings to 4-forms we have been considering, and which underlies the discrete symmetry of the system. We are interested in its behavior in the large k limit. Consistent scaling of the monodromy relations for large k requires that

$$\phi_i \sim k^{1/2} \,. \quad (6.100)$$

This is the generalization of the scaling for b_i in (6.75), and provides the complexified counterpart of our scalings for v_i in (6.97) (which recovered those in (6.75)). We point out that the fact that the two components of complex moduli have identical scalings with large flux quanta fits nicely with results on asymptotic flux compactification [145]. It is fascinating that this result follows from just the discrete symmetry in the present context.

Motivated by this, we can use a similar argument to extract the scaling of the dilaton multiplet in the large k limit. From (6.99) we get

$$\xi_a \sim k^{3/2} \,. \quad (6.101)$$

This is the complexification of a similar dependence of the dilaton, which thus reproduces (6.75).

Interestingly, with this information, which in particular implies the scaling (6.76), i.e. $M_s \sim k^{-3/2} M_{P,4}$, we obtain the scaling of gauge couplings (6.94), (6.96)

$$g_2 \sim k^{-15/4} \,,\; g_{6,\tilde{i}} \sim k^{-11/4} \,,\; g \sim k^{-15/4} \,, \quad (6.102)$$

providing a nice version of the WCC for domain walls.

Note, however, that when including the H_3 fluxes, the above discussion is equivalent to the inclusion of additional topological couplings $p_a\xi_a F_4$. In other words, D2-brane domain walls, in the presence of H_3 flux, can annihilate in sets of p_a by nucleating a string given by a D4-brane wrapped on the 3-cycle α_a, due to the FW inconsistency of the latter. The presence of these couplings spoils the structure of continuous and discrete 3-form gauge symmetries found in the Kähler moduli sector. In other words, the coupling of F_4 to a different linear combination of axions implies that the former continuous symmetry is actually also broken by the new additional axion, given by the linear combination of

All the scalings can be found looking at Eq. (3.34) and substituting the corresponding scalings with respect to the F_4 flux:

$$\frac{1}{g_0^2} = \frac{\pi e^{-K}}{8M_P^4} \sim k^{15/2} \,,$$
$$\frac{1}{g_i^2} = \frac{\pi e^{-K}}{8M_P^4 (v^i)^2} \sim k^{13/2} \,,$$
$$\frac{1}{g_{\tilde{i}}^2} = \frac{\pi e^{-K} (v^i)^2}{8M_P^4 \tilde{\mathcal{V}}^2} \sim k^{11/2} \,,$$
$$\frac{1}{g_4^2} = \frac{\pi e^{-K}}{8M_P^4 \tilde{\mathcal{V}}^2} \sim k^{9/2} \,,$$

however, here they have been obtained only looking at the discrete symmetries and using the WGC for the DW.

ξ_a. We skip the detailed discussion of the resulting complete discrete symmetry group. Note, however, that for large k the effects of both m and p are sub-leading in an $1/k$ expansion, so the $\mathbb{Z}_k$ symmetry we have been using prevails.

Since we have recovered the scalings of the Kähler and complex structure moduli, it is a simple exercise to use the expressions of 4d supergravity to derive others like (6.77), and eventually recover the scale separation (6.81). On the other hand, the 4d approach has been criticized as potentially hiding subtleties of the 10d solution. Therefore, in the following we use an alternative approach, and exploit properties of BPS domain walls to recover the vacuum energy.

6.6.4 Discrete symmetries and scale separation

In this section, we exploit the interplay between the tensions of domain walls and the vacuum energy, and study the interplay of discrete symmetries and scale separation. We argue through explicit examples that AdS vacua with trivial discrete symmetry for domain walls do not have scale separation; this is true even if there are non-trivial discrete symmetries for particles or strings, and in general for real codimension higher than 1 objects. On the other hand, we show that the above type IIA modes with non-trivial discrete symmetry for domain walls, with the corresponding scaling for moduli, do have vacuum energy with scale separation. We extend this general relation and put forward the following refined version of the swampland constraint (6.72), as follows:

Conjecture 6.2 [$\mathbb{Z}_k$ Refined SADC ($\mathbb{Z}_k$ RSADC])**.**

Consider quantum gravity on an AdS vacuum with a $\mathbb{Z}_k$ discrete symmetry for domain walls (with k large). In the flat-space limit $\Lambda \to 0$ (with $\Lambda k \to 0$ as well) there exists an infinite tower of states at a scale M_{cutoff}, with the relation

$$\Lambda \sim \frac{M_{\text{cutoff}}^2}{k} \,. \tag{6.103}$$

We now proceed to check this conjecture in the examples of supersymmetric AdS vacua of this chapter, by deriving their vacuum energies from the properties of domain walls.

6.6.4.1 Vacuum energy from domain walls

Let us describe our main tool to evaluate the vacuum energies without invoking an underlying scalar potential. There is a general relation between domain wall tensions and vacuum energies, which essentially follows from the junction conditions in general relativity. We refer the reader to Appendix A for a discussion well adapted to our application in AdS. The key point is that the domain wall tension T is the variation of certain quantities λ, see (A.9), whose square essentially gives the vacuum

energy Λ, see (A.8). In the supersymmetric setup, and for BPS domain walls, these statements become the familiar

$$\lambda = e^{\mathcal{K}/2}W\ ,\ T = \Delta(e^{\mathcal{K}/2}W) = \Delta\lambda\ ,\ \Lambda = -3e^{\mathcal{K}}|W|^2 \sim -|\lambda|^2\ . \quad (6.104)$$

We consider BPS domain walls whose quantized charge describes the change in some field strength flux n as one crosses the domain wall. In the limit of large flux n, the tension T provides the derivative of $d\lambda/dn$. We can then solve to obtain the scaling with n of λ, and thus of its square, Λ.

6.6.4.2 Warm-up examples: no scale separation

We now turn to discuss the AdS examples of Sections 6.3 and 6.4, **deriving** their AdS radius from the above strategy, and showing there is no scale separation. This is in agreement with our RSADC, as these examples have discrete symmetries for particles (and for their dual real codimension 2 objects) but not for domain walls.

6.6.4.2.1 Type IIB on $\mathbf{S}^5/\mathbb{Z}_k$

Consider type IIB on $\mathbf{S}^5/\mathbb{Z}_k$ with N units of RR 5-form flux and

$$R^4 \sim M_s^{-4} g_s N k\ . \quad (6.105)$$

This is of course the class of theories considered in Section 6.3, but we are now not imposing the solution for the 5d vacuum, rather we are deriving its vacuum energy from the domain wall properties. In passing, we also discuss the gauge coupling of the 3-forms and draw conclusions regarding the WCC.

We consider a BPS domain wall given by a D3-brane in 5d. Its tension is

$$T_{\rm D3} \sim M_s^4 g_s^{-1} \sim M_{P,5}^4 N^{-5/3} k^{-1/3}\ . \quad (6.106)$$

The same result is obtained from the BPS condition

$$T_{\rm D3} = g Q_{\rm D3} \quad (6.107)$$

upon computation of the gauge coupling of the 5d RR 4-form under which the D3-brane is charged. Since the tension essentially agrees with the gauge coupling, we observe an interesting WCC scaling for g (in that respect, recall that the relevant large order discrete symmetry is $\mathbb{Z}_N$). This is interesting, since the discrete symmetry acts on particles/membranes, whereas g is a 3-form gauge coupling. It would be interesting to explore the interplay between discrete and continuous symmetries of different degrees; we hope to come back to this in future work.

Since this domain wall interpolates between vacua with N and $N+1$, one can now obtain

$$\frac{d\lambda}{dN} \sim N^{-5/3} k^{-1/3} \quad \Rightarrow \quad \lambda \sim N^{-2/3} k^{-1/3} \quad \Rightarrow \quad \Lambda \sim M_{P,5}^2 N^{-4/3} k^{-2/3}\ . \quad (6.108)$$

Using (6.28) we have

$$\Lambda \sim R^{-2}\ . \quad (6.109)$$

Hence the AdS radius is the same as that of the internal space, and there is no decoupling of scales. This is the strong ADC statement in [83].

Note that, even though there are discrete gauge symmetries in the system, their orders do not enter the ratio of scales. This is in agreement with our RSADC, since these discrete symmetries involve particles and membranes, not domain walls.

6.6.4.2.2 M-theory on $\mathbf{S}^7/\mathbb{Z}_k$

Let us consider M-theory on $\mathbf{S}^7/\mathbb{Z}_k$ with N units of flux (or Nk in the covering space) and

$$R^6 \sim M_{P,11}^{-6} Nk\,. \tag{6.110}$$

This is of course the same system as in Section 6.4, but again we wish to **derive** the 4d vacuum energy from the relevant BPS domain walls. We consider a BPS domain wall given by an M2-brane in 4d. Its tension is

$$T_{\text{M2}} \sim M_{P,11}^3 \sim M_{P,4}^3 N^{-7/4} k^{-1/4}\,. \tag{6.111}$$

where we used (6.41). The same result is obtained from the BPS condition

$$T_{\text{M2}} = g Q_{\text{M2}} \tag{6.112}$$

upon computation of the gauge coupling g for the 4d 3-form. Recalling the relevant large order discrete symmetry is $\mathbb{Z}_N$, we note again that we get an interesting WCC scaling for g.

Since the M2-brane domain wall interpolates between vacua with N and $N+1$ units of flux, we have

$$\frac{d\lambda}{dN} \sim N^{-7/4} k^{-1/4} \Rightarrow \lambda \sim N^{-3/4} k^{-1/4} \Rightarrow \Lambda \sim M_{P,4}^2 N^{-3/2} k^{-1/2} \sim R^{-2}\,. \tag{6.113}$$

In the last relation, we have used (6.41). Again, we recover the result that the AdS radius is of the same order of magnitude as the KK scale of the internal space. Also, notice that there are discrete symmetries in the theory, but they involve particles and strings, rather than domain walls. Hence, they do not alter the relation between scales, in agreement with our RSADC.

6.6.4.2.3 Type IIA on $\mathbb{CP}^3$

We would like to repeat the previous computation in the type IIA picture. Let us consider type IIA theory on $\mathbb{CP}^3$ with N units of F_6 RR flux over $\mathbb{CP}^3$ and k units of F_2 RR flux over $\mathbb{CP}^1 \subset \mathbb{CP}^3$ and

$$R_s^2 \sim M_s^{-2} N^{1/2} k^{-1/2}\,. \tag{6.114}$$

This is the same system as in Section 6.4.2. The relevant BPS domain wall is a D2-brane in 4d, whose tension is

$$T_{\text{D2}} \sim M_s^3 g_s^{-1} \sim M_{p,4}^3 N^{-7/4} k^{-1/4}\,. \tag{6.115}$$

This is the same scaling as the M2-brane in the previous section, and the D2-brane domain wall interpolates vacua with N and $N+1$ units of flux,

so we recover

$$\Lambda \sim M_{p,4}^2 N^{-3/2} k^{-1/2} \sim R_s^{-2} \,. \tag{6.116}$$

The AdS radius is the same as that of the internal space, with no scale separation, in agreement with our RSADC.

6.6.4.3 Revisiting the Scale Separation in type IIA CY flux compactifications

Consider now the configurations with the large k discrete $\mathbb{Z}_k$ symmetry for domain walls in Section 6.6.2. We wish to derive the scaling of the vacuum energy with k, just using the scaling of moduli VEVs (6.75), (6.76) derived in Section 6.6.3 from the $\mathbb{Z}_k$ symmetry.

We consider the BPS domains wall given by a D4-brane wrapped on the combination of 2-cycles $\sum_i \bar{e}_i \tilde{\Sigma}_i$. This domain wall interpolates between vacua with F_4 flux given by k and $k+1$. Notice that the F_4-flux is not monodromic, hence the D4-branes are stable against nucleation of strings, and can provide BPS objects (in contrast to, e.g., D2- and D6-brane domain walls encountered in earlier sections).

The tension of these domain walls can be obtained from the BPS equation and the gauge couplings, computed in detail in Section 3.2.1. Here we carry out a simplified derivation, taking the toroidal case for concreteness. The gauge coupling of a D4$_i$-brane domain wall is

$$\frac{1}{g_{4,i}^2} = M_s^2 \bar{\mathcal{V}} (M_s^{-3} v_i^{-1})^2 = M_s^{-4} \bar{\mathcal{V}} v_i^{-2} \sim k^{13/2} \,. \tag{6.117}$$

As usual, in the first equality, the first term comes from the reduction of the 10d coupling, and the parenthesis from the charge normalization. Note that the scaling is common for all i, so by the BPS condition we get the tension

$$T_{\rm DW} \sim k^{-13/4} \,. \tag{6.118}$$

Notice that, if interpreted in terms of gauge couplings, this implies an interesting WCC, as in earlier examples. From the above tension, we get

$$\frac{d\lambda}{dk} \sim k^{-13/4} \Rightarrow \lambda \sim k^{-9/4} \Rightarrow \Lambda \sim k^{-9/2} \,. \tag{6.119}$$

So we recover the scaling (6.77) for Λ (the reader can check those of $\mathcal{K}$ and W as well). Once $m_{\rm KK}$ is recovered as in (6.78), this reproduces the scale separation (6.81), in agreement with our RSADC.

Dynamical tadpoles and swampland

Dynamical Tadpoles and Weak Gravity Constraints

7

Non-supersymmetric string models are plagued with tadpoles for dynamical fields, which signal uncanceled forces sourced by the vacuum. We argue that in certain cases, uncanceled dynamical tadpoles can lead to inconsistencies with QG, via violation of swampland constraints. We describe an explicit realization in a supersymmetric toroidal $\mathbb{Z}_2 \times \mathbb{Z}_2$ orientifold with D7-branes, where the dynamical tadpole generated by displacement of the D7-branes off its minimum leads to violation of the axion Weak Gravity Conjecture. In these examples, cancellation of dynamical tadpoles provides consistency conditions for the configuration, of dynamical nature (as opposed to the topological conditions of topological tadpoles, such as RR tadpole cancellation in compact spaces). We show that this approach provides a re-derivation of the Z-minimization criterion for AdS vacua giving the gravitational dual of a-maximization in 4d $\mathcal{N} = 1$ toric quiver SCFTs.

The chapter is organized as follows. In Section 7.2 we point out that the condition of Z-minimization in AdS_5 vacua (which is the gravity duals of a-maximization for 4d $\mathcal{N} = 1$ quiver SCFTs, as reviewed in Section 1.1.4) can be recasted as a requirement for the WGC of BPS particles to be fulfilled. In Section 7.3 we consider D-brane backreaction effects, both in the supersymmetric (Section 7.3.1) and the non-supersymmetric setups (Section 7.3.2). In Section 7.4, we describe a class of models and discuss how mistreatment of its dynamical tadpole can lead to naive violations of the WGC. In Section 7.4.1 we describe the supersymmetric toroidal orientifolds with D7-branes and 3-form fluxes. In Section 7.4.2 we discuss the dynamical tadpole generated when D7-branes move off its minimum, and discuss its backreaction. In Section 7.4.3 we argue that computation of the backreaction only in the internal space can lead to violation of the WGC for different classes of ED3-brane instantons. In Section 7.5 we construct and explicit orientifold of $\mathbf{T}^6/(\mathbb{Z}_2 \times \mathbb{Z}_2)$ realizing this idea. In Sections 7.5.1 and 7.5.2 we review different discrete choices in toroidal orientifolds, and in Section 7.5.3 we employ them to build our explicit example, which is equipped with suitable fluxes in Section 7.5.4. We conclude with some final considerations in Section 7.6.

7.1 Preliminaries

Supersymmetry breaking has proven a formidable challenge since the early days of string theory. Leaving aside the potential appearance of tachyons, the supersymmetry breaking ingredients often produce tadpole sources for dynamical fields, unstabilizing the vacuum [146, 147]. In terms of underlying supersymmetric moduli space, this can be described in terms of a non-trivial potential for the moduli, with the tadpole signaling that the theory is sitting on a slope, rather than at a minimum (or an otherwise tachyonic extremum). Simple realizations arise in early models of supersymmetry breaking using antibranes in type II (orientifold) compactifications [148–151]. As in these models such tadpoles arise for

fields in the NSNS sector, they are usually known as NSNS tadpoles. However, since similar phenomena arise in more general contexts e.g. for open string moduli (or in other constructions like heterotic or M-theory), we refer to them as **dynamical tadpoles**.

They are in contrast with non-dynamical tadpoles, i.e. tadpoles for non-propagating p-form fields (such as the familiar RR tadpoles), which lead to topological consistency conditions on string vacua. Instead, dynamical tadpoles indicate not an inconsistency of the theory, but the fact that equations of motion are not obeyed in the proposed configuration, which should be modified to a spacetime dependent solution, e.g. rolling down the slope of the potential (see e.g. [152, 153] for this approach in the above context). Hence, they are often treated more lightly, or directly ignored/hidden under the rug.

In this work we argue that such a mistreatment of dynamical tadpoles has a dramatic impact on the consistency of the theory, and in particular can lead to stark contradiction with QG, in the form of violations of some of the best established swampland constraints [82, 105] (see [77, 78] for reviews), in particular the WGC [84].

We illustrate these ideas in an explicit example of a type IIB orientifold compactification with NSNS and RR 3-form fluxes [42, 154], with D7-branes, and admitting a supersymmetric minimum. We focus on supersymmetric instantons given by euclidean D3-branes (ED3-branes) wrapped on 4-cycles, satisfying the axion WGC [84], and in fact saturating it as the BPS relation [111]. We consider toroidal models (and orbifolds thereof), on which D7-branes have position 'moduli' which are in fact stabilized by the fluxes [155–158]. The potential arises by the axion monodromy mechanism [70, 121, 159, 160], with the axion played by the periodic D7-brane position. Moving the D7-branes slightly off this minimum leads to a controlled supersymmetry breaking due to flux-induced extra tension on the D7-brane worldvolume, and the generation of dynamical tadpoles, in particular for the D7-brane position 'modulus' itself. This kind of displacement has been exploited in the construction of models of inflation [161, 162].

The key point is that the flux-induced extra energy density stored on the D7-brane worldvolume sources corrections to the geometry, which are usually encoded in a corrected internal warp factor (see [163], based on [164] in the supersymmetric setup). We show that this procedure implies brooming a dynamical tadpole under the rug, and that it leads to a contradiction with QG; concretely, it produces corrections to the action of ED3-brane instantons which violate the axion WGC.

The problem lies in the assumption that the backreaction of the supersymmetry breaking source is fully encoded in an internal warp factor, with no effect on the non-compact spacetime configuration, hence ignoring the dynamical tadpole sourced by supersymmetry breaking. QG is thus reminding us that consistent configurations must necessarily include spacetime dependence to account the dynamical tadpole.

Although we shown this for a concrete model, we expect the general ideas to hold in more general configurations, and even genuinely non-supersymmetric vacua. In fact, we advocate that these general ideas must play a crucial role in understanding how swampland constraints on vacua

extend to 'moduli' spaces with non-trivial scalar potential. In particular, unless a proper treatment of the dynamical tadpoles is implemented, the familiar formulation of swampland constraints such as the WGC can be expected to hold **only** in vacua.

One can turn this logic around and consider that the condition to satisfy the WGC in its familiar formulation can be equivalent to the condition to sit at a vacuum, i.e. minimizing the corresponding scalar potential. This is indeed what happens in our D7-brane case study, and we expect this to hold in more generality.[56] In fact, we provide extra support for this idea in an amusingly unrelated setup; we show that the condition of Z-minimization [25, 33], which in holographic dualities provides the gravitational dual of a-maximization of 4d $\mathcal{N}=1$ SCFTs [37] in terms of type IIB $AdS_5 \times \mathbf{X}_5$ vacua, introduced in Section 1.1.4, follows from applying the WGC for D3-branes wrapped on 3-cycles of the internal variety $\mathbf{X}_5$.

56: This view aligns with the recent progress in relating swampland constraints on spacetime configurations and on properties of states defined on them, see for instance [165, 166].

7.2 Z-minimization and a-maximization from WGC

Z-minimization has been introduced in Section 1.1.4.

We start with an observation that in certain string models, configurations away from the vacuum lead to an uncanceled dynamical tadpole which manifests as a non-fulfillment of the WGC. Hence, the condition to satisfy the WGC by minimizing the action of suitable charged states turns out to be equivalent to minimization of the scalar potential. In this section we explain how this idea explains the condition of Z-minimization in the context of AdS vacua in holography. We point out that in this context the deviation from the vacuum is not a modulus or light scalar direction, but rather involves modes with masses comparable with the cutoff, i.e. the KK scale; this suggests a more general validity of our arguments beyond their use in effective field theory. We are going to use this argument as a warm-up for what will follow in the next sections.

We now show that the above condition of Z-minimization is equivalent to the requirement that the WGC is satisfied for a suitable set of charged states in the AdS theory. For this purpose, we consider type IIB theory compactified on $AdS_5 \times \mathbf{X}_5$, with the volume of $\mathbf{X}_5$ relative to that of $\mathbf{S}^5$ (of the same radius as the AdS, R) given by the function $Z(\xi)$, which is minimized at the vacuum.

We now consider a set of states whose masses depend on the Reeb vector. As explained in Section 1.1.4, we can take D3-branes wrapped on 3-cycles Σ_i of $\mathbf{X}_5$. The ratio of the masses $m_i/m_{i;0}$ of such state for a general trial Reeb vector, and for the vacuum one is

$$\frac{m_i}{m_{i;0}} = \frac{\mathrm{Vol}(\Sigma_i)}{\mathrm{Vol}_{\min}(\Sigma_i)} \,. \tag{7.1}$$

In order to express it in a WGC format, we need to obtain the gauge couplings of the $U(1)_R$ under which these are charged. By dimensional reduction from 10d we have

$$g^{-2} = M_s^8 g_s^{-2} \mathrm{Vol}(\mathbf{X}_5) R^2 \,, \tag{7.2}$$

where the last R^2 is just a standard normalization factor.

We can also compute the 5d Planck mass by reduction from 10d to get

$$M_{P,5}^3 = M_s^8 g_s^{-2} \mathrm{Vol}(\mathbf{X}_5)\,. \tag{7.3}$$

They are related by

$$g M_{P,5}^{3/2} = R^{-1}\,, \tag{7.4}$$

independently of $\mathrm{Vol}(\mathbf{X}_5)$. This is useful, since in this system the free parameters in the Reeb vector are not actual moduli in this configuration (their masses are of the order of the KK scale), so their change is not really a deformation in a given effective theory. Hence, it is questionable to use the same or different values for g and $M_{P,5}$ in comparing the vacuum and configurations away from it. The above relation allows us to circumvent this discussion and proceed to the result.

We now use that the wrapped D3-branes are BPS states at the vacuum and satisfy

$$m_{i;0} = g Q M_{P,5}^{3/2} = \frac{Q}{R}\,. \tag{7.5}$$

where Q denotes its charge under $\mathrm{U}(1)_R$. Hence, at the configuration away from the vacuum we have

$$m_i = g Q M_{P,5}^{3/2} \frac{\mathrm{Vol}(\Sigma_i)}{\mathrm{Vol}_{\min}(\Sigma_i)}\,. \tag{7.6}$$

Due to the convexity of the volume functions with respect to the Reeb vector ξ [25, 33] (see also [35, 167, 168]), the only way to satisfy the WGC is to take the value $\xi = \xi_{\min}$. In other words, we recover the Z-minimization condition from WGC considerations.

7.3 D-brane backreactions in local models

In our examples, the dynamical tadpole is sourced by D-branes, hence its proper discussion requires accounting for the D-brane backreaction. In this section we consider several examples of backreaction of D-branes on other D-branes, in cases where they preserve a common supersymmetry, or not. For our examples in later sections we need to focus on backreaction effects on ED3's, so we restrict to this case in this section, although the ideas generalize easily to other branes. We also mainly focus on local models, leaving the discussion of global models, and the issues of the resulting dynamical tadpoles, to Section 7.4.

7.3.1 Warm up: Supersymmetric backreactions

We start with a review of supergravity backgrounds sourced by D-branes (D3-branes, D7-branes, and bound states thereof), and the backreaction effects on ED3-branes preserving a common supersymmetry. In these supersymmetric cases, the discussion in this section is related to alternative description in terms of generalized calibrations, see [169–176].

7.3.1.1 D7 on ED3

Consider type IIB theory on $M_4 \times \mathbf{X}_4 \times \mathbb{R}^2$, with $\mathbf{X}_4$ a compact K3 or $\mathbf{T}^4$, and consider N_{D7} D7-branes spanning the directions 01234567 and transverse to 89 (see below for remarks on the bounds on N_{D7}). In this theory, there is a BPS instanton given by an euclidean D3-branes (ED3) spanning $\mathbf{X}_4$ and localized in 0123 and 89, in general not coinciding with the D7-brane in those coordinates. The fact that the ED3 is BPS is easy to verify from the common solutions to the supersymmetry conditions of the D7 and the ED3. In an alternative view, there is a 'no-force' condition, which is easy to check from the open string perspective, from the vanishing of the 1-loop annulus amplitude. Here we are instead interested in the closed string perspective, in which we check that the supergravity background created by the D7-brane exerts 'no net force' on the ED3 (in more proper language, the action of the ED3 is independent of its position with respect to the D7).

We consider the background created by the D7-branes. Denoting by z the complex plane in 89, and using $r = |z|$, the metric has the general brane solution structure

$$ds^2 = Z(r)^{-1/2}\eta_{\mu\nu}dx^\mu dx^\nu + Z(r)^{-1/2}ds^2_{\mathbf{X}_4} + Z(r)^{1/2}dzd\bar{z}\,. \tag{7.7}$$

The function $Z(r)$ obeys the 2d Laplace equation with a point source at the origin. In the non-compact case, for N_{D7} D7-branes, we have

$$Z = -\frac{N_{D7}}{2\pi}\log(r/L) + \dots\,, \tag{7.8}$$

where L is a scale set by e.g. by the global compactification (see Section 7.4 for a related discussion), and the dots correspond to extra contributions due to possible distant sources. In addition, there is a non-trivial background for the dilaton

$$e^{-\phi} = Z(r) \tag{7.9}$$

and for the 10d axion. These are more easily described by combining them into the 10d complex coupling $\tau = C_0 + ie^{-\phi}$. For the case in Eq. (7.8), it is given by

$$\tau = \frac{N_{D7}}{2\pi i}\log(z/L) + \dots \tag{7.10}$$

This encodes the shift $C_0 \to C_0 + 1$ upon the shift $z \to e^{2\pi i}z$ as one surrounds one D7.

This is a good approximation for a small number of D7-branes; due to the non-flat asymptotics, larger N_{D7} overcloses the transverse space to a compact structure better described in F-theory [177]. In our description we will deal with one D7-brane and, if necessary, we consider the compact configuration close to the weakly coupled IIB limit of the orientifold of $\mathbf{T}^2$ by $\Omega\mathcal{R}(-1)^{F_L}$, where $\mathcal{R} : z \to -z$ introducing O7-planes [178]. In such situation, the above function Z should be replaced by a $\mathbf{T}^2$ Green's function, see later for analogous examples.

It is now straightforward to consider an ED3 in the probe approximation, and to evaluate its action to check it is independent of its position relative to the D7-brane. Concretely, the effect of the backreaction is to introduce

factors of Z which cancel off

$$S_{\text{ED3}} = \frac{\left(Z^{-1/4}\right)^4 \text{Vol}(\mathbf{X}_4)}{Z^{-1} g_s} = \frac{\text{Vol}(\mathbf{X}_4)}{g_s} \,. \tag{7.11}$$

This is the closed string version of the BPS property.

As usual, the open string description is more suitable for inter-brane distances below the string scale, while the closed string exchange description is better suited for larger distances. In this case the discussion is equivalent in both pictures, due to the large amount of supersymmetry in the system.

7.3.1.2 D3 on ED3

Les us now consider a different example. Consider again type IIB theory on $M_4 \times \mathbf{X}_4 \times \mathbb{R}^2$ as above, with $\mathbf{X}_4$ compact, and consider N_{D3} D3-branes along 4d Minkowski space. Although the discussion can be carried out in more generality, we are interested in smearing the D3-branes as a constant density along $\mathbf{X}_4$. The backreaction thus depends only on the radial direction in the complex plane $z = re^{i\theta}$ spanned by 89. This is similar to the above D7-brane case, and in fact both are related by 'T-duality'[57] in $\mathbf{X}_4$. Adapting the celebrated D3-brane supergravity solution to the case of a warp factor obeying a 2d Laplace equation, we have

57: This would be Fourier-Mukai in case $\mathbf{X}_4$ =K3.

$$ds^2 = Z(r)^{-1/2} \eta_{\mu\nu} dx^\mu dx^\nu + Z(r)^{1/2} ds^2_{\mathbf{X}_4} + Z(r)^{1/2} dz d\bar{z} \,, \tag{7.12}$$

with

$$Z(r) = -\frac{g_s N_{\text{D3}}}{2\pi} \log(r/L) + \dots \tag{7.13}$$

Here the dots denote extra pieces, due to global structure e.g. due to possible distant sources, and L again denotes a global (e.g. compactification) scale.

The D3-branes also source the RR 4-form C_4. Given its self-duality, the background can be expressed in terms of the components of C_4 along $\mathbf{X}_4$. This leads to the following profile with the polar angle θ

$$\varphi \equiv \int_{\mathbf{X}_4} C_4 = \frac{N_{\text{D3}}}{2\pi} \theta + \dots \tag{7.14}$$

We now consider a BPS instanton given by an ED3 wrapped on $\mathbf{X}_4$, and describe the effect of the backreaction. The ED3 feels the warping in the metric, and couples directly to the axion φ, so its Dirac-Born-Infeld (DBI) + CS action picks up a factor

$$\frac{1}{g_s}\left(-\frac{g_s N_{\text{D3}}}{2\pi} \log r\right) - i \frac{N_{\text{D3}}}{2\pi} \text{Im} \;\; \log z + \dots = -\frac{N_{\text{D3}}}{2\pi} \log z + \dots \tag{7.15}$$

In this case, it is the holomorphy of the result that encodes the BPS nature of the ED3. Our computation is essentially that in [164]; indeed, using (7.15) as the corrected instanton action, for e.g. $N_{\text{D3}} = 1$ the 4d non-perturbative contribution to e.g. the superpotential gives

$$W = z e^{-S^0_{\text{ED3}}} \,, \tag{7.16}$$

where the factor 2π has been reabsorbed and $S^0_{\rm ED3}$ is the instanton action in the absence of correction. For the open string perspective on this result, see [135–137, 179].

7.3.1.3 D7/D3 on ED3

By combining the results of the previous two sections, it is straightforward to study the backreaction of BPS bound states of D7- and D3-branes (namely, magnetized D7-branes [132, 180, 181]). The gravitational backreaction is obtained using the harmonic superposition rule in supergravity [182]

$$ds^2 = Z_{\rm D7}^{-1/2} Z_{\rm D3}^{-1/2} \eta_{\mu\nu} dx^\mu dx^\nu + Z_{\rm D7}^{-1/2} Z_{\rm D3}^{1/2} ds^2_{\mathbf{X}^4} + Z_{\rm D7}^{1/2} Z_{\rm D3}^{1/2} dz d\bar{z} \,, \quad (7.17)$$

with

$$Z_{\rm D7} = -\frac{N_{\rm D7}}{2\pi} \log(r/L) \,, \;\; Z_{\rm D3} = -\frac{g_s N_{\rm D3}}{2\pi} \log(r/L) \,, \quad (7.18)$$

where we are ignoring the dots. In addition, we have backgrounds for the IIB complex coupling τ and the axion φ as in Eq. (7.14)

$$\tau = \frac{N_{\rm D7}}{2\pi i} \log(z/L) \,, \;\; \varphi = \frac{N_{\rm D3}}{2\pi} {\rm Im}\,(\log z) \,. \quad (7.19)$$

In the ED3 action, the dilaton background cancels with the D7-brane metric backreaction factor $Z_{\rm D7}$, leaving a net effect due only to the D3-branes, given by (7.15).

The generalization of results of the previous sections to global supersymmetric setups is clear, by simply replacing $Z_{\rm D7}$, $Z_{\rm D3}$ by the corresponding solutions of the Laplace equation

$$-\Delta Z_{\rm D3/7}\left(x^8, x^9\right) = \rho_{\rm D3/7}\left(x^8, x^9\right) \,. \quad (7.20)$$

The above examples correspond to the local solutions of

$$\rho_{\rm D3/7} \sim N_{\rm D3/7} \delta_2(z, \bar{z}) \,. \quad (7.21)$$

In global compact setups, the Laplace equation implies some non-trivial integrability conditions on the sources, which are closely related to the dynamical tadpoles. We thus postpone their discussion to Section 7.4.

7.3.2 Non-supersymmetric backreactions

In this section we consider supersymmetry breaking sources, including anti-D3-branes (dubbed $\overline{\rm D3}$-branes in the following), and their backreaction effect on ED3's. Our aim is to obtain the backreaction of D7-branes with induced D3/$\overline{\rm D3}$-brane charge, as arises in the presence of NSNS 2-form field backgrounds (ubiquitous in compactifications with NSNS and RR 3-form fluxes [42, 154]). Our results provide a simple re-derivation of [163] (to which we refer the reader for a detailed discussion), and generalize easily to some further effects not considered therein.

7.3.2.1 Anti-D3 on ED3

Consider the setup of type IIB theory on $M_4 \times \mathbf{X}_4 \times \mathbb{R}^2$ as in Section 7.3.1.2, but with $N_{\overline{\text{D3}}}$ $\overline{\text{D3}}$-branes instead of D3-branes. We consider the model locally, so that we ignore global tadpoles. Since the $\overline{\text{D3}}$-branes have the same tension but opposite charge compared with D3-branes, their backreaction on the metric is given by (7.12) with

$$Z(r) = -\frac{g_s N_{\overline{\text{D3}}}}{2\pi} \log(r/L) + \dots \tag{7.22}$$

and the backreaction on the RR 4-form equals to Eq. (7.14) with an extra sign

$$\varphi = -\frac{N_{\overline{\text{D3}}}}{2\pi}\theta + \dots . \tag{7.23}$$

The effect on an ED3 located at position z is multiplication by a factor

$$-\frac{N_{\text{D3}}}{2\pi} \log(\bar{z}/L) + \dots . \tag{7.24}$$

This anti-holomorphic dependence reflects the fact that locally, the ED3 and $\overline{\text{D3}}$ preserve common supersymmetries, albeit those opposite to the ED3/D3 system (and globally, by the CY threefold compactification).

7.3.2.2 D7/D3/anti-D3 on ED3

We could now consider the backreaction of D3/$\overline{\text{D3}}$ pairs. However, these systems are strongly unstable due to tachyons, and we prefer to consider a more tractable alternative, which in fact is our main setup in future sections. We consider type IIB theory on $M_4 \times \mathbf{X}_4 \times \mathbb{R}^2$ with a D7-brane wrapped on $\mathbf{X}_4$ with equal smeared (in $\mathbf{X}_4$) D3/$\overline{\text{D3}}$ charge distributions. These arise in the presence of a worldvolume gauge background with field strength F_2 and/or pullbacked NSNS 2-form background B_2, which combine into

$$\mathcal{F}_2 = 2\pi\alpha' F_2 + B_2 \,. \tag{7.25}$$

The D3/$\overline{\text{D3}}$ charge distributions cancel locally when it satisfies

$$\mathcal{F}_2 \wedge \mathcal{F}_2 = 0 \,. \tag{7.26}$$

The individual D3- and $\overline{\text{D3}}$-brane contributions are obtained by extracting the self- and anti-selfdual pieces

$$\mathcal{F}_{2,\pm} = \frac{1}{2}(\mathcal{F}_2 \pm \star_4 \mathcal{F}_2) \,, \tag{7.27}$$

where $\star_4$ is Hodge in $\mathbf{X}_4$. In particular, we have

$$N_{\text{D3}} = \int_{\mathbf{X}_4} \mathcal{F}_{2,+} \wedge \mathcal{F}_{2,+} \,, \quad N_{\overline{\text{D3}}} = -\int_{\mathbf{X}_4} \mathcal{F}_{2,-} \wedge \mathcal{F}_{2,-} \tag{7.28}$$

and (7.26) implies $N_{\text{D3}} = N_{\overline{\text{D3}}}$, as anticipated.

Since both contribute in the same way to the gravitational background, it

is useful to introduce

$$N_3 = \int_{\mathbf{X}_4} |\mathcal{F}_2|^2 = N_{\mathrm{D3}} + N_{\overline{\mathrm{D3}}} = 2N_{\mathrm{D3}} \,. \tag{7.29}$$

To compute the backreaction, we superimpose the effects of the corresponding brane charges, as computed in earlier sections. This is the leading contribution in an expansion with the sources (flux densities) as a perturbative parameter; this implies ignoring the corrections that would involve, e.g., solving the gravitational background of a source in the background created by another source. The present expansion fits well with the regime needed for the coming sections and agrees with the detailed analysis in [163].

The result is that the correction to the ED3 action is controlled by a factor $-\frac{N_3}{2\pi}\log(r/L)$. Particularizing to toroidal $\mathbf{X}_4 = \mathbf{T}^4$ and constant backgrounds, we have

$$S_{\mathrm{ED3}} = \left[1 - \frac{1}{2\pi}|\mathcal{F}_2|^2 \log(r/L) + \dots\right] S^0_{\mathrm{ED3}} \,, \tag{7.30}$$

where for future convenience, we have added a constant piece in the prefactor, so that the action is S^0_{ED3} when $\mathcal{F}_2 = 0$. The above result is easily understood from different perspectives. The D7-brane backreaction on the dilaton and metric cancel out, leaving an effective D3- and $\overline{\mathrm{D3}}$-brane distribution, whose backreaction on C_4 cancels exactly, and whose backreaction on the metric adds up. As anticipated, we recover the result in [163].

7.3.2.3 D5/anti-D5 on ED3

We now consider an effect present in this setup, but not included in [163]. In the presence of the worldvolume background $\mathcal{F}_2$, there is an induced D5- or $\overline{\mathrm{D5}}$-brane density, which also must backreact on the geometry. For simplicity and future use, we consider $\mathbf{X}_4 = \mathbf{T}^4$ (or an orbifold thereof), and consider constant $\mathcal{F}_2$, so that the D5-brane charge is smeared, and the solution does not depend on internal coordinates in $\mathbf{X}_4$. We also focus on induced D5-brane charge, and the results will extend easily to D5/$\overline{\mathrm{D5}}$ setups needed later on.

The supergravity background created by a D5-brane (e.g. along 45 and transverse to 67 in $\mathbf{X}_4$) is determined by a 2d harmonic function $Z_{\mathrm{D5}}(r)$ as

$$\begin{aligned} ds^2 &= Z_{\mathrm{D5}}^{-1/2}\eta_{\mu\nu}dx^\mu dx^\nu + Z_{\mathrm{D5}}^{-1/2}ds^2_{45} + Z_{\mathrm{D5}}^{1/2}ds^2_{67} + Z_{\mathrm{D5}}^{1/2}dzd\bar{z} \,, \\ e^{-2\phi} &= Z_{\mathrm{D5}} \,. \end{aligned} \tag{7.31}$$

In local $\mathbb{R}^2$ we have

$$Z_{\mathrm{D5}} = -\frac{g_s N_{\mathrm{D5}}}{2\pi}\log(r/L) + \dots \,. \tag{7.32}$$

The above backreaction superimposes to D7/D3/$\overline{\mathrm{D3}}$ as discussed earlier.

There is also a RR 2-form background, which will not be relevant to our setups. In fact, we are interested in obtaining the correction to the action of an ED3 (along 4567) from the above background, and the latter does not couple to the RR 2-form. Note also that in this case there is no correction coming from the backreacted metric, since the $Z_{\rm D5}$ factors have inverse power for 45 and 67, and they cancel off. One is thus left with the correction to the dilaton, which gives a correction to $S^0_{\rm ED3}$ by a factor

$$S^0_{\rm ED3} \to \left[1 - \frac{1}{4\pi}|\mathcal{F}_2| \log(r/L) + \dots\right] S^0_{\rm ED3}\,, \tag{7.33}$$

where we expanded $Z^{1/2}_{\rm D5}$ to first order in the induced D5-brane charge, and we already included the constant piece 1, as above.

In the above expressions we have been sloppy concerning the numerical factors, which are not essential to our analysis below, since it is enough to keep track of the parametric dependence with induced charges. The signs of the different contributions are on the other hand crucial.

7.4 Dynamical tadpoles and WGC in D7-brane models

7.4.1 A D7-brane model

We are considering the model with D7-brane and 3-form fluxes in [157], which we now review. Although the specific model fulfilling the conditions we need is discussed in Section 7.5, we here discuss the general class of type IIB orientifolds of $\mathbf{T}^6$, or rather orbifolds thereof, like $\mathbf{T}^2 \times \mathbf{T}^4/\mathbb{Z}_2$, or $\mathbf{T}^6/(\mathbb{Z}_2 \times \mathbb{Z}_2)$. For concreteness, we carry out the description in terms of the latter, although we also discuss the simpler alternatives when indicated. We take a factorized $(\mathbf{T}^2)^3$ structure, with coordinates $0 \le x^i, y^i \le 1$, $i = 1, 2, 3$ for each $\mathbf{T}^2$, and complexify them as $z^i = x^i + \tau_i y^i$. We mod out by $\Omega\mathcal{R}(-1)^{F_L}$, where $\mathcal{R}$ flips all $\mathbf{T}^6$ coordinates, $z^i \to -z^i$, which introduces 64 O3-planes. In addition, in the presence of orbifold quotients, e.g., $\mathbb{Z}_2 \times \mathbb{Z}_2$, there are additional sets of 4 O7$_i$-planes localized on the i$^{\rm th}$ $\mathbf{T}^2$. The O3-plane charge is canceled against contributions from the upcoming 3-form fluxes, and D3-branes if necessary, which can be located at arbitrary positions. The models typically also contain D7$_i$-branes, transverse to the i$^{\rm th}$ $\mathbf{T}^2$. These can be located at arbitrary positions, provided we include the corresponding orbifold and orientifold images, and that we comply with the flux stabilization discussed next.

Following [157] we introduce a specific choice of NSNS and RR 3-form fluxes,

$$\begin{aligned} F_3 &= 4\pi^2\alpha' N \left(dx^1 \wedge dx^2 \wedge dy^3 + dy^1 \wedge dy^2 \wedge dy^3\right)\,, \\ H_3 &= 4\pi^2\alpha' N \left(dx^1 \wedge dx^2 \wedge dx^3 + dy^1 \wedge dy^2 \wedge dx^3\right)\,. \end{aligned} \tag{7.34}$$

Although naively $N \in \mathbb{Z}$ due to flux quantization, it must actually be some suitable multiple of some $N_{\rm min}$ due to the diverse quotients; for instance, $N \in 2\mathbb{Z}$ for $\mathbf{T}^6$ orientifolds with standard (i.e. negatively

charged) O3-planes [183], and $N \in 4\mathbb{Z}, 8\mathbb{Z}$ in $\mathbf{T}^6/(\mathbb{Z}_2 \times \mathbb{Z}_2)$ orientifolds [184, 185], as we recall in Section 7.5.4.

The flux superpotential admits supersymmetric minima for

$$\tau_1 \tau_2 = -1 \,, \;\; \tau_3 \tau = -1 \,, \tag{7.35}$$

where τ is the 10d IIB complex coupling.

The fluxes also stabilize some of the D7-brane moduli as follows. The presence of the fluxes introduces an in general non-zero pullback of the NSNS 2-form on the D7-branes. For instance, for a $D7_1$ at a generic position $\left(x^1, y^1\right)$, in a suitable gauge, we have

$$B|_{D7_1} = 4\pi^2 \alpha' N \left(x^1 dx^2 \wedge dx^3 + y^1 dy^2 \wedge dx^3\right) \,. \tag{7.36}$$

The supersymmetry condition [186] requires that (7.25) is primitive, and of type $(1,1)$ when expressed in complex components. This is clearly satisfied at the origin $z^1 = 0$, where $D7_1$-branes can thus be stabilized. However, as emphasized in [157] it is possible to locate them at other positions $\left(x^1, y^1\right)$ if $N x^1, N y^1 \in \mathbb{Z}$, by compensating (7.36) with suitably quantized worldvolume gauge fluxes. For our purposes, we just need some D7-brane to be located at the origin, and we can consider a general distribution for the rest. For concreteness, using the above freedom, and the fact that N is even from flux quantization, we choose to locate the $D7_1$-branes distributed in sets of 8 on top of the $O7_1$-planes to have local charge cancellation (see Section 7.5.3 for an explicit example).

For orientifolds of $\mathbf{T}^6/(\mathbb{Z}_2 \times \mathbb{Z}_2)$ there are typically[58] additional kinds of D7-branes, that we now discuss. $D7_2$-brane behave similar to the $D7_1$-branes above, and introduce no qualitative new features. On the other hand, for $D7_3$-branes, the motion away from the origin is compatible with supersymmetry and corresponds to a flat direction. This is because the induced B-field is $(1,1)$ (and primitive), hence satisfies the supersymmetry conditions. Our focus is on supersymmetry breaking effects, so we will not be interested in exploring this possibility.

58: Albeit, not in the specific example to be constructed in Section 7.5.

Focusing again on $D7_1$-branes, we also note that, despite the induced B-fields, there is no net induced D3-brane charge, since (7.36) wedges to zero with itself, c.f. (7.26). In fact in other models, or even in this model but for the motion of the $D7_3$-branes, there is a non-zero net induced D3-brane charge, proportional to the displacement squared. This is compatible with the cancellation of tadpoles for the RR 4-form due to a mechanism unveiled in [162]: the backreaction of the induced D5-brane charges on the D7-brane modifies the RR 3-form flux F_3, changing the flux contribution to the tadpole in precisely the right amount. In our examples, we focus on D7-brane motions not involving induced net D3-brane charge, and hence no such modification of the F_3 flux background.

7.4.2 Moving off the minimum and the dynamical tadpole

We now start addressing our main point by introducing a source of supersymmetry breaking, which triggers a dynamical tadpole. A simple

way to achieve this is to consider moving away from the minimum of the potential. Among the different ways to climb up the potential, we focus on the motion of $D7_1$-branes because they lead to better understood backreaction effects, of the kind discussed in Section 7.3 (clearly, $D7_2$-brane motion leads to similar results).

Consider the above type IIB orientifold, and consider a fixed point at which some $D7_1$-branes sit, which without loss of generality we take to be the origin $x^1 = y^1 = 0$. To be precise, we consider regular D7-branes with respect to the relevant orbifold group, so that they can move off into the bulk (see Section 7.5 for a detailed discussion of constructions allowing this motion) e.g. in the first complex plane, to the position

$$z^1 = \pm\varepsilon \in \mathbb{R}\,, \tag{7.37}$$

where the two signs correspond to a D7-brane and its image.

This motion is along a massive direction, off the minimum of the potential, due to the non-trivial B-field (7.36) on the $D7_1$-brane worldvolume. Since there is no net D3-brane charge, this can be regarded as a D3/$\overline{\text{D3}}$-brane tension localized at $z^1 = \pm\varepsilon$, and proportional to $N^2|\varepsilon|^2$, backreacting on the metric, as in Section 7.3.2.1. This is also the scaling of the potential energy stored in the configuration. In addition, there is an induced D5-brane change on the D7-brane (and its corresponding $\overline{\text{D5}}$-brane in its image), which implies a backreaction on the dilaton, as in Section 7.3.2.3. We are now interested in computing the backreaction of these extra sources. Since everything will be happening in a complex plane, from now on we denote z^1 and τ_1 by z and τ (hoping for no confusion with the IIB complex coupling).

Since we consider a motion $|\varepsilon| \ll L$, where L sets the size of the $(\mathbf{T}^2)_1$ directions, we can start with a local model as in Section 7.3. Note that we still consider $M_s \ll \varepsilon$ so that we can use the supergravity description to obtain the backreaction. In general, there is a non-trivial supergravity background created by the D3-branes and O3-planes in the configuration, the D7-branes and O7-planes, and finally the induced D3/$\overline{\text{D3}}$-branes, and D5- (and $\overline{\text{D5}}$-) branes. In the coming sections we are interested in the effect of this background on $ED3_1$-branes,[59] for which most of these contributions cancel. As discussed in Section 7.3.2, the key backreaction effects are in the warp factor Z sourced only by the induced tension on the D7-brane worldvolume, and the induced D5-brane backreaction on the dilaton. They schematically read

$$\begin{aligned} Z &\simeq 1 - \frac{N^2|\varepsilon|^2}{2\pi}\left[\log(|z-\varepsilon|/L) + \log(|z+\varepsilon|/L)\right] + \dots \\ g_s^{-1} &\simeq 1 - \frac{N|\varepsilon|}{4\pi}\left[\log(|z-\varepsilon|/L) + \log(|z+\varepsilon|/L)\right] + \dots \end{aligned} \tag{7.38}$$

where we introduce the constant term 1 to recover the trivial backreaction for $\varepsilon = 0$. Here the overall prefactors depending on $N|\varepsilon|$ provide the induced brane density, and the dots hide the global features to which turn next. Note that in these and coming expressions, we are only interested in the parametric dependence, and we skip order 1 numerical factors, in particular in the coefficients of the log terms for the metric and dilaton profiles. On the other hand, the explicit minus sign and the structure of the bracket of logs itself are identical for both backgrounds, as it is

59: In Section 7.4.3.3 we also consider ED(−1)-brane instantons. These are also BPS with respect to the supersymmetric D3/O3 and D7/O7 background, and again disappear in the relevant part of the backreaction.

determined by the solution of a Laplace equation in $\mathbb{R}^2$ with sources at $z = \pm\varepsilon$.

The above expression is valid for small ε, since we take the linear/quadratic approximation for the induced D5/D3-brane density. The result can however, be extended to a larger ε by using the full DBI contribution, e.g. for the 3-brane charge we sketchily change

$$|\varepsilon|^2 \to 2\left(\sqrt{1+|\varepsilon|^2}-1\right) . \tag{7.39}$$

We will nevertheless stick to small ε, since it controls the expansion of weak supersymmetry breaking sources employed in the computation of the leading backreaction effect. In any event, the only relevant information is that the coefficients of the logs are positive definite (up to the explicitly indicated sign) for any value of ε, and vanish at $\varepsilon = 0$ at least as $\mathcal{O}(\varepsilon)$.

We now turn to a very important point. We eventually need the backreaction at a general position z, not necessarily close to the origin. Hence, even if ε is small, we need to consider the global compactification. For this, in principle, one would simply promote the previous logarithmic backreaction to a solution of the Laplace equation with a delta function source c.f. (7.20). However, this leads to a problem of integrability of the equation, as the left-hand side integrates to zero in a compact space, and the right-hand side does not. This is nothing but the dynamical tadpole problem presented in the introduction: there is a vacuum energy stored in the internal space, which leads to an inconsistency of the equations of motion.

A usual procedure (see [163], based on [164] in the supersymmetric setup) is to modify the equations of motion (the Laplace equation) by introducing a constant distribution of background source compensating the delta function (i.e. so that the right-hand side integrates to zero). In other words, we promote

$$\log\left(\frac{|z+\varepsilon|}{L}\right)+\log\left(\frac{|z-\varepsilon|}{L}\right) \to G_2\left(\frac{|z+\varepsilon|}{L}\right)+G_2\left(\frac{|z-\varepsilon|}{L}\right) , \tag{7.40}$$

where $G_2(z)$ is the 2d Green's function, satisfying

$$\Delta G_2\,(z-z') = \delta_2\,(z-z') - \frac{1}{L^2 \mathrm{Im}\,\tau} . \tag{7.41}$$

Here, L is explicitly the length of the $\mathbf{T}^2$ sides, set to $L = 1$ in what follows for simplicity. The solution is given by (see, e.g., [163, 187], also [188] in a different context)

$$G_2(z) = \frac{1}{2\pi}\log\left|\frac{\vartheta_1(z|\tau)}{\eta(\tau)}\right| - \frac{(\mathrm{Im}\,z)^2}{2\mathrm{Im}\,\tau} , \tag{7.42}$$

where $\vartheta_1(z|\tau)$ and $\eta(\tau)$ are defined, respectively in Eqs. (D.8) and (D.10) and where an additive integration constant has been fixed to have the Green function integrated to zero (so that a constant density of source gives rise to no correction).

The above trick is a well-defined mathematical procedure, but its physical meaning is questionable. It corresponds to introduce by hand in (7.41) a constant negative tension background in the internal geometry, which

indeed sounds troublesome. Alternatively, it corresponds to ignoring the dynamical tadpole (potential for the D7-brane position off its minimum) and to insist that the configuration still admits a solution with distortions only in the internal space, keeping the external 4d Minkowski spacetime. In the following section, we argue that these are not just subtle technicalities, but, rather than putting the dynamical tadpole under the rug, can lead to a direct contradiction with quantum gravitational swampland constraints, in particular the Weak Gravity conjecture.

7.4.3 The clash with the WGC

In this section we show that in the theory there are objects that implement the WGC in the vacuum, but for which the above discussed backreaction (with the tadpole hidden under the rug) induces corrections in the **wrong** direction, so that the configuration no longer obeys the WGC.

A simple possibility is to focus on BPS objects at the supersymmetric minimum, and to track their properties in the displaced configuration. As anticipated in Section 7.3.2, we consider the axion WGC and focus on the ED3-brane instantons wrapped on $\mathbf{X}_4$, and transverse to the z^1-complex plane. We consider two possibilities to be discussed, in turn, regular ED3-branes, which are mobile and can be located at different positions in z^1, and fractional ED3-branes, which are stuck at a given fixed point (and can be regarded as ED3/ED(−1) bound states).

7.4.3.1 The regular ED3

Consider a regular ED3, namely one that can be located at any position in z^1, before the introduction of fluxes (since the latter lead to localization, as will be mentioned soon). In the case of a $\mathbf{T}^6$ orientifold, this is achieved by introducing an orientifold image, and if there are orbifold quotients this requires a specific choice of Chan-Paton actions, whose details we skip (see Section 7.5 for an extensive discussion).

At the supersymmetric minimum, the action for the BPS ED3-brane instanton is

$$S_0 = \mathrm{Im}\, T\,, \tag{7.43}$$

where T is the 4-cycle modulus of the underlying $\mathbf{T}^6$. The BPS relation ensures these instantons saturate the axion WGC, in fact also for arbitrary instanton charge (e.g., multiply wrapped ED3s).

Although the above observations apply for instantons located at arbitrary z^1, the introduction of 3-form fluxes leads to a localization effect, since, e.g. away from $z^1 = 0$ the ED3 picks up a B-field exactly as in (7.36), which contributes to increase its action. This contribution grows quadratically with $|z^1|$ and is not suppressed for small ε, so it dominates over ε-dependent backreaction corrections. Hence, in the following we focus on the effect of backreactions on ED3 located at $z^1 = 0$, where the direct flux-induced localization vanishes (however, we advance that ED3s at other possible locations will bite back in Section 7.4.3.2).

When we move the D7-brane off its minimum, the backreaction (7.38) enters as a multiplicative factor in the instanton action. Hence, the

correction to the ED3 action at $z = 0$ is

$$\Delta S = -C \left(\log |\varepsilon|\right) \mathrm{Im}\, T \,, \tag{7.44}$$

with a positive definite coefficient C, vanishing for $\varepsilon \to 0$, with the sketchy structure

$$C \sim \frac{N|\varepsilon|}{2\pi} + \frac{N^2|\varepsilon|^2}{\pi} \,. \tag{7.45}$$

Note that $N|\varepsilon|, N^2|\varepsilon|^2 \mathrm{Im}\, T$ encodes the total induced 5-brane and 3-brane tensions, and correspond to N_5, N_3 in (7.32) and (7.29), respectively.

Since we have small ε, this gives a positive correction ΔS positive, thus increasing the action of the instanton. Actually, this is not yet problematic. In fact, since (7.44) follows from just the local model approximation, there is no finite 4d Planck scale and hence no contradiction with the WGC so far. Notice also that the dynamical tadpole has not yet been ignored, since the Laplace equation in non-compact spaces does not require the cancellation of sources, hence the introduction of the fake background to cancel the tadpole. This agrees with our picture that it is the mistreatment of the dynamical tadpole that leads to problems with quantum gravitational constraints.

7.4.3.2 Going compact: The ED3 landscape

In this section we consider the compact $\mathbf{T}^2$ model, and the modification it implies for the ED3-brane action and its interplay with the axion WGC.

As we have explained, to describe the backreaction in the compact $\mathbf{T}^2$ we have to promote the logs in earlier expressions to solutions of the 2d Laplace equation c.f. (7.40), which leads to the dynamical tadpole problem. Getting rid of it as described above, the effect of the backreaction on the action of an ED3 at a general location z is

$$-C G_{\text{tot.}}(z;\varepsilon) \equiv -C \left[G_2(z+\varepsilon|\tau) + G_2(x-\varepsilon|\tau)\right] \,, \tag{7.46}$$

where $G_{\text{tot.}}$ is the total Green's function due to the two sources at $z = \pm\varepsilon$. This by itself does not lead to a substantial modification, since its local behavior near $z = 0$ is just the above logs, so we recover the same correction to the action of the ED3 at $z = 0$. However, there is an important novelty in the compact model, since there are locations away from $z = 0$ where the B-field induced on the volume of the ED3-brane can be canceled by a suitable worldvolume magnetic flux, giving a vanishing (7.25) on the ED3. Namely, recalling (7.36), we see that for an ED3 at $x^1 = n_1/N$, $y^1 = n_2/N$, with $n_i \in \mathbb{Z}$, we may cancel the induced B-field by choosing

$$F_2 = -\left(n_1 dx^2 \wedge dx^3 + n_2 dy^2 \wedge dx^3\right) \,. \tag{7.47}$$

This is nothing but the ED3 version of the open string landscape of [157]. These ED3s are in the same topological charge sector as the original ED3 at $z = 0$ because $\int_{\mathbf{X}_4} F_2 \wedge F_2 = 0$. Hence, the condition that we actually obtain a violation of the WGC is that the backreacted ED3 action increases for all points of the ED3 open string landscape. In terms of (7.46), the condition is that the value of $G_{\text{tot.}}$ is negative at **all** the ED3 open string landscape points.

Since flux quantization in orientifolds of $\mathbf{T}^6$ requires that N must be at least a multiple of 2 (and possibly for 4 or 8, in further orbifolds), the ED3 open string landscape points include at least the four points $z = 0, 1/2, \tau/2, (1+\tau)/2$. This is non-trivial, since recall the integral of the Green's function integrates to zero over $\mathbf{T}^2$, hence scans over both positive and negative values. In fact, we have performed extended numerical checks for different values of ε and τ, and have always found that the above condition seems impossible to fulfill. In other words, even if the value of $G_{\text{tot.}}$ can be made negative at one or even several of these points, there is always at least one of them where $G_{\text{tot.}}$ is positive. In Figures 7.1, 7.2 we provide typical examples for $\tau = 2i$, $\varepsilon = 0.1, 0.2$, and $N = 2, 4$.

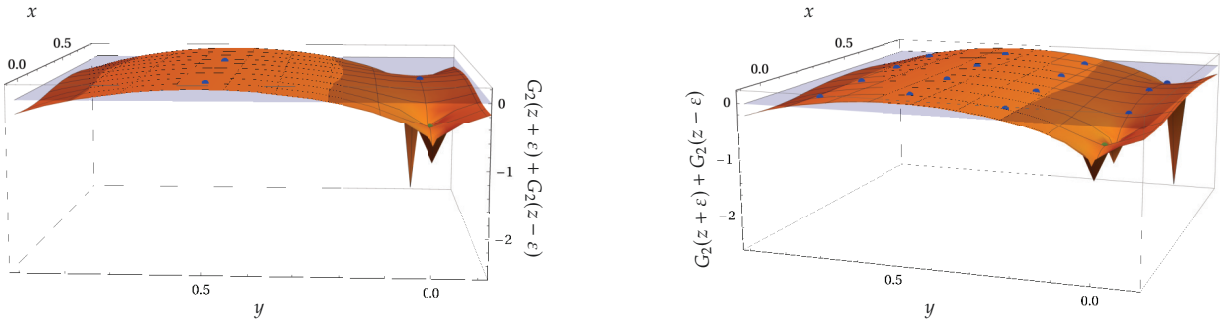

(a) $N = 2$.

(b) $N = 4$.

Figure 7.1: Plot of $G_{\text{tot.}}$ for $\tau = 2i$ and $\varepsilon = 0.1$. The blue dots are the ED3 open string landscape points, and the green one $z = 0$.

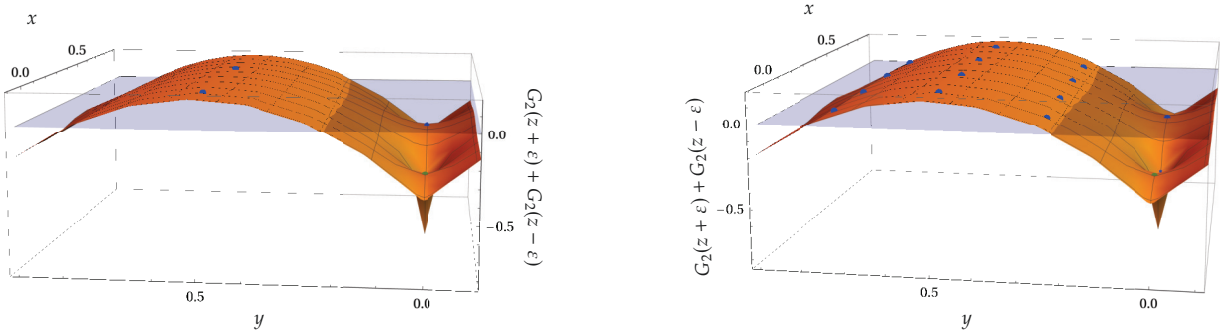

(a) $N = 2$.

(b) $N = 4$.

Figure 7.2: Plot of $G_{\text{tot.}}$ for $\tau = 2i$ and $\varepsilon = 0.1$. The blue dots are the ED3 open string landscape points, and the green one $z = 0$.

The pattern is clear and shows that there is no violation of the WGC in this sector of axion charges. Although it could be interesting to have a direct analytical proof of this result, we instead move the discussing the WGC in other closely related charge sectors.

7.4.3.3 The fractional ED3/ED(−1) sector

The discussion in the previous section makes it clear that the WGC for regular ED3s is satisfied precisely because they are free to move in the $\mathbf{T}^2$, so that there is always a representative of the charge sector with small enough action. In this section we seek further and consider fractional ED3-branes, which can be stuck at fixed points, and show that the corresponding WGC is violated.

In orientifolds of toroidal orbifolds, in addition to the regular ED3-branes there may be fractional ED3-branes, stuck at the orbifold fixed points. These arise when it is possible to endow the ED3-branes with Chan-Paton indices not in the regular representation of the orbifold group. On general grounds, it is not obvious that one can build models in which D7-branes can be mobile (as we need, to move off the minimum) while admitting fractional ED3-branes stuck at the orbifold points. We postpone this technical discussion and the construction of an explicit model to Section 7.5, and here proceed with those aspects related to the WGC.

For our purposes in this section, it suffices to note that flux quantization in orbifolds ensures that the orbifold points lie at possible ED3 open string landscape positions, so that (suitably magnetized) fractional ED3s maintain their minimal action, without suffering an increase due to the pullbacked B-field. Hence, since these ED3's are stuck at such position, it would naively seem straightforward to find values of parameters τ, ε, such that the $G_{\text{tot.}}$ at that particular location is negative. Some obvious examples are given by the figures above. This would seem to lead to direct violation of the WGC.

However, although the final conclusion is correct, this is not exactly how things work, due to important subtleties. Recall the intuition that fractional branes cannot move off the fixed point because they carry charges under RR fields in the orbifold twisted sector (geometrically, they are secretly wrapped on the cycles collapsed at the orbifold singularity). In other words, they can be regarded as ED3/ED(−1)-brane bound states. We are thus dealing with a multi-charge sector, and must hence consider the multi-axion version of the WGC. This is described in terms of the convex hull WGC [85, 122, 189]. In the following, we sketch the discussion in the simplified situation that there is only one twisted axion,[60] since the generalization to several introduces no new features. Also, we abuse language to use the more familiar particle WGC terminology, such as 'state' or 'mass' (instead of instanton and action).

Consider the situation before the introduction of the 3-form fluxes. We can consider the set of BPS (possibly fractional) ED3/ED(−1)-brane bound states, for arbitrary charges. The BPS condition ensures that all these states saturate the WGC condition, and that their charge to mass ratio lie in the extremal region given by the unit ball. Namely, for any rational direction in charge space, there is a BPS state saturating the WGC, namely with unit charge to mass ratio. This is illustrated in Figure 7.3a.

Let us now consider including the backreaction effects. In the direction of the purely untwisted charge, the discussion is as in the previous section, and although the fractional ED3 at the orbifold point does not satisfy the WGC bound, the theory does contain other states satisfying the strict inequality. Hence, the curve of former BPS states is deformed outward along that direction, with the deformation controlled by the small parameter ε.

In the direction of the purely twisted charge, the charged states are (fractional and regular) ED(−1)-branes. Although we have not discussed them in Section 7.3, the backreaction effects are straightforward to describe. Since they have no extended dimensions, the ED(−1)-branes are insensitive to the warp factor sourced by the induced D3-brane

60: We are also skipping the discussion of the 10d axion, to which ED(−1)-brane instantons couple; again they do not significantly change the argument or its conclusion.

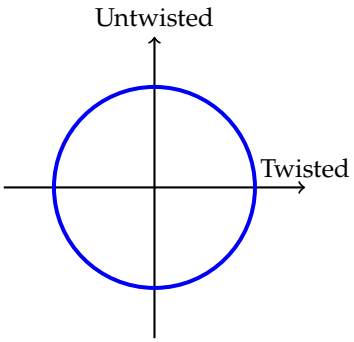

(a) In the BPS case, the solid line describes the set of BPS states, saturating the WGC for any rational direction.

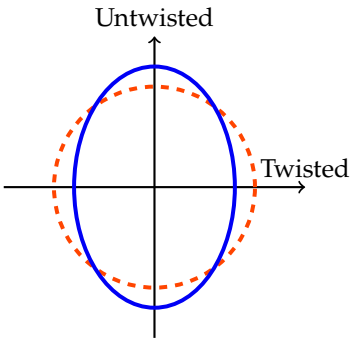

(b) After including the backreaction, the curve of the former BPS states is deformed away from the unit circle. In the purely untwisted charge direction, the WGC is satisfied, but it is violated in the purely twisted charge direction.

Figure 7.3: The 2-axion convex hull WGC before and after including the backreaction.

charge; on the other hand, their action is controlled by g_s^{-1}, which gets corrected due to the induced D5-brane charge. Promoting its value (7.38) to the global setup, we find a correction given by (7.46), with a positive definite coefficient $C \sim N|\varepsilon|$ from the 5-brane source. In analogy with the argument for ED3s, this correction increases the action for fractional ED(-1) brane instantons, again with the deviation controlled by ε. Since we are dealing with twisted charges, there are no representatives in this charge sector in other locations, so there is no charged states satisfying the WGC in this charge sector. Combining results for general rational charge vectors, the WGC diagram looks like Figure 7.3b. The unit ball is squashed by an amount controlled by ε, and there is a violation of the WGC in the direction close enough to the purely twisted axion charge vector.

We can be more precise about Figure 7.3. In Figure 7.3a we are showing all possible states with charges (n, m) under the untwisted and twisted axions given by bound states of ED3-branes wrapped n times on $\mathbf{T}^2$ and m fractional ED(-1)-brane instantons. Since they are BPS they fill out the round circle. In Figure 7.3b, the corrections controlled by ε go in opposite directions for the untwisted and twisted directions, and the states fill out the ellipse. Since now the convex hull does not contain the unit ball, there is a violation of the WGC, in particular close to the twisted axion charge vector.

As a final remark, note that we have not discussed the values of the Planck scale and axion decay constants. In fact, since we are working in the effective theory of the supersymmetric vacuum, and have simply changed a scalar VEV, the axion decay constants remain fixed; or more precisely, any change in the axion decay constant should be encoded in a dependence on the scalars. This would lead to a discussion in terms of the scalar WGC (see [90], also [190, 191] for variants, and [78] for the axion version). However, this does not help to satisfy the constraint since e.g. for a single axion the scalar WGC reads [78]

$$f^2 S^2 + f^2 (\partial_\phi S)^2 M_P^2 \leq M_P^2 \,. \tag{7.48}$$

Hence the scalar contribution is positive definite and adds to the gravitational contribution.

The simplest explanation for the non-fulfillment of the WGC in the configuration is thus that it does not provide a consistent background, due to the artificial removal of the dynamical tadpole. In other words, the configuration makes the inconsistency of the background manifest as an incompatibility with QG, namely with the swampland constraint.

In the next section, we build an explicit orientifold with the features described above. Readers not interested in the details are advised to jump to the conclusions in Section 7.6.

7.5 An explicit $\mathbb{Z}_2 \times \mathbb{Z}_2$ orientifold example

In this section, we build an orientifold of $\mathbf{T}^6/(\mathbb{Z}_2 \times \mathbb{Z}_2)$ with mobile D7_1-branes which allows for fractional ED3 branes stuck at some fixed points, hence provides an explicit realization of the above ideas. As we

will see, the fact that we are interested in D7- and ED3-branes associated to the same 4-cycle in $\mathbf{T}^6$ makes it non-trivial to allow mobile D7s and stuck ED3s. For the benefit of the reader, we take the opportunity to review the key points of type IIB orientifolds, and some of the main models illustrating them, to better explain our eventual choice of the final model realizing mobile D7-branes and stuck ED3-branes.

7.5.1 Choice of discrete torsion

Orientifolds of $\mathbf{T}^6/(\mathbb{Z}_2 \times \mathbb{Z}_2)$ have been studied for decades, and illustrate the wealth of possible discrete parameters in defining orientifolds of orbifold varieties. On one hand, the $\mathbf{T}^6/(\mathbb{Z}_2 \times \mathbb{Z}_2)$ orbifold admits a choice of $\mathbb{Z}_2$ discrete torsion [192–194]. The two resulting models are distinguished by a parameter $\varepsilon = \pm 1$ determining the action of the generator θ of one of the $\mathbb{Z}_2$'s on the states of the sector twisted by the generator ω of the second $\mathbb{Z}_2$ (equivalently, as a relative weight between two disjoint $\mathrm{SL}(2,\mathbb{Z})$ orbits of contributions to the torus partition function). Since the twisted sector of ω contains 2-cycles (collapsed at the orbifold singularities) and 3-cycles (given by the 2-cycles times a 1-cycle in the unrotated $\mathbf{T}^2$), the choice of discrete torsion determines if the θ projection keeps the ω-twisted 2-cycles or the 3-cycles. Including a similar analysis for the three different twisted sectors, and the untwisted contributions, the resulting CY 3-folds have Hodge numbers $(h_{1,1}, h_{2,1}) = (3, 51)$ for one choice (which we will refer to as without discrete torsion, and denote with $\varepsilon = +1$) and $(h_{1,1}, h_{2,1}) = (51, 3)$ for the other choice (which we will refer to as with discrete torsion, and denote with $\varepsilon = -1$). We warn the reader that the convention of 'with/without' is not uniform in the literature, and that we follow the one used in part of the literature on orientifolds (see later), which is opposite to e.g. [194].

From a geometric perspective, a fractional ED3-brane wrapped on a holomorphic 4-cycle stuck at orbifold fixed points must be secretly wrapped on a collapsed 2-cycle at the singularity. Hence, to allow for them, the underlying orbifold model must contain blowup 2-cycles, namely, it must be the $(h_{1,1}, h_{2,1}) = (51, 3)$ choice (with discrete torsion or $\varepsilon = -1$, in our conventions).

This means that the $\mathbf{T}^6/(\mathbb{Z}_2 \times \mathbb{Z}_2)$ orientifold we need is **not** the one constructed in [195], which corresponds to the model $(h_{1,1}, h_{2,1}) = (3, 51)$ (without discrete torsion, or $\varepsilon = +1$, in our convention). This can be checked by noticing that the Chan-Paton matrices defining the orbifold actions on the D-branes give not a true representation of the orbifold group, but a projective one, as explained in [196, 197] (the 'with/without' convention there is opposite to ours, and follows [194]). Instead, we must focus on models based on the choice $(h_{1,1}, h_{2,1}) = (51, 3)$ (with discrete torsion, or $\varepsilon = -1$, in our convention). This may sound troublesome, since models with this choice of discrete torsion tend to have positively charged orientifold planes, and hence require the introduction of antibranes [198, 199] (see also [148–150, 200, 201] for examples in other orientifolds). We will later on see how our model does not suffer from this problem.

7.5.2 Choice of vector structure

When performing the orientifold quotient, there are further discrete choices to consider.[61] In the twisted sectors of a general orbifold element $\mathbb{Z}_n$, the orientifold usually acts by exchanging oppositely twisted sectors.[62] This implies that the sector twisted by an order 2 orbifold element R is mapped to itself, and there is a discrete choice of sign for the corresponding orientifold action Ω' (where the prime indicates that the worldsheet parity is in general accompanied by geometric, or other, actions) [203]. As explained in this reference, this manifests in the open string sector of a Dp-brane as the following condition on the Chan-Paton matrices

$$\gamma_{R,p} = \pm\gamma_{\Omega',p}\gamma_{R,p}^{T}\gamma_{\Omega',p}^{-1}\,. \tag{7.49}$$

The choices $+/-$ are (this time, universally) known as with/without vector structure, see [204] (also [205]) for geometric interpretation underlying the naming. An important aspect is that the choice is correlated with a choice of the orientifold action on the closed string sector, hence the sign choice in the open sector must hold for **all** D-branes in the model.

A typical choice of Chan-Paton matrices for any of these branes in models without vector structure is, in a suitable basis,

$$\gamma_{R,p} = \mathrm{diag}(i\mathbb{1}_n, -i\mathbb{1}_n)\,,\ \gamma_{\Omega',p} = \begin{pmatrix} & \mathbb{1}_n \\ \mathbb{1}_n & \end{pmatrix} \text{ or } \gamma_{\Omega',p} = \begin{pmatrix} & i\mathbb{1}_n \\ -i\mathbb{1}_n & \end{pmatrix}, \tag{7.50}$$

where n denotes the number of D-branes in a given set fixed under the orbifold and orientifold actions, and the two choices of $\gamma_{\Omega',p}$ are symmetric/antisymmetric for the SO/Sp projections. For instance, the 6d $\mathbf{T}^4/\mathbb{Z}_2$ model in [206, 207] corresponds to the above action for $n = 16$ on 32 coincident D-branes mapped to themselves by the orbifold and orientifold actions. Similarly, in the 4d model in [195] the orientifold action on each $\mathbb{Z}_2$ orbifold twist is of this kind (albeit in a not simultaneously diagonalizable way, as befits the projective representation required for the discrete torsion choice of the model). Generalizations to other orbifold groups have also been constructed [208] (see also [209]).

As is clear from the template (7.50), the orientifold acts by exchanging the two different kinds of fractional branes of the underlying $\mathbb{Z}_2$ orbifold. Hence, a consistent orientifold action requires that the orbifold action on D-branes is in the regular representation, namely, $\mathrm{tr}\,\gamma_{R,p} = 0$, and hence one cannot have stuck fractional D-branes. For our purposes in the main text, this would be fine to allow for mobile D7-branes, but it forbids having stuck ED3-branes. Note that, in the particular case of the model in [195], this also agrees with our earlier discussion of the absence of fractional 4-cycles for that choice of discrete torsion.

Hence, for our purposes in the main text, we are interested in models where the orientifold action on an orbifold element rotating the first complex plane is with vector structure. Models with vector structure have been considered, starting from [203] (see [210] for 4d examples) and they involve an extra subtlety. In the D9-brane description, the orbifold fixed points, also fixed under this orientifold action with vector structure, have a positive RR charge. Hence, as shown in [203], a consistent supersymmetric model can be achieved only if 8 of the 16 fixed points have orientifold

61: Actually, the most obvious choice would be the SO/Sp projection. In the discussion below, we assume we take the projection corresponding to negatively charged orientifold planes, to the extent allowed by the other discrete choices (which in some cases force some of these orientifold planes to be positively charged).

62: See [202] for a notable exception.

action with vector structure, and the other 8 have orientifold action without vector structure (with the difference implemented by a suitable Wilson line). The model thus contains D9-branes, but no D5-branes. The model has a T-dual with D5-branes and no D9-branes, which had been constructed in [211]. We now turn to the construction of this 6d model, but in terms of D7-branes, to later employ it to build a 4d model with mobile D7-branes and admitting stuck ED3s.

The construction of the 6d model is as follows. Take $\mathbf{T}^4$ parameterized by (z_1, z_2) with $z_i = x_i + \tau_i y_i$, and x_i, y_i with periodicities 1. We have a $\mathbb{Z}_2$ orbifold action generated by $\theta : (z_1, z_2) \to (-z_1, -z_2)$, with 16 orbifold fixed points at the locations $x_i = 0, \frac{1}{2}$, $y_i = 0, \frac{1}{2}$. We orientifold by $\Omega R_1 (-1)^{F_L}$ with $R_1 : (z_1, z_2) \to \left(-z_1 + \frac{1}{2}, z_2\right)$. This leads to 4 $O7_1$-planes (which we take negatively charged), located at $x_1 = \frac{1}{4}, \frac{3}{4}$, $y_1 = 0, \frac{1}{2}$, and spanning z_2. There are 32 $D7_1$-branes, whose distribution in the z_1 plane should respect the symmetries and will be discussed later on. The orbifold fixed points do not sit on top of the $O7_1$-planes, so the orientifold action exchanges them. The orientifold group also includes the element $\Omega R_1 \theta (-1)^{F_L}$, which is however freely acting since $R_1 \theta : (z_1, z_2) \to \left(z_1 + \frac{1}{2}, -z_2\right)$. Hence, there are no crosscap RR tadpoles, namely, no $O7_2$-planes, and hence no $D7_2$-branes need to be introduced. This reproduces the cancellation of untwisted tadpoles with only one kind of brane, as in the T-duals [203, 211]. On the other hand, since the orientifold planes do not coincide with the orbifold fixed points, they do not induce twisted RR tadpoles. Hence, the $D7_1$-branes can be located anywhere in the z_1-plane, for instance as 8 independent D7-branes with their corresponding orbifold and orientifold images. If they are located on top of an orbifold or orientifold fixed point, their symmetry is enhanced. For instance, locating 16 D7-branes on top of an orientifold plane and 16 on top of its orbifold image, one gets SO(16) vector multiplets of 6d $\mathcal{N} = 1$, with one adjoint hypermultiplet. If we locate 16 D7-branes on top of an orbifold point, and 16 at its orientifold image, the cancellation of RR disk twisted tadpoles enforces

$$\mathrm{tr}\, \gamma_{\theta,7_1} = 0 \to \gamma_{\theta,7_1} = \mathrm{diag}(\mathbb{1}_8, -\mathbb{1}_8)\,, \tag{7.51}$$

at each of the two orbifold fixed points. In this case, the gauge group is $U(8)^2$, with two hypermultiplets in the $(\,\square\,,\,\overline{\square}\,)$. Although sitting at the orbifold fixed point, the $D7_1$-branes can be moved off into the bulk, and this corresponds to Higgsing with the bifundamental down to less symmetric patterns, possibly down to the generic $U(1)^8$. As a related comment, note that the equality of +1 and -1 entries in (7.51) is not enforced by the orientifold action (which is merely mapping one orbifold fixed point to the other), but by the disk RR tadpole condition. This implies that it is perfectly consistent to have a D3-brane wrapped on the directions z_2 and sitting at an orbifold fixed point in z_1 (with another D3-brane at its orientifold image position) with

$$\mathrm{tr}\, \gamma_{\theta,3} \neq 0 \to \text{ e.g. } \gamma_{\theta,3} = 1\,. \tag{7.52}$$

This D3-brane sources a twisted tadpole, but there are non-compact dimensions transverse to it in which the flux lines can escape to infinity. The fact that the D3-brane sources this charge implies it cannot be moved off the orbifold fixed point. Indeed, the open string sector does not contain any matter fields for the choice (7.52). This wrapped D3-brane

corresponds to a BPS string in the 6d theory, and is to become a stuck ED3 in the upcoming 4d model, by wrapping its two dimensions on the extra $\mathbf{T}^2$.

7.5.3 The 4d model

It is now easy to combine different above ingredients to build a 4d model with mobile D7-branes and admitting stuck ED3s. We consider a factorized $\mathbf{T}^6$ parameterized by (z_1, z_2, z_3) with $z_i = x_i + \tau_i y_i$, and x_i, y_i with periodicities 1. We mod out by the $\mathbb{Z}_2 \times \mathbb{Z}_2$ orbifold action generated by θ: $(z_1, z_2, z_3) \to (-z_1, -z_2, z_3)$ and ω: $(z_1, z_2, z_3) \to (z_1, -z_2, -z_3)$. This leads to the familiar 16×3 orbifold fixed planes, and as explained in Section 7.5.1, we choose the model leading to $(h_{1,1}, h_{2,1}) = (51, 3)$ (i.e. with discrete torsion or $\varepsilon = -1$, in our convention).

We now perform an orientifold $\Omega R_1 (-1)^{F_L}$, with R_1: $(z_1, z_2, z_3) \to (-z_1 + 1/2, z_2, z_3)$. As explained in Section 7.5.2, this leads to 4 $O7_1$-planes located at $x_1 = 1/4, 3/4$, $y_1 = 0, 1/2$, and spanning z_2. On the other hand, $\Omega R_1 \theta (-1)^{F_L}$ and $\Omega R_1 \theta\omega (-1)^{F_L}$ act with a shift in the coordinate z_1, hence are freely acting and do not introduce $O7_2$- and $O7_3$-planes. Finally, $\Omega R_1 \omega (-1)^{F_L}$ acts geometrically as $R_1\omega$: $(z_1, z_2, z_3) \to (-z_1 + 1/2, -z_2, -z_3)$, and leads to 64 O3-planes, at $x_1 = 1/4, 3/4$, $y_1 = 0, 1/2$, $x_i, y_i = 0, 1/2$ for $i = 2, 3$. Note that the $O7_1$ planes exchange the θ-fixed orbifold points (and similarly for the $\omega\theta$-fixed points), but maps each ω-fixed plane to itself (and similarly for the O3-planes). In particular, notice that there are points which are simultaneously fixed under the ω action and the O3-plane (or $O7_1$-plane) action.

We must now specify the discrete choices for these orientifold actions to achieve the desired result. We take negatively charged $O7_1$-planes to have a total of 32 $D7_1$-branes, as counted in the covering space. Since we seek to have mobile $D7_1$-branes and stuck ED3-branes in z_1, we need the action of $\Omega R_1 (-1)^{F_L}$ on the θ orbifold to be with vector structure, just as in the last 6d example discussed above. On the other hand, the action of $\Omega R_1 (-1)^{F_L}$ on the ω orbifold cannot be with vector structure, since this would lead to positively charged O3-planes, whose RR charge cannot be canceled in a supersymmetric way. Hence, this sector should have Chan-Paton matrices without vector structure. The orientifold action on the $\theta\omega$ sector follows from the above, and is without vector structure.

Notice that this pattern matches the observation in [198] that in orientifolds of $\mathbf{T}^6/(\mathbb{Z}_2 \times \mathbb{Z}_2)$ there are three discrete sign choices ε_i determining the orientifold action on the corresponding orbifold element, morally $\varepsilon_i = +1$ (resp. $\varepsilon_i = -1$) implies the corresponding orientifold planes are negatively (resp. positively) charged. These signs are correlated with the discrete torsion parameter ε by $\varepsilon_1 \varepsilon_2 \varepsilon_3 = \varepsilon$. Our model has a discrete torsion $\varepsilon = -1$, and hence requires that at least one orientifold action has $\varepsilon_i = -1$. However, the model cleverly evades the need to introduce positively charged orientifolds planes, because the $\varepsilon_i = -1$ action corresponds to the θ orbifold sector, where the orientifold action is freely acting and no actual orientifold planes appear. The two $\varepsilon_i = +1$ sectors are the $\theta\omega$ sector, without orientifold planes, and the ω, with negatively charged O3-planes.

To make the above description more explicit, let us describe the Chan-Paton action on the 32 D3-branes. In the actual model in the main text, the D3-branes will actually be replaced by 3-form fluxes, see Section 7.5.4, so they are here used just to illustrate the effect of discrete choices in open string sectors.

We consider 16 D3-branes located at and O3-plane, and 16 at the image under the orbifold action θ (or $\theta\omega$). Each set is mapped to itself by the action ω and by $\Omega' \equiv \Omega R_1 (-1)^{F_L}$, which should be represented by matrices $\gamma_{\omega,3}$, $\gamma_{\Omega',3}$ of the form (7.50). On the other hand, if we include the 16+16 set in a single matrix $\gamma_{\theta,3}$ to describe the action of θ, its interplay with $\Omega R_1 (-1)^{F_L}$ should be with vector structure. Finally, recall that the matrices $\gamma_{\theta,3}$, $\gamma_{\omega,3}$ should provide a non-projective representation of the orbifold group, due to the choice of discrete torsion. A simple choice satisfying these properties is

$$\gamma_{\theta,3} = \begin{pmatrix} & \mathbb{1}_{16} \\ \mathbb{1}_{16} & \end{pmatrix}, \quad \gamma_{\omega,3} = \mathrm{diag}\,(i\mathbb{1}_8, -i\mathbb{1}_8; i\mathbb{1}_8, -i\mathbb{1}_8)\,,$$
$$\gamma_{\Omega',3} = \begin{pmatrix} & i\mathbb{1}_8 & & \\ -i\mathbb{1}_8 & & & \\ & & & i\mathbb{1}_8 \\ & & -i\mathbb{1}_8 & \end{pmatrix}. \tag{7.53}$$

Although $\gamma_{\theta,3}$ and $\gamma_{\omega,3}$ commute, we have not diagonalized the former to maintain the 16+16 split manifest. The matrices satisfy (7.49) with + sign for $\gamma_{\theta,3}$ and − sign for $\gamma_{\omega,3}$. We have chosen the antisymmetric $\gamma_{\Omega',3}$ corresponding to an Sp projection.

For $D7_1$ branes, we choose to locate 8 on top of each $O7_1$-plane, which we recall are exchanged pairwise by θ. The Chan-Paton matrices in the corresponding 8+8 set are similar to the above, but with symmetric $\gamma_{\Omega',7}$, namely

$$\gamma_{\theta,7_1} = \begin{pmatrix} & \mathbb{1}_8 \\ \mathbb{1}_8 & \end{pmatrix}, \quad \gamma_{\omega,7_1} = \mathrm{diag}\,(i\mathbb{1}_4, -i\mathbb{1}_4; i\mathbb{1}_4, -i\mathbb{1}_4)\,,$$
$$\gamma_{\Omega',7_1} = \begin{pmatrix} & \mathbb{1}_4 & & \\ \mathbb{1}_4 & & & \\ & & & \mathbb{1}_4 \\ & & \mathbb{1}_4 & \end{pmatrix}. \tag{7.54}$$

7.5.4 Introducing 3-form fluxes

As already mentioned, and is clear in the main text, the model must include NSNS and RR 3-form fluxes, which contribute to the RR 4-form tadpole cancellation. In particular, in the normalization (7.34), we have

$$N_{\rm flux} = \frac{1}{(2\pi)^4 \alpha'^2} \int_{\mathbf{X}_6} F_3 \wedge H_3 = 2N^2\,. \tag{7.55}$$

The RR tadpole condition is

$$N_{\rm flux} + N_{\rm D3} = 32\,, \tag{7.56}$$

where $N_{\rm D3}$ is the number of D3-branes, as counted in the covering space. Hence, the condition for the flux contribution not to overshoot[63] the RR

63: Notice that a moderate overshoot can actually be allowed, and still maintain supersymmetry, if one includes suitably magnetized D9-branes, as implemented in [212, 213] to solve a similar overshooting problem in [184, 185, 214].

tadpole is that $N \leq 4$.

One may fear that this bound is too small for an orientifold of $\mathbf{T}^6/(\mathbb{Z}_2\times\mathbb{Z}_2)$, due to flux quantization conditions. As mentioned in the main text, it was argued in [183] that in orientifolds of $\mathbf{T}^6$, NSNS and RR fluxes must be quantized in multiples of 2, if the model has all negatively charged O3-planes, while odd quanta are allowed only if other (positively charged) exotic O3-planes are included. In addition, the $\mathbb{Z}_2$ orbifold projections in general allow for smaller 3-cycles than in the underlying $\mathbf{T}^6$, leading to more strict quantization conditions. In fact, as shown in [184, 185] the orientifold of the $\mathbf{T}^6/(\mathbb{Z}_2 \times \mathbb{Z}_2)$ with $(h_{11}, h_{21}) = (3, 51)$ (without discrete torsion, or $\varepsilon = 1$, in our convention) requires 3-form fluxes to be quantized in multiples of 8, leading to an overshoot of their RR tadpole contribution. However, happily, for the $\mathbf{T}^6/(\mathbb{Z}_2 \times \mathbb{Z}_2)$ we are actually using, with $(h_{11}, h_{21}) = (51, 3)$ (with discrete torsion, or $\varepsilon = -1$, in our convention), it was shown in [184] that 3-form fluxes must be quantized in multiples of 4. Thus, the minimum amount of flux available for this model leads to $N = 4$, which precisely saturates the RR tadpole cancellation, without need of D3-branes.

We would like to finish with an important observation, which relates flux quantization with the 'energetics' of the stuck ED3-branes of interest in the main text. The 3-form fluxes (7.34) are clearly invariant under the orbifold and orientifold transformations. However, this invariance is not manifest once we write down explicit expressions for the NSNS 2-form gauge potential. For instance, let us redefine the origin in the z^1-plane, so that the origin $z^1 = 0$ corresponds to an orientifold plane, as in the main text. Then, we may write

$$B = 4\pi^2\alpha' N \left(x^1 dx^2 \wedge dx^3 + y^1 dy^2 \wedge dx^3\right) , \tag{7.57}$$

c.f. (7.36). This is invariant under the orientifold action, but not invariant under the orbifold action (which in the z_1-plane acts as a reflection with respect to e.g. $(x^1, x^2) = (1/4, 0)$. Clearly, this is just because (7.57) holds in a local patch, and we are allowed to make gauge transformations among different patches. Hence, near $(x^1, x^2) = (1/4, 0)$ we may fix a different gauge and represent the same H_3 with

$$B = 4\pi^2\alpha' N \left(\left(x^1 - \tfrac{1}{4}\right) dx^2 \wedge dx^3 + y^1 dy^2 \wedge dx^3\right) , \tag{7.58}$$

which is invariant under the orbifold, but not the orientifold action. The question now is, if we consider ED3-brane instantons stuck at the orbifold fixed point, which of the two expressions for the B-field should we consider? This is relevant, because its pullback on the ED3 worldvolume provides a contribution to the ED3 action, and hence seems to have an impact on whether the WGC is satisfied. The answer is simply that both expressions are valid, if we consider not just a given ED3, but rather the whole set of magnetized ED3s, with different magnetization quanta. Indeed, the shift in the B-field upon the gauge transformation can be translated into a change in the magnetization of an ED3 by an amount

$$-\frac{1}{4} N dx^2 \wedge dx^3 . \tag{7.59}$$

This can be absorbed by a properly quantized worldvolume magnetic flux precisely thanks to the 3-form flux quantization condition $N = 4$ (or

a multiple thereof, in general).

An equivalent description is in terms of axion monodromy, with the 'axion' given by the position of the ED3-branes; considering the full tower of magnetized ED3-branes, the tower at $z^1 = 1/4$ is identical to the tower at $z^1 = 0$ modulo ED3-branes with different magnetization $F_2 = n dx^2 \wedge dx^3$ changing as $n \to n - 1$. Another equivalent description is in the language of [157] c.f. Section 7.4.3.2, as follows. In terms of the B-field (7.57), there is an open string landscape of BPS ED3's at points $x^1 N \in \mathbb{Z}$, $y^1 N \in \mathbb{Z}$; hence, for $N = 4$, the orbifold fixed point $z^1 = 1/4$ is one of the open string landscape points where some ED3 with suitable magnetization can cancel the corresponding B-field. This cancellation is made manifest in the alternative local expression (7.58). Notice that a similar mechanism is exploited for the $D7_1$-branes so that their distribution in sets of 8 on top of the $O7_1$-planes, as discussed in Section 7.5.3, remains a valid supersymmetric background in the presence of fluxes.

7.6 Final remarks

In this chapter, we have considered the backreaction of supersymmetry breaking effects and the corresponding dynamical tadpole in explicit examples of type IIB toroidal orientifolds. We have shown that the resulting configurations seem to violate the WGC for certain axions. We have argued that the underlying problem is due to the unphysical assumption of ignoring the effects of the dynamical tadpoles on the 4d spacetime configuration, restricting the backreaction to the internal space. Hence, these are examples of theories in which dynamical tadpoles manifest as direct incompatibility with QG, via swampland constraints.

These examples and the above interpretation open up many new avenues, among others:

- Our source of supersymmetry breaking is based on moving slightly off the minimum of an otherwise supersymmetric theory. It would be nice to carry out the arguments in this chapter in a genuinely non-supersymmetric model.
- It would be interesting to find models where the spacetime dependence sourced by the dynamical tadpole can be solved, and to address the formulation of the WGC in those backgrounds. In particular, it may well be possible that the WGC does not hold in its usual formulation. For instance, the usual black hole arguments for the WGC for particles is based on the stability of remnants, a feature which is sensitive to new effects if one is considering e.g. time-dependent configurations.
- We have also encountered models where the dynamical tadpole does not seem to lead to violation of the WGC. It would be interesting to explore if they violate some other swampland constraint. Conversely, these models could potentially be used to uncover new swampland constraints not considered hitherto.
- Cancellation of topological tadpoles (such as RR tadpoles), which are often associated to cancellation of anomalies in the spacetime theory, or on suitable probes [134]. The ED3 and ED(−1)-brane

instantons in our examples are reminiscent of probes of the dynamical tadpoles, albeit in a dynamical rather than a topological way. It would be interesting to explore the interplay of dynamical tadpoles and probes in more general setups.

These and other related questions seem capable of shedding new light in the long-standing problem of dynamical tadpoles in string theory.

Conclusions

Conclusiones

En esta tesis hemos analizado múltiples aspectos de simetrías discretas y las hemos relacionado con el programa de Ciénaga. Hemos señalado también que ignorar la presencia de tadpoles dinámicos en compatificaciones de TC puede conducir a violaciones de la CGD, señalando una incompatibilidad con GC.

La tesis se divide en tres partes principales.

La primera parte contiene desde el Capítulo 1 al Capítulo 4. Presentaban el material de referencia necesario para entender los resultados principales de la tesis. En el Capítulo 1 hemos examinado los conceptos básicos de la correspondencia AdS / TCC que sienta las bases de las teorías y los instrumentos que habríamos usado en los capítulos siguientes. Hemos analizado también cuáles son las condiciones para una compatificación consistente de tipo II sobre CY con orientifolds y flujos, centrándonos en particular en la TC de tipo IIA.
En el Capítulo 2 hemos introducido el concepto de teoría de gauge con quivers y, para las teoría de gauge tórica, las hemos descrito usando diagramas de dimers y sus duales, quiver periódicos. En la Sección 2.3 y 2.3.1 hemos descrito una nueva manera para obtener simetrías U(1) globales a partir de propiedades topológicas de los dimers (o quiver periódicos), usando lo que hemos llamado identidades geométricas.
En el Capítulo 3 hemos analizado simetrías discretas de gauge, en particular cómo la simetrías discretas de gauge surgen naturalmente en la compactificación de TC. Hemos introducido los acoplamientos DKS en 4d que señalan la presencia de simetrías discretas, bajo las cuales las paredes de dominios tienen carga. Desde el punto de vista de las TsCC, hemos introducido el grupo de Heisenberg discreto que surge en la 4d TsCC definida en las D3-branas que sondan singularidades de orbifolds generales para generales CYs 3-folds toricas.
En el Capítulo 4 hemos elegido resumir el programa de Ciénaga en su objetivo y características principales. Nos hemos centrado en las principales conjeturas, y en particular sobre las principales versiones de la CGD que juegan una función importante en los siguientes capítulos de esta tesis.

La segunda parte trata sobre la relación entre simetrías discretas y el programa del Ciénaga. Primero, hemos estudiado las simetrías discretas globales en TsCC en 4d en el Capítulo 5 y, luego, hemos estudiado simetrías discretas de gauge en compatificación de TC en el Capítulo 6. De hecho, en el Capítulo 5, hemos aplicado las técnicas de los diagramas dimer para descubrir las simetrías discretas globales en las teorías de campos sobre D3-branas en singularidades dadas por orbifolds generales de singularidades de CY 3-fold tóricas generales.
Primero hemos descrito cómo es posible definir las simetrías discretas desde el espacio de cobertura de la teoría con el orbifold, y luego hemos encontrado una manera algorítmica de definir las cargas de los campos quirales que tienen carga bajo las simetrías discretas del grupo de Heisenberg. Se presentan muchos ejemplos como prueba de la universalidad de nuestra técnica por cualquier orbifold que preserva

por lo menos $\mathcal{N} = 1$ de supersimetría en 4d. Hemos concluido con unos comentarios sobre el dual gravitacional. Este dual ha sido usado en el Capítulo 6 como apoyo para nuestras conjeturas. Estas conjeturas son la primera formulación precisa de la importancia de las simetrías discretas en el programa del Ciénaga.
La primera conjetura es la $\mathbb{Z}_k$ CAD en la Conjetura 6.1. Dicha conjetura dice que en una teoría de GQ con una simetría discreta $\mathbb{Z}_k$ de gauge y una simetría U(1) de gauge con acoplamiento g, el acopiamiento de gauge escala como $g\ k^{-\alpha}$, con α un número de orden 1. Hemos mostrado ejemplos para apoyar dicha conjetura. Por ejemplo todos los duales gravitacionales de las teorías que tienen un grupo discreto de Heisenberg satisfacen la conjetura. Otro ejemplo es el modelo ABJM, ambos en la formulación de tipo IIA y de teoría M, que satisface la conjetura.
La segunda conjetura es la $\mathbb{Z}_k$ RCDAF en la Conjetura 6.2. Esta conjetura es un refinamiento de la CDAF en el caso en el cual hay una simetría de gauge discreta $\mathbb{Z}_k$. En particular, dicha simetría discreta está relacionada con paredes de dominio en 4d, asociadas a 3-formas. La declaración exacta de la conjetura es que en una teoría de GQ sobre un vacío de AdS, con una simetría discreta $\mathbb{Z}_k$ para paredes de dominio, en el límite de espacio plano, la constante cosmológica L escala con M2k.1, donde M es la masa de una torre infinita de estados que muestran que la TCE se está rompiendo. Esto es un resultado importante que puede explicar la presencia de la separación de escala en vacíos de AdS en compactificación de TC. Para apoyar nuestra conjetura hemos usado fórmulas de uniones (presentadas en el Apéndice A) que nos permiten calcular el comportamiento de la constante cosmológica en completa generalidad.

Hay interesantes argumentos que pueden ser desarrollados partiendo de los resultados del Capítulo 6. Aquí podemos comentar dos:

- Una consecuencia directa de la CAD es que es posible hacer el acoplamiento de gauge de una simetría de gauge U(1) arbitrariamente pequeño si hay una simetría discreta $\mathbb{Z}_k$ con k arbitrariamente grande. Esto puede resultar en una violación de la CGD, y sería interesante encontrar un límite del orden de la simetría discreta de manera que las teorías efectivas permanecen consistentes con los principios de la gravedad cuántica.
- Todos los vacíos que hemos estudiado cuando hemos propuesto nuestras conjeturas son en AdS y en una configuración supersimétrica. Esperamos que la CAD sea verdadera también cuando hay otros fondos y sería interesante comporbar si es verdadera también en casos no supersimétricos. En estos escenarios no siempre es fácil identificar la torre que se convierte en ligeras cuando la teoría se rompe, además, hay meno control de las masas de las partículas cargadas bajo las simetrías consideradas. Sin embargo, puede ser importante investigar ulteriormente tales configuraciones para conectar con nuestro Universo.

La tercera y última parte contiene el Capítulo 7. Hemos estudiado el comportamiento de la CGD por axiones en compactificaciones de tipo IIB sobre toros con orientifolds y flujos que admiten D7-branas móviles. Cuando las D7-branas se mueven fuera del mínimo, se forma un tadpole dinámico, y si se ha ignorado, se viola la CGD. Primero hemos dado un argumento heurístico usando el dual gravitacional del laa-maximización,

es decir la minimización del volumen, explicado en la Sección 1.1.4. Si consideramos D3-branas que envuelven 3-ciclos holomorfos, hemos mostrado que la CGD se satisface solo si imponemos las ecuaciones del movimiento, es decir si minimizamos el volumen del ciclo. Esto ha sido usado como un indicio que la CGD, tal y como está formulada, podría ser válida solo al mínimo de un potencial.
Luego hemos estudiado las reacciones de D-branas en la geometría y los otros campos en compatificaciones de tipo IIB. Como calentamiento, hemos estudiado primero los casos supersimétricos, sin flujos, y luego hemos hecho los casos no supersimétricos con flujos. Hemos construido una compatificación explicita sobre toros con orientifolds y flujos que permiten por D7-branas móviles. Hemos estudiado la reacción proveniente desde las D7-branas, cuando estaban fuera de la posición de equilibrio, sobre branas instantónicas. Si elegimos ignorar el tadpole dinámico que se forma cuando la D7-brana está fuera del mínimo, hay estados que violan la Convex Hull CGD para axioness. Pero, hemos encontrado también modelos donde los tadpoles dinámicos no parecían conducir a una violación de la CGD. Sería interesante explorar si violan otras conjeturas del Ciénaga. Además, estos modelos pueden potencialmente conducir a nuevas limitaciones del Ciénaga que no hemos considerado hasta ahora.

En esta tesis hemos hecho progresos en el entendimiento de GC, en particular hemos enseñado cómo las simetrías discretas pueden jugar un papel en el programa del Ciénaga y en GC en general. Por ejemplo, pueden explicar porqué hay separación de escala en el modelo DGKT de estabilización de módulos. Además, está claro que también las simetrías continuas se ven afectadas por la presencia de las simetrías discretas, entonces su física tiene que ser investigada ulteriormente.
El estudio de la relación entre la presencia de tadpoles dinámicos y el programa de Ciénaga es también importante. De hecho, uno de los fines del programa de Ciénaga es refinar sus conjeturas con el fin de delimitar lo máximo posible la frontera entre el Ciénaga y el Panorama. El hecho de que hayamos encontrado violaciones en la CGD cuando los tadpoles dinámicos han sido ignorados permite una doble interpretación: por un lado GC parece ser consciente de que la solución que ha sido usada no era la correcta, porque el tadpole dinámico ha sido ignorado. Por otro lado, es posible que la CGD tenga que ser modificada para que sea verdadera en todo el espacio de los campos.
Esta tesis ha dado respuesta a unas preguntas, pero también ha formulado nuevas interesantes preguntas cuya respuesta puede contribuir a esta nueva era de Fenomenología de TC.

Conclusions

In this thesis, we have analyzed multiple aspects of discrete symmetries and related them to the Swampland program. We have also pointed out that ignoring the presence of dynamical tadpoles in ST compactifications may lead to violations of the WGC, signaling an incompatibility with QG.

The thesis is divided in three main parts.

The first part contains Chapters 1 to 4. They were reviewing the background material that was necessary to understand the main results of the thesis. In Chapter 1 we reviewed the basic concepts of the AdS / CFT correspondence to lay the foundations to the theories and the tools that we would have used in the following chapters. We have also reviewed what are the conditions for a consistent tree-level type II compactification on CY orientifold with fluxes, focusing in particular, on type IIA ST.
In Chapter 2 we have introduced the concept of quiver gauge theories and, for toric gauge theories, we have also described them in terms of dimer diagrams and their dual periodic quivers. It is in Sections 2.3 and 2.3.1 that we described a new way to get global U(1) symmetries from the topological properties of dimer diagrams (or periodic quivers), using what we called geometric identities.
In Chapter 3 we reviewed discrete gauge symmetries, in particular, how gauge discrete symmetries arise naturally in string theory compactifications. We introduce the DKS couplings in 4d that signal the presence of discrete symmetries, under which domain walls are charged. From the SCFT point of view, we introduced the discrete Heisenberg group that arise in 4d SCFTs defined on the worldvolume of D3-branes probing general orbifold singularities for general toric CY 3-folds.
In Chapter 4 we decided to review the Swampland program in its aim and main characteristics. We focused on the principal conjectures, and in particular, on the various version of the WGC that played a major rôle in the following chapters of this thesis.

The second part discussed the interplay between the discrete symmetries and the Swampland program. We first studied global discrete symmetries in 4d SCFTs in Chapter 5 and, then, we studied gauge discrete symmetries in ST compactifications in Chapter 6.
Indeed, in Chapter 5, we applied dimer diagram techniques to uncover discrete global symmetries in the fields theories on D3-branes at singularities given by general orbifolds of general toric CY 3-fold singularities. We first described how it was possible to define discrete symmetries from the covering space of the orbifolded theory, and then we found an algorithmic way to define the charges for the chiral fields under the discrete symmetries of the Heisenberg group. Many examples were also given that prove the universality of our technique for any kind of orbifold that preserves at least $\mathcal{N} = 1$ supersymmetry in 4d. We concluded with some remarks on the gravity dual. The gravity dual of these theories has been also used in Chapter 6 to provide support to our conjectures. These conjectures are the first precise formulation proving that discrete symmetries are important in the Swampland program.

The first conjecture is the $\mathbb{Z}_k$ WCC in Conjecture 6.1. Such conjecture states that in a theory of QG with a discrete $\mathbb{Z}_k$ gauge symmetry and a U(1) gauge symmetry with coupling g, the gauge coupling scales as $g \sim k^{-\alpha}$, with α some order 1 coefficient. We provided examples that support such conjecture. For instance, all the gravity dual theories that have a discrete Heisenberg group satisfy the conjecture. Another example is the ABJM model, both in the type IIA and in the M-theory formulation, that satisfies the conjecture.
The second conjecture is the $\mathbb{Z}_k$ RSADC in Conjecture 6.2. This conjecture is a refinement of the SADC in the case in which a $\mathbb{Z}_k$ gauge symmetry is present. In particular, such discrete symmetry is related to domain walls in 4d, so associated to 3-forms. The precise statement of the conjecture is that in a theory of QG on an AdS vacuum, with a $\mathbb{Z}_k$ discrete symmetry for domain walls, in the flat-space limit the cosmological constant Λ scale with $M^2 k^{-1}$, where M is the mass of an infinite tower of states signaling the breaking of the EFT. This is an important result because it can explain the presence of scale separation in AdS vacua ST compactifications. To support our conjecture, we used junctions formulas (reviewed in Appendix A) that allowed us to compute the scaling behavior of the cosmological constant in complete generality.

There are interesting topics that may be developed starting from the results of Chapter 6. Here we can comment on two of them:

- A direct consequence of the WCC is that it is in principle possible to make the gauge coupling of a U(1) gauge symmetry arbitrarily small if there exists a discrete symmetry $\mathbb{Z}_k$ with k arbitrarily large. Such effect may lead to violation of the WGC, and it would be interesting to find a bound on the order of the discrete symmetry so that the effective theories remain consistent with quantum gravity principles.
- All the vacua that we studied when we proposed our conjectures are in AdS and in a supersymmetric set up. We expect that the WCC is true also when there are other backgrounds, and it would be interesting to see if it is true also in non-supersymmetric cases. In these scenarios it is not always easy to identify the tower that is becoming light when the theory is breaking down, moreover, there is less control on the masses of the particles charged under the considered symmetries. Nevertheless, it could be important to further investigate such set-ups to make contact with our universe.

The third (and last) part contains Chapter 7. We studied the behavior of the axion WGC in type IIB compactifications on tori with orientifolds, fluxes and mobile D7-branes. When the D7-branes are moved off-shell, a dynamical tadpole is forming, and if ignored, the WGC is violated. We first gave an heuristic argument using the gravity dual of the a-maximization, i.e., volume minimization, reviewed in Section 1.1.4. If we consider D3-branes wrapping holomorphic 3-cycles, we showed that the WGC is satisfied only if impose the EoM, i.e. we minimize the volume of the cycle. This has been used as a hint that the WGC, as it is formulated, might be valid only at the minimum of a potential.
We, then, studied the backreactions of D-branes on the geometry and other fields in type IIB compactifications. As a warm-up, we first studied the supersymmetric cases without fluxes, and then we moved on to the non-supersymmetric cases with fluxes. We constructed an explicit

toroidal compactification with orientifolds and fluxes that allowed for mobile D7-branes. We studied the backreaction coming from the D7-branes moved from their stable position on instanton branes. If we decide to ignore the dynamical tadpole that forms once the D7-branes are off-shell, there are states that violate the Convex Hull WGC for axions. However, we have encountered models where the dynamical tadpole does not seem to lead to violation of the WGC. It would be interesting to explore if they violate some other swampland constraint. Moreover, these models could potentially lead to new swampland constraints not considered so far.

In this thesis, we made progress in the understanding of QG, in particular, we showed how discrete symmetries may play an important rôle in the Swampland program and QG in general. For instance, they provide an explanation for the scale separated vacua in DGKT moduli stabilization. Moreover, it is clear that also continuous symmetries are affected by the presence of discrete symmetries, so their physics should be investigated more.
The study of the interplay between the presence of dynamical tadpoles and the Swampland program is also important. One of the purposes of the Swampland program is to refine its conjectures and to delineate as much as possible the border between the Swampland and the Landscape. The fact that we found violations of the WGC when dynamical tadpoles are ignored allows for a duple interpretation: on one hand QG seems to be aware that the solution that has been used was not the correct one, since the dynamical tadpole was ignored. On the other hand, it is possible that the WGC might be modified to be true in all field space.
This thesis provided answers to some questions but also raised new interesting questions whose answers may contribute to this new era of String Phenomenology.

Appendix

Junction conditions for AdS vacua

A

Here we adapt to the 4d set-up, the discussion of [215], which studies a Randall-Sundrum construction [216, 217] with an arbitrary number of branes (domain walls). The discussion is also similar to systems of D8-branes in type I' theory [218].

Consider a 4d spacetime with N parallel domain walls with tensions T_i, located at positions y_i in a coordinate y. The region between the i-th and $(i+1)$-th brane has cosmological constant Λ_i. A solution of the 4d Einstein equation

$$\sqrt{-G}\mathcal{G}_{MN} = -\frac{1}{4M_{P,4}^2}\left[\sum_{i=1}^{N}\Lambda_i[\theta(y-y_i)-\theta(y-y_{i+1})]\sqrt{-G}G_{MN}+ \right. \\ \left. + \sum_{i=1}^{N} T_i\sqrt{-g^{(i)}}g^{(i)}_{\mu\nu}\delta^{\mu}_{M}\delta^{\nu}_{N}\delta(y-y_i)\right], \tag{A.1}$$

where $\mathcal{G}_{MN} = R_{MN} - \frac{1}{2}G_{MN}R$, is given by the ansatz

$$ds^2 = e^{-2\sigma(y)}\eta_{\mu\nu}dx^{\mu}dx^{\nu} + r_c^2 dy^2\,. \tag{A.2}$$

The warp factor in the above expression is given by the following piecewise linear function

$$\sigma(y) =(\lambda_1-\lambda_0)(y-y_1)\theta(y-y_1) + (\lambda_2-\lambda_1)(y-y_2)\theta(y-y_2)+ \\ + \ldots + (\lambda_N-\lambda_{N-1})(y-y_N)\theta(y-y_N)\,, \tag{A.3}$$

where λ_0 and λ_N provide the asymptotic behavior at $y = \mp\infty$. In any region between two domain walls, we can perform a change of coordinates

$$\frac{x_0}{r_c} = e^{\sigma(y)}\,, \tag{A.4}$$

to bring the metric (A.2) to a more standard form, i.e.

$$ds^2 = \frac{r_c^2}{x_0^2}\left(\eta_{\mu\nu}dx^{\mu}dx^{\nu} + dx_0^2\right)\,, \tag{A.5}$$

from which it is clear that the solution describes slices of AdS_4 with different values of the cosmological constant, made explicit below.

From (A.1), we obtain the following constraints for $\sigma(y)$ [215]:

$$(\sigma'(y))^2 = -\frac{r_c^2}{12M_{P,4}^2}\sum_{i=1}^{N}\Lambda_i\left[\theta(y-y_i)-\theta(y-y_{i+1})\right]\,, \tag{A.6}$$

$$\sigma''(y) = \frac{r_c}{8M_{P,4}^2}\sum_{i=1}^{N}T_i\delta(y-y_i)\,. \tag{A.7}$$

Substituting (A.3) in (A.6) and (A.7), we obtain the relations

$$\lambda_i = \pm\sqrt{\frac{-\Lambda_i r_c^2}{12M_{P,4}^2}}\,, \tag{A.8}$$

$$\frac{T_i r_c}{8M_{P,4}^2} = \lambda_i - \lambda_{i-1}\,. \tag{A.9}$$

Hence these junction conditions relate the variation of the cosmological constant to the potential of the branes that give us the domain walls. This is a general interpretation of what we proposed in Section 6.6.4.

Toric Geometry B

In this appendix we collect the main definitions of toric geometry useful for Chapters 2 and 5.

Appendix B is based on [219–221] and references therein.

B.1 Toric variety

The definition of **toric variety** is [220]:

Definition B.1 [Toric Variety]**.**

A toric variety $\mathbf{X}$ is a complex algebraic variety containing an algebraic torus $\mathbf{T} = (\mathbb{C}^*)^r$ as a dense open set, together with an action of $\mathbf{T}$ on $\mathbf{X}$ whose restriction to $\mathbf{T} \subset \mathbf{X}$ is just the usual multiplication on $\mathbf{T}$.

$\mathbb{C}^* = \mathbb{C} \setminus \{0\}$

It usually considers a generalization of a projective space $\mathbb{CP}^n$, defined as

$$\mathbb{CP}^n = \frac{\mathbb{C}^{n+1} \setminus \{0, 0, \ldots, 0\}}{\mathbb{C}^*}\,, \tag{B.1}$$

and the action of $\mathbb{C}^*$ is to multiply all the coordinates of $\mathbb{C}^{n+1}$ by a $\lambda \in \mathbb{C}^*$, i.e.

$$(z_0, \ldots z_n) \to (\lambda z_0, \ldots, \lambda z_n)\,. \tag{B.2}$$

In the case of a toric variety, it is necessary to specify which points are removed from $\mathbb{C}^m$ and there could be several $\mathbb{C}^*$ actions that give an **algebraic torus**,

$$\mathbf{T} = \mathbb{C}^* \times \ldots \times \mathbb{C}^* \simeq (\mathbb{C}^*)^r\,. \tag{B.3}$$

For these reasons, usually, a toric variety of dimension n is expressed as [219, 221]

$$\mathbf{X} = \frac{\mathbb{C}^m \setminus Z_\Delta}{(\mathbb{C}^*)^r \times \Gamma}\,, \tag{B.4}$$

where Z_Δ is a set of points removed from $\mathbb{C}^m$, and $r = m - n$. We have also added Γ, which is an Abelian subgroup related to the **orbifold** singularities.

B.2 Fans, toric diagram and (p, q)-web diagrams

Toric varieties can be described by a **fan**, and projective toric varieties can all be described by lattice points in a **polytope** [220]. Let us consider a lattice $N \simeq \mathbb{Z}^m$ and the vector space $N_{\mathbb{R}} = N \times \mathbb{R}$ obtained allowing for real coefficients.

Definition B.2 [Cone]**.**

A strongly convex rational polyhedral cone $\sigma \subset N_{\mathbb{R}}$ is a set

$$\sigma = \left\{ \sum_i a_i v_i \middle| a_i \geq 0 \right\} , \tag{B.5}$$

where $\{v_i\}$ are a set of vectors in N. We also ask the **strong convexity** condition, i.e., $\sigma \cap (-\sigma) = \{0\}$.

Definition B.3 [Fan].

A collection Σ of strongly convex rational polyhedral cones in $N_{\mathbb{R}}$ is called a fan if

1. each face of a cone in Σ is also a cone in Σ;
2. the intersection of two cones in Σ is a face of each.

Let us try to construct Eq. (B.4) using the definition of the fan. First, we consider a fan with m vectors, of dimensions n. The 1-dimensional cones of a fan Σ, i.e., $\Sigma(1)$ correspond to vectors in N. They are set $\{v_i\}$, with $i = 1, \ldots m$. To each vector v_i it is associated a **homogeneous coordinate** t_i. For any subset of $\Sigma(1)$, that does not generate a cone in Σ we associate an algebraic set defined by $t_{i1} = \ldots = t_{il} = 0$, where t_{i1} to t_{il} are the vectors in the subset. The union of all the subsets is Z_Δ.
Let us, now, define $G = (\mathbb{C}^*)^{m-n} \times \Gamma = \tilde{G} \times \Gamma$. We introduce a map

$$\phi : \mathbb{C}^m \to \mathbb{C}^n , \tag{B.6}$$

that acts on the coordinates t_i as

$$(t_1, \ldots t_m) \to \left(\prod_{i=1}^m t_i^{v_i^1}, \ldots \prod_{i=1}^m t_i^{v_i^n} \right) , \tag{B.7}$$

where we have denoted the vector $v_i = \left(v_i^1, \ldots, v_i^n\right)$. The group $\tilde{G}$ is the kernel of ϕ, i.e.

$$\tilde{G} = \ker\left(\phi\right) . \tag{B.8}$$

In other words, let us define the action of $\tilde{G}$ on the homogeneous coordinates as

$$\tilde{G} \cdot (t_1, \ldots t_m) = \left(\lambda^{\omega_1^a} t_1, \ldots \lambda^{\omega_m^a} t_m \right) , \tag{B.9}$$

the charge vectors ω^a are in the kernel of ϕ, i.e.

$$\sum_i \left(v_i^k\right) \omega_i^a = 0 . \tag{B.10}$$

For a fan with m vectors in N, we must find n linear relations among them, and the coefficients of the relations are the ω_i^a. On the other hand, the discrete subgroup Γ is associated to **orbifold** singularities.
The easiest way to understand these definitions is through an example. Let us consider the toric fan for the first del Pezzo, dP_1, with vectors

This is also the first Hirzebruch F_1.

$$v_1 = (1,0)\,,\ v_2 = (0,1)\,,\ v_3 = (-1,-1) \text{ and } v_4 = (0,-1)\,. \tag{B.11}$$

The vectors $\{v_1, v_3\}$ and $\{v_2, v_4\}$ do not span a cone in the fan (see Figure B.1), we conclude that

$$Z_\Delta = \{t_1 = t_3 = 0\} \cup \{t_2 = t_4 = 0\}\ . \tag{B.12}$$

The group $\tilde{G}$ is the kernel of the function ϕ acting on the homogeneous coordinates as

$$\phi\,(t_1,t_2,t_3,t_4) = \left(t_1 t_3^{-1}, t_2 t_3^{-1} t_4^{-1}\right)\ . \tag{B.13}$$

We identify, then, $\tilde{G}$ with the action

$$\tilde{G}\cdot(t_1,t_2,t_3,t_4) = \left(\lambda_1 t_1, \lambda_2 t_2, \lambda_1 t_3, \lambda_1^{-1}\lambda_2 t_4\right)\ , \tag{B.14}$$

we obtain two $\mathbb{C}^*$ actions associated to the parameters λ_1 with charges $\omega_1 = (1,0,1,-1)$ and λ_2 with charges $\omega_2 = (0,1,0,1)$.

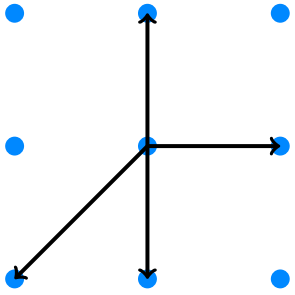

Figure B.1: Fan of dP_1.

Proposition B.1 [TORIC CALABI-YAU VARIETY]**.**

The toric variety X_Δ is Calabi-Yau if and only if all the vectors v_i of Σ end on the same hyperplane in N.

As a consequence,

$$\sum_i \omega_i^a = 0\,. \tag{B.15}$$

Considering, for instance, the complex cone over a dP_1, this would correspond to increase the dimension of the lattice from 2-dimensional to 3-dimensional. The vectors in Eq. (B.11) may become, for instance

$$v_1 = (1,0,1)\,,\ v_2 = (0,1,1)\,,\ v_3 = (-1,-1,1) \text{ and } v_4 = (0,-1,1)\,. \tag{B.16}$$

There is only one $\mathbb{C}^*$ action for these four vectors, and the corresponding charges are, for instance, $\omega = (2,-1,2,-3)$. Projecting the fan on the plane $(0,0,1)$, we obtain the so-called **toric diagram**, in Figure B.2a.

Finally, one can draw the dual of the toric diagram, i.e., the **(p,q)-web**, by simply drawing the perpendicular lines to the edges of the toric diagram. In Figure B.2b we show the unresolved (p,q)-web of the complex cone over dP_1.

It might be worth to stress that the first del Pezzo is **compact**, i.e., its fan spans the whole $N_\mathbb{R}$. In the following we will construct toric varieties that are CYs, and this can happen only if

$$\sum_i \omega_i^a = 0\,.$$

The toric CY associated to a del Pezzo surface is the complex cone constructed over the del Pezzo. This is a toric non-compact space, and it is CY.

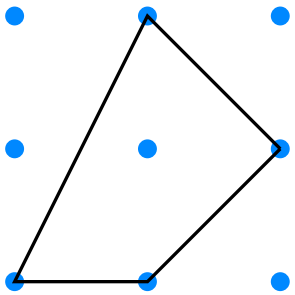

(a) Toric diagram.

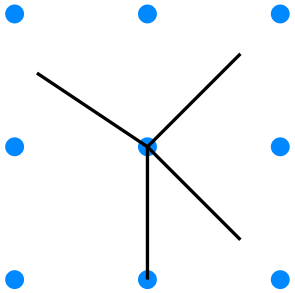

(b) Unresolved (p,q)-web.

Figure B.2: Toric diagram and unresolved (p,q)-web of $C_\mathbb{C}(dP_1)$.

Freed-Witten anomaly and Hanany-Witten construction

C

Section C.1 is based on [51, 64, 65] and references therein.

C.1 Freed-Witten anomaly

Recall the example in Section 3.2 of the D6-brane domain wall in 4d coming from the compactification of B_2 over a basis of 2-cycles. We concluded that such a brane must be present because of the presence of FW anomaly coming from the wrapped NS5-brane and the Roman mass. Freed and Witten showed in [64], indeed, that D-branes cannot wrap a submanifold which supports some units of NSNS 3-form flux, since this configuration is anomalous. What was later showed in [65] is that such an anomaly can be cancelled if we assume the presence of other D-branes wrapping specific cycles. Let us be more concrete using the notation of [65].
FW anomaly is telling us that a D-brane can wrap a cycle $\mathcal{W}'$ in the presence of a NSNS 3-form flux in the class $[H]|_{\mathcal{W}'}$ only if

$$W_3(\mathcal{W}') + [H]|_{\mathcal{W}'} = 0\,, \tag{C.1}$$

where $W_3(\mathcal{W}')$ is the integral Stiefel-Whitney class of $T\mathcal{W}'$.[64]
Suppose that we want to wrap a D-brane on $\mathcal{W}'$. The anomaly can be cancelled if there is a magnetic source F on $\mathcal{W} \subset \mathcal{W}'$ such that

$$\mathrm{PD}\left(\mathcal{W} \subset \mathcal{W}'\right) = W_3(\mathcal{W}') + [H]|_{\mathcal{W}'}\,. \tag{C.2}$$

The magnetic source is given by a D-brane ending on $\mathcal{W}$. The consequence is that a D-brane wrapping $\mathcal{W}$ propagates in time, and ends on the D-brane wrapping $\mathcal{W}'$. Such D-brane is then unstable and it might decay due to the presence of the D-brane wrapping $\mathcal{W}'$.
In Section 3.2 we generalized the discussion of the possible domain walls associated to the DKS couplings coming from the compactification. Such discussion may be rewritten in terms of FW anomaly as follows.

Suppose to have a NS5-brane with worldvolume Σ_6 and the presence of a background RR-flux $F_p^{\text{flux}}|_\Sigma$, such that $\Sigma \subset \Sigma_6$.[65] Then, the NS5-brane will emit D$(6-p)$-branes spanning the Poincaré dual class of Σ.

It is clear that it is the same phenomenon described above but from the opposite perspective. Other possibilities may be obtained T-dualizing and S-dualizing this case. For completeness, we list them all in the following [51]:

- A Dp-brane with worldvolume Σ_{p+1} and non-trivial NSNS 3-form flux $H_3^{\text{flux}}|_\Sigma$, with $\Sigma \subset \Sigma_{p+1}$, must emit D$(p-2)$-branes on $\mathrm{PD}\big(\Sigma \subset \Sigma_{p+1}\big)$.
- Finally, a Dp-brane with worldvolume Σ_{p+1} and non-trivial RR-flux $F_p^{\text{flux}}|_\Sigma$, emits F1-strings along the Poincaré dual class of $\Sigma \subset \Sigma_{p+1}$ [222].

64: We add it for completeness but in the cases discuss in Section 3.2 and Chapter 6 we have not considered torsion classes, so this term may be ignored.

65: Remember that in the case of type IIA string theory p can be only even, but this argument works also for type IIB where p is odd.

It is an exercise to obtain these versions of the FW anomalies from the one in the box by a set of T- and S-dualizations.

C.2 Hanany-Witten construction

Section C.2 is based on [51, 112] and references therein.

FW anomaly may be regarded also as the consistency condition for the creation and annihilation of branes by HW transition [112]. The HW transition comes from the possibility of engineering 3d $\mathcal{N} = 4$ Supersymmetric Quantum Field Theories (SQFTs) via string theory constructions. We will first review the original technique, and we later mention the relations between the two effects.
Let us consider a set of NS5-branes and D5-branes as in Table C.1.

Table C.1: Possible configuration of the original HW construction. The – represents where the branes extend.

	x^0	x^1	x^2	x^3	x^4	x^5	x^6	x^7	x^8	x^9
NS5	–	–	–	–	–	–				
D5	–	–	–				–	–	–	

The D5-branes and the NS5-branes may cross along direction x^9, and such crossing generate a D3-brane along the directions showed in Table C.2.

Table C.2: Possible configuration of the original HW construction with the presence of D3-branes. The – represents where the branes extend.

	x^0	x^1	x^2	x^3	x^4	x^5	x^6	x^7	x^8	x^9
NS5	–	–	–	–	–	–				
D5	–	–	–				–	–	–	
D3	–	–	–							–

This phenomenon of brane creation is due to the presence of a source of flux coming from one of the two branes that the other brane picks up when they cross. In the compact case, FW anomaly imposes that a D3-brane must be present as a consistent condition.
As an interesting aside from a configuration like that in Table C.2 it is possible to construct 3d $\mathcal{N} = 4$ theories leaving on the worldvolume of the D3-brane after a dimensional reduction along x^9. The SO(3) × SO(3) R-symmetry of 3d $\mathcal{N} = 4$ theories comes from the rotational symmetries of the plane (x^2, x^3, x^4) and (x^6, x^7, x^8). The gauge theory can be read using what is called HW cartoon, showed in Figure C.1 as an example.

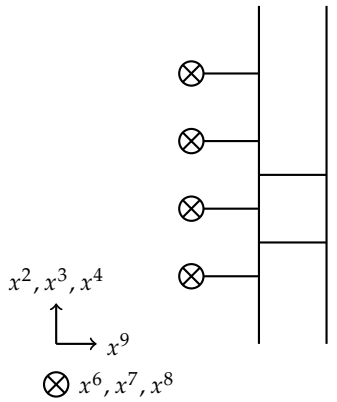

Figure C.1: Example of a HW cartoon. The horizontal lines represent D3-branes, the vertical lines are NS5-branes and the circled crosses are D5-branes.

The identification of the 3d field theory can proceed as follows. For every region between two NS5-branes, the number N_i of horizontal lines (i.e., the number of D3-branes) corresponds to U(N_i) gauge group. Vector multiplets are strings starting from a D3-brane in a cell, to another (or the same) D3-brane cell in the same cell. Bifundamental matter is instead given by strings starting from a D3-brane in a cell and ends on another D3-brane in another cell. Flavors are given by strings starting from a D3-brane in a cell and ends on a D3-brane attached to a D5-brane. For these reasons, the theory in Figure C.1 is the HW cartoon of the 3d $\mathcal{N} = 4$ U(2) gauge theory with 4 flavors.
Brane creation and annihilation may be used to move the branes in the cartoon around and obtain different branches of the same theory.[66]
We end this section with the generalization of the HW construction by use of a set of T- and S-dualizations. In general, the brane creation or annihilation goes as follows [51].

66: We are not entering into details, but in order not to break supersymmetry, when moving around the branes it is necessary to respect the **s-rule** [112, 223]. In 3d, this rule states that there cannot be more than one D3-brane stretching between an NS5-brane and a D5-brane. It is easy to see that such a rule is satisfied in Figure C.1.

Consider a NS5-brane along directions 012345 and a D($p+3$)-brane along $01\ldots p678$, for $p \leq 5$. These branes can cross along x^9, creating a D($p+1$)-brane along $01\ldots p9$.

A dual version of this set-up is given, considering a Dp-brane along $01\ldots p$ and a D($8-p$)-brane along $0(p+1)\ldots 8$. Once again they can cross at x^9 where an F1-string is created spanning 09. All these set-ups are related to the consistency conditions given by FW anomaly.

Modular functions D

Here we collect the definitions of the modular functions used in Chapter 7. Modular functions are functions of a complex parameter τ which transforms under the $\mathrm{SL}(2,\mathbb{Z})$ modular group [9]

$$\tau \to \frac{a\tau + b}{c\tau + d} \text{ with } a,\, b,\, c,\, d \in \mathbb{Z} \text{ and } ad - bc = 1\,. \tag{D.1}$$

The generators of the group are

$$\begin{aligned} T &: \tau \to \tau + 1\,, \\ S &: \tau \to -\frac{1}{\tau}\,. \end{aligned} \tag{D.2}$$

It is usually useful to introduce the **nome**

$$q = e^{2\pi i \tau}\,, \tag{D.3}$$

and we will now follow [224] in order to define the principal modular functions. The first function we introduce is the **theta** function

$$\vartheta(z,\tau) = \sum_{n=-\infty}^{\infty} e^{\pi i n^2 \tau} e^{2\pi i n z}\,, \tag{D.4}$$

which enjoys the following properties:

$$\vartheta(z+1,\tau) = \vartheta(z,\tau)\,, \tag{D.5a}$$

$$\vartheta(z+\tau,\tau) = e^{-\pi i \tau - 2\pi i z}\vartheta(z,\tau)\,, \tag{D.5b}$$

$$\vartheta(z,\tau+1) = \vartheta\left(z+\frac{1}{2},\tau\right)\,, \tag{D.5c}$$

$$\vartheta\left(\frac{z}{\tau},-\frac{1}{\tau}\right) = (-i\tau)^{1/2} e^{\pi i z^2/\tau}\vartheta(z,\tau)\,. \tag{D.5d}$$

In terms of the nome (D.3), it can be written as a product

$$\begin{aligned} \vartheta(z,\tau) &= \prod_{n=1}^{\infty}\left(1-q^m\right)\left(1+e^{2\pi i z}q^{m-1/2}\right)\left(1+e^{-2\pi i z}q^{m-1/2}\right) \\ &= \prod_{n=1}^{\infty}\left(1-q^m\right)\left(1+2\cos(2\pi z)q^{m-1/2}+q^{2m}\right)\,. \end{aligned} \tag{D.6}$$

The theta function in (D.4) usually is refined with two characteristics θ and ϕ, becoming

$$\vartheta\begin{bmatrix}\theta\\ \phi\end{bmatrix}(z,\tau) = e^{\pi i\theta^2\tau + 2\pi i\theta(z+\phi)}\vartheta(z+\theta\tau+\phi,\tau)\,, \tag{D.7}$$

that can be used to define the function $\vartheta_1(z,\tau)$:

$$\begin{aligned}\vartheta_1(z|\tau) \equiv -\vartheta \begin{bmatrix} 1/2 \\ 1/2 \end{bmatrix}(z,\tau) &= i \sum_{n=-\infty}^{\infty} (-1)^n q^{(n-1/2)^2} e^{2\pi i (n-1/2)z} \\ &= 2q^{1/8}\sin(\pi z)\prod_{m=1}^{\infty}\left(1-q^m\right)\left(1-2\cos(2\pi z)q^m+q^{2m}\right) .\end{aligned} \tag{D.8}$$

From Eq. (D.5), we can derive the following quasi-periodicity relations:

$$\vartheta_1(z+1|\tau) = -\vartheta_1(z|\tau) \tag{D.9a}$$

$$\vartheta_1(z+\tau|\tau) = -q^{-1/2}e^{-2\pi i z}\vartheta_1(z|\tau) . \tag{D.9b}$$

There are other particular theta functions that can be obtained from Eq. (D.7) and the reader may find them in standard string theory books such as [9, 224, 225]. Finally, we can introduce the **Dedekind eta** function

$$\eta(\tau) = q^{1/24}\prod_{m=1}^{\infty}(1-q^m) , \tag{D.10}$$

that has the following modular transformations

$$\eta(\tau+1) = e^{i\pi/12}\eta(\tau) , \tag{D.11a}$$

$$\eta\left(-\frac{1}{\tau}\right) = (-i\tau)^{1/2}\eta(\tau) . \tag{D.11b}$$

Bibliography

Here are the references in citation order.

[1] Eduardo García-Valdecasas, Alessandro Mininno, and Ángel M. Uranga. "Discrete Symmetries in Dimer Diagrams". In: *JHEP* 10 (2019), p. 091. DOI: 10.1007/JHEP10(2019)091. arXiv: 1907.06938 [hep-th] (cited on pages v, 61, 98, 104).

[2] Ginevra Buratti, José Calderón, Alessandro Mininno, and Ángel M. Uranga. "Discrete Symmetries, Weak Coupling Conjecture and Scale Separation in AdS Vacua". In: *JHEP* 06 (2020), p. 083. DOI: 10.1007/JHEP06(2020)083. arXiv: 2003.09740 [hep-th] (cited on pages v, 24, 65).

[3] Alessandro Mininno and Ángel M. Uranga. "Dynamical Tadpoles and Weak Gravity Constraints". In: *JHEP* 05 (2021), p. 177. DOI: 10.1007/JHEP05(2021)177. arXiv: 2011.00051 [hep-th] (cited on pages v, 25, 65).

[4] Federico Carta and Alessandro Mininno. "No go for a flow". In: *JHEP* 05 (2020), p. 108. DOI: 10.1007/JHEP05(2020)108. arXiv: 2002.07816 [hep-th] (cited on page v).

[5] Federico Carta, Alessandro Mininno, Nicole Righi, and Alexander Westphal. "Gopakumar-Vafa hierarchies in winding inflation and uplifts". In: *JHEP* 05 (2021), p. 271. DOI: 10.1007/JHEP05(2021)271. arXiv: 2101.07272 [hep-th] (cited on page v).

[6] Federico Carta, Simone Giacomelli, Noppadol Mekareeya, and Alessandro Mininno. "Conformal Manifolds and 3d Mirrors of Argyres-Douglas theories". In: (May 2021). arXiv: 2105.08064 [hep-th] (cited on page v).

[7] Georges Aad et al. "Observation of a new particle in the search for the Standard Model Higgs boson with the ATLAS detector at the LHC". In: *Phys. Lett. B* 716 (2012), pp. 1–29. DOI: 10.1016/j.physletb.2012.08.020. arXiv: 1207.7214 [hep-ex] (cited on page 11).

[8] Michael E. Peskin and Daniel V. Schroeder. *An Introduction to quantum field theory*. Reading, USA: Addison-Wesley, 1995 (cited on pages 11, 55).

[9] Luis E. Ibáñez and Ángel M. Uranga. *String theory and particle physics: An introduction to string phenomenology*. Cambridge University Press, 2012. URL: http://www.cambridge.org/de/knowledge/isbn/item6563092/?site_locale=de_DE (cited on pages 11–13, 28, 30, 31, 33, 58, 112, 175, 176).

[10] Matthew D. Schwartz. *Quantum Field Theory and the Standard Model*. Cambridge University Press, Mar. 2014 (cited on pages 11, 55).

[11] Charles W. Misner, K. S. Thorne, and J. A. Wheeler. *Gravitation*. San Francisco: W. H. Freeman, 1973 (cited on page 11).

[12] Robert M. Wald. *General Relativity*. Chicago, USA: Chicago Univ. Pr., 1984. DOI: 10.7208/chicago/9780226870373.001.0001 (cited on page 11).

[13] B. P. Abbott et al. "Observation of Gravitational Waves from a Binary Black Hole Merger". In: *Phys. Rev. Lett.* 116.6 (2016), p. 061102. DOI: 10.1103/PhysRevLett.116.061102. arXiv: 1602.03837 [gr-qc] (cited on page 11).

[14] Matteo Bertolini. *Lectures on Supersymmetry*. https://people.sissa.it/~bertmat/susycourse.pdf. May 2021 (cited on page 11).

[15] Juan Martin Maldacena. "The Large N limit of superconformal field theories and supergravity". In: *Int. J. Theor. Phys.* 38 (1999), pp. 1113–1133. DOI: 10.1023/A:1026654312961. arXiv: hep-th/9711200 (cited on page 21).

[16] Edward Witten. "Anti-de Sitter space and holography". In: *Adv. Theor. Math. Phys.* 2 (1998), pp. 253–291. DOI: 10.4310/ATMP.1998.v2.n2.a2. arXiv: hep-th/9802150 [hep-th] (cited on pages 21, 23, 27, 107).

[17] Ofer Aharony, Steven S. Gubser, Juan Martin Maldacena, Hirosi Ooguri, and Yaron Oz. "Large N field theories, string theory and gravity". In: *Phys. Rept.* 323 (2000), pp. 183–386. DOI: 10.1016/S0370-1573(99)00083-6. arXiv: hep-th/9905111 (cited on pages 21–24, 107).

[18] Yuji Tachikawa. *AdS/CFT Correspondence with Eight Supercharges*. https://member.ipmu.jp/yuji.tachikawa/transp/thesis-corrected.pdf. July 2006 (cited on pages 21–23, 25).

[19] Martin Ammon and Johanna Erdmenger. *Gauge/gravity duality: Foundations and applications*. Cambridge: Cambridge University Press, Apr. 2015 (cited on page 21).

[20] Joseph Polchinski. "Tasi lectures on D-branes". In: *Theoretical Advanced Study Institute in Elementary Particle Physics (TASI 96): Fields, Strings, and Duality*. Nov. 1996, pp. 293–356. arXiv: hep-th/9611050 (cited on page 21).

[21] Constantin P. Bachas. "Lectures on D-branes". In: *A Newton Institute Euroconference on Duality and Supersymmetric Theories*. June 1998, pp. 414–473. arXiv: hep-th/9806199 (cited on page 21).

[22] Gary T. Horowitz and Andrew Strominger. "Black strings and P-branes". In: *Nucl. Phys. B* 360 (1991), pp. 197–209. DOI: 10.1016/0550-3213(91)90440-9 (cited on page 22).

[23] Cyril Closset. "Studies of fractional D-branes in the gauge/gravity correspondence & flavored Chern-Simons quivers for M2-branes". PhD thesis. Brussels U., PTM, 2010 (cited on pages 22–24).

[24] Sergio Benvenuti, Sebastian Franco, Amihay Hanany, Dario Martelli, and James Sparks. "An Infinite family of superconformal quiver gauge theories with Sasaki-Einstein duals". In: *JHEP* 06 (2005), p. 064. DOI: 10.1088/1126-6708/2005/06/064. arXiv: hep-th/0411264 [hep-th] (cited on pages 23, 47).

[25] Dario Martelli, James Sparks, and Shing-Tung Yau. "Sasaki-Einstein manifolds and volume minimisation". In: *Commun. Math. Phys.* 280 (2008), pp. 611–673. DOI: 10.1007/s00220-008-0479-4. arXiv: hep-th/0603021 (cited on pages 23, 25, 129, 130).

[26] James Sparks. "Sasaki-Einstein Manifolds". In: *Surveys Diff. Geom.* 16 (2011), pp. 265–324. DOI: 10.4310/SDG.2011.v16.n1.a6. arXiv: 1004.2461 [math.DG] (cited on page 23).

[27] Philip Candelas and Xenia C. de la Ossa. "Comments on Conifolds". In: *Nucl. Phys. B* 342 (1990), pp. 246–268. DOI: 10.1016/0550-3213(90)90577-Z (cited on page 23).

[28] Edward Witten. "Baryons and branes in anti-de Sitter space". In: *JHEP* 07 (1998), p. 006. DOI: 10.1088/1126-6708/1998/07/006. arXiv: hep-th/9805112 [hep-th] (cited on pages 23, 24).

[29] Sergei Gukov, Mukund Rangamani, and Edward Witten. "Dibaryons, strings and branes in AdS orbifold models". In: *JHEP* 12 (1998), p. 025. DOI: 10.1088/1126-6708/1998/12/025. arXiv: hep-th/9811048 [hep-th] (cited on pages 23, 24, 61, 62, 74, 93, 98, 104, 105).

[30] Andrei Mikhailov. "Giant gravitons from holomorphic surfaces". In: *JHEP* 11 (2000), p. 027. DOI: 10.1088/1126-6708/2000/11/027. arXiv: hep-th/0010206 [hep-th] (cited on pages 23, 93).

[31] John McGreevy, Leonard Susskind, and Nicolaos Toumbas. "Invasion of the giant gravitons from Anti-de Sitter space". In: *JHEP* 06 (2000), p. 008. DOI: 10.1088/1126-6708/2000/06/008. arXiv: hep-th/0003075 [hep-th] (cited on pages 23, 105).

[32] Ofer Aharony, Oren Bergman, Daniel Louis Jafferis, and Juan Maldacena. "N=6 superconformal Chern-Simons-matter theories, M2-branes and their gravity duals". In: *JHEP* 10 (2008), p. 091. DOI: 10.1088/1126-6708/2008/10/091. arXiv: 0806.1218 [hep-th] (cited on pages 24, 25, 98, 108–111).

[33] D. Martelli, J. Sparks, and Shing-Tung Yau. "The Geometric dual of a-maximisation for Toric Sasaki-Einstein manifolds". In: *Commun. Math. Phys.* 268 (2006), pp. 39–65. DOI: 10.1007/s00220-006-0087-0. arXiv: hep-th/0503183 (cited on pages 25, 26, 129, 130).

[34] Masahito Yamazaki. "Brane Tilings and Their Applications". In: *Fortsch. Phys.* 56 (2008), pp. 555–686. DOI: 10.1002/prop.200810536. arXiv: 0803.4474 [hep-th] (cited on page 25).

[35] Richard Eager. "Equivalence of A-Maximization and Volume Minimization". In: *JHEP* 01 (2014), p. 089. DOI: 10.1007/JHEP01(2014)089. arXiv: 1011.1809 [hep-th] (cited on pages 25, 130).

[36] Yuji Tachikawa. "Lectures on 4d $\mathcal{N}$=1 dynamics and related topics". In: Dec. 2018. arXiv: 1812.08946 [hep-th] (cited on page 25).

[37] Kenneth A. Intriligator and Brian Wecht. "The Exact superconformal R symmetry maximizes a". In: *Nucl. Phys. B* 667 (2003), pp. 183–200. DOI: 10.1016/S0550-3213(03)00459-0. arXiv: hep-th/0304128 (cited on pages 26, 27, 129).

[38] M. Henningson and K. Skenderis. "The Holographic Weyl anomaly". In: *JHEP* 07 (1998), p. 023. DOI: 10.1088/1126-6708/1998/07/023. arXiv: hep-th/9806087 (cited on page 27).

[39] S. S. Gubser, Igor R. Klebanov, and Alexander M. Polyakov. "Gauge theory correlators from noncritical string theory". In: *Phys. Lett. B* 428 (1998), pp. 105–114. DOI: 10.1016/S0370-2693(98)00377-3. arXiv: hep-th/9802109 (cited on page 27).

[40] Mariana Grana. "Flux compactifications in string theory: A Comprehensive review". In: *Phys. Rept.* 423 (2006), pp. 91–158. DOI: 10.1016/j.physrep.2005.10.008. arXiv: hep-th/0509003 (cited on pages 28, 31, 33, 58).

[41] Juan Martin Maldacena and Carlos Nunez. "Supergravity description of field theories on curved manifolds and a no go theorem". In: *Int. J. Mod. Phys. A* 16 (2001). Ed. by Michael J. Duff, J. T. Liu, and J. Lu, pp. 822–855. DOI: 10.1142/S0217751X01003937. arXiv: hep-th/0007018 (cited on page 28).

[42] Steven B. Giddings, Shamit Kachru, and Joseph Polchinski. "Hierarchies from fluxes in string compactifications". In: *Phys. Rev.* D66 (2002), p. 106006. DOI: 10.1103/PhysRevD.66.106006. arXiv: hep-th/0105097 [hep-th] (cited on pages 28, 30, 128, 133).

[43] Tristan Hubsch. *Calabi-Yau manifolds: A Bestiary for physicists*. Singapore: World Scientific, 1994 (cited on page 31).

[44] Thomas W. Grimm and Jan Louis. "The Effective action of N = 1 Calabi-Yau orientifolds". In: *Nucl. Phys. B* 699 (2004), pp. 387–426. DOI: 10.1016/j.nuclphysb.2004.08.005. arXiv: hep-th/0403067 (cited on pages 31, 33).

[45] Thomas W. Grimm and Jan Louis. "The Effective action of type IIA Calabi-Yau orientifolds". In: *Nucl. Phys. B* 718 (2005), pp. 153–202. DOI: 10.1016/j.nuclphysb.2005.04.007. arXiv: hep-th/0412277 (cited on pages 31, 33, 35).

[46] Thomas W. Grimm. "The Effective action of type II Calabi-Yau orientifolds". In: *Fortsch. Phys.* 53 (2005), pp. 1179–1271. DOI: 10.1002/prop.200510253. arXiv: hep-th/0507153 (cited on pages 31, 33).

[47] Yang-Hui He. "The Calabi-Yau Landscape: from Geometry, to Physics, to Machine-Learning". In: (Dec. 2018). arXiv: 1812.02893 [hep-th] (cited on page 31).

[48] Oliver DeWolfe, Alexander Giryavets, Shamit Kachru, and Washington Taylor. "Type IIA moduli stabilization". In: *JHEP* 07 (2005), p. 066. DOI: 10.1088/1126-6708/2005/07/066. arXiv: hep-th/0505160 (cited on pages 33, 39, 59, 98, 114–116, 119).

[49] Michael R. Douglas and Shamit Kachru. "Flux compactification". In: *Rev. Mod. Phys.* 79 (2007), pp. 733–796. DOI: 10.1103/RevModPhys.79.733. arXiv: hep-th/0610102 (cited on pages 33, 58).

[50] Ralph Blumenhagen, Boris Kors, Dieter Lust, and Stephan Stieberger. "Four-dimensional String Compactifications with D-Branes, Orientifolds and Fluxes". In: *Phys. Rept.* 445 (2007), pp. 1–193. DOI: 10.1016/j.physrep.2007.04.003. arXiv: hep-th/0610327 (cited on pages 33, 58).

[51] M. Berasaluce-Gonzalez, P. G. Camara, F. Marchesano, and A. M. Uranga. "Zp charged branes in flux compactifications". In: *JHEP* 04 (2013), p. 138. DOI: 10.1007/JHEP04(2013)138. arXiv: 1211.5317 [hep-th] (cited on pages 33, 55, 56, 59, 74, 97, 117, 171, 172).

[52] Dagoberto Escobar, Fernando Marchesano, and Wieland Staessens. "Type IIA flux vacua and α'-corrections". In: *JHEP* 06 (2019), p. 129. DOI: 10.1007/JHEP06(2019)129. arXiv: 1812.08735 [hep-th] (cited on pages 33, 55, 59).

[53] Nigel J. Hitchin. "Lectures on special Lagrangian submanifolds". In: *AMS/IP Stud. Adv. Math.* 23 (2001). Ed. by Cumrun Vafa and S. -T. Yau, pp. 151–182. arXiv: math/9907034 (cited on page 36).

[54] Michael R. Douglas and Gregory W. Moore. "D-branes, quivers, and ALE instantons". In: (1996). arXiv: hep-th/9603167 [hep-th] (cited on page 43).

[55] Amihay Hanany and Kristian D. Kennaway. "Dimer models and toric diagrams". In: (2005). arXiv: hep-th/0503149 [hep-th] (cited on pages 43, 74).

[56] Sebastian Franco, Amihay Hanany, Kristian D. Kennaway, David Vegh, and Brian Wecht. "Brane dimers and quiver gauge theories". In: *JHEP* 01 (2006), p. 096. DOI: 10.1088/1126-6708/2006/01/096. arXiv: hep-th/0504110 [hep-th] (cited on pages 43, 74).

[57] Kristian D. Kennaway. "Brane Tilings". In: *Int. J. Mod. Phys.* A22 (2007), pp. 2977–3038. DOI: 10.1142/S0217751X07036877. arXiv: 0706.1660 [hep-th] (cited on pages 43, 74).

[58] Luis E. Ibáñez, R. Rabadan, and A. M. Uranga. "Anomalous U(1)'s in type I and type IIB D = 4, N=1 string vacua". In: *Nucl. Phys.* B542 (1999), pp. 112–138. DOI: 10.1016/S0550-3213(98)00791-3. arXiv: hep-th/9808139 [hep-th] (cited on page 44).

[59] M. Bertolini, F. Bigazzi, and A. L. Cotrone. "New checks and subtleties for AdS/CFT and a-maximization". In: *JHEP* 12 (2004), p. 024. DOI: 10.1088/1126-6708/2004/12/024. arXiv: hep-th/0411249 [hep-th] (cited on page 47).

[60] Robert G. Leigh and Matthew J. Strassler. "Exactly marginal operators and duality in four-dimensional N=1 supersymmetric gauge theory". In: *Nucl. Phys.* B447 (1995), pp. 95–136. DOI: 10.1016/0550-3213(95)00261-P. arXiv: hep-th/9503121 [hep-th] (cited on page 51).

[61] Yosuke Imamura, Hiroshi Isono, Keisuke Kimura, and Masahito Yamazaki. "Exactly marginal deformations of quiver gauge theories as seen from brane tilings". In: *Prog. Theor. Phys.* 117 (2007), pp. 923–955. DOI: 10.1143/PTP.117.923. arXiv: hep-th/0702049 [hep-th] (cited on page 51).

[62] Martin Schmaltz. "Duality of nonsupersymmetric large N gauge theories". In: *Phys. Rev.* D59 (1999), p. 105018. DOI: 10.1103/PhysRevD.59.105018. arXiv: hep-th/9805218 [hep-th] (cited on page 51).

[63] Ángel M. Uranga. "Brane configurations for branes at conifolds". In: *JHEP* 01 (1999), p. 022. DOI: 10.1088/1126-6708/1999/01/022. arXiv: hep-th/9811004 [hep-th] (cited on page 51).

[64] Daniel S. Freed and Edward Witten. "Anomalies in string theory with D-branes". In: *Asian J. Math.* 3 (1999), p. 819. arXiv: hep-th/9907189 (cited on pages 55, 58, 171).

[65] Juan Martin Maldacena, Gregory W. Moore, and Nathan Seiberg. "D-brane instantons and K theory charges". In: *JHEP* 11 (2001), p. 062. DOI: 10.1088/1126-6708/2001/11/062. arXiv: hep-th/0108100 (cited on pages 55, 58, 171).

[66] Gia Dvali. "Three-form gauging of axion symmetries and gravity". In: (2005). arXiv: hep-th/0507215 [hep-th] (cited on pages 55, 58, 99, 115).

[67] Tom Banks and Nathan Seiberg. "Symmetries and Strings in Field Theory and Gravity". In: *Phys. Rev.* D83 (2011), p. 084019. DOI: 10.1103/PhysRevD.83.084019. arXiv: 1011.5120 [hep-th] (cited on pages 55, 56, 65, 74, 97).

[68] Mikel Berasaluce González. "Discrete gauge symmetries in string theory". PhD thesis. U. Autonoma, Madrid (main), 2014 (cited on page 55).

[69] Mirjam Cvetič and Ling Lin. "TASI Lectures on Abelian and Discrete Symmetries in F-theory". In: *PoS* TASI2017 (2018), p. 020. DOI: 10.22323/1.305.0020. arXiv: 1809.00012 [hep-th] (cited on page 55).

[70] Nemanja Kaloper and Lorenzo Sorbo. "A Natural Framework for Chaotic Inflation". In: *Phys. Rev. Lett.* 102 (2009), p. 121301. DOI: 10.1103/PhysRevLett.102.121301. arXiv: 0811.1989 [hep-th] (cited on pages 58, 99, 115, 128).

[71] Anamaría Font, Alvaro Herráez, and Luis E. Ibáñez. "The Swampland Distance Conjecture and Towers of Tensionless Branes". In: *JHEP* 08 (2019), p. 044. DOI: 10.1007/JHEP08(2019)044. arXiv: 1904.05379 [hep-th] (cited on pages 59, 61).

[72] Alvaro Herráez, Luis E. Ibáñez, Fernando Marchesano, and Gianluca Zoccarato. "The Type IIA Flux Potential, 4-forms and Freed-Witten anomalies". In: *JHEP* 09 (2018), p. 018. DOI: 10.1007/JHEP09(2018)018. arXiv: 1802.05771 [hep-th] (cited on pages 60, 115, 119).

[73] Benjamin A. Burrington, James T. Liu, and Leopoldo A. Pando Zayas. "Finite Heisenberg groups in quiver gauge theories". In: *Nucl. Phys.* B747 (2006), pp. 436–454. DOI: 10.1016/j.nuclphysb.2006.04.022. arXiv: hep-th/0602094 [hep-th] (cited on pages 61–63, 74, 93, 98, 104).

[74] Benjamin A. Burrington, James T. Liu, and Leopoldo A. Pando Zayas. "Central extensions of finite heisenberg groups in cascading quiver gauge theories". In: *Nucl. Phys.* B749 (2006), pp. 245–265. DOI: 10.1016/j.nuclphysb.2006.05.020. arXiv: hep-th/0603114 [hep-th] (cited on pages 61, 62, 104).

[75] Benjamin A. Burrington, James T. Liu, Manavendra Mahato, and Leopoldo A. Pando Zayas. "Finite Heisenbeg groups and Seiberg dualities in quiver gauge theories". In: *Nucl. Phys.* B757 (2006), pp. 1–18. DOI: 10.1016/j.nuclphysb.2006.06.030. arXiv: hep-th/0604092 [hep-th] (cited on pages 61, 62, 104).

[76] Benjamin A. Burrington, James T. Liu, and Leopoldo A. Pando Zayas. "Finite Heisenberg groups from nonAbelian orbifold quiver gauge theories". In: *Nucl. Phys.* B794 (2008), pp. 324–347. DOI: 10.1016/j.nuclphysb.2007.11.004. arXiv: hep-th/0701028 [hep-th] (cited on pages 61, 62, 74, 104).

[77] T. Daniel Brennan, Federico Carta, and Cumrun Vafa. "The String Landscape, the Swampland, and the Missing Corner". In: *PoS* TASI2017 (2017), p. 015. DOI: 10.22323/1.305.0015. arXiv: 1711.00864 [hep-th] (cited on pages 65, 68, 74, 97, 128).

[78] Eran Palti. "The Swampland: Introduction and Review". In: *Fortsch. Phys.* 67.6 (2019), p. 1900037. DOI: 10.1002/prop.201900037. arXiv: 1903.06239 [hep-th] (cited on pages 65, 66, 68–70, 74, 97, 100, 128, 144).

[79] Marieke van Beest, José Calderón-Infante, Delaram Mirfendereski, and Irene Valenzuela. "Lectures on the Swampland Program in String Compactifications". In: (Feb. 2021). arXiv: 2102.01111 [hep-th] (cited on pages 65, 66, 68).

[80] Tom Banks and Lance J. Dixon. "Constraints on String Vacua with Space-Time Supersymmetry". In: *Nucl. Phys.* B307 (1988), pp. 93–108. DOI: 10.1016/0550-3213(88)90523-8 (cited on pages 65, 74).

[81] Daniel Harlow and Hirosi Ooguri. "Symmetries in quantum field theory and quantum gravity". In: (Oct. 2018). arXiv: 1810.05338 [hep-th] (cited on pages 66, 74, 75, 97).

[82] Hirosi Ooguri and Cumrun Vafa. "On the Geometry of the String Landscape and the Swampland". In: *Nucl. Phys.* B766 (2007), pp. 21–33. DOI: 10.1016/j.nuclphysb.2006.10.033. arXiv: hep-th/0605264 [hep-th] (cited on pages 66, 97, 128).

[83] Dieter Lüst, Eran Palti, and Cumrun Vafa. "AdS and the Swampland". In: *Phys. Lett. B* 797 (2019), p. 134867. DOI: 10.1016/j.physletb.2019.134867. arXiv: 1906.05225 [hep-th] (cited on pages 67, 75, 98, 114, 123).

[84] Nima Arkani-Hamed, Lubos Motl, Alberto Nicolis, and Cumrun Vafa. "The String landscape, black holes and gravity as the weakest force". In: *JHEP* 06 (2007), p. 060. DOI: 10.1088/1126-6708/2007/06/060. arXiv: hep-th/0601001 [hep-th] (cited on pages 67–69, 97, 100, 128).

[85] Clifford Cheung and Grant N. Remmen. "Naturalness and the Weak Gravity Conjecture". In: *Phys. Rev. Lett.* 113 (2014), p. 051601. DOI: 10.1103/PhysRevLett.113.051601. arXiv: 1402.2287 [hep-ph] (cited on pages 68, 103, 143).

[86] Ben Heidenreich, Matthew Reece, and Tom Rudelius. "Sharpening the Weak Gravity Conjecture with Dimensional Reduction". In: *JHEP* 02 (2016), p. 140. DOI: 10.1007/JHEP02(2016)140. arXiv: 1509.06374 [hep-th] (cited on pages 68, 69, 100).

[87] Miguel Montero, Gary Shiu, and Pablo Soler. "The Weak Gravity Conjecture in three dimensions". In: *JHEP* 10 (2016), p. 159. DOI: 10.1007/JHEP10(2016)159. arXiv: 1606.08438 [hep-th] (cited on page 68).

[88] Ben Heidenreich, Matthew Reece, and Tom Rudelius. "Evidence for a sublattice weak gravity conjecture". In: *JHEP* 08 (2017), p. 025. DOI: 10.1007/JHEP08(2017)025. arXiv: 1606.08437 [hep-th] (cited on pages 68, 100).

[89] Stefano Andriolo, Daniel Junghans, Toshifumi Noumi, and Gary Shiu. "A Tower Weak Gravity Conjecture from Infrared Consistency". In: *Fortsch. Phys.* 66.5 (2018), p. 1800020. DOI: 10.1002/prop.201800020. arXiv: 1802.04287 [hep-th] (cited on page 68).

[90] Eran Palti. "The Weak Gravity Conjecture and Scalar Fields". In: *JHEP* 08 (2017), p. 034. DOI: 10.1007/JHEP08(2017)034. arXiv: 1705.04328 [hep-th] (cited on pages 69, 144).

[91] Ben Heidenreich, Matthew Reece, and Tom Rudelius. "Weak Gravity Strongly Constrains Large-Field Axion Inflation". In: *JHEP* 12 (2015), p. 108. DOI: 10.1007/JHEP12(2015)108. arXiv: 1506.03447 [hep-th] (cited on page 70).

[92] L. F. Abbott and Mark B. Wise. "Wormholes and Global Symmetries". In: *Nucl. Phys. B* 325 (1989), pp. 687–704. DOI: 10.1016/0550-3213(89)90503-8 (cited on page 74).

[93] Sidney R. Coleman and Ki-Myeong Lee. "Wormholes made without massless matter fields ". In: *Nucl. Phys.* B329 (1990), pp. 387–409. DOI: 10.1016/0550-3213(90)90149-8 (cited on page 74).

[94] Renata Kallosh, Andrei D. Linde, Dmitri A. Linde, and Leonard Susskind. "Gravity and global symmetries". In: *Phys. Rev.* D52 (1995), pp. 912–935. DOI: 10.1103/PhysRevD.52.912. arXiv: hep-th/9502069 [hep-th] (cited on page 74).

[95] Mark G. Alford and Frank Wilczek. "Aharonov-Bohm Interaction of Cosmic Strings with Matter". In: *Phys. Rev. Lett.* 62 (1989), p. 1071. DOI: 10.1103/PhysRevLett.62.1071 (cited on pages 74, 97).

[96] Lawrence M. Krauss and Frank Wilczek. "Discrete Gauge Symmetry in Continuum Theories". In: *Phys. Rev. Lett.* 62 (1989), p. 1221. DOI: 10.1103/PhysRevLett.62.1221 (cited on pages 74, 97).

[97] Mark G. Alford, John March-Russell, and Frank Wilczek. "Discrete Quantum Hair on Black Holes and the Nonabelian Aharonov-Bohm Effect". In: *Nucl. Phys.* B337 (1990), pp. 695–708. DOI: 10.1016/0550-3213(90)90512-C (cited on pages 74, 97).

[98] John Preskill and Lawrence M. Krauss. "Local Discrete Symmetry and Quantum Mechanical Hair". In: *Nucl. Phys.* B341 (1990), pp. 50–100. DOI: 10.1016/0550-3213(90)90262-C (cited on page 74).

[99] Mark G. Alford, Katherine Benson, Sidney R. Coleman, John March-Russell, and Frank Wilczek. "The Interactions and Excitations of Nonabelian Vortices". In: *Phys. Rev. Lett.* 64 (1990). [Erratum: Phys. Rev. Lett.65,668(1990)], p. 1632. DOI: 10.1103/PhysRevLett.65.668.2,10.1103/PhysRevLett.64.1632 (cited on pages 74, 97).

[100] Mark G. Alford, Sidney R. Coleman, and John March-Russell. "Disentangling nonAbelian discrete quantum hair". In: *Nucl. Phys.* B351 (1991), pp. 735–748. DOI: 10.1016/S0550-3213(05)80042-2 (cited on pages 74, 97).

[101] Mark G. Alford and John March-Russell. "Discrete gauge theories". In: *Int. J. Mod. Phys.* B5 (1991), pp. 2641–2674. DOI: 10.1142/S021797929100105X (cited on pages 74, 97).

[102] Mark G. Alford, Kai-Ming Lee, John March-Russell, and John Preskill. "Quantum field theory of nonAbelian strings and vortices". In: *Nucl. Phys.* B384 (1992), pp. 251–317. DOI: 10.1016/0550-3213(92)90468-Q. arXiv: hep-th/9112038 [hep-th] (cited on pages 74, 97).

[103] Daniel Harlow and Hirosi Ooguri. "Constraints on Symmetries from Holography". In: *Phys. Rev. Lett.* 122.19 (2019), p. 191601. DOI: 10.1103/PhysRevLett.122.191601. arXiv: 1810.05337 [hep-th] (cited on pages 74, 75, 97).

[104] Nathaniel Craig, Isabel García García, and Seth Koren. "Discrete Gauge Symmetries and the Weak Gravity Conjecture". In: *JHEP* 05 (2019), p. 140. DOI: 10.1007/JHEP05(2019)140. arXiv: 1812.08181 [hep-th] (cited on pages 74, 97).

[105] Cumrun Vafa. "The String landscape and the swampland". In: (2005). arXiv: hep-th/0509212 [hep-th] (cited on pages 74, 97, 128).

[106] Pablo G. Camara, Luis E. Ibáñez, and Fernando Marchesano. "RR photons". In: *JHEP* 09 (2011), p. 110. DOI: 10.1007/JHEP09(2011)110. arXiv: 1106.0060 [hep-th] (cited on pages 74, 107).

[107] Mikel Berasaluce-Gonzalez, Luis E. Ibáñez, Pablo Soler, and Ángel M. Uranga. "Discrete gauge symmetries in D-brane models". In: *JHEP* 12 (2011), p. 113. DOI: 10.1007/JHEP12(2011)113. arXiv: 1106.4169 [hep-th] (cited on pages 74, 97, 112).

[108] L. E. Ibáñez, A. N. Schellekens, and A. M. Uranga. "Discrete Gauge Symmetries in Discrete MSSM-like Orientifolds". In: *Nucl. Phys.* B865 (2012), pp. 509–540. DOI: 10.1016/j.nuclphysb.2012.08.008. arXiv: 1205.5364 [hep-th] (cited on pages 74, 97).

[109] Mikel Berasaluce-Gonzalez, Miguel Montero, Ander Retolaza, and Ángel M. Uranga. "Discrete gauge symmetries from (closed string) tachyon condensation". In: *JHEP* 11 (2013), p. 144. DOI: 10.1007/JHEP11(2013)144. arXiv: 1305.6788 [hep-th] (cited on page 74).

[110] M. Berasaluce-Gonzalez, P. G. Camara, F. Marchesano, D. Regalado, and A. M. Uranga. "Non-Abelian discrete gauge symmetries in 4d string models". In: *JHEP* 09 (2012), p. 059. DOI: 10.1007/JHEP09(2012)059. arXiv: 1206.2383 [hep-th] (cited on pages 74, 97, 107).

[111] Hirosi Ooguri and Cumrun Vafa. "Non-supersymmetric AdS and the Swampland". In: *Adv. Theor. Math. Phys.* 21 (2017), pp. 1787–1801. DOI: 10.4310/ATMP.2017.v21.n7.a8. arXiv: 1610.01533 [hep-th] (cited on pages 75, 97, 102, 128).

[112] Amihay Hanany and Edward Witten. "Type IIB superstrings, BPS monopoles, and three-dimensional gauge dynamics". In: *Nucl. Phys.* B492 (1997), pp. 152–190. DOI: 10.1016/S0550-3213(97)00157-0,10.1016/S0550-3213(97)80030-2. arXiv: hep-th/9611230 [hep-th] (cited on pages 93, 172).

[113] Davide Forcella, Amihay Hanany, and Alberto Zaffaroni. "Baryonic Generating Functions". In: *JHEP* 12 (2007), p. 022. DOI: 10.1088/1126-6708/2007/12/022. arXiv: hep-th/0701236 [HEP-TH] (cited on page 93).

[114] Agostino Butti, Davide Forcella, Amihay Hanany, David Vegh, and Alberto Zaffaroni. "Counting Chiral Operators in Quiver Gauge Theories". In: *JHEP* 11 (2007), p. 092. DOI: 10.1088/1126-6708/2007/11/092. arXiv: 0705.2771 [hep-th] (cited on page 93).

[115] Davide Forcella, Amihay Hanany, Yang-Hui He, and Alberto Zaffaroni. "The Master Space of N=1 Gauge Theories". In: *JHEP* 08 (2008), p. 012. DOI: 10.1088/1126-6708/2008/08/012. arXiv: 0801.1585 [hep-th] (cited on page 93).

[116] Davide Forcella, Amihay Hanany, Yang-Hui He, and Alberto Zaffaroni. "Mastering the Master Space". In: *Lett. Math. Phys.* 85 (2008), pp. 163–171. DOI: 10.1007/s11005-008-0255-6. arXiv: 0801.3477 [hep-th] (cited on page 93).

[117] Sebastian Franco, Eduardo García-Valdecasas, and Ángel M. Uranga. "Bipartite field theories and D-brane instantons". In: *JHEP* 11 (2018), p. 098. DOI: 10.1007/JHEP11(2018)098. arXiv: 1805.00011 [hep-th] (cited on page 93).

[118] Davide Forcella, Iñaki García-Etxebarria, and Ángel Uranga. "E3-brane instantons and baryonic operators for D3-branes on toric singularities". In: *JHEP* 03 (2009), p. 041. DOI: 10.1088/1126-6708/2009/03/041. arXiv: 0806.2291 [hep-th] (cited on page 93).

[119] Georges Obied, Hirosi Ooguri, Lev Spodyneiko, and Cumrun Vafa. "De Sitter Space and the Swampland". In: (2018). arXiv: 1806.08362 [hep-th] (cited on page 97).

[120] Ginevra Buratti, Eduardo García-Valdecasas, and Ángel M. Uranga. "Supersymmetry Breaking Warped Throats and the Weak Gravity Conjecture". In: *JHEP* 04 (2019), p. 111. DOI: 10.1007/JHEP04(2019)111. arXiv: 1810.07673 [hep-th] (cited on page 97).

[121] Fernando Marchesano, Gary Shiu, and Ángel M. Uranga. "F-term Axion Monodromy Inflation". In: *JHEP* 09 (2014), p. 184. DOI: 10.1007/JHEP09(2014)184. arXiv: 1404.3040 [hep-th] (cited on pages 97, 99, 115, 128).

[122] Miguel Montero, Ángel M. Uranga, and Irene Valenzuela. "Transplanckian axions!?" In: *JHEP* 08 (2015), p. 032. DOI: 10.1007/JHEP08(2015)032. arXiv: 1503.03886 [hep-th] (cited on pages 97, 143).

[123] Ginevra Buratti, José Calderón, and Ángel M. Uranga. "Transplanckian axion monodromy!?" In: *JHEP* 05 (2019), p. 176. DOI: 10.1007/JHEP05(2019)176. arXiv: 1812.05016 [hep-th] (cited on page 97).

[124] Sidney R. Coleman, John Preskill, and Frank Wilczek. "Quantum hair on black holes". In: *Nucl. Phys.* B378 (1992), pp. 175–246. DOI: 10.1016/0550-3213(92)90008-Y. arXiv: hep-th/9201059 [hep-th] (cited on page 98).

[125] Isabel García García. "Properties of Discrete Black Hole Hair". In: *JHEP* 02 (2019), p. 117. DOI: 10.1007/JHEP02(2019)117. arXiv: 1809.03527 [gr-qc] (cited on page 98).

[126] Gia Dvali. "Black Holes and Large N Species Solution to the Hierarchy Problem". In: *Fortsch. Phys.* 58 (2010), pp. 528–536. DOI: 10.1002/prop.201000009. arXiv: 0706.2050 [hep-th] (cited on pages 100, 102, 104, 105).

[127] Julian S. Schwinger. "On gauge invariance and vacuum polarization". In: *Phys. Rev.* 82 (1951). Ed. by K. A. Milton, pp. 664–679. DOI: 10.1103/PhysRev.82.664 (cited on page 100).

[128] William A. Hiscock and Lance D. Weems. "Evolution of Charged Evaporating Black Holes". In: *Phys. Rev. D* 41 (1990), p. 1142. DOI: 10.1103/PhysRevD.41.1142 (cited on page 100).

[129] G. W. Gibbons. "Vacuum Polarization and the Spontaneous Loss of Charge by Black Holes". In: *Commun. Math. Phys.* 44 (1975), pp. 245–264. DOI: 10.1007/BF01609829 (cited on page 100).

[130] Miguel Montero, Thomas Van Riet, and Gerben Venken. "Festina Lente: EFT Constraints from Charged Black Hole Evaporation in de Sitter". In: *JHEP* 01 (2020), p. 039. DOI: 10.1007/JHEP01(2020)039. arXiv: 1910.01648 [hep-th] (cited on page 101).

[131] G. Aldazabal, S. Franco, Luis E. Ibáñez, R. Rabadan, and A. M. Uranga. "Intersecting brane worlds". In: *JHEP* 02 (2001), p. 047. DOI: 10.1088/1126-6708/2001/02/047. arXiv: hep-ph/0011132 [hep-ph] (cited on page 104).

[132] G. Aldazabal, S. Franco, Luis E. Ibáñez, R. Rabadan, and A. M. Uranga. "D = 4 chiral string compactifications from intersecting branes". In: *J. Math. Phys.* 42 (2001), pp. 3103–3126. DOI: 10.1063/1.1376157. arXiv: hep-th/0011073 [hep-th] (cited on pages 104, 133).

[133] Miguel Montero, Ángel M. Uranga, and Irene Valenzuela. "A Chern-Simons Pandemic". In: *JHEP* 07 (2017), p. 123. DOI: 10.1007/JHEP07(2017)123. arXiv: 1702.06147 [hep-th] (cited on page 111).

[134] Ángel M. Uranga. "D-brane probes, RR tadpole cancellation and K theory charge". In: *Nucl. Phys.* B598 (2001), pp. 225–246. DOI: 10.1016/S0550-3213(00)00787-2. arXiv: hep-th/0011048 [hep-th] (cited on pages 113, 151).

[135] Ralph Blumenhagen, Mirjam Cvetic, and Timo Weigand. "Spacetime instanton corrections in 4D string vacua: The Seesaw mechanism for D-Brane models". In: *Nucl. Phys.* B771 (2007), pp. 113–142. DOI: 10.1016/j.nuclphysb.2007.02.016. arXiv: hep-th/0609191 [hep-th] (cited on pages 114, 133).

[136] L. E. Ibáñez, A. N. Schellekens, and A. M. Uranga. "Instanton Induced Neutrino Majorana Masses in CFT Orientifolds with MSSM-like spectra". In: *JHEP* 06 (2007), p. 011. DOI: 10.1088/1126-6708/2007/06/011. arXiv: 0704.1079 [hep-th] (cited on pages 114, 133).

[137] Bogdan Florea, Shamit Kachru, John McGreevy, and Natalia Saulina. "Stringy Instantons and Quiver Gauge Theories". In: *JHEP* 05 (2007), p. 024. DOI: 10.1088/1126-6708/2007/05/024. arXiv: hep-th/0610003 [hep-th] (cited on pages 114, 133).

[138] Shamit Kachru, Renata Kallosh, Andrei D. Linde, and Sandip P. Trivedi. "De Sitter vacua in string theory". In: *Phys. Rev.* D68 (2003), p. 046005. DOI: 10.1103/PhysRevD.68.046005. arXiv: hep-th/0301240 [hep-th] (cited on page 114).

[139] Vijay Balasubramanian, Per Berglund, Joseph P. Conlon, and Fernando Quevedo. "Systematics of moduli stabilisation in Calabi-Yau flux compactifications". In: *JHEP* 03 (2005), p. 007. DOI: 10.1088/1126-6708/2005/03/007. arXiv: hep-th/0502058 [hep-th] (cited on page 114).

[140] Pablo G. Camara, A. Font, and L. E. Ibáñez. "Fluxes, moduli fixing and MSSM-like vacua in a simple IIA orientifold". In: *JHEP* 09 (2005), p. 013. DOI: 10.1088/1126-6708/2005/09/013. arXiv: hep-th/0506066 [hep-th] (cited on pages 114, 115).

[141] Fernando Marchesano and Joan Quirant. "A Landscape of AdS Flux Vacua". In: *JHEP* 12 (2019), p. 110. DOI: 10.1007/JHEP12(2019)110. arXiv: 1908.11386 [hep-th] (cited on page 114).

[142] Dagoberto Escobar, Fernando Marchesano, and Wieland Staessens. "Type IIA Flux Vacua with Mobile D6-branes". In: *JHEP* 01 (2019), p. 096. DOI: 10.1007/JHEP01(2019)096. arXiv: 1811.09282 [hep-th] (cited on page 115).

[143] Anamaría Font, Alvaro Herráez, and Luis E. Ibáñez. "On scale separation in type II AdS flux vacua". In: *JHEP* 03 (2020), p. 013. DOI: 10.1007/JHEP03(2020)013. arXiv: 1912.03317 [hep-th] (cited on page 116).

[144] Gerardo Aldazabal and Anamaría Font. "A Second look at N=1 supersymmetric AdS(4) vacua of type IIA supergravity". In: *JHEP* 02 (2008), p. 086. DOI: 10.1088/1126-6708/2008/02/086. arXiv: 0712.1021 [hep-th] (cited on page 116).

[145] Thomas W. Grimm, Chongchuo Li, and Irene Valenzuela. "Asymptotic Flux Compactifications and the Swampland". In: *JHEP* 06 (2020). [Erratum: JHEP 01, 007 (2021)], p. 009. DOI: 10.1007/JHEP06(2020)009. arXiv: 1910.09549 [hep-th] (cited on page 120).

[146] W. Fischler and Leonard Susskind. "Dilaton Tadpoles, String Condensates and Scale Invariance". In: *Phys. Lett. B* 171 (1986), pp. 383–389. DOI: 10.1016/0370-2693(86)91425-5 (cited on page 127).

[147] Willy Fischler and Leonard Susskind. "Dilaton Tadpoles, String Condensates and Scale Invariance. 2." In: *Phys. Lett. B* 173 (1986), pp. 262–264. DOI: 10.1016/0370-2693(86)90514-9 (cited on page 127).

[148] Shigeki Sugimoto. "Anomaly cancellations in type I D-9 - anti-D-9 system and the USp(32) string theory". In: *Prog. Theor. Phys.* 102 (1999), pp. 685–699. DOI: 10.1143/PTP.102.685. arXiv: hep-th/9905159 [hep-th] (cited on pages 127, 145).

[149] Ignatios Antoniadis, E. Dudas, and A. Sagnotti. "Brane supersymmetry breaking". In: *Phys. Lett.* B464 (1999), pp. 38–45. DOI: 10.1016/S0370-2693(99)01023-0. arXiv: hep-th/9908023 [hep-th] (cited on pages 127, 145).

[150] G. Aldazabal and A. M. Uranga. "Tachyon free nonsupersymmetric type IIB orientifolds via Brane - anti-brane systems". In: *JHEP* 10 (1999), p. 024. DOI: 10.1088/1126-6708/1999/10/024. arXiv: hep-th/9908072 [hep-th] (cited on pages 127, 145).

[151] Ángel M. Uranga. "Comments on nonsupersymmetric orientifolds at strong coupling". In: *JHEP* 02 (2000), p. 041. DOI: 10.1088/1126-6708/2000/02/041. arXiv: hep-th/9912145 [hep-th] (cited on page 127).

[152] E. Dudas, G. Pradisi, M. Nicolosi, and A. Sagnotti. "On tadpoles and vacuum redefinitions in string theory". In: *Nucl. Phys. B* 708 (2005), pp. 3–44. DOI: 10.1016/j.nuclphysb.2004.11.028. arXiv: hep-th/0410101 (cited on page 128).

[153] J. Mourad and A. Sagnotti. "AdS Vacua from Dilaton Tadpoles and Form Fluxes". In: *Phys. Lett. B* 768 (2017), pp. 92–96. DOI: 10.1016/j.physletb.2017.02.053. arXiv: 1612.08566 [hep-th] (cited on page 128).

[154] Keshav Dasgupta, Govindan Rajesh, and Savdeep Sethi. "M theory, orientifolds and G - flux". In: *JHEP* 08 (1999), p. 023. DOI: 10.1088/1126-6708/1999/08/023. arXiv: hep-th/9908088 [hep-th] (cited on pages 128, 133).

[155] Lars Gorlich, Shamit Kachru, Prasanta K. Tripathy, and Sandip P. Trivedi. "Gaugino condensation and nonperturbative superpotentials in flux compactifications". In: *JHEP* 12 (2004), p. 074. DOI: 10.1088/1126-6708/2004/12/074. arXiv: hep-th/0407130 (cited on page 128).

[156] Pablo G. Camara, L.E. Ibáñez, and A.M. Uranga. "Flux-induced SUSY-breaking soft terms on D7-D3 brane systems". In: *Nucl. Phys. B* 708 (2005), pp. 268–316. DOI: 10.1016/j.nuclphysb.2004.11.035. arXiv: hep-th/0408036 (cited on page 128).

[157] Jaume Gomis, Fernando Marchesano, and David Mateos. "An Open string landscape". In: *JHEP* 11 (2005), p. 021. DOI: 10.1088/1126-6708/2005/11/021. arXiv: hep-th/0506179 (cited on pages 128, 136, 137, 141, 151).

[158] S. Bielleman, L. E. Ibáñez, F. G. Pedro, and I. Valenzuela. "Multifield Dynamics in Higgs-otic Inflation". In: *JHEP* 01 (2016), p. 128. DOI: 10.1007/JHEP01(2016)128. arXiv: 1505.00221 [hep-th] (cited on page 128).

[159] Eva Silverstein and Alexander Westphal. "Monodromy in the CMB: Gravity Waves and String Inflation". In: *Phys. Rev.* D78 (2008), p. 106003. DOI: 10.1103/PhysRevD.78.106003. arXiv: 0803.3085 [hep-th] (cited on page 128).

[160] Arthur Hebecker, Sebastian C. Kraus, and Lukas T. Witkowski. "D7-Brane Chaotic Inflation". In: *Phys. Lett.* B737 (2014), pp. 16–22. DOI: 10.1016/j.physletb.2014.08.028. arXiv: 1404.3711 [hep-th] (cited on page 128).

[161] Luis E. Ibáñez and Irene Valenzuela. "The inflaton as an MSSM Higgs and open string modulus monodromy inflation". In: *Phys. Lett.* B736 (2014), pp. 226–230. DOI: 10.1016/j.physletb.2014.07.020. arXiv: 1404.5235 [hep-th] (cited on page 128).

[162] Luis E. Ibáñez, Fernando Marchesano, and Irene Valenzuela. "Higgs-otic Inflation and String Theory". In: *JHEP* 01 (2015), p. 128. DOI: 10.1007/JHEP01(2015)128. arXiv: 1411.5380 [hep-th] (cited on pages 128, 137).

[163] Manki Kim and Liam McAllister. "Monodromy Charge in D7-brane Inflation". In: *JHEP* 10 (2020), p. 060. DOI: 10.1007/JHEP10(2020)060. arXiv: 1812.03532 [hep-th] (cited on pages 128, 133, 135, 139).

[164] Daniel Baumann, Anatoly Dymarsky, Igor R. Klebanov, Juan Martin Maldacena, Liam P. McAllister, and Arvind Murugan. "On D3-brane Potentials in Compactifications with Fluxes and Wrapped D-branes". In: *JHEP* 11 (2006), p. 031. DOI: 10.1088/1126-6708/2006/11/031. arXiv: hep-th/0607050 (cited on pages 128, 132, 139).

[165] Alvaro Herráez. "A Note on Membrane Interactions and the Scalar potential". In: *JHEP* 10 (2020), p. 009. DOI: 10.1007/JHEP10(2020)009. arXiv: 2006.01160 [hep-th] (cited on page 129).

[166] Stefano Lanza, Fernando Marchesano, Luca Martucci, and Irene Valenzuela. "Swampland Conjectures for Strings and Membranes". In: (June 2020). arXiv: 2006.15154 [hep-th] (cited on page 129).

[167] Agostino Butti and Alberto Zaffaroni. "R-charges from toric diagrams and the equivalence of a-maximization and Z-minimization". In: *JHEP* 11 (2005), p. 019. DOI: 10.1088/1126-6708/2005/11/019. arXiv: hep-th/0506232 (cited on page 130).

[168] Agostino Butti, Alberto Zaffaroni, and Davide Forcella. "Deformations of conformal theories and non-toric quiver gauge theories". In: *JHEP* 02 (2007), p. 081. DOI: 10.1088/1126-6708/2007/02/081. arXiv: hep-th/0607147 (cited on page 130).

[169] J. Gutowski and G. Papadopoulos. "AdS calibrations". In: *Phys. Lett. B* 462 (1999), pp. 81–88. DOI: 10.1016/S0370-2693(99)00878-3. arXiv: hep-th/9902034 (cited on page 130).

[170] J. Gutowski, G. Papadopoulos, and P.K. Townsend. "Supersymmetry and generalized calibrations". In: *Phys. Rev. D* 60 (1999), p. 106006. DOI: 10.1103/PhysRevD.60.106006. arXiv: hep-th/9905156 (cited on page 130).

[171] Jerome P. Gauntlett, Nakwoo Kim, Dario Martelli, and Daniel Waldram. "Five-branes wrapped on SLAG three cycles and related geometry". In: *JHEP* 11 (2001), p. 018. DOI: 10.1088/1126-6708/2001/11/018. arXiv: hep-th/0110034 (cited on page 130).

[172] Jerome P. Gauntlett, Dario Martelli, Stathis Pakis, and Daniel Waldram. "G structures and wrapped NS5-branes". In: *Commun. Math. Phys.* 247 (2004), pp. 421–445. DOI: 10.1007/s00220-004-1066-y. arXiv: hep-th/0205050 (cited on page 130).

[173] Jerome P. Gauntlett, Dario Martelli, and Daniel Waldram. "Superstrings with intrinsic torsion". In: *Phys. Rev. D* 69 (2004), p. 086002. DOI: 10.1103/PhysRevD.69.086002. arXiv: hep-th/0302158 (cited on page 130).

[174] Dario Martelli and James Sparks. "G structures, fluxes and calibrations in M theory". In: *Phys. Rev. D* 68 (2003), p. 085014. DOI: 10.1103/PhysRevD.68.085014. arXiv: hep-th/0306225 (cited on page 130).

[175] Gianguido Dall'Agata and Nikolaos Prezas. "N = 1 geometries for M theory and type IIA strings with fluxes". In: *Phys. Rev. D* 69 (2004), p. 066004. DOI: 10.1103/PhysRevD.69.066004. arXiv: hep-th/0311146 (cited on page 130).

[176] Juan F.G. Cascales and Ángel M. Uranga. "Branes on generalized calibrated submanifolds". In: *JHEP* 11 (2004), p. 083. DOI: 10.1088/1126-6708/2004/11/083. arXiv: hep-th/0407132 (cited on page 130).

[177] Cumrun Vafa. "Evidence for F theory". In: *Nucl. Phys. B* 469 (1996), pp. 403–418. DOI: 10.1016/0550-3213(96)00172-1. arXiv: hep-th/9602022 (cited on page 131).

[178] Ashoke Sen. "F theory and orientifolds". In: *Nucl. Phys. B* 475 (1996), pp. 562–578. DOI: 10.1016/0550-3213(96)00347-1. arXiv: hep-th/9605150 (cited on page 131).

[179] Ori J. Ganor. "A Note on zeros of superpotentials in F theory". In: *Nucl. Phys. B* 499 (1997), pp. 55–66. DOI: 10.1016/S0550-3213(97)00311-8. arXiv: hep-th/9612077 (cited on page 133).

[180] C. Angelantonj, Ignatios Antoniadis, E. Dudas, and A. Sagnotti. "Type I strings on magnetized orbifolds and brane transmutation". In: *Phys. Lett. B* 489 (2000), pp. 223–232. DOI: 10.1016/S0370-2693(00)00907-2. arXiv: hep-th/0007090 (cited on page 133).

[181] Ralph Blumenhagen, Lars Goerlich, Boris Kors, and Dieter Lust. "Noncommutative compactifications of type I strings on tori with magnetic background flux". In: *JHEP* 10 (2000), p. 006. DOI: 10.1088/1126-6708/2000/10/006. arXiv: hep-th/0007024 (cited on page 133).

[182] Tomas Ortin. *Gravity and Strings*. 2nd ed. Cambridge Monographs on Mathematical Physics. Cambridge University Press, July 2015. DOI: 10.1017/CBO9781139019750 (cited on page 133).

[183] Andrew R. Frey and Joseph Polchinski. "N=3 warped compactifications". In: *Phys. Rev. D* 65 (2002), p. 126009. DOI: 10.1103/PhysRevD.65.126009. arXiv: hep-th/0201029 (cited on pages 137, 150).

[184] Ralph Blumenhagen, Dieter Lust, and Tomasz R. Taylor. "Moduli stabilization in chiral type IIB orientifold models with fluxes". In: *Nucl. Phys. B* 663 (2003), pp. 319–342. DOI: 10.1016/S0550-3213(03)00392-4. arXiv: hep-th/0303016 (cited on pages 137, 149, 150).

[185] Juan F.G. Cascales and Ángel M. Uranga. "Chiral 4d string vacua with D branes and NSNS and RR fluxes". In: *JHEP* 05 (2003), p. 011. DOI: 10.1088/1126-6708/2003/05/011. arXiv: hep-th/0303024 (cited on pages 137, 149, 150).

[186] Marcos Marino, Ruben Minasian, Gregory W. Moore, and Andrew Strominger. "Nonlinear instantons from supersymmetric p-branes". In: *JHEP* 01 (2000), p. 005. DOI: 10.1088/1126-6708/2000/01/005. arXiv: hep-th/9911206 (cited on page 137).

[187] Chang-Shou Lin and Chin-Lung Wang. "Elliptic functions, Green functions and the mean field equations on tori". In: *Annals of Mathematics* (2010), pp. 911–954 (cited on page 139).

[188] David Andriot and Dimitrios Tsimpis. "Gravitational waves in warped compactifications". In: *JHEP* 06 (2020), p. 100. DOI: 10.1007/JHEP06(2020)100. arXiv: 1911.01444 [hep-th] (cited on page 139).

[189] Tom Rudelius. "Constraints on Axion Inflation from the Weak Gravity Conjecture". In: *JCAP* 1509.09 (2015), p. 020. DOI: 10.1088/1475-7516/2015/09/020,10.1088/1475-7516/2015/9/020. arXiv: 1503.00795 [hep-th] (cited on page 143).

[190] Eduardo Gonzalo and Luis E. Ibáñez. "A Strong Scalar Weak Gravity Conjecture and Some Implications". In: *JHEP* 08 (2019), p. 118. DOI: 10.1007/JHEP08(2019)118. arXiv: 1903.08878 [hep-th] (cited on page 144).

[191] Eduardo Gonzalo and Luis E. Ibáñez. "Pair Production and Gravity as the Weakest Force". In: *JHEP* 12 (2020), p. 039. DOI: 10.1007/JHEP12(2020)039. arXiv: 2005.07720 [hep-th] (cited on page 144).

[192] Cumrun Vafa. "Modular Invariance and Discrete Torsion on Orbifolds". In: *Nucl. Phys. B* 273 (1986), pp. 592–606. DOI: 10.1016/0550-3213(86)90379-2 (cited on page 145).

[193] A. Font, Luis E. Ibáñez, and F. Quevedo. "$Z(N)$ X Z(m) Orbifolds and Discrete Torsion". In: *Phys. Lett. B* 217 (1989), pp. 272–276. DOI: 10.1016/0370-2693(89)90864-2 (cited on page 145).

[194] Cumrun Vafa and Edward Witten. "On orbifolds with discrete torsion". In: *J. Geom. Phys.* 15 (1995), pp. 189–214. DOI: 10.1016/0393-0440(94)00048-9. arXiv: hep-th/9409188 (cited on page 145).

[195] Micha Berkooz, Michael R. Douglas, and Robert G. Leigh. "Branes intersecting at angles". In: *Nucl. Phys. B* 480 (1996), pp. 265–278. DOI: 10.1016/S0550-3213(96)00452-X. arXiv: hep-th/9606139 (cited on pages 145, 146).

[196] Michael R. Douglas. "D-branes and discrete torsion". In: (July 1998). arXiv: hep-th/9807235 (cited on page 145).

[197] Michael R. Douglas and Bartomeu Fiol. "D-branes and discrete torsion. 2." In: *JHEP* 09 (2005), p. 053. DOI: 10.1088/1126-6708/2005/09/053. arXiv: hep-th/9903031 (cited on page 145).

[198] C. Angelantonj, Ignatios Antoniadis, G. D'Appollonio, E. Dudas, and A. Sagnotti. "Type I vacua with brane supersymmetry breaking". In: *Nucl. Phys. B* 572 (2000), pp. 36–70. DOI: 10.1016/S0550-3213(00)00052-3. arXiv: hep-th/9911081 (cited on pages 145, 148).

[199] Mathias Klein and Raul Rabadan. "Orientifolds with discrete torsion". In: *JHEP* 07 (2000), p. 040. DOI: 10.1088/1126-6708/2000/07/040. arXiv: hep-th/0002103 (cited on page 145).

[200] Carlo Angelantonj, Ralph Blumenhagen, and Matthias R. Gaberdiel. "Asymmetric orientifolds, brane supersymmetry breaking and nonBPS branes". In: *Nucl. Phys.* B589 (2000), pp. 545–576. DOI: 10.1016/S0550-3213(00)00518-6. arXiv: hep-th/0006033 [hep-th] (cited on page 145).

[201] R. Rabadan and A. M. Uranga. "Type IIB orientifolds without untwisted tadpoles, and nonBPS D-branes". In: *JHEP* 01 (2001), p. 029. DOI: 10.1088/1126-6708/2001/01/029. arXiv: hep-th/0009135 [hep-th] (cited on page 145).

[202] Ángel M. Uranga. "A New orientifold of C**2 / Z(N) and six-dimensional RG fixed points". In: *Nucl. Phys. B* 577 (2000), pp. 73–87. DOI: 10.1016/S0550-3213(00)00127-9. arXiv: hep-th/9910155 (cited on page 146).

[203] Joseph Polchinski. "Tensors from K3 orientifolds". In: *Phys. Rev. D* 55 (1997), pp. 6423–6428. DOI: 10.1103/PhysRevD.55.6423. arXiv: hep-th/9606165 (cited on pages 146, 147).

[204] Micha Berkooz, Robert G. Leigh, Joseph Polchinski, John H. Schwarz, Nathan Seiberg, and Edward Witten. "Anomalies, dualities, and topology of D = 6 N=1 superstring vacua". In: *Nucl. Phys. B* 475 (1996), pp. 115–148. DOI: 10.1016/0550-3213(96)00339-2. arXiv: hep-th/9605184 (cited on page 146).

[205] Edward Witten. "Toroidal compactification without vector structure". In: *JHEP* 02 (1998), p. 006. DOI: 10.1088/1126-6708/1998/02/006. arXiv: hep-th/9712028 (cited on page 146).

[206] Gianfranco Pradisi and Augusto Sagnotti. "Open String Orbifolds". In: *Phys. Lett. B* 216 (1989), pp. 59–67. DOI: 10.1016/0370-2693(89)91369-5 (cited on page 146).

[207] Eric G. Gimon and Joseph Polchinski. "Consistency conditions for orientifolds and d manifolds". In: *Phys. Rev. D* 54 (1996), pp. 1667–1676. DOI: 10.1103/PhysRevD.54.1667. arXiv: hep-th/9601038 (cited on page 146).

[208] G. Aldazabal, A. Font, Luis E. Ibáñez, and G. Violero. "D = 4, N=1, type IIB orientifolds". In: *Nucl. Phys. B* 536 (1998), pp. 29–68. DOI: 10.1016/S0550-3213(98)00666-X. arXiv: hep-th/9804026 (cited on page 146).

[209] Gysbert Zwart. "Four-dimensional N=1 Z(N) x Z(M) orientifolds". In: *Nucl. Phys. B* 526 (1998), pp. 378–392. DOI: 10.1016/S0550-3213(98)00288-0. arXiv: hep-th/9708040 (cited on page 146).

[210] Matthias Klein and Raul Rabadan. "D = 4, N=1 orientifolds with vector structure". In: *Nucl. Phys. B* 596 (2001), pp. 197–230. DOI: 10.1016/S0550-3213(00)00698-2. arXiv: hep-th/0007087 (cited on page 146).

[211] Atish Dabholkar and Jaemo Park. "An Orientifold of type IIB theory on K3". In: *Nucl. Phys. B* 472 (1996), pp. 207–220. DOI: 10.1016/0550-3213(96)00199-X. arXiv: hep-th/9602030 (cited on page 147).

[212] Fernando Marchesano and Gary Shiu. "MSSM vacua from flux compactifications". In: *Phys. Rev. D* 71 (2005), p. 011701. DOI: 10.1103/PhysRevD.71.011701. arXiv: hep-th/0408059 (cited on page 149).

[213] Fernando Marchesano and Gary Shiu. "Building MSSM flux vacua". In: *JHEP* 11 (2004), p. 041. DOI: 10.1088/1126-6708/2004/11/041. arXiv: hep-th/0409132 (cited on page 149).

[214] Juan F.G. Cascales and Ángel M. Uranga. "Chiral 4-D string vacua with D-branes and moduli stabilization". In: *10th Marcel Grossmann Meeting on Recent Developments in Theoretical and Experimental General Relativity, Gravitation and Relativistic Field Theories (MG X MMIII)*. Nov. 2003, pp. 1048–1067. arXiv: hep-th/0311250 (cited on page 149).

[215] Hisaki Hatanaka, Makoto Sakamoto, Motoi Tachibana, and Kazunori Takenaga. "Many brane extension of the Randall-Sundrum solution". In: *Prog. Theor. Phys.* 102 (1999), pp. 1213–1218. DOI: 10.1143/PTP.102.1213. arXiv: hep-th/9909076 [hep-th] (cited on page 165).

[216] Lisa Randall and Raman Sundrum. "A Large mass hierarchy from a small extra dimension". In: *Phys. Rev. Lett.* 83 (1999), pp. 3370–3373. DOI: 10.1103/PhysRevLett.83.3370. arXiv: hep-ph/9905221 [hep-ph] (cited on page 165).

[217] Lisa Randall and Raman Sundrum. "An Alternative to compactification". In: *Phys. Rev. Lett.* 83 (1999), pp. 4690–4693. DOI: 10.1103/PhysRevLett.83.4690. arXiv: hep-th/9906064 [hep-th] (cited on page 165).

[218] Joseph Polchinski and Edward Witten. "Evidence for heterotic - type I string duality". In: *Nucl. Phys.* B460 (1996), pp. 525–540. DOI: 10.1016/0550-3213(95)00614-1. arXiv: hep-th/9510169 [hep-th] (cited on page 165).

[219] Brian R. Greene. "String theory on Calabi-Yau manifolds". In: *Theoretical Advanced Study Institute in Elementary Particle Physics (TASI 96): Fields, Strings, and Duality*. June 1996, pp. 543–726. arXiv: hep-th/9702155 (cited on page 167).

[220] K. Hori, S. Katz, A. Klemm, R. Pandharipande, R. Thomas, C. Vafa, R. Vakil, and E. Zaslow. *Mirror symmetry*. Vol. 1. Clay mathematics monographs. Providence, USA: AMS, 2003 (cited on page 167).

[221] Cyril Closset. "Toric geometry and local Calabi-Yau varieties: An Introduction to toric geometry (for physicists)". In: (Jan. 2009). arXiv: 0901.3695 [hep-th] (cited on page 167).

[222] Edward Witten. "D-branes and K theory". In: *JHEP* 12 (1998), p. 019. DOI: 10.1088/1126-6708/1998/12/019. arXiv: hep-th/9810188 (cited on page 171).

[223] Oren Bergman, Amihay Hanany, Andreas Karch, and Barak Kol. "Branes and supersymmetry breaking in three-dimensional gauge theories". In: *JHEP* 10 (1999), p. 036. DOI: 10.1088/1126-6708/1999/10/036. arXiv: hep-th/9908075 (cited on page 172).

[224] J. Polchinski. *String theory. Vol. 1: An introduction to the bosonic string*. Cambridge Monographs on Mathematical Physics. Cambridge University Press, Dec. 2007. DOI: 10.1017/CBO9780511816079 (cited on pages 175, 176).

[225] J. Polchinski. *String theory. Vol. 2: Superstring theory and beyond*. Cambridge Monographs on Mathematical Physics. Cambridge University Press, Dec. 2007. DOI: 10.1017/CBO9780511618123 (cited on page 176).

Notation

α'	$1/(2\pi M_s^2)$
κ_{10}	$\frac{(2\pi)^7 \alpha'^4}{2}$
$\mathcal{L}$	Lagrangian density
g_s	VEV of the spacetime dilaton $\phi(x)$, defined $e^{\phi(x)}$
l_s	$1/M_s$
M_s	String scale
$M_{P,d}$	Planck mass in d dimensions
S	Action

Glossary

ABJM Aharony-Bergman-Jafferis-Maldacena. 15, 16, 21, 24, 25, 97, 98, 108–110, 118, 119, 160
ADC AdS Distance Conjecture. 67, 99, 123
AdS Anti-de Sitter. 14–17, 21–28, 41, 55, 66, 67, 74, 75, 97–99, 104–109, 114–116, 121–124, 127, 129, 159, 160, 165

BH Black Hole. 68
BPS Bogomol'nyi–Prasad–Sommerfield. 16, 97–99, 101, 106, 109, 110, 112, 115, 119, 121–124, 127, 128, 130–133, 138, 140, 143, 144, 148, 151
BSM Beyond Standard Model. 97

CFT Conformal Field Theory. 21, 24, 25, 55, 66, 104, 106, 109, 159
CS Chern-Simons. 15, 24, 34, 40, 58, 60, 74, 108, 111, 112, 117, 119, 132
CY Calabi-Yau. 13–16, 23, 25, 28–33, 35–39, 43, 59, 63, 73, 74, 93, 97, 98, 113–115, 117–120, 134, 145, 159, 169

DBI Dirac-Born-Infeld. 132, 139
DGKT DeWolfe-Giryavets-Kachru-Taylor. 15, 16, 39, 116, 161
DKS Dvali-Kaloper-Sorbo. 16, 58, 59, 99, 115, 159, 171
DoF Degree of Freedom. 33, 37
dS de Sitter. 28
DW Domain Wall. 16, 120

EFT Effective Field Theory. 11–14, 65, 68, 69, 160
EoM Equation of motion. 15, 28, 29, 160

FW Freed-Witten. 17, 58, 59, 111, 120, 171–173

GCD Greatest Common Divisor. 41
GKP Giddings-Kachru-Polchinski. 28, 30, 31
GR General Relativity. 11, 12

HW Hanany-Witten. 17, 59, 62, 93, 172

IR Infrared. 21
ISD Imaginary Self-Dual. 30, 31

KK Kaluza-Klein. 28, 41, 58, 60, 74, 98, 99, 104–114, 116, 123, 129, 130

MSSM Minimal Supersymmetric Standard Model. 11, 14, 74

NSNS Neveu–Schwarz − Neveu–Schwarz. 24, 29, 33, 38, 39, 51, 58, 98, 114, 115, 117, 128, 133, 134, 136, 137, 149, 150, 171

QFT Quantum Field Theory. 11, 12, 55
QG Quantum Gravity. 12, 14, 16, 65, 74, 97, 99, 103, 127, 128, 144, 151, 159–161

RR Ramond − Ramond. 24, 25, 29, 33, 36–40, 51, 58–60, 98, 105, 111–115, 117, 122, 123, 127, 128, 132–134, 136, 137, 143, 148–151, 171
RSADC Refined Strong AdS Distance Conjecture. 16, 41, 99, 121–124, 160

SADC Strong AdS Distance Conjecture. 16, 67, 97, 98, 121, 160
SCFT Supersymmetric Conformal Field Theory. 15, 16, 23, 24, 26, 27, 43, 51, 55, 61, 62, 98, 106, 107, 114, 127, 129, 159
SDC Swampland Distance Conjecture. 66, 67, 103, 104

SE Sasaki-Einstein. 15, 21, 23, 25–27, 43, 47, 93, 98
SM Standard Model. 11, 12, 14, 73
SQFT Supersymmetric Quantum Field Theory. 172
ST String Theory. 12–16, 159, 160
SUGRA Supergravity. 12, 13
SYM SuperYang-Mills. 15, 21, 22, 43

UV Ultraviolet. 11, 12, 14, 65

VEV Vacuum Expectation Value. 11, 28, 34, 55, 66, 124, 144

WCC Weak Coupling Conjecture. 16, 25, 98, 99, 103, 104, 106–108, 110–115, 120, 122–124, 160
WGC Weak Gravity Conjecture. 16, 17, 65, 67–70, 97, 98, 100–103, 106, 109, 110, 112, 120, 127–130, 136, 140–144, 150, 151, 159–161
WS Worldsheet. 12